INVESTIGATING NOVEL DRUG TREATMENTS FOR HEART FAILURE

By

HANNAH NOORDALI

A thesis submitted to the University of Birmingham
For the degree of DOCTOR OF PHILOSOPHY

Institute of Cardiovascular Sciences
School of Clinical and Experimental Medicine
College of Medical and Dental Sciences
University of Birmingham
January 2018

Abstract

Perhexiline is a metabolic modulator considered to be an alternative pharmacotherapeutic agent in heart failure (HF), a debilitating condition characterised by severe metabolic disturbances (i.e. impaired substrate utilisation and energy production) in which morbidity and mortality are high. However, perhexiline therapy requires regular plasma monitoring, which is clinically unattractive. Moreover, its exact cardioprotective mechanism(s) remains unknown. The work in this thesis aimed to investigate the protective effects and underlying molecular mechanism(s) of perhexiline *ex vivo*, in Langendorff-perfused mouse hearts and *in vivo*, in the abdominal aortic constriction model of HF, and to determine whether the effects could be replicated by the novel perhexiline derivative, fluoroperhexiline-1 (FPER-1), which has better pharmacokinetics. *Ex vivo*, 2 µM perhexiline or 10 µM FPER-1 perfusion increased cardiac contractility and relaxation pre-ischaemia and improved post-ischaemic haemodynamics and hypercontracture magnitude. This involved enhancing the contractility-relaxation pathway (phospholamban (PLB) deactivation) pre-ischaemia and improving glucose metabolism (pyruvate dehydrogenase (PDH) activation and glycogen synthase kinase 3αβ (GSK3αβ) deactivation) during ischaemia. *In vivo*, 4-week gavage with 70 mg/kg perhexiline or FPER-1 attenuated hypertrophy and cardiac remodelling at end-diastole whilst decreasing the expression of uncoupling protein 3 (UCP3), a redox-sensitive protein. Additionally, perhexiline alone improved systolic function (i.e. improved left ventricular ejection fraction and fractional shortening) in parallel with PLB deactivation. Taken together these results provide novel evidence that perhexiline protects the heart against ischaemic injury and delays progression from hypertrophy to failure by metabolic and non-metabolic (PLB) mechanisms, most of which were replicated by FPER-1.

Acknowledgements

I would first and foremost like to thank my supervisors Professor Michael Frenneaux and Dr Iain Greig (of Signal Pharma) for the opportunity to undertake such a compelling and stimulating research project and for always offering their guidance and expertise during this PhD. I would also like to express my deepest gratitude to my supervisor Professor Janice Marshall for her kindness and all the support, advice and guidance she has given me. She has truly been an inspiration throughout my academic career and has not only taught me to believe in my abilities but to also believe in myself.

Special thanks also goes to those who have assisted with the different aspects of my research; Dr Sian Lax for her help with thesis editing, Dr Larissa Fabritz and Dr Fahima Syeda for the echocardiographic training, Dr James Clark and Dr Alexander Brill for their guidance with *in vivo* surgery, Dr Patricia Lalor and Dr Julie Rayes for their expertise on liver histology, Professor Benedetta Sallustio for conducting the drug pharmacokinetics and lastly Professor Gerard Nash for his support during the final year of my PhD.

To my ever-changing lab group who have been the soul of this PhD; Dr Jenna Bailey, Dr Alessandra Borgognone, Dr Safa Abdul Ghani, Dr Fiona Ashford, Dr Eakkapote Prompunt, Miss Rosie May Hayes and Miss Sophie Worrall, thank you for all the countless laughs and memories that we have created and shared together. You have all made this PhD a truly enjoyable and memorable experience.

Most of all, thank you to my family who I am irrevocably indebted to; my father for always believing I could achieve anything I put my mind to, my mother for being my rock and for all her strength and encouragement and my brother Farhan, whose witty sense of humour has kept me smiling and motivated throughout my PhD.

And lastly, God, thank you for blessing me with the determination to embark on and complete this PhD.

List of Publications

The following publications have been made based on the work/information presented in this thesis.

1. **Noordali, H.**, Greig, I.R., Frenneaux, M.P. and Madhani, M. (2015) Abstract n° P-15-17: The anti-ischaemic effects of perhexiline in the murine heart. *J Mol Cell Cardiol*, p. S47.

2. Loudon, B.L.*, **Noordali, H.***, Gollop, N.D., Frenneaux, M.P. and Madhani, M. (2016) Present and future pharmacotherapeutic agents in heart failure: an evolving paradigm. *Br J Pharmacol*, 173 (12), pp. 1911-1924.

*Joint first authors

3. Tseng, C.C., **Noordali, H.**, Sani, M., Madhani, M., Grant, D.M. and Frenneaux, M.P. et al. (2017) Development of Fluorinated Analogues of Perhexiline with Improved Pharmacokinetic Properties and Retained Efficacy. *J Med Chem*, 60 (7), pp. 2780-2789.

4. **Noordali, H.**, Loudon, B.L., Frenneaux, M.P. and Madhani, M. (2018) Cardiac metabolism—A promising therapeutic target for heart failure. *Pharmacol Ther*, 182, pp. 95 – 114.

Table of Contents

List of Figures

Chapter 3

Chapter 4

Chapter 5

Chapter 6

Chapter 7

List of Tables

Abbreviations

AAC	Abdominal aortic constriction
ACC	Acetyl-coenzyme A carboxylase
ACE	Angiotensin converting enzyme
ADP	Adenosine diphosphate
Akt	Protein kinase B
ALT	Alanine transaminase
AMPK	5' adenosine monophosphate-activated protein kinase
ANOVA	Analysis of variance
ANT	Adenine nucleotide translocase
AP	Action potential
APS	Acetate plate sealer
ARB	Angiotensin receptor blocker
ASPA	Animals Scientific Procedures Act
ATP	Adenosine triphosphate
B-mode	Bright mode
BNP	Brain natriuretic peptide
bpm	beats per minute
BSA	Bovine serum albumin
BW	Body weight
Ca^{2+}	Calcium ion
CABG	Coronary artery bypass grafting
CFR	Coronary flow rate
CK	Creatine kinase
CO	Cardiac output
CO_2	Carbon dioxide
CoA	Coenzyme A
CoQ10	Coenzyme Q10
CPT	Carnitine palmitoyltransferase
CYP2D6	Cytochrome P450 2D6
DCA	Dichloroacetate
DCM	Dilated cardiomyopathy
DHPR	Dihydropyridine receptor
DMSO	Dimethyl sulfoxide
DNA	Deoxyribonucleic acid

EC	Excitation-contraction
ECM	Extracellular matrix
EDTA	Ethylenediaminetetraacetic acid
EDV	End-diastolic volume
EF	Ejection fraction
EIA	Enzyme immunoassay
ERK1/2	Extracellular signal-regulated kinase 1/2
ESC	European Society of Cardiology
ETC	Electron transport chain
FA	Fatty acid
$FADH_2$	Flavin adenine dinucleotide
FPER	Fluoroperhexiline
FS	Fractional shortening
G6P	Glucose-6-phosphate
GIK	Glucose-Insulin-Potassium
GLP-1	Glucagon-like peptide-1
GLUT	Glucose transporter
GSK3αβ	Glycogen synthase kinase 3αβ
GTN	Glyceryl trinitrate
h	Hour
H^+	Hydrogen ion
HCM	Hypertrophic cardiomyopathy
H&E	Haematoxylin and Eosin
HERG	Human ether-ago-go-related gene
HIF1α	Hypoxia-inducible factor 1α
HF	Heart failure
HFrEF	Heart Failure with reduced Ejection Fraction
HFmEF	Heart Failure with mid-range Ejection Fraction
HFpEF	Heart Failure with preserved Ejection Fraction
HRP	Horseradish peroxidase
HPLC	High performance liquid chromatography
HW	Heart weight
i.p	Intraperitoneally
IVS	Interventricular septal wall
K^+	Potassium ion
KHB	Krebs-Henseleit buffer
KLF14	Krüppel-like factor 14

LA	Long axis
LV	Left ventricular
LVAW	Left ventricular anterior wall
LVDP	Left ventricular developed pressure
LVdp/dt	Change in left ventricular pressure over time
LVEDP	Left ventricular end-diastolic pressure
LVEF	Left ventricular ejection fraction
LVID	Left ventricular internal diameter
LVP	Left ventricular pressure
LVPW	Left ventricular posterior wall
MCD	Malonyl-coenzyme A decarboxylase
MI	Myocardial infarction
min	Minute
M-mode	Movie/motion mode
MRA	Mineralocorticoid receptor antagonist
mRNA	Messenger ribonucleic acid
mTORC1	Mammalian target of rapamycin complex 1
Na^+	Sodium ion
NaCMC	Sodium carboxymethyl cellulose
NADH	Nicotinamide adenine dinucleotide
NADPH	Nicotinamide adenine dinucleotide phosphate
Na_2CO_3	Sodium carbonate
$NaHCO_3$	Sodium bicarbonate
NO	Nitric oxide
NOS	Nitric oxide synthase
NOX	Nicotinamide adenine dinucleotide phosphate oxidase
NT-proBNP	N-terminal prohormone of brain natriuretic peptide
NYHA	New York Heart Association
O_2	Oxygen
OCR	Oxygen consumption rate
OD	Optical density
OH-perhexiline	Hydroxy-perhexiline
PARP	Poly (adenosine diphosphate-ribose) polymerase
PBS	Phosphate buffered saline
PBST	Phosphate buffered saline with 0.1% Tween
PCr	Phosphocreatine
PGC-1	Peroxisome proliferator activated receptor-γ coactivator-1

PDH	Pyruvate dehydrogenase
PDK	Pyruvate dehydrogenase kinase
PDP	Pyruvate dehydrogenase phosphatase
PKG	Protein kinase G
PLB	Phospholamban
PM	Poor metaboliser
PPAR	Peroxisome proliferator-activated receptor
p.o	Per os/orally
PVDF	Polyvinylidene difluoride
PW	Pulse-wave
qPCR	Quantitative polymerase chain reaction
RAAS	Renin-angiotensin-aldosterone-system
RCT	Randomised controlled trial
RISK	Reperfusion Injury Salvage Kinase
ROS	Reactive oxygen species
RYR	Ryanodine receptor
SA	Short axis
SA-HRP	Streptavidin-horseradish peroxidase
SDS	Sodium dodecyl sulphate
sec	Second
SEM	Standard error of the mean
SERCA	Sarco-endoplasmic reticulum calcium-ATPase
SNA	Sympathetic nerve activity
SR	Sarcoplasmic reticulum
SS31	Szeto-Schiller peptide 31
STEMI	Acute AT-segment elevation myocardial infarction
SV	Stroke volume
TAC	Thoracic aortic constriction
TAG	Triacylglycerol
TCA	Tricarboxylic acid
TMB	Tetramethylbenzidine
Trx2	Thioredoxin 2
TTC	Triphenyltetrazolium chloride
TXNIP	Thioredoxin-interacting protein
UCP	Uncoupled protein
UK	United Kingdom
VTI	Velocity time integral

Chapter 1: Introduction

Chapter 1: Introduction

1.1. Overview

Heart failure (HF) is a highly debilitating disease which affects a large proportion of the population, particularly the elderly (≥65 years). Despite the existence of evidence-based pharmacological treatments for HF, aimed at reversing neurohormonal dysregulation, morbidity and mortality remain high. Therefore, a novel pharmacological target has been sought. Growing evidence suggests that cardiac metabolism and energetics are impaired in HF, and correcting these disturbances may improve cardiac function. Consequently, the overall focus of the work in this PhD thesis was to investigate a well-known metabolic modulator, perhexiline, and its newly developed analogue fluoroperhexiline-1 (FPER-1), in an established *ex vivo* global ischaemia model and *in vivo* HF model to determine the efficacy and accompanying molecular mechanisms of these agents.

1.2. The mammalian heart

The heart is a pivotal organ, which, alongside the intricate pulmonary and systemic vasculature forms the cardiovascular system (Levick, 2009). The primary role of the heart is to pump oxygenated and nutrient-rich blood to the systemic organs, in a manner that can be increased to meet metabolic demand (Kemp and Conte, 2012). The volume of blood pumped by the heart per minute is called the cardiac output (CO). The human heart pumps ~7,500 L of blood daily, beating on average 100,000 times a day (BHF, 2018). This continuous pumping is made efficient by the hearts specialised structure and cells.

1.2.1. Basic structure and blood flow in the heart

In the mammalian heart, the right side is involved with transporting deoxygenated blood from the systemic circulation to the pulmonary circulation for reoxygenation and in parallel, the left side is responsible for transporting the freshly oxygenated blood from the lungs back to the systemic organs **[Figure 1.1]** (Levick, 2009; Katz, 2010). The oxygenated blood enters the left ventricle following opening of the mitral valve and upon ventricular contraction, blood is pushed through the aortic valve into the aorta for transport to the systemic circulation. A greater force is required to pump blood into the systemic circulation given its greater resistance; therefore, the left ventricle is thicker than the right side. The two ventricular chambers are also separated by the interventricular septal wall (Iaizzo, 2015).

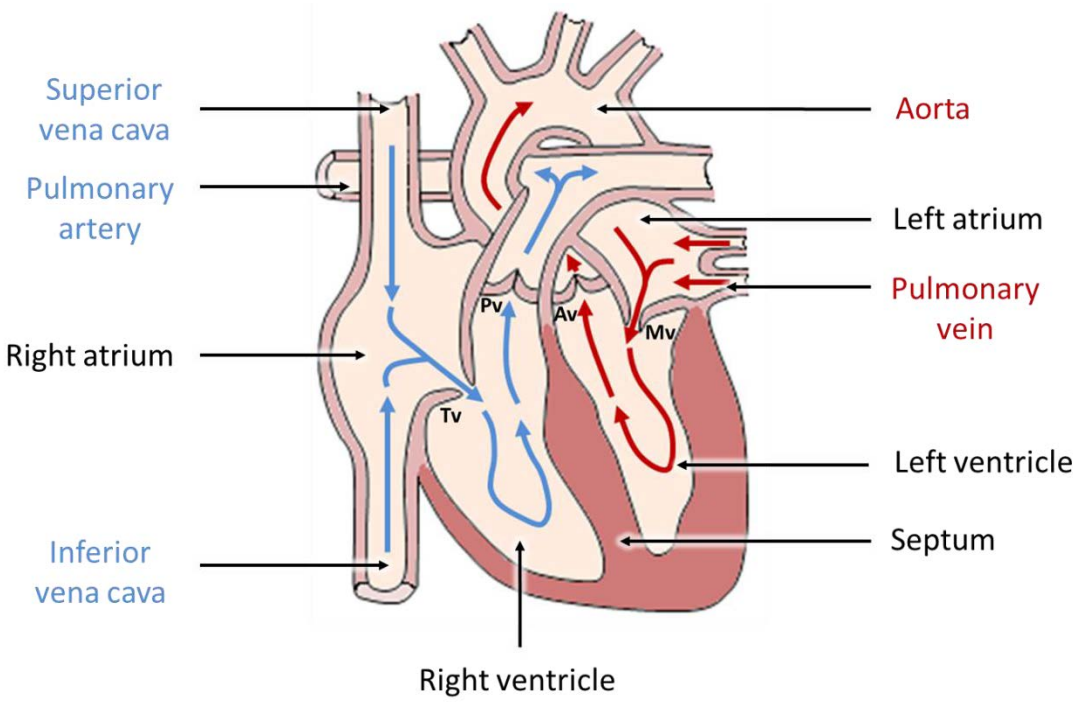

Figure 1.1. Basic structure and blood flow of the heart

The mammalian heart consists of four chambers and transports blood to the pulmonary and systemic circulation. The blue arrows outline the transport of deoxygenated blood which arrives from the systemic circulation into the right side of the heart though the vena cava, for transport to the lungs by the pulmonary artery, for reoxygenation. The red arrows outline the transport of oxygenated blood which arrives from the pulmonary circulation and enters the left side of the heart through the pulmonary vein, to be delivered to the body by entering the systemic circulation through the aorta.

Av, aortic valve; Mv, mitral valve; Pv, pulmonary valve; Tv, tricuspid valve.

The heart itself receives a constant supply of oxygenated and nutrient-rich blood from the coronary circulation; a network of coronary arteries present on the outer heart wall (Levick, 2009). The heart wall has three layers: the outer epicardium, the middle myocardium and the inner endocardium (Katz, 2010). The middle layer consists of the cardiac muscle which forms the bulk tissue of the heart and is responsible for cardiac contractions (discussed in section 1.3.2).

1.2.2. The cardiac muscle

The cardiac muscle contains two cell types: ~1% pacemaker cells and ~99% cardiomyocytes (Pinnel et al., 2007; Levick, 2009). Pacemakers are part of the heart's electrical conducting system and are responsible for initiating contractions and/or determining the cardiac rhythm. Cardiomyocytes are striated contractile muscle cells; each consisting of myofibrils, which are made of repetitive regular chains of contractile units known as sarcomeres **[Figure 1.2]** (Stenger and Spiro, 1961). In turn, the sarcomeres comprise of fibrous contractile myofilaments, actin and myosin, which are stacked in a specialised formation that enables uniformed contraction and relaxation (Pinnell et al., 2007). Cardiomyocytes are also connected to one another by intercalated discs which facilitate rapid electrical and mechanical conduction, thereby enabling synchronized cardiac contraction, fundamental for healthy cardiac function (Stenger and Spiro, 1961).

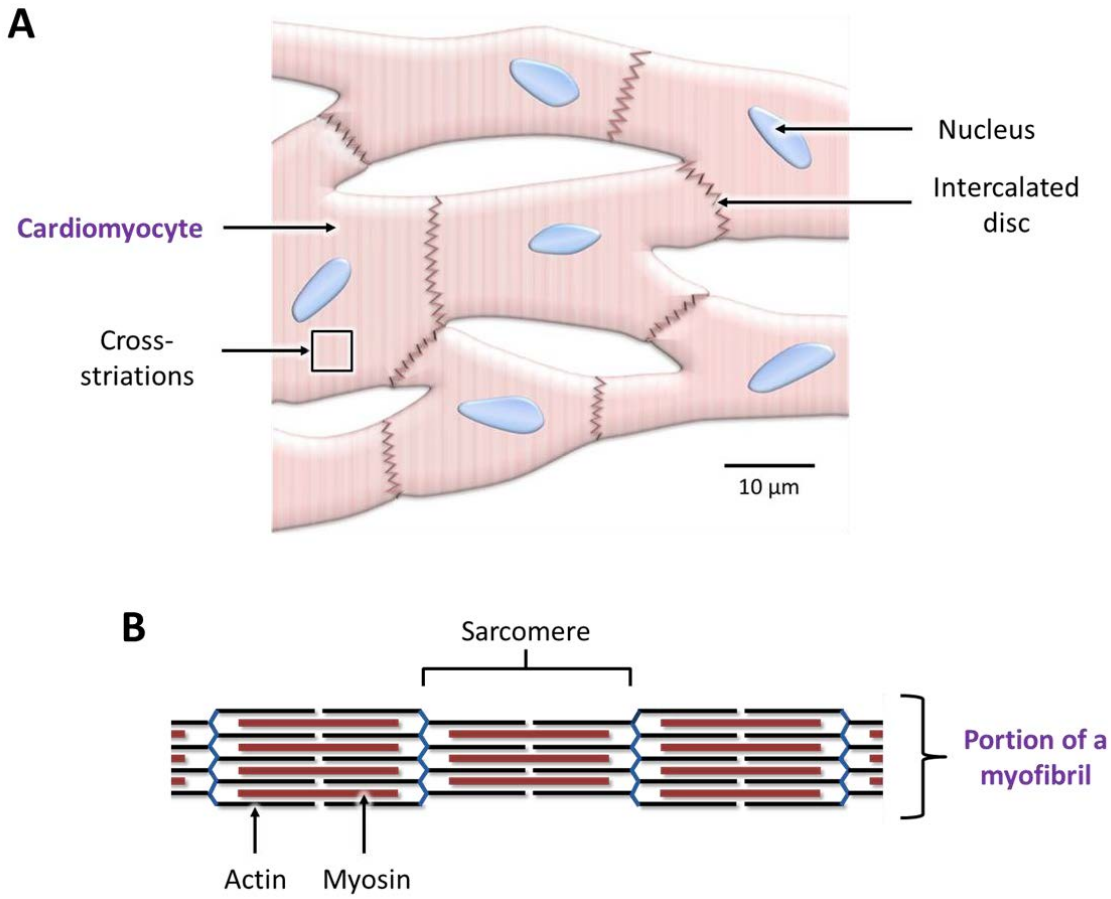

Figure 1.2. Schematic of the cardiac muscle fibre and sarcomere

A: A series of cardiomyocytes which are connected to one another by intercalated discs, forming the cardiac muscle fibre. **B:** Repeating chains of sarcomeres which form the myofibrils present in cardiomyocytes. Each sarcomere consists of the overlapping myofilaments actin and myosin, which give rise to the striated appearance of the cardiac muscle.

1.3. Cardiac function in the healthy heart

The synchronised contraction and relaxation of the atria and ventricles with every heart beat forms the cardiac cycle. In this cycle, cardiac contraction and ejection of blood is referred to as 'systole' whilst cardiac relaxation and filling is called 'diastole'. The cardiac cycle also involves coordinated pressure changes within the chambers (Levick, 2009). Understanding these fundamental processes is important in recognising the detrimental changes in function that take place during cardiovascular diseases such as HF.

1.3.1. Cardiac haemodynamics

Haemodynamics refers to the movement of blood within the cardiovascular system which is governed by pressure changes created initially by the heart and modified by the vasculature (Borlaug and Kass, 2009). The clinical assessment of cardiac haemodynamics, through either non-invasive Doppler echocardiography or invasive Swan-Ganz catheterisation, is used for evaluating myocardial systolic and diastolic function (Sutton, 2010). Pressure within the left ventricle is particularly important given its role in determining systemic perfusion. The left ventricular end-diastolic pressure (LVEDP), i.e. the pressure at end-diastole and cardiac filling, reflects left ventricular (LV) compliance and thus an increase in this pressure is commonly seen in LV failure (Borlaug and Kass, 2009). The LVEDP and the volume present at end-diastole (EDV) also determine the systolic pressure and force of contraction that the heart can generate via the Frank-Starling mechanism. This mechanism describes that the greater the EDV, the greater the stretch of the myocardial muscle fibres (preload) which stimulates a greater force of contraction (Sequeira and van der Velden, 2015). An increase in contractile force contributes to an increase in stroke volume (SV) and therefore CO (CO = SV x heart rate). During contraction, the myocardium generates and sustains a pressure that propels blood into the aorta. This pressure and force must overcome the resistance within the vasculature, known as the afterload, and is best described as the ventricular wall stress (Norton, 2001). The afterload can be formally defined by Laplace's law: Wall stress = (Pressure x Ventricular radius)/2 x Wall thickness (Norton, 2001). When afterload rises to high levels, the SV (and thus CO) become inversely related, i.e. the greater the afterload, the lower the SV (and CO). In addition to heart rate, preload and afterload, the CO is also dependent on the contractility of the heart itself (Borlaug and Kass, 2009).

1.3.2. Cardiac contractility

Cardiac contractility or 'inotropy' is the unique and intrinsic ability of the cardiac muscle to generate a force independent of preload and afterload and is governed by the degree to which the myocardial fibres can shorten following activation by the sympathetic system (i.e. strength of contraction) (Sequeira and van der Velden, 2015). An increase in sympathetic nerve activity (SNA) leads to an increase in noradrenaline release at the cardiac nerve terminals and circulating catecholamine levels. The released catecholamines bind to β-adrenergic receptors located on the cardiomyocyte sarcolemma, activating an intracellular signalling cascade that increases the intracellular Ca^{2+} ion levels (Triposkiadis et al., 2009). Inotropy is largely dependent on the cytosolic Ca^{2+} ion concentration which converts the electrical energy from an action potential (AP) into mechanical energy (contraction), and is termed excitation-contraction (EC) coupling **[Figure 1.3]** (Eisner et al., 2017). Therefore, an increase in Ca^{2+} cycling increases the rate (chronotropy) and strength of cardiac contractility (inotropy) and relaxation (lusitropy).

In brief, APs initiated by the pacemaker cells cause cardiomyocyte depolarisation which activates voltage-dependent Ca^{2+} ion channels known as dihydropyridine receptors (DHPR) located on the sarcolemma, thereby allowing Ca^{2+} ions to enter the cell. This influx of Ca^{2+} stimulates the release of additional Ca^{2+} ions within the sarcoplasmic reticulum (SR) through Ca^{2+}-release channels called ryanodine receptors (RYR). This process is termed calcium-induced-calcium-release (Endo et al., 1970; Eisner et al., 2017). The cytosolic Ca^{2+} ions bind to troponin-C present on actin myofilaments, enabling the binding of actin to myosin and cross-bridge formation. The cyclic movement of the actin over myosin, following adenosine

triphosphate (ATP) hydrolysis, leads to shortening of the sarcomere length and thus contraction (Rassier, 2017). This activity continues until the Ca^{2+} ions are removed, inducing cardiac relaxation, either by extrusion through sarcolemmal Ca^{2+}/Na^{+} ion exchangers, sarcolemmal uniport Ca^{2+}-ATPase or sequestration into the SR via the sarco-endoplasmic reticulum Ca^{2+}-ATPase 2a (SERCA2a) following ATP hydrolysis (Eisner et al., 2017). SERCA2a activity is responsible for removal of >70% of the cytosolic Ca^{2+} ion levels. Dysregulation of this protein is commonly seen in HF (Eisner et al., 2017).

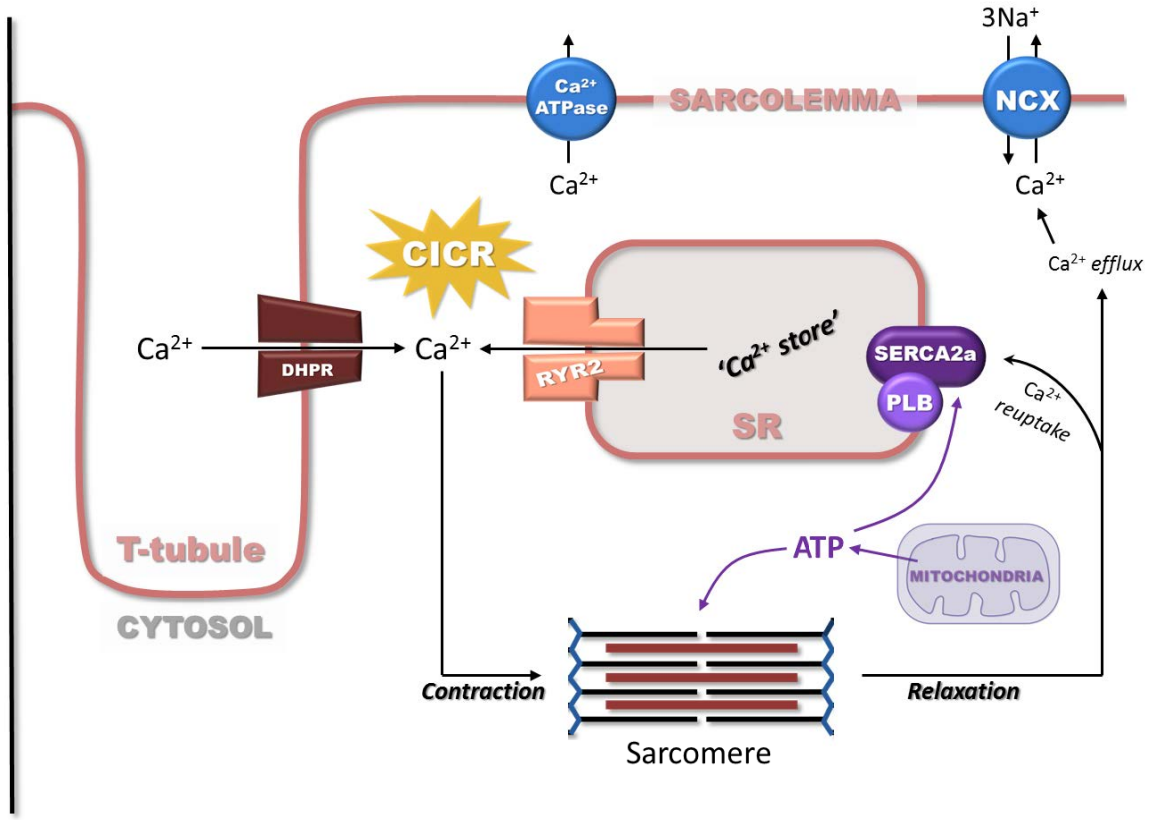

Figure 1.3. A simplified schematic of excitation-contraction coupling

Excitation-contraction coupling is an energetic process which involves Ca^{2+} cycling within the cardiomyocytes, generating a contractile force by enhancing sarcomere shortening. Cardiac relaxation is achieved by Ca^{2+} sequestration either extracellularly or into the sarcoplasmic reticulum via SERCA.

ATP, adenosine triphosphate; Ca^{2+}, calcium ion; CICR, calcium-induced-calcium-release, DHPR, dihydropyridine receptor; PLB, phospholamban; NCX, Na^{+}/Ca^{2+} exchanger; RYR2, ryanodine receptor 2; SERCA2a, sarco-endoplasmic reticulum Ca^{2+}-ATPase 2a; SR, sarcoplasmic reticulum.

SERCA2a activity is regulated by transmembrane protein phospholamban (PLB). When dephosphorylated PLB binds to and inhibits SERCA2a. Following PLB phosphorylation at either Ser16 or Thr17 (Colyer, 1998) this inhibition is relieved, increasing the SR Ca^{2+} ion flux, thereby enhancing cardiac contractility and relaxation. Thus, changes in the expression and/or activity of proteins such as PLB are useful experimental markers of changes in cardiac contractility and relaxation.

Clinically, the inotropic state of the heart is assessed by measuring the left ventricular ejection fraction (LVEF); the percentage of blood ejected from the ventricles upon each contraction, using echocardiography (Borlaug and Kass, 2011). Experimentally, echocardiography is also used to measure *in vivo* cardiac function in small animals (Ram et al., 2011). However *ex vivo* assessment of cardiac function in isolated perfused hearts still dominate experimental studies due to the simplicity and high reproducibility. Furthermore, isolated heart perfusion models allow for functional assessments in the absence of confounding and complex vascular and neurohormonal responses observed *in vivo* (Liao et al., 2012). The Langendorff is one of such models, highly used for both cardiovascular and pharmacological research (Liao et al., 2012).

1.3.3. The Langendorff: an experimental model to assess cardiac function

The Langendorff model, developed by Oskar Langendorff in 1895, involves the retrograde perfusion of a specialised ion and nutrient-rich solution through the cannulated aorta (Langendorff, 1897). The alternative isolated heart perfusion model, i.e. the 'working/ejecting heart', uses antegrade perfusion as both the pulmonary artery and aorta

are cannulated, thus this model requires greater skill to set-up (Neely et al., 1967). Nonetheless haemodynamics, such as LVEDP, can be easily assessed in the Langendorff model by insertion of a fluid-filled balloon (connected to a pressure transducer) into the LV chamber (Gottlieb and Magnus, 1904) and was therefore adequate for assessing the effects of pharmacological intervention on cardiac function *ex vivo* in this thesis. Small rodents i.e. mice are more commonly used; their hearts can be easily subjected to ischaemia to replicate functional and molecular changes that occur in diseases such as HF (Bell et al., 2011).

1.4. Heart failure

Chronic HF is a highly prevalent, severe and debilitating clinical syndrome which affects around 900,000 people within the UK alone (NICE, 2010; NHS, 2014) and up to 26 million worldwide (Ambrosy et al., 2014). The prevalence is expected to rise as demographic aging continues to increase. This complex condition describes the inability of the cardiac muscle to pump blood efficiently and maintain an adequate CO to meet the metabolic demand of the body (Kemp and Conte, 2012). In milder cases, this insufficiency may only manifest upon exertion whilst, in severe cases, the CO can be impaired even at rest. In addition to being an age-related condition, predominately affecting those ≥65 years, HF also develops secondary to cardiovascular insults such as hypertension, myocardial infarction (MI) and cardiomyopathy (van Riet et al., 2016).

1.4.1. The general pathophysiological changes in heart failure

In HF, the clinical manifestations may include exercise intolerance, dyspnoea, fatigue, and peripheral oedema with the symptomatic severity clinically described using the New York

Heart Association (NYHA) functional classification (Class I to IV; IV representing most severe) (Ponikowski et al., 2016). These symptoms stem from the pathophysiological changes that take place locally within the cardiac muscle as well as systemically (Kemp and Conte, 2012). Molecular changes within the cardiac muscle include dysregulation of the SERCA/PLB complex discussed in section 1.3.2. A decrease in SERCA2a expression (Lipskaia et al., 2014; Gattoni et al., 2017; Bennett et al., 2014) and SERCA2a activity (Qin et al., 2014; Sande et al., 2002; Schwinger et al., 1995; Schmidt et al., 1999) were observed in failing mouse hearts, failing rat hearts and failing human hearts respectively. Moreover, undesirable decreases in PLB phosphorylation at Ser16 and/or Thr17 were observed in LV samples from patients with end-stage HF (Ling et al., 2012), in mice with thoracic aortic constriction (TAC)-induced HF (Pereira et al., 2013; Chen et al., 2016; Aoyama et al., 2016), in failing rat hearts (Sande et al., 2002) and failing dog hearts (Mishra et al., 2003). The combined changes in the SERCA/PLB complex during HF lead to dysregulated Ca^{2+} cycling and uptake into the SR which reduces the rate of cardiac relaxation and contractility, ultimately causing diastolic and systolic dysfunction (Haghighi et al., 2014).

In addition to these molecular alterations, the general maladaptive changes in HF include: neurohormonal dysregulation i.e. increased SNA and activation of the renin-angiotensin-aldosterone system (RAAS), aberrant cardiac remodelling, and cardiac and vascular dysfunction **[Figure 1.4]**. However, HF is a complex disorder and it is now recognised that fundamental pathophysiological differences exist between subsets of HF patients, particularly in relation to the LVEF (Noordali et al., 2018).

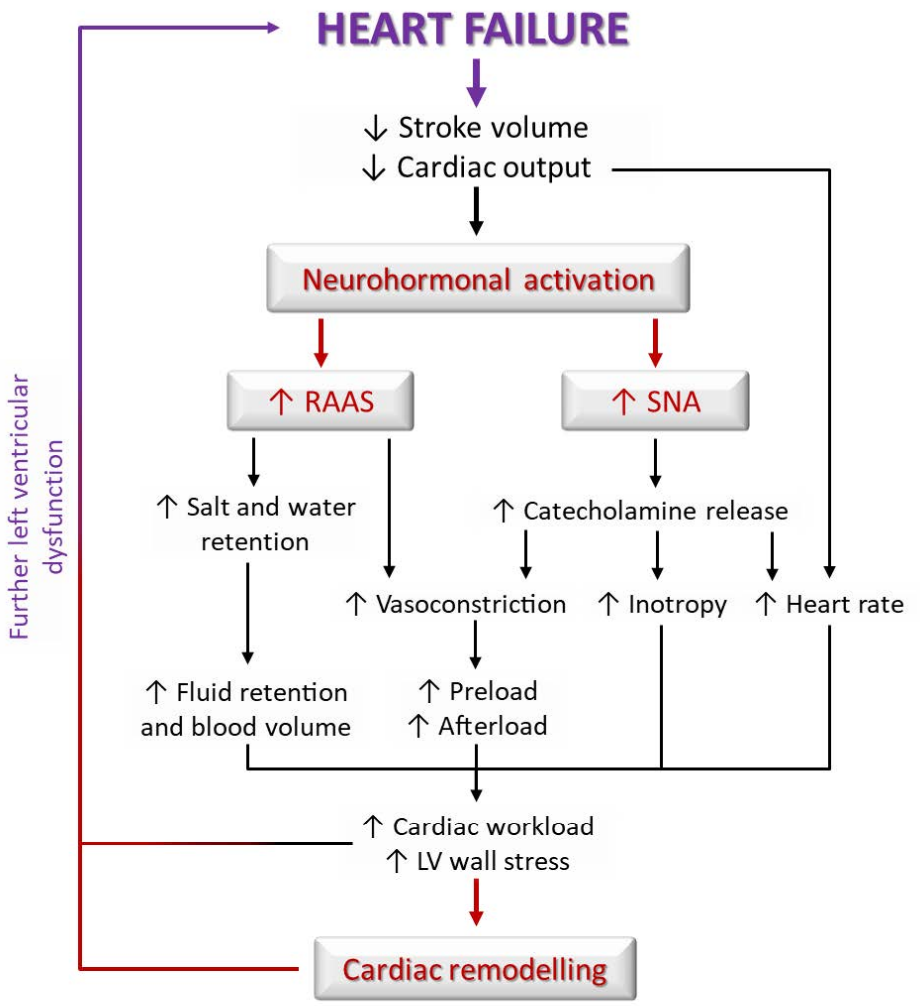

Figure 1.4. The general pathophysiological changes in heart failure

A simplified outline of the general compensatory changes that occur in heart failure (red text and arrows), which together aim to increase cardiac output. Overtime these changes become maladaptive and counterproductive, further exacerbating left ventricular dysfunction and failure (purple arrow).

RAAS, renin-angiotensin-aldosterone-system; SNA, sympathetic nerve activity.

1.4.2. Ejection fraction is used to classify heart failure

The LVEF, which provides a non-invasive echocardiographic measure of systolic function with strong correlation to HF mortality, is now commonly used to classify patients with HF (Solomon et al., 2005). HF with a LVEF of <40% is classed as heart failure with reduced ejection fraction (HFrEF): patients with this condition make up less than half of the HF

population. In contrast, just over half of HF patients have an LVEF ≥50%: heart failure with preserved ejection fraction (HFpEF) (Borlaug and Kass, 2011). More recently, HF with a LVEF in the mid-range of 40-49% (HFmEF) was also identified: this affects around 15% of HF patients (Ponikowski et al., 2016).

Despite both HFrEF and HFpEF sharing similar signs and symptoms as outlined above (section 1.4.1), they do not share a common aetiology (Borlaug and Redfield, 2011). Current pharmacological therapies have proven successful in the treatment and management of HFrEF, but have failed to produce similar benefits for HFpEF (Owan et al., 2006; Senni et al., 2017). Furthermore, despite the wide range of pharmacological treatments available for HFrEF, prognosis remains unfavorable and there are currently no evidence-based treatments for HFpEF (Loudon et al., 2016; van Riet et al., 2016; Senni et al., 2017). It is therefore evident that novel therapies are required.

In recent years, the role of cardiac energetic impairment in the pathophysiology and progression of HF has gained increasing attention (Neubauer et al., 2007; Hunter et al., 2016; Pascual and Coleman, 2016). As such, pharmacological agents which have the potential to correct metabolic dysfunction by altering cardiac substrate utilisation, increasing energy transfer from the mitochondria to cytosol, or improving mitochondrial electron transport chain (ETC) function have been considered (Siddiqi et al., 2013; Tuomainen and Tavi, 2017). To date, several metabolic modulators have shown promise in HFrEF, and are under experimental and/or clinical investigation for HFpEF: this includes perhexiline (Chong et al., 2016; Noordali et al., 2018).

1.5. The pathophysiology of HFrEF versus HFpEF

Although HFrEF and HFpEF are now both characterised by systolic and diastolic dysfunction and cardiac remodelling, they are phenotypically distinct forms of HF with different underlying pathophysiological mechanisms **[Figure 1.5]** (Borlaug and Kass, 2011; Noordali et al., 2018). However, despite the different clinical characteristics, the prognosis and survival outcome of HFrEF and HFpEF patients are similar (Abebe et al., 2016).

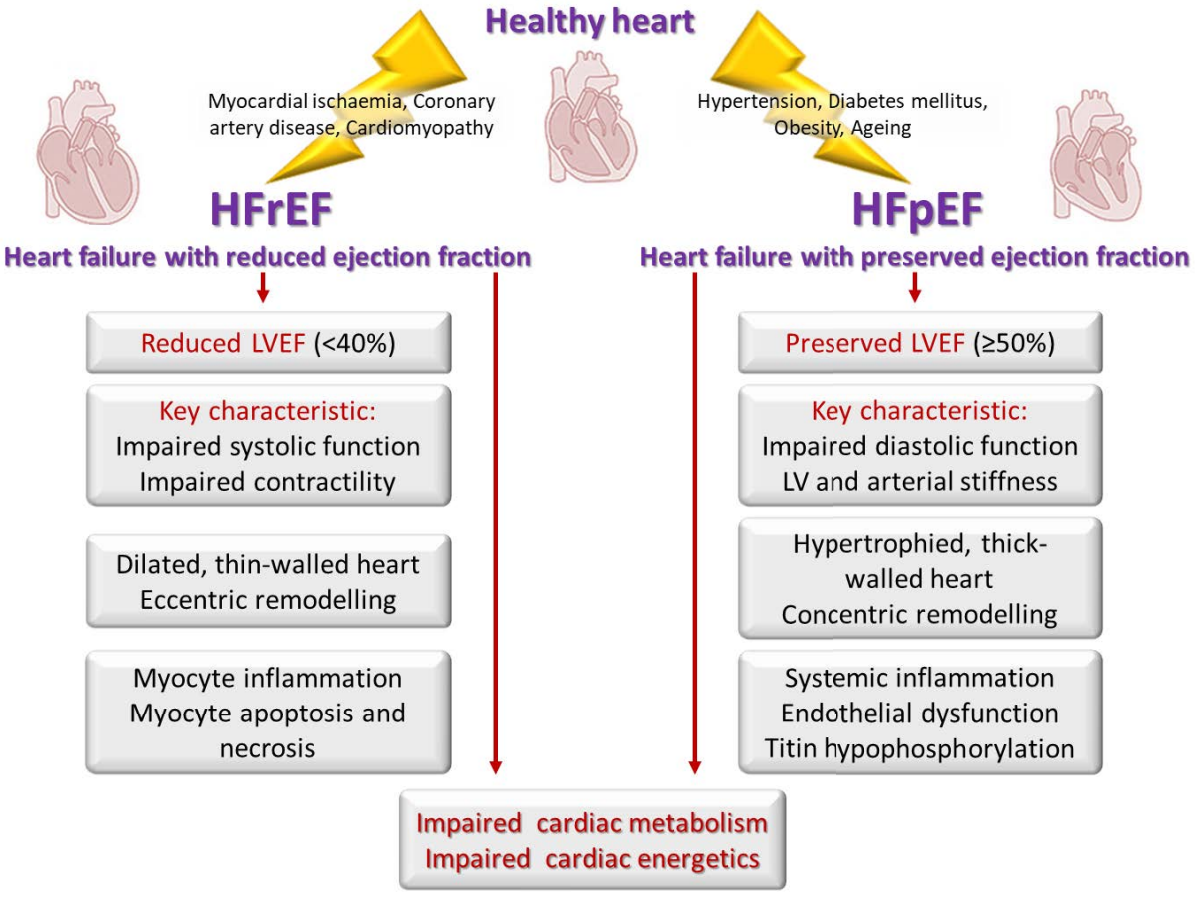

Figure 1.5. The pathophysiological differences between HFrEF and HFpEF

HFrEF and HFpEF are two phenotypically distinct forms of heart failure with different underlying pathophysiology. However, it has now been proposed that disturbances in cardiac metabolism and energetics may engender both diseases. As such, cardiac metabolism provides a novel and promising pharmacological target for the treatment and management of both types of heart failure.

HFpEF, heart failure with preserved ejection fraction; HFrEF, heart failure with reduced ejection fraction; LV, left ventricular; LVEF, left ventricular ejection fraction.

1.5.1. Heart failure with reduced ejection fraction (HFrEF)

HFrEF typically develops following a direct myocardial insult such as ischaemia, coronary artery disease or cardiomyopathy (van Riet et al., 2016). The condition was originally termed 'systolic HF' due to the clinical feature of severely reduced LVEF which occurs as a result of impaired cardiac inotropy, cardiac remodelling and dysfunctional ventricular-vascular coupling (Kass et al., 1987; Ky et al., 2013). An LVEF of <40% culminates in decreased CO and CO reserve with a parallel increase in LVEDP and LVEDV (Borlaug and Kass, 2009). As discussed in section 1.3.1, an increase in LVEDV causes activation of the Frank-Starling mechanism, which during HF acts as a compensatory mechanism to increase inotropy leading to an increased SV, which helps correct the fall in CO (Sequeira and van der Velden, 2015). Unfortunately, this response is only beneficial at rest where contractile and filling reserve can be recruited to increase CO, but is ineffective in exercise as CO reserve has already been expended at rest (Lele et al., 1996; Sumimoto et al., 1997). The deficiency in cardiovascular reserve leads to exercise intolerance in HFrEF patients.

Moreover, the fall in CO causes a reduction in arterial blood pressure such that the baroreceptor reflex is stimulated, increasing SNA and inhibiting parasympathetic vagal nerve activity (Jackson et al., 2000). The increase in SNA also stimulates the renal granular cells, contributing to RAAS activation (Triposkiadis et al., 2009). The reduced CO also leads to end-organ hypoperfusion, which in the kidney acts as an additional stimulus to release renin and consequently generate vasoconstrictor angiotensin 2 and release aldosterone via the RAAS (Kemp and Conte, 2012). Unloading of the arterial baroreceptors also activates the parvocellular neurosecretory neurons within the hypothalamic paraventricular nucleus to release the osmoregulator, vasopressin (Sharma et al., 2016). This compensatory activation

of the neurohormonal system (increase in RAAS and SNA) initially functions to retain water and sodium (to increase preload and activate the Frank-Starling mechanism), induce peripheral vasoconstriction to maintain cerebral blood pressure and improve cardiac function by increasing inotropy, lusitropy and chronotropy **[see Figure 1.4]** (Jackson et al., 2000; Kemp and Conte, 2012). However, as HF progresses this activation becomes maladaptive as the Frank-Starling mechanism becomes exhausted and cardiac work overtly increased (Kemp and Conte, 2012). Hyperactivation of the sympathetic system in HFrEF also causes a reduction in cardiac β1-adrenoreceptor density (Bristow et al., 1982) and receptor desensitisation (Lohse, 1995) thereby reducing the cardiac muscle response to β-adrenergic stimulation. Chronically elevated catecholamine levels are also toxic by inducing Ca^{2+} overload and apoptosis as well as being arrhythmogenic (Mann et al., 1992). In combination, this translates into decompensation with autonomic dysfunction, further exacerbating chronotropic incompetence and exercise intolerance.

The cardiac muscle of HFrEF patients is also characterised by ventricular remodelling in the form of LV cavity dilatation and thinned walls (eccentric remodelling), as a result of raised LVEDV, which weaken cardiac function (Kemp and Conte, 2012). The dilated chambers increase aortic pressure, thus raising the afterload/wall stress according to Laplace's law (Norton, 2001). The increase in ventricular wall stress leads to further compensatory SNA and RAAS activation and angiotensin 2 generation which promotes remodelling by increasing inflammation, protein synthesis and interstial fibrosis (Paul et al., 2006). Ventricular dyssynchrony may also occur as a result of pathological remodelling of the electrical components of the heart, further exacerbating LV contractility (Noordali et al., 2018).

1.5.2. Heart failure with preserved ejection fraction (HFpEF)

HFpEF is more prevalent in women and older hypertensives with underlying cardiovascular morbidities such as diabetes mellitus, obesity and endothelial dysfunction (Borlaug and Kass, 2011; Mohammed et al., 2012a; Eaton et al., 2016). Initially, HFpEF was thought to be a condition of purely LV diastolic dysfunction, and as it commonly occurs in the presence of systemic hypertension, it was also believed to be caused primarily by static 'afterload excess' (Hart et al., 2001). However, it is now understood that HFpEF is a disease of both cardiac and extra cardiac components and maintains many similarities to HFrEF such as systolic dysfunction, reduced cardiovascular reserve (Borlaug et al., 2010), exercise intolerance (Phan et al., 2009a), neurohormonal dysregulation (Burkhoff, 2011; Bishu et al., 2012), abnormal ventricular-vascular coupling (Redfield et al., 2005; Lam et al., 2007), impaired β-adrenergic signalling, chronotropic incompetence (Borlaug et al., 2006; Phan et al., 2010), endothelial dysfunction (Hundley et al., 2007) and inflammation (Paulus and Tschope, 2013; Upadhya and Kitzman, 2017).

Despite a preserved LVEF at rest, HFpEF is still characterised by some degree of systolic dysfunction and reduced systolic performance, in particular long axis dysfunction, and mechanical dyssynchrony (Baicu et al., 2005; Vinereanu et al., 2005; Garcia et al., 2006; Tan et al., 2009; Santos et al., 2014). Nonetheless, impaired LV relaxation, LV stiffness (reduced compliance) and arterial stiffness are the key hallmarks of HFpEF (Hess et al., 1979; Hanrath et al., 1980; Soufer et al., 1985; Zile et al., 2004; Westermann et al., 2008). Impaired relaxation occurs in part, due to SERCA/PLB dysregulation (Reil et al., 2013), which is a common mechanism in HF as discussed in section 1.4.1. However, the increase in LV

stiffness, which determines passive filling of the ventricles, also involves changes in macro-cytoskeletal protein titin, collagen and the myocardial extracellular matrix (ECM) (Reil et al., 2013; Zile et al., 2015; Franssen and González Miqueo, 2016). In human hearts, two isoforms of titin exist: N2BA isoform which is longer and more compliant, and N2B which is smaller and stiffer (Franssen and González Miqueo, 2016). Increased N2B expression was observed in rats with diastolic muscle stiffness (Yamamoto et al., 2002). Hypophosphorylation of titin, which alters its distensability and thus stiffness, was also observed both in humans with HFpEF (Borbély et al., 2009) and rats with HFpEF (Hamdani et al., 2013), and is in part caused by oxidative stress (Upadhya and Kitzman, 2017). Detrimental changes in the ECM include increased collagen deposition (predominately type 1) and increased cross-linking (Kato et al., 1995; Kasner et al., 2011), which also contribute to LV diastolic dysfunction. This increased LV stiffness is associated with a raised LVEDP and thus preload. In parallel, arterial stiffness is elevated in HFpEF (Kawaguchi et al., 2003) and this causes a reduction in vasodilator reserve (Borlaug et al., 2010) and further reduces exercise capacity in these patients (Hundley et al., 2001; Phan et al., 2009a). Altered ventricular-arterial coupling is also a feature of HFpEF (Frenneaux and Williams, 2007).

It has been proposed that the comorbidities that occur in HFpEF induce a state of systemic inflammation, resulting in oxidative stress and inflammation of the coronary endothelium (Paulus and Tschope, 2013). This differs to HFrEF, in which inflammation initially occurs at the level of the cardiomyocyte, inducing cellular apoptosis and necrosis, only becoming systemic at a later stage. In HFpEF, endothelial inflammation leads to a reduction in nitric oxide (NO) bioavailability culminating in reduced protein kinase G (PKG) activity in the

adjacent cardiomyocytes (van Heerebeek et al., 2012). Reduced PKG activity contributes to LV stiffness by inducing titin hypophosphorylation and hypertrophy of the cardiomyocytes (Yu et al., 2002; Bhatia et al., 2006; Steinberg et al., 2012). Inflammation also induces increased collagen deposition within the ECM. As such, in contrast to HFrEF, the cardiac remodelling observed in HFpEF is of uncontrolled hypertrophy and commonly of a concentric nature with normal cavity radius (Melenovsky et al., 2007; Heinzel, 2015). Hypertrophy reduces wall stress and thus afterload is lower in HFpEF. However, as discussed above, LVEDP is raised due to increased LV stiffness, and this reflects back into the left atrium and the pulmonary circulation, causing pulmonary hypertension/oedema, increased risk of atrial fibrillation and right ventricular dysfunction (Guazzi and Borlaug, 2012).

1.5.3. Dysregulated metabolism: a shared pathophysiological mechanism

Detrimental alterations in cardiac metabolism are now suggested to accompany both HFrEF and HFpEF, and contribute to the exercise intolerance (Neubauer et al., 1992; Sharma and Kass, 2014). Impaired cardiac energetics, i.e. low phosphocreatine (PCr)/ATP ratio was observed in HFrEF and HFpEF patients, indicating an increased use of energy reserve (PCr) to meet metabolic demand (Neubauer et al., 1992; Phan et al., 2009a). Multiple mechanisms are involved in this metabolic impairment, and are discussed in depth in section 1.7.

1.6. Current pharmacological agents for HFrEF

The current pharmacotherapeutic agents available for HF are geared towards correcting neurohormonal dysregulation **[Figure 1.6]**. Such agents are approved and recommended by the European Society of Cardiology (ESC) Guidelines 2016 for the treatment and

management of HFrEF based on the large and robust clinical evidence-base, obtained through randomised controlled trials (RCT) (Ponikowski et al., 2016). However, these agents have not proven successful in HFpEF (see below) (Upadhya and Kitzman, 2017).

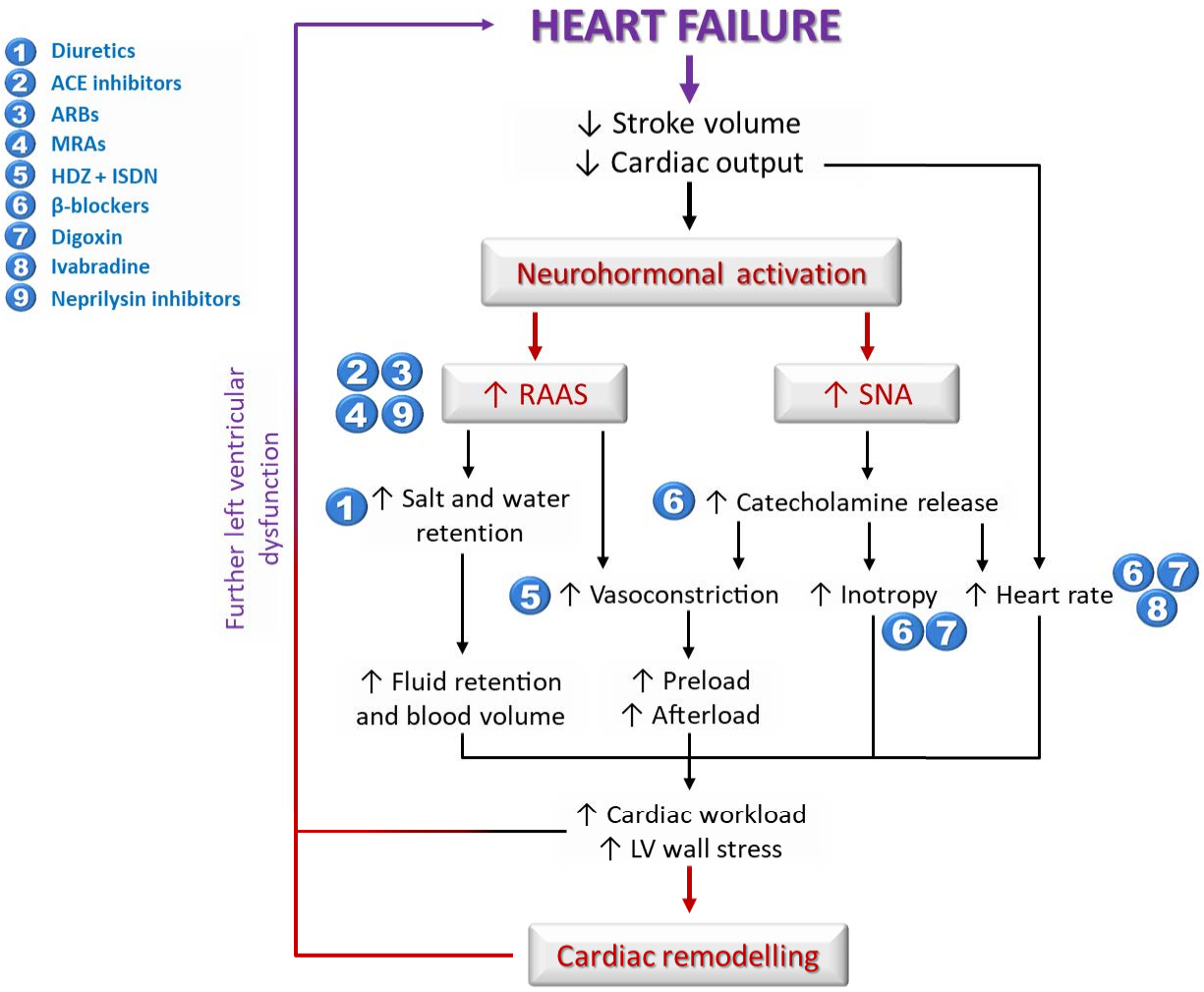

Figure 1.6. The target mechanisms of current drugs in heart failure

An overview of the point of action of current pharmacological agents as indicated in blue numbered circles at the respective maladaptive compensatory changes that take place in heart failure (red and black text and arrows). Unfortunately, these drugs have only showed promise in heart failure with reduced ejection fraction (HFrEF) and have been largely unsuccessful in heart failure with preserved ejection fraction (HFpEF).

ACE, angiotensin converting enzyme; ARBs, angiotensin receptor blockers; HDZ + ISDN, hydralazine + isosorbide dinitrate; LV, left ventricular; MRAs, mineralocorticoid receptor antagonists; RAAS, renin–angiotensin–aldosterone system; SNA, sympathetic nerve activity.

1.6.1. Diuretics

Diuretics work by reducing the circulating blood volume, which reduces cardiac workload and fluid congestion by increasing urine production and is commonly used for symptom relief in HF (Lonn and Mckelvie, 2009). Unfortunately in a randomised trial on patients with acute decompensated HF, furosemide therapy did not significantly improve HF symptoms (Felke et al., 2011). However in the Japanese clinical trial (J-MELODIC), azosemide reduced the risk of cardiovascular mortality and hospitalisation when compared to furosemide in HF patients (Masuyama et al., 2012).

1.6.2. Angiotensin converting enzyme inhibitors

During HF, RAAS activation generates vasoconstrictor angiotensin 2, which ultimately increases afterload, and induces cardiac hypertrophy and inflammation. On activation of the RAAS, angiotensin 1 is first converted into angiotensin 2 by the angiotensin converting enzyme (ACE) (Furberg and Yusuf, 1985). ACE inhibitors therefore work by reducing circulating angiotensin 2 levels and their systemic effects. A series of RCTs in patients with HFrEF have demonstrated the benefits of ACE inhibitors such as enalapril (The CONSENSUS Trial Study Group, 1987; The SOLVD Investigators, 1991), ramipril (SAVE trial, Pfeffer et al., 1992) and captopril (The AIRE Study Investigators, 1993), which reduced hospital admission and/or mortality. However, in a RCT in HFpEF patients aged ≥70, enalapril therapy did not improve exercise capacity or quality of life (Kitzman et al., 2010). Furthermore, in HFpEF patients aged ≥70, although the long acting ACE inhibitor perindopril did reduce hospital admission, the benefit on morbidity and mortality was uncertain, probably because the study was underpowered (PEP-CHF study, Cleland et al., 2006).

1.6.3. Angiotensin receptor blockers

Angiotensin receptor blockers (ARBs) have a similar therapeutic application as ACE inhibitors but work by antagonising angiotensin 2 action, thus providing an alternative option for patients intolerant of ACE inhibitors. In the Val-HeFT trial valsartan therapy in HFrEF patients improved LVEF, the NYHA functional class and reduced hospital admission (Cohn and Tognoni, 2001). Furthermore, in the CHARM-alternative trial in HFrEF patients, candesartan, therapy reduced cardiovascular death and hospitalisation (Granger et al., 2003). In contrast, in HFpEF patients, candesartan only had moderate impact on reducing hospital readmission in the CHARM-preserved trial (Yusuf et al., 2003) whilst irbesartan treatment in the I-PRESERVE trial did not improve mortality or hospitalisation rates (Massie et al., 2008).

1.6.4. Mineralocorticoid receptor antagonists

Aldosterone release following RAAS activation in HF promotes fluid retention which increases preload and cardiac work, promoting interstitial collagen deposition and fibrosis. Mineralocorticoid receptor antagonists (MRAs) work by directly blocking aldosterone activity in the kidneys and heart (Lainscak et al., 2015). In HFrEF patients, spironolactone treatment (RALES trial, Pitt et al., 1999) and eplerenone therapy (EPHESUS trial, Pitt et al., 2003) reduced mortality and improved symptoms. In the more recent EMPHASIS RCT trial, eplerenone combined with standard HF therapy reduced morbidity and hospitalisation (Zannad et al., 2011). In contrast, in the Aldo-DHF study in HFpEF patients, spironolactone did not improve exercise capacity, symptoms or quality of life despite evidence of improved diastolic function (Edelmann et al., 2013). Similar observations were made in the RAAM-PEF RCT following eplerenone treatment (Deswal et al., 2011). In further trials on HFpEF patients,

the OPTIMIZE-HF registry, aldosterone antagonism did not improve clinical outcome (Patel et al., 2013), and the large TOPCAT RCT, spironolactone did not significantly reduce mortality or hospitalisation (Pitt et al., 2014).

1.6.5. Hydralazine and Isosorbide dinitrate

The combined use of arterial vasodilator hydralazine and arteriolar venodilator isosorbide dinitrate aims to reduce systemic vascular resistance and thus afterload in HF (Loudon et al., 2016). In the V-HeFT I trial, this drug combination significantly reduced mortality at 2 years and improved LV function in HFrEF (Cohn et al., 1986). The V-HeFT II trial also observed similar benefits (Cohn et al., 1991). Furthermore, in the African-American (A-HeFT) trial in HFrEF patients, hydralazine and isosorbide dinitrate therapy reduced all-cause mortality and hospitalisation at 3 years (Taylor et al., 2004). By contrast, in HFpEF patients, isosorbide mononitrate therapy in the NEAT-HF trial did not improve exercise capacity or quality of life (Redfield et al., 2015), and more recently, isosorbide dinitrate therapy with or without hydralazine did not reduce LV remodelling or improve exercise tolerance in HFpEF (Zamani et al., 2017).

1.6.6. β-Blockers

Sympathetic hyperactivity is a key compensatory feature of HF which becomes maladaptive chronically. β-Blockers counteract this excessive SNA (Triposkiadis et al., 2009). The CIBIS-II (1999), the MERIT-HF (1999), the COPERNICUS (2002) and the SENIORS (2005) are four cornerstone trials in HFrEF patients, which assessed the β-Blockers bisoprolol, metoprolol and carvedilol respectively. All four trials demonstrated significant reductions in mortality

and/or hospitalisation following drug treatment (CIBIS-II Investigators and Committees, 1999; MERIT-HF Study Group, 1999; Packer et al., 2001; Flather et al., 2005). However, in HFpEF patients, carvedilol did not improve mortality in the J-DHF study (K. Yamamoto et al., 2013), and nebivolol did not improve exercise capacity, symptoms or quality of life relative to placebo (Conraads et al., 2012).

1.6.7. Cardiac glycosides

Cardiac glycosides (e.g. digoxin) are organic compounds with positive inotropic effects. In the large clinical trial in HF patients (Digitalis Investigation Group trial), digoxin therapy reduced hospitalisation due to worsening HF, but all-cause mortality was unaltered (Digitalis Investigation Group, 1997). However, a later post-hoc analysis on this study revealed that mortality was reduced in patients with digoxin plasma levels at the lowest end of the therapeutic range, but not at the higher end (Vamos et al., 2015). Nonetheless, in HFpEF patients, digoxin treatment had no effect on all-cause mortality or hospitalisation (Ahmed et al., 2006).

1.6.8. Neprilysin inhibitors

Neprilysin is an innate enzyme which breaks down vasoactive substances such as atrial natriuretic peptide and brain natriuretic peptide (BNP) which are released in HF to reduce systemic vascular resistance and counteract neurohormonal over-activation (Selim et al., 2017). Neprilysin inhibition therefore aims to prevent the breakdown of these vasodilators. However, neprilysin also degrades angiotensin 2 and thus inhibition of this enzyme holds the risk of increasing the levels of this vasoconstrictor. However, when 8442 HFrEF patients

received a combination therapy of neprilysin inhibition (sacubitril) and ARB (valsartan), referred to as LCZ696, this achieved an impressive 20% reduction in cardiovascular death or hospitalisation (PARADIGM-HF trial, McMurray et al., 2014). In contrast, in the PARAMOUNT trial on HFpEF patients, LCZ696 showed only a trend of improvement in NYHA functional class, but did significantly lower levels of the N-terminal prohormone of BNP (NT-proBNP; HF marker) (Solomon et al., 2012).

1.6.9. Ivabradine

Ivabradine, a selective inhibitor of the I*f* current in the sinoatrial node (the pacemaker), works by reducing heart rate, but has a unique property in that the cardiac conduction system and contractility remain uninfluenced (Selim et al., 2017). In the SHIFT trial, ivabradine treatment in HFrEF patients with a resting heart rate of ≥70 beats per minute reduced cardiovascular-related deaths and hospitalisation (Swedberg et al., 2012). Regarding HFpEF, in a small study on 61 patients , ivabradine increased exercise capacity and improved the LV filling pressure (Kosmala et al., 2013), but in another short-term RCT, ivabradine significantly *reduced* submaximal exercise capacity thus exacerbating the HF symptom (Pal et al., 2015).

To summarise, despite the wide array of treatments available for HFrEF, mortality remains high and to date, there are no established pharmacological treatments for HFpEF (Loudon et al., 2016). So far, treatment has been limited to lifestyle interventions such as weight loss and exercise, and symptom management with diuretics (Senni et al., 2017). It is therefore evident that an alternative therapeutic target is required for HF. In recent years,

disturbances in myocardial metabolism and energetics have attracted more attention and as these changes occur in both HFrEF and HFpEF, they may provide a novel and promising therapeutic target (Noordali et al., 2018).

1.7. Cardiac metabolism in the healthy heart versus failing heart

The cardiac muscle requires a constant supply of energy in the form of ATP, to maintain continuous contractile function and fuel ion channel activity (predominately those involved with Ca^{2+} handling), cycling around 6 kg of ATP per day **[Figure 1.7]** (Neubauer, 2007). ATP generated within the mitochondrial ETC is transported into the cytosol and stored as PCr following an enzyme reaction catalysed by creatine kinase (CK) (ATP + Creatine ⟷ ADP + PCr). PCr acts as an energy reserve which can be converted back into ATP upon demand in a reaction which takes place more rapidly than *de novo* ATP generation (Doenst et al., 2013). The high turnover of myocardial ATP is met through the metabolism of various metabolic substrates; in the post-absorptive state, the metabolism of free fatty acids (FA) accounts for approximately 70% of cardiac ATP production (discussed in sections 1.7.2 and 1.7.4), whilst 20% is achieved through carbohydrate (primarily glucose) metabolism (discussed in section 1.7.5) and the remaining by oxidation of ketones, lactate and specific amino acids (Bing et al., 1954; Lopaschuk et al., 1994).

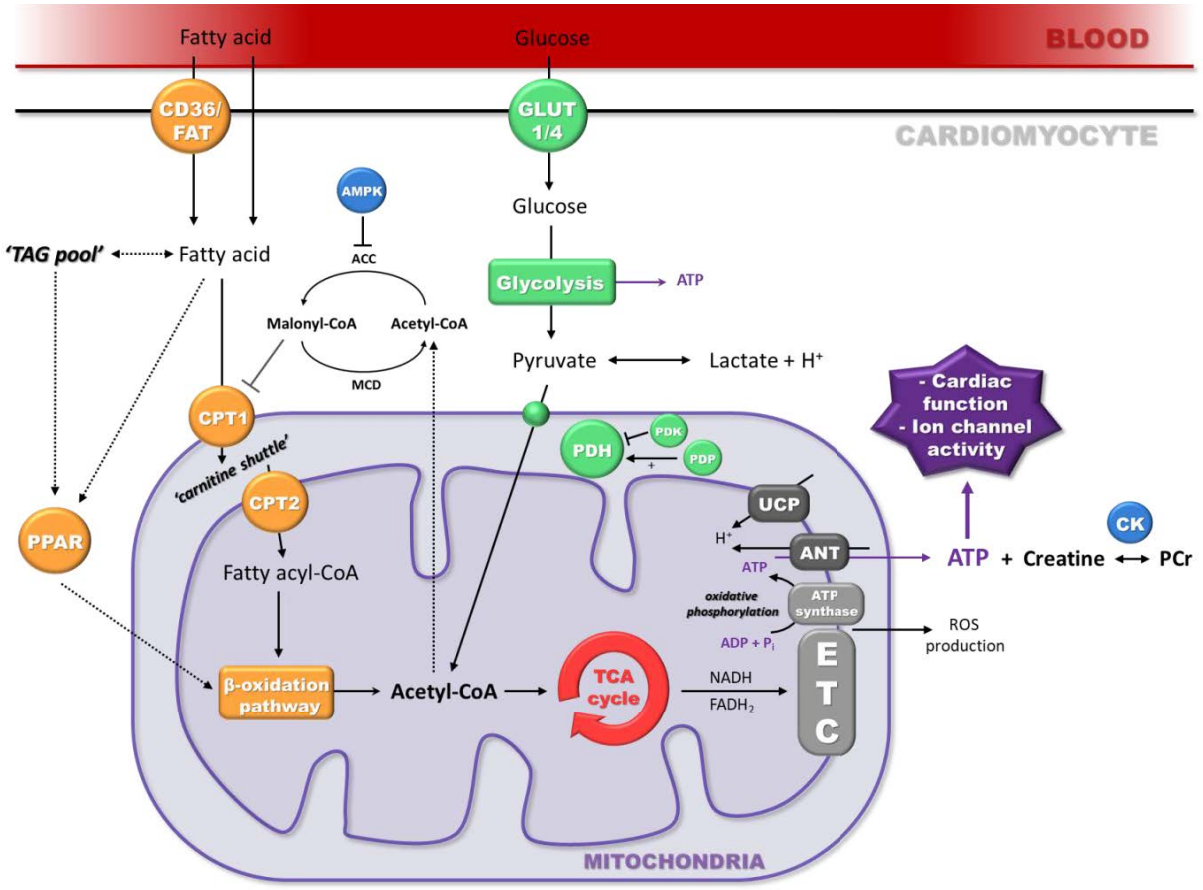

Figure 1.7. An overview of cardiac metabolism in the healthy heart

Cardiac metabolism in the healthy heart involves the oxidation of fatty acids and glucose within the mitochondria, leading to the generation of high levels of ATP, essential for fuelling cardiac function and ion channel activity.

ACC, acetyl-coenzyme A carboxylase; ADP, adenosine diphosphate; AMPK, 5' adenosine monophosphate-activated protein kinase; ANT, adenine nucleotide translocase; ATP, adenosine triphosphate; CK, creatine kinase; CoA, coenzyme A; CPT, carnitine palmitoyltransferase; ETC, electron transport chain; $FADH_2$, flavin adenine dinucleotide; FAT, fatty acid transporter; GLUT, glucose transporter; H^+, hydrogen ion; MCD, malonyl-coenzyme A decarboxylase; PCr, phosphocreatine; P_i, inorganic phosphate; PDH, pyruvate dehydrogenase; PDK, pyruvate dehydrogenase kinase; PDP, pyruvate dehydrogenase phosphatase; PPAR, peroxisome-proliferator activated receptor; ROS, reactive oxygen species; TAG, triacylglycerol; TCA, tricarboxylic acid; UCP, uncoupled protein.

The cardiac muscle has a unique characteristic of being able to switch substrate utilisation based on availability. For example, following exercise, lactate utilisation increases (Gertz et al., 1988), whereas after a carbohydrate-rich meal, metabolism can switch to an almost

exclusive use of carbohydrates (Singh et al., 2014). Oxidation of both FAs and carbohydrates produce acetyl-coenzyme A (CoA) which enters the tricarboxylic acid cycle (TCA), generating electrons required to drive oxidative phosphorylation and thus ATP production within the mitochondria (discussed in section 1.7.7) (Lopaschuk et al., 2010). However, carbohydrate metabolism is more efficient with regards to ATP yield per oxygen atom consumed than FA metabolism (Faadiel Essop and Opie, 2004).

1.7.1. Impaired cardiac energetics

There is now a wide range of evidence from both experimental and clinical studies which demonstrate severe disturbances in cardiac metabolism and impaired energetic status during HF (Doenst et al., 2013). The PCr energy reserve levels were dramatically lower, relative to healthy controls, in explanted failing human hearts and in failing rat hearts (Neubauer et al., 1999). Similar results were obtained in a porcine pressure overload model of HF (Xiong et al., 2015) and in dogs with tachycardia-induced HF (Jameel et al., 2016). Myocardial PCr levels were also decreased by 35% in patients with LV hypertrophy and HF (Smith et al., 2006). Furthermore, the PCr/ATP ratio was reduced in patients with HF caused by dilated cardiomyopathy (DCM) and the degree of reduction correlated with the NYHA functional class and mortality (Neubauer et al., 1997). Similar decreases in the PCr/ATP ratio were described in the inherited condition hypertrophic cardiomyopathy (HCM), changes in energetics often preceding the onset of hypertrophy (de Roos et al., 1992). Importantly, substantial reductions in the PCr/ATP ratio were also demonstrated in patients with HFpEF (Phan et al., 2009b). Several mechanisms, such as oxidative stress and altered substrate

metabolism **[Figure 1.8]**, have been identified which contribute to the energetic impairment during HF, as outlined below (section 1.7.1.1 to 1.7.1.5).

1.7.1.1. Microvascular dysfunction

Reduced oxygen delivery caused by microvascular dysfunction was reported to exacerbate impaired myocardial energetics during exercise (Levelt et al., 2015). Vascular dysfunction is well-defined in HFrEF and detrimental alterations in the microvasculature are now also observed in patients with HFpEF (Lee et al., 2016).

1.7.1.2. Energy wasting mechanisms

Cardiac remodelling such as cardiac enlargement results in greater energy expenditure, whereas hypertrophic growth requires glycolytic intermediates and other metabolic by-products to be re-routed to support the increased protein synthesis (Tuomainen and Tavi, 2017). Moreover, mechanical dyssynchrony, both intra-ventricular (Phan et al., 2009a) and inter-ventricular (Atherton et al., 1997) has been reported in many patients with HF and is considered an energy 'wasting' mechanism.

1.7.1.3. Impaired energy transfer

Energy transfer from the mitochondria to the site of utilisation within the cytosol is often impaired in HF as a direct result of changes in the CK system (Ingwal, 1984). These changes include a reduction in the Na^+-creatine cotransporter levels and diminished cytosolic CK activity caused by oxidative stress (Ashrafian et al., 2007a; Ventura-Clapier et al., 2011).

1.7.1.4. Oxidative and nitrosative stress

Excessive production of reactive oxygen species (ROS) is a prominent feature of HF. Elevations in ROS occur as a result of alterations in the mitochondrial ETC complexes, increased activity of cytosolic enzymes such as xanthine oxidase and nicotinamide adenine dinucleotide phosphate (NADPH) oxidase and uncoupling of nitric oxide synthase (NOS) (Tsutsui et al., 2011). This culminates in oxidative and nitrosative stress which leads to mitochondrial structural and functional damage, including mitochondrial deoxyribonucleic acid (DNA) damage.

1.7.1.5. Disruptions in cardiac substrate utilisation

The precise cause for the switch in substrate utilisation that occurs in HF has not been determined and is considered one of the most complex changes. However it also offers the most potential for pharmacological modulation (Doehner et al., 2014). Some have argued that these metabolic alterations are compensatory and protective whereas others propose that they are maladaptive (Doenst et al., 2013). Overall, the evidence suggests that in advanced HF, metabolism reverts back to a foetal metabolic profile with a downregulation of FA metabolism in spite of preserved cellular FA uptake and increased glucose uptake and glycolysis **[see figure 1.8]** (Razeghi et al., 2001). Nonetheless, a downregulation in glucose oxidation is also reported alongside the reduction in FA oxidation in the mitochondria. Such downregulations limit the ability of the cardiac muscle to generate ATP (Pascual and Coleman, 2016), and these changes are highlighted below (section 1.7.2 to 1.7.6)

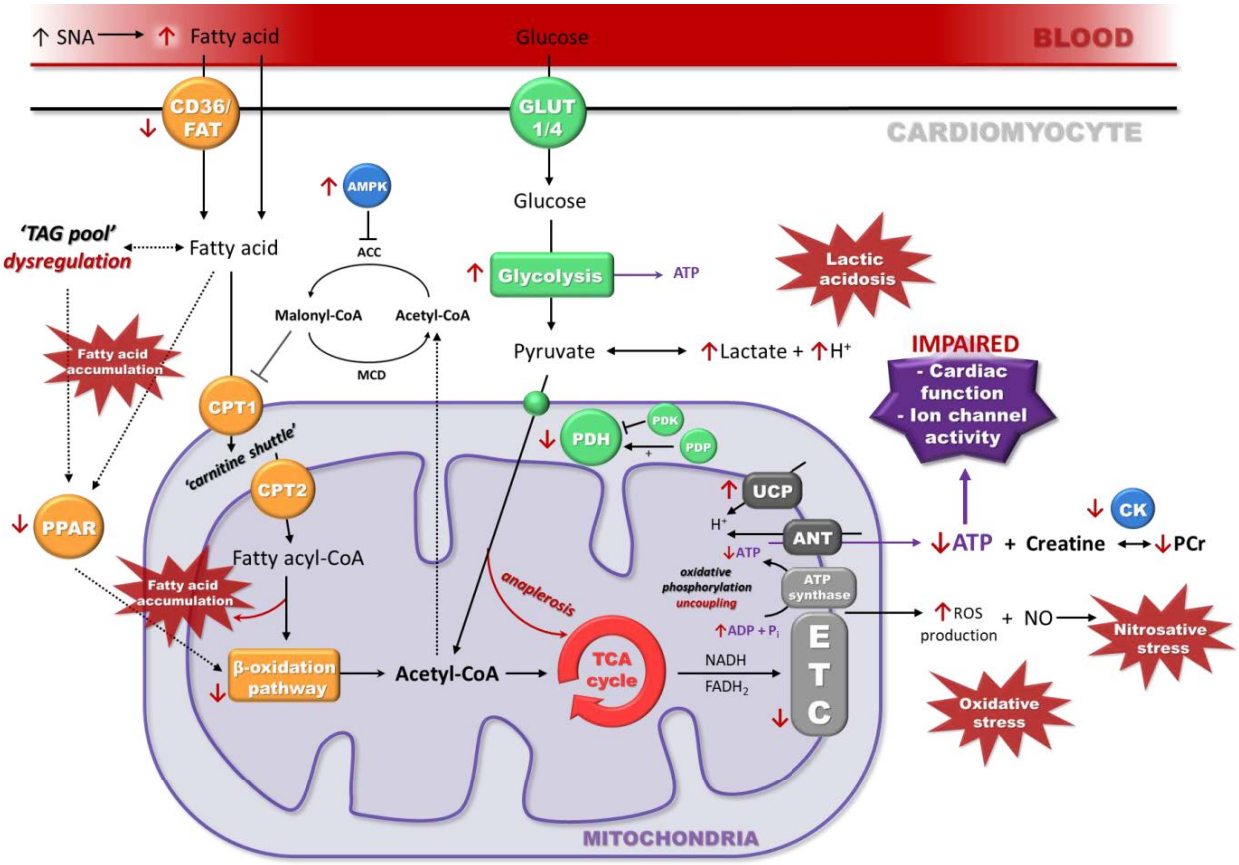

Figure 1.8. An overview of cardiac metabolism in the failing heart

The failing heart is characterised by severe disturbances in cardiac metabolism, leading to a dramatic decrease in ATP production. The key disruptions include a decrease in fatty acid and glucose oxidation in parallel to an increase in glycolysis and ROS generation.

ACC, acetyl-coenzyme A carboxylase; ADP, adenosine diphosphate; AMPK, 5' adenosine monophosphate-activated protein kinase; ANT, adenine nucleotide translocase; ATP, adenosine triphosphate; CK, creatine kinase; CoA, coenzyme A; CPT, carnitine palmitoyltransferase; ETC, electron transport chain; $FADH_2$, flavin adenine dinucleotide; FAT, fatty acid transporter; GLUT, glucose transporter; H^+, hydrogen ion; MCD, malonyl-coenzyme A decarboxylase; NO, nitric oxide; PCr, phosphocreatine; P_i, inorganic phosphate; PDH, pyruvate dehydrogenase; PDK, pyruvate dehydrogenase kinase; PDP, pyruvate dehydrogenase phosphatase; PPAR, peroxisome-proliferator activated receptor; ROS, reactive oxygen species; SNA, sympathetic nerve activity; TAG, triacylglycerol; TCA, tricarboxylic acid; UCP, uncoupled protein.

1.7.2. Fatty acid metabolism in the healthy heart

Free FAs derived from the bloodstream enter the cardiomyocytes through passive diffusion, or facilitated uptake by FA translocases (primarily CD36) and plasma membrane FA binding proteins **[see Figure 1.7]** (Lopaschuk et al., 2010). Within the cytosol, the free FAs are

esterified into short or long chain fatty acyl-CoA depending on their original FA carbon chain length. The long chain fatty acyl-CoA can be further esterified into triacylglycerol (TAG) and stored as an additional source of free long chain FAs when uptake from the blood is reduced (Lopaschuk et al., 2010).

Short chain fatty acyl-CoA enters the mitochondria by diffusion through the inner mitochondrial membrane whereas long chain fatty acyl-CoA must be shuttled across the mitochondrial membrane by entering the 'carnitine shuttle' (van der Vusse et al., 2000). The carnitine shuttle involves the conjugation of carnitine to the esterified long chain fatty acyl-CoA by the carnitine palmitoyltransferase (CPT) 1 enzyme. This generates long chain acyl-carnitine which is able to traverse the outer mitochondrial membrane. Consequently, CPT1 is the rate limiting enzyme for FA metabolism. The CPT2 enzyme, located on the inner mitochondrial membrane, cleaves the carnitine (which is transported back into the cytosol) thereby restoring the fatty acyl-CoA molecule which enters the mitochondrial matrix (Lopaschuk et al., 2010). Within the matrix, the long chain fatty acyl-CoA undergoes a series of recurring oxidation steps in the β-oxidation pathway, generating acetyl-CoA, nicotinamide adenine dinucleotide (NADH) and flavin adenine dinucleotide ($FADH_2$). Acetyl-CoA then enters the TCA cycle.

The transport of long chain fatty acyl-CoA into the mitochondria by CPT1 is a closely regulated process, the rate being dependent on energy demand. In the presence of excess energy, CPT1 activity can be potently inhibited by allosteric binding of the endogenous molecule malonyl-CoA (Foster et al., 2012). Malonyl-CoA is synthesised from acetyl-CoA by

acetyl-CoA carboxylase (ACC) and degraded by malonyl-CoA decarboxylase (MCD). The balance between the activities of these two enzymes determines the cytosolic concentration of malonyl-CoA and thus the extent of CPT1 inhibition (Lopaschuk et al., 2010; Foster et al., 2012). For example, in the presence of low energy, the cellular energy sensor 5' adenosine monophosphate-activated protein kinase (AMPK) becomes activated and inhibits ACC which in turn reduces malonyl-CoA levels and thus CPT1 inhibition is relieved (Stanley et al., 2005).

1.7.3. Fatty acid metabolism in the failing heart

In HF, the dysregulation in FA metabolism appears to stem from reduced activity of FA metabolic regulator proteins, discussed in section 1.7.4, leading to a downregulation of the β-oxidation enzymes **[see Figure 1.8]** (Pellieux et al., 2006). Sack and colleagues (1996) were first to identify a downregulation in the β-oxidation pathway when assessed in LV biopsies from patients with terminal HF (>40% decrease) and rats with LV hypertrophy (>70% decrease). A decrease in FA oxidation and enzyme expression was also reported in rats with abdominal aortic constriction (AAC)-induced HF (Akki et al., 2008). Furthermore, reduced FA uptake and oxidation was observed in dogs with tachycardia-induced HF (Osorio et al., 2002) and rats with high salt diet-induced HF (Kato et al., 2010). Similar observations were made in patients with DCM and symptoms of HF (Neglia et al., 2007), with up to 70% decrease in FA oxidation reported in these patients (Yazaki et al., 1999). In addition, the expression and/or activity of key enzymes required for FA uptake and oxidation, such as CPT1, were downregulated in HF (Lionetti et al., 2005; de Brouwer et al., 2006; Pellieux et al., 2006). Moreover, Shibayama and co-workers (2015) recently demonstrated significant reductions in cardiac mitochondrial FA and carnitine levels in dogs with pacing-induced HF. Reductions in

myocardial carnitine levels were also reported clinically in patients with HCM and chronic HF (Regitz et al., 1990).

However, not all studies have shown similar downregulations in FA metabolism, and it is suggested that the experimental procedure used for HF induction and/or the disease severity may determine the course of metabolic alteration (Doenst et al., 2013). For example, in rats with coronary artery ligation-induced HF, palmitate oxidation was unchanged despite the development of LV dysfunction (Remondino et al., 2000). Furthermore, in patients with congestive HF, mitochondrial FA uptake and oxidation was increased by approximately 40% despite no increase in coronary blood flow (Paolisso et al., 1994).

The TAG pool turnover and dynamics are also dysregulated in HF (O'Donnell et al., 2008; Chokshi et al., 2012). Given that the TAG pool is a vital source of FAs which serve as ligands for the peroxisome proliferator-activated receptor α (PPARα), an important regulator in FA metabolism (Haemmerle et al., 2011), dysregulated TAG turnover results in reduced PPARα signalling **[see Figure 1.8]** (Lahey et al., 2014).

1.7.4. Fatty acid metabolic regulation in the healthy and failing heart

The expression of proteins involved in FA metabolism, including CPT and those of the β-oxidation pathway, is driven by regulatory proteins such as PPARα, β/δ and γ (Braissant et al., 1996): a family of transcription factors regulated by free FA levels and interaction with transcription co-factor PPAR-γ coactivator-1 (PGC-1) (Arumugam et al., 2016). PGC-1 itself is

a master regulator of mitochondrial biogenesis and energy metabolism. Interestingly, downregulation of both PPARα and PGC-1 were reported in mice with HF (Young et al., 2001). A decrease in PPARα expression and activity was also observed in hearts from TAC mice (Barger et al., 2000). PPARα expression was also reduced in failing human hearts (Karbowska et al., 2003) and in mice with chronic angiotensin 2-stimulated HF (Pellieux et al., 2006), the latter study also demonstrated decreases in messenger ribonucleic acid (mRNA) expression of FA metabolic enzymes such as CPT1. Notably, in a TAC model of HF, PGC-1β knock-out mice progressed more rapidly towards HF with severe mitochondrial dysfunction, diminished cardiac efficiency and elevated oxidative stress than wild-type littermates subjected to TAC (Riehle et al., 2011). Similar results were obtained in other studies on TAC mice deficient in PGC-1α (Arany et al., 2006; Lu et al., 2010). However, PPARα and PGC-1 cardiac protein levels did not change compared to control hearts in dogs with tachycardia-induced HF (Lionetti et al., 2005).

1.7.5. Glucose metabolism in the healthy heart

Glucose is taken up from the bloodstream into the cardiomyocytes by membrane bound glucose transporters; GLUT1 and GLUT4 **[see Figure 1.7]** (Doenst et al., 2013). Within the cytosol, glucose is first phosphorylated into glucose-6-phosphate (G6P) by hexokinase where it can be stored as glycogen, enter the pentose phosphate pathway which produces NADPH (essential for ROS detoxification) (Ussher et al., 2012), enter the hexosamine biosynthesis pathway (for increasing cellular biomass), or enter anaerobic glycolysis to generate pyruvate (Doenst et al., 2013). Pyruvate is transported into the mitochondria by pyruvate translocase, followed by decarboxylation via the rate limiting pyruvate dehydrogenase (PDH) complex

which generates acetyl-CoA (which is also the end-product of FA β-oxidation as described in section 1.7.2). PDH activity is negatively regulated by PDH kinase (PDK) and positively by PDH phosphatase (Kolobova et al., 2001), whilst it is allosterically inhibited by acetyl-CoA and NADH; its by-products (Stanley et al., 2005).

Under induced hypoxic conditions or as a result of mitochondrial dysfunction, ATP production declines and thus the cytosolic ATP/adenosine diphosphate (ADP) ratio is reduced and this consequently activates glycolysis, which can generate smaller quantities of ATP (Maldonado and Lemasters, 2014). Hypoxia also inhibits degradation of the ubiquitous hypoxia-inducible factor 1α (HIF1α), leading to HIF1α accumulation, followed by translocation into the nucleus where the expression of PDK1 is upregulated alongside many other glycolytic enzymes (Lei et al., 2008).

1.7.6. Glucose metabolism in the failing heart

HF is highly correlated with insulin resistance and type 2 diabetes mellitus which is in part caused by the compensatory increase in SNA (Tenenbaum and Fisman, 2004; Ashrafian et al., 2007a). Despite a reduction in insulin-stimulated glucose uptake, there is evidence that insulin-independent uptake mechanisms (e.g. GLUT1 upregulation or AMPK signalling) may compensate. Indeed many studies have suggested that in HF, both glucose uptake and glycolysis are in fact maintained or even increased (Tenenbaum and Fisman, 2004). However, interestingly, in rats with TAC-induced HF, the increase in glycolysis was not accompanied by an increase in flux through PDH thereby revealing the uncoupling of glycolysis from glucose oxidation **[see Figure 1.8]** (Sorokina et al., 2007). In addition, the decrease in glucose

oxidation was accompanied by an increase in compensatory anaplerosis (Sorokina et al., 2007); a pathway involved in replenishing the TCA cycle intermediates which would have been used for biosynthesis as a result of hypertrophic growth in the failing hearts (Kolwicz et al., 2012). Therefore, the overall effect in that study, despite the availability of glucose, was impaired energy production from carbohydrate metabolism. Similar uncoupling was observed in TAC mice (Dai et al., 2012) and AAC rats (Seymour et al., 2015). A 66% decrease in cardiac glucose oxidation was also reported in TAC mice (Zhabyeyev et al., 2013) and in rats with pressure overload-induced HF (Doenst et al., 2010). Such results may be explained by the decreases in PDH expression and activity which were observed by Lei and co-workers (2004) in dogs with pacing-induced HF. A downregulation of PDH expression was also observed in rats with high salt diet-induced HF, and this downregulation included other metabolic proteins such as GLUT4 (Kato et al., 2010).

Upregulation of glycolysis has also been attributed to the elevations in HIF1α, which occur secondary to hypoxia in HF (Holscher et al., 2012). The uncoupling of glycolysis-glucose oxidation in HF leads to increases in pyruvate to lactate and H^+ ion conversion and thus cellular acidosis (Fillmore and Lopaschuk, 2013). This uncoupling can be further exacerbated by high plasma FA levels, but also by the fall in FA oxidation (discussed in section 1.7.3) due to the Randle cycle (Fillmore and Lopaschuk, 2013), which refers to the reciprocal relationship between cellular FA β-oxidation and glucose oxidation, such that inhibiting one increases the other (Randle et al., 1963). In this phenomenon, increased production of acetyl-CoA from β-oxidation can inhibit PDH activity and thus glucose metabolism. In contrast, an increase in acetyl-CoA from glucose metabolism can be converted into cytosolic

malonyl-CoA which inhibits CPT1 activity and therefore FA metabolism (Jaswal et al., 2011). However, despite all the evidence suggesting that glucose metabolism is impaired in HF, it should be noted that not all HF studies have demonstrated this. For example, Osorio and colleagues (2002) observed an increase in the rate of glucose oxidation in dogs with tachycardia-induced HF.

1.7.7. The tricarboxylic acid cycle and oxidative phosphorylation in the healthy heart

Oxidation of both FAs and glucose terminates in acetyl-CoA production which feeds into the TCA cycle, generating electron carriers NADH and $FADH_2$ **[see Figure 1.7]** (Schwarz et al., 2014). High energy electrons are donated from both NADH and $FADH_2$ and transferred to electron acceptors in complex I to IV, which form the ETC within the inner mitochondrial membrane. This process drives the extrusion of protons (i.e. H^+ ions) across the mitochondrial inner membrane to generate an electrochemical gradient, activating ATP synthase. ATP synthase is responsible for phosphorylation of ADP into ATP in a reaction accompanied by the oxidation of H^+ ions into water, thereby coupling oxidation to phosphorylation (Doenst et al., 2013). Oxidative phosphorylation accounts for an astounding 95% of ATP production within the myocardium (Beer et al., 2002).

The ETC is a major site of premature electron leakage and subsequent binding to oxygen can often lead to ROS formation, which although signalling molecules in their own right, when elevated, culminate in oxidative stress which is deleterious to mitochondrial structure and function (Schwarz et al., 2014). Even in normal hearts, post-translational modification of ETC complex I and III contributes to increased ROS (i.e. superoxide) production (Holmstrom and

Finkel, 2014). However, counter-regulatory mechanisms of mitochondrial-generated ROS exist including uncoupling proteins (UCP) and adenine nucleotide translocase (ANT) – both of which dissipate the proton gradient across the inner mitochondrial membrane thereby balancing the charge at the intermembrane space (Akhmedov et al., 2015), and also ROS detoxifying enzymes such as mitochondrial superoxide dismutase and NADPH (Azzu and Brand, 2010; Circu and Aw, 2010). Furthermore, membrane phospholipid cardiolipin has an essential role in ensuring the organisation of the respiratory chain complexes into functional units termed respirasomes, enabling coordinated ETC activity (Szeto, 2014). Respirasome dissociation therefore causes increased ROS production and reduced ATP generation (Lee and Tian, 2015).

1.7.8. Oxidative phosphorylation and the mitochondria in the failing heart

During HF, oxidative phosphorylation is impaired and thus ATP generation is diminished **[see Figure 1.8]**. This occurs as a result of abnormal changes in mitochondrial structure and function (Fillmore and Lopaschuk, 2013; Pereira et al., 2014). Bugger and colleagues (2010) observed detrimental changes in mitochondrial volume density and morphology in parallel to reduced expression of 53% of ETC proteins in TAC rats with HFrEF. ETC complex activity was also reduced in dogs with tachycardia-induced HF (Ide et al., 1999) and in LV biopsies from HF patients (Scheubel et al., 2002). The ETC complex organisation into respirasomes is also impaired in HF which contributes to electron leak and ROS formation; such dysfunction may be related to a reduced expression of cardiolipin and altered cardiolipin-respiratory complex interaction (Rosca and Hoppel, 2013; Szeto, 2014). Oxidative stress also results in

disruption to the EC coupling mechanism, by modulating the SERCA/PLB complex, thereby contributing to LV dysfunction in failing hearts (Akhmedov et al., 2015).

In response to elevated ROS and oxidative stress, cardiomyocytes develop a defence mechanism, one of which involves compensatory increases in UCP expression, in particular UCP2 and UCP3 (Ruiz-Ramírez et al., 2016), which prevents activation of ROS-mediated pro-apoptotic pathways (Deng et al., 2012). Unfortunately, increased UCP3 levels lead to increased heat generation rather than ATP generation, thereby rendering oxidative phosphorylation less efficient (Vettor et al., 2002). Furthermore, an increase in UCP3 has been associated with elevated free FA levels in the plasma of rats with chronically failing hearts (Murray et al., 2008) and in failing human hearts (Murray et al., 2004), which may be caused by the elevated FA levels stimulating PPARα signalling which in turn upregulates UCP expression (Akhmedov et al., 2015). UCP3 also interacts with other redox regulators such as thioredoxin 2 (Trx2) (Hirasaka et al., 2011). Knock-out of Trx2 in mice resulted in a gradual decline in LV function and death by HF 4 months on, whilst a downregulation of Trx2 was observed in patients with DCM (Huang et al., 2015). This effect may be associated with the upregulation of the thioredoxin-interacting protein (TXNIP) in HF, which is a natural inhibitor of Trx2 (Chong et al., 2014). Moreover, TXNIP is associated with inducing oxidative stress (Wang and Yoshioka, 2017) and was implicated in inhibiting glucose uptake and utilisation (Yu et al., 2010). Therefore, the changes in the expression and/or activity of these proteins can be useful markers of oxidative stress during ischaemia and HF.

The detrimental changes in mitochondrial structure, morphology and function discussed above are also in part due to the shifts in cardiac substrate metabolism themselves. To elaborate, the reduction in FA β-oxidation causes FA accumulation within the cytosol and mitochondria, which combined with the high levels of ROS causes lipid peroxide formation and lipotoxicity (Schrauwen et al., 2001; Ventura-Clapier et al., 2011). In parallel, the decrease in glucose oxidation which is associated with a build-up of lactate and H^+ ions induces cellular acidosis (Münzel et al., 2015). In combination, the lipotoxicity and acidosis result in damage to the mitochondrial membrane and proteins (Dai et al., 2012). Furthermore, lipid peroxides may also trigger fibrotic and hypertrophic pathways (Siddiqi et al., 2013). Consequently, pharmacologically targeting the metabolic disturbances of HF has the potential to prevent the perturbation of mitochondrial function, biogenesis, and energy transfer and improve ATP production.

1.8. Novel pharmacological agents for heart failure: metabolic modulators

Correcting metabolic dysfunction and impaired energetics has received considerable attention as an alternative strategy for treating and managing HF. A range of metabolic modulating agents exist which target the different components of cardiac metabolism discussed in section 1.7 **[Figure 1.9]**.

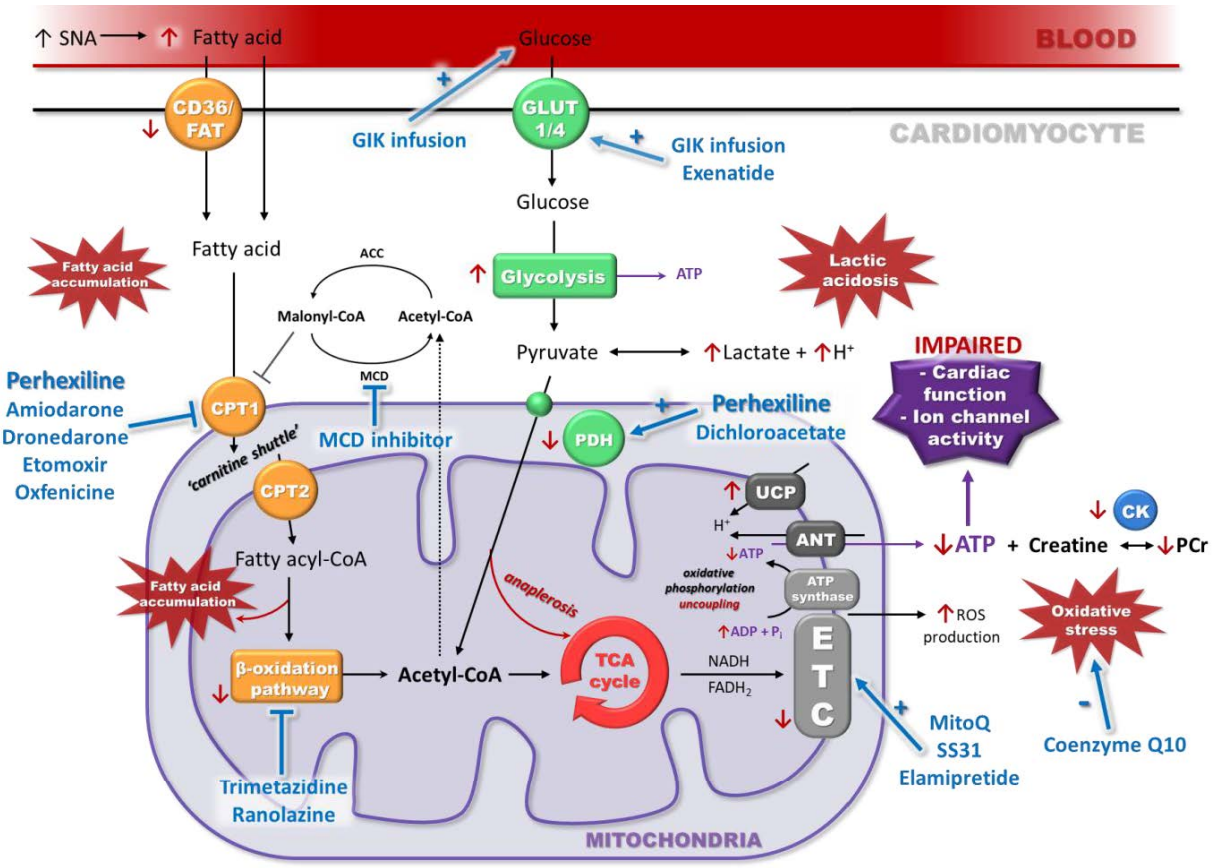

Figure 1.9. The target sites of metabolic modulators in the failing heart

Metabolic modulating agents (blue text and arrows) aim to correct the metabolic disturbances that take place in the cardiomyocytes of failing hearts in order to improve ATP production and/or reduce ROS formation. Current strategies focus on reducing fatty acid oxidation and/or increasing glucose oxidation.

ACC, acetyl-coenzyme A carboxylase; ADP, adenosine diphosphate; ANT, adenine nucleotide translocase; ATP, adenosine triphosphate; CK, creatine kinase; CoA, coenzyme A; CPT, carnitine palmitoyltransferase; ETC, electron transport chain; $FADH_2$, flavin adenine dinucleotide; FAT, fatty acid transporter; GIK, Glucose-Insulin-Potassium; GLUT, glucose transporter; H^+, hydrogen ion; MCD, malonyl-coenzyme A decarboxylase; PCr, phosphocreatine; P_i, inorganic phosphate; PDH, pyruvate dehydrogenase; ROS, reactive oxygen species; SNA, sympathetic nerve activity; SS31, Szeto-Schiller peptide 31; TCA, tricarboxylic acid; UCP, uncoupled protein.

It has been proposed that inhibition of FA metabolism with a parallel increase in glucose metabolism may be the most beneficial approach (Doehner et al., 2014). This idea is based on evidence demonstrating that FA utilisation is associated with increased oxidative stress and thus cardiac damage (Schonfield and Wojtczak, 2007). In addition, because FA oxidation consumes more oxygen than glucose oxidation, a shift towards glucose metabolism would

increase the efficiency of energy production by creating an oxygen sparing effect (Faadiel Essop and Opie, 2004). Discussed below are examples of renowned metabolic modulators. Of these only perhexiline, trimetazidine and ranolazine are currently used clinically. As perhexiline is the focus of this thesis and is a CPT1 inhibitor, this category is discussed last in section 1.8.7.

1.8.1. Partial fatty acid oxidation inhibitors

These pharmacological agents inhibit FA metabolism via CPT1-*independent* mechanisms. Trimetazidine and ranolazine are two well-investigated partial FA oxidation inhibitors used as anti-anginal agents (Chong et al., 2016) and work by inhibiting the 3-ketoacyl-CoA thiolase enzyme of the β-oxidation pathway (Kantor et al., 2000). In HFrEF patients, trimetazidine treatment enhanced LV function and improved NYHA functional class (Fragasso et al., 2006). In another clinical study in patients with idiopathic DCM and HFrEF, trimetazidine improved LVEF and in parallel, increased myocardial glucose oxidation (Tuunanen et al., 2008). In a meta-analysis conducted by Zhang and colleagues (2012) on 16 RCTs in patients with chronic HF, trimetazidine therapy increased LVEF, improved NYHA functional class, attenuated LV remodelling and reduced hospitalisation, despite no change in all-cause mortality. Although rare, a pitfall of trimetazidine therapy is the potential adverse effect in causing Parkinsonian symptoms (e.g. tremors and bradykinesia) (Martí Massó et al., 2005).

Ranolazine had similar benefits such as improved LVEF in 70% of patients with HFrEF (Murray and Colombo, 2014) and enhancing LV function and ameliorating BNP levels in rats with chronic ischaemic HF (Feng et al., 2016). Importantly, in patients with HFpEF, 30-min

ranolazine infusion in the RALI-DHF study attenuated LVEDP, but had no effect on LV end-systolic pressure or systemic vascular resistance (Maier et al., 2013).

1.8.2. Malonyl-CoA decarboxylase inhibitors

Malonyl-CoA, the natural inhibitor of CPT1, is converted into acetyl-CoA by the MCD enzyme. MCD inhibition thus increases natural CPT1 inhibition resulting in reduced FA oxidation and in parallel increased glucose oxidation through the Randle cycle (Fillmore and Lopaschuk, 2013). In rats with cardiac dysfunction induced by MI, MCD inhibition via gene silencing improved LVEF, increased energy reserve (PCr/ATP ratio) and reduced lactic acidosis (Wu et al., 2014). In MCD knock-out mice with coronary artery ligation-induced HF, LVEF was 31% higher and ATP production greater than their wild-type littermates subjected to the same ligation procedure (Masoud et al., 2014). Currently, only pre-clinical data exists for the use of MCD inhibition in HF, but they, nonetheless highlight that CPT1 inhibition could be effective in HF.

1.8.3. Glucose-Insulin-Potassium infusion

Combined infusion of glucose, insulin and potassium (GIK) has been used as a therapeutic agent following MI (Fath-Ordoubadi and Beat, 1977). Its proposed mechanism of action involves increasing plasma glucose levels and glucose uptake whilst also reducing plasma free FAs and lipolysis, which improves overall cardiac energetics by decreasing oxygen consumption and ROS accumulation (Cave et al., 2000). However, in a large scale clinical trial (CREATE-ECLA) GIK infusion did not significantly reduce mortality in patients with acute AT-segment elevation myocardial infarction (STEMI), this being consistent in patients with and

without HF (Mehta et al., 2005). Conversely, in patients with HFrEF caused by ischaemic cardiomyopathy, GIK therapy *did* improve LVEF and reduce BNP levels (Kalay et al., 2008). Nicolas-Robin and colleagues (2008) also observed an increase in LVEF following GIK infusion in patients with severe HF following brain death.

1.8.4. Glucagon-like peptide-1 analogues

Glucagon-like peptide-1 (GLP-1) is an innate hormone which enhances insulin secretion; GLP-1 analogues (e.g. exenatide) mimic this function to improve glycaemic control (Gupta, 2013). In patients with severe HF, Sokos and colleagues (2006) demonstrated improvements in LVEF and quality of life following 5-week GLP-1 infusion. Furthermore, in a phase II clinical trial on patients with HFrEF and type 2 diabetes intravenous infusion of exenatide increased cardiac index (Nathanson et al., 2012). However, in non-diabetic patients with congestive HF, recombinant GLP-1 did not alter LVEF or cardiac index and hypoglycaemia was a common adverse effect (Halbirk et al., 2010). A meta-analysis also revealed that only 3 of 7 HF trials showed LVEF improvements in HF (Wroge and Williams, 2016).

1.8.5. Dichloroacetate

Dichloroacetate (DCA) is a pyruvate analogue and inhibitor of PDK, which is responsible for inhibitory phosphorylation of PDH (Fillmore and Lopaschuk, 2013). On this basis, DCA therapy aims to increase glucose oxidation which is downregulated in HF, and to reduce lactate accumulation and lactic acidosis by reducing pyruvate availability for this conversion and directing it towards the TCA cycle (Durkot et al., 1995). Accordingly, in rats with LV hypertrophy and failure induced by high salt diet, DCA treatment enhanced glucose uptake

which was accompanied by improvements in cardiac function and survival (Kato et al., 2010). The same group also showed that DCA reduced oxidative stress in cultured rat cardiomyocytes. Furthermore, in a phase II clinical trial, 30-min DCA infusion increased LV function whilst decreasing myocardial oxygen consumption in patients with congestive HF (Bersin et al., 1994). However, long-term use of DCA requires caution as it can cause peripheral neuropathy which limits its clinical use (Calcutt et al., 2009).

1.8.6. Mitochondrial-targeted antioxidants

Coenzyme Q10 (CoQ10) is an endogenous substance and a component of the mitochondrial ETC. CoQ10 also has an important role in oxidative phosphorylation, which is speculated to be involved in its ability to enhance ATP generation in HF, whilst its antioxidant and free radical scavenging properties may reduce ROS and oxidative stress (Oleck and Ventura, 2016). Moreover, CoQ10 deficiency has been observed in HF; the severity of this deficiency strongly correlates with the severity of HF (Oleck and Ventura, 2016). Initial clinical studies in patients with HFrEF suggested improvements in LVEF and CO following CoQ10 supplementation, but with minimal effects on mortality (Morisco et al., 1994; Munkholm et al., 1999). A meta-analysis conducted by Fotino and co-workers (2013) reported that CoQ10 increased cardiac performance and improved NYHA functional class in HF, but concluded that the effects on mortality and survival remain unclear. In a more recent RCT (Q-SYMBIO), patients with moderate to severe HF treated with CoQ10 for 2 years had reduced mortality and hospitalisation compared to placebo (Mortensen et al., 2014). Nonetheless, it would appear that larger RCTs are necessary to determine the efficacy of CoQ10 in HF.

MitoQ and SS31 (a Szeto-Schiller peptide) are other antioxidants considered for treating HF, but in contrast to CoQ10, they accumulate selectively in the mitochondria due to their lipophilic nature and negative charge (Münzel et al., 2015). In spontaneously hypertensive rats with HF, MitoQ reduced cardiac hypertrophy and oxidative stress (Graham et al., 2009). Furthermore, MitoQ therapy in rats with doxorubicin-induced HF reduced ROS and oxidative stress (Chandran et al., 2009). Similarly, SS31 attenuated cardiac hypertrophy, fibrosis and diastolic dysfunction in mice with HF (Dai et al., 2011) and had similar effects in TAC mice, as well as abolishing mitochondrial oxidative damage (Dai et al., 2013). These protective effects were attributed to SS31's ability to stabilise cardiolipin and facilitate the maintenance of mitochondrial respirasome organisation, thereby promoting oxidative phosphorylation (Szeto et al., 2014). Elamipretide is another selective mitochondrial-targeted antioxidant with similar cardiolipin stabilising properties as SS31 (Szeto et al., 2014). In dogs with microembolization-induced HF, elamipretide treatment increased LVEF and ATP synthesis whilst also reducing plasma BNP and ROS formation (Sabbah et al., 2016). However, only pre-clinical data currently exists for MitoQ, SS31 and elamipretide.

1.8.7. Carnitine palmitoyltransferase 1 inhibitors

This group of metabolic modulators are perhaps the most well-investigated and work by directly inhibiting CPT1, thus reducing FA transport and oxidation (Chong et al., 2016). Reducing FA mitochondrial levels may also reduce lipid peroxide-induced mitochondrial toxicity, although this may also result in tissue phospholipidosis (Ashrafian et al., 2007b).

Amiodarone and dronedarone are CPT1 inhibitors that are used as anti-arrhythmic agents. Amiodarone therapy increased LVEF and exercise tolerance in a small trial on patients with HFrEF (Hamer et al., 1989). However, retrospective analysis of the COMET trial revealed that amiodarone therapy in HF was associated with increasing the risk of death due to circulatory failure (Torp-Pederson et al., 2007). Dronedarone has faced similar safety concerns as in patients with severe HFrEF dronedarone treatment was associated with increased mortality compared to placebo (Køber et al., 2008).

Etomoxir is an irreversible CPT1 inhibitor (Steggal et al., 2017). In rats with aortic constriction-induced HF, long-term etomoxir treatment increased contractile performance, reduced wall stress (Turcani and Rupp, 1997), increased LV function and prevented LV remodeling (Turcani and Rupp, 1999). Moreover, improved LVEF and central haemodynamics at rest and during exercise were observed in the first clinical trial using etomoxir therapy in 10 patients with chronic HFrEF (Schmidt-Schweda and Holubarsch, 2000). However, etomoxir has since been withdrawn from clinical use due to severe hepatotoxicity occurring in some patients in the ERGO trial on moderate HF (Holubarsch et al., 2007). Oxfenicine is another irreversible CPT1 inhibitor, demonstrated to reduce LV remodelling, ameliorate haemodynamic alteration, and delay progression towards end-stage failure in dogs with pacing-induced HF (Lionetti et al., 2005). There are currently no clinical trials on the use of oxfenicine in patients with HF.

Perhexiline is another potent reversible CPT1 inhibitor with well-documented anti-ischaemic and therapeutic properties (Horowitz et al., 2010; Steggal et al., 2017). Therefore,

perhexiline is one particular metabolic drug which has gained increasing attention for use as a novel agent in HF. An in depth discussion of perhexiline and its proposed mechanisms of action are explored below in section 1.9 to 1.11.

1.9. Perhexiline: a history of an old drug

Perhexiline (2-(2,2-dicyclohexylethyl)piperidine) is a synthetic amphiphilic drug developed in the late 1960s by Richardson-Merrell Pharmaceuticals **[Figure 1.10]**.

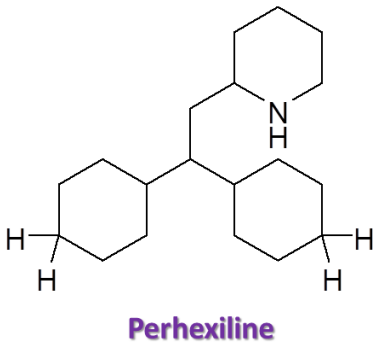

Figure 1.10. The chemical structure of perhexiline

The chemical structure of perhexiline includes two saturated cyclohexane rings and one pyridine ring. Hydroxylation by the cytochrome P450 2D6 (CYP450 2D6) enzyme occurs on one or both cyclohexyl rings.

It was first prescribed clinically in the 1970s as an anti-anginal agent, its introduction to the UK taking place in 1975 (Ashrafian et al., 2007b). Early *in vivo* experiments in the open-chest and close-chest canine models revealed that perhexiline was capable of inducing systemic and coronary vasodilation and this response was a result of direct action on the vascular smooth muscle, independent of SNA (Hudak et al., 1970). Increased coronary flow following intravenous perhexiline infusion was also observed not only in the ischaemic canine myocardium (Klassen et al., 1976), but also in the normal heart of open-chest dogs (Ono et al., 1982). The latter study also observed an increase in LV mechanical efficiency following

perhexiline infusion, an effect which was not achieved by glyceryl trinitrate (GTN) – a coronary vasodilator and anti-anginal drug. Furthermore, in a right-heart perfusion canine model, LV work (blood pressure x CO) and the index of LV efficiency (change in LV work/change in myocardial oxygen consumption) was increased following intravenous perhexiline infusion (Cho et al., 1970). Based on such effects, perhexiline was judged to be a successful and valuable pharmacological agent for angina (Ashrafian et al., 2007b). Consistent with this, several clinical studies demonstrated perhexiline's antianginal effects, including a reduction in incidence and severity of attack (Hirshleifer et al., 1969; de Oliveira and Amado, 1970; Winsor, 1970; Lyon et al., 1971; Burns-Cox et al., 1971; Bleifer et al., 1972; Brown et al., 1976; Horowitz et al., 1986). In addition, perhexiline had greater efficacy in treating angina when compared to β-blockers such as propranolol (Armstrong, 1973; Horowitz and Mashford, 1979) and oxprenolol (Pilcher, 1978), and was also effective in patients with angina who were non-responders to β-blocker therapy (White and Lowe, 1983) or other traditional anti-anginal drugs (Alcocer et al., 1973).

Further interest in perhexiline was associated with its unique ability to produce improvements in cardiac function and coronary flow that were not accompanied by intolerable reductions in heart rate or blood pressure (Hudak et al., 1970; Ashrafian et al., 2007b). Indeed, perhexiline was reported to have negative chronotropic effects in humans, only following exercise-induced tachycardia (Grupp et al., 1970; Winsor, 1970), but not at rest (Pepine et al., 1974). Perhexiline also increased SV and exercise tolerance in patients with coronary heart disease and angina (Pepine et al., 1973; Pepine et al., 1974). These clinical findings spurred an increase in the use of perhexiline, until it surfaced in the 1980s

that perhexiline therapy led to a series of adverse effects with potential for severe neuro- and hepatotoxicity (Shah et al., 1982) (outlined in section 1.10.1). The appearance of these severe side effects led to the rapid decline and eventual withdrawal of perhexiline from clinical use and perhexiline's removal from the UK market in 1985. However, it was later identified that perhexiline-mediated toxicity stemmed from its ability to inhibit CPT1 (discussed in section 1.9.1), a potentially useful property (Ashrafian et al., 2007b).

1.9.1. Perhexiline is a carnitine palmitoyltransferase 1 inhibitor

Observations made in early studies on dogs suggested that perhexiline may have metabolic modulating properties as it increased cardiac metabolic efficiency (Cho et al., 1970), reduced myocardial oxygen consumption (Klassen et al., 1970; Ono et al., 1982) and enhanced lactate uptake (Klassen et al., 1976). Similarly, Pepine and co-workers (1974) reported reduced coronary lactate extraction following perhexiline therapy, despite constant oxygen extraction in patients with coronary artery disease and angina. Such findings implied that perhexiline shifted cardiac metabolism towards carbohydrate utilisation and away from FA metabolism, thereby increasing metabolic efficiency (Kennedy et al., 1996; Faadiel Essop and Opie, 2004).

In 1994, perhexiline's property as a FA inhibitor was revealed as FA β-oxidation was inhibited *in vitro* and *in vivo* in mice and also in *ex vivo* cultured rat heart and hepatocyte preparations following perhexiline treatment (Deschamps et al., 1994). The latter study also showed that perhexiline concentrated within the mitochondria. Similarly, Jeffrey and colleagues (1995) reported an increase in lactate uptake with a concomitant reduction in FA oxidation in the isolated working rat heart. Following a hypothesis put forward by Professor John Horowitz

(Ashrafian et al., 2007b), it was finally determined in isolated rat cardiac and hepatic homogenates that perhexiline is a competitive reversible CPT1 (and CPT2) inhibitor (with an IC_{50} of 77 and 148 µmol/L respectively), with greater potency than amiodarone and able to induce a 35% decrease in FA utilisation (Kennedy et al., 1996). However, the CPT1 enzyme exists as three isoforms: hepatic isoform CPT1A, skeletal and cardiac muscle isoform CPT1B and brain isoform CPT1C (Bonnefont et al., 2004). Therefore, the potential for perhexiline to have non-cardiac specific effects existed and these were later found to be responsible for perhexiline-mediated toxicity.

1.10. Perhexiline-mediated toxicity

1.10.1 Neurotoxicity and hepatotoxicity of perhexiline

Initial clinical studies had shown minor short-term adverse effects arising from perhexiline therapy including nausea, lethargy, headaches and insomnia (Shah et al., 1982). However, it was the emergence of individual patient case studies depicting severe neuro- and hepatotoxicity which culminated in perhexiline's withdrawal from clinical use (Shah et al., 1982). Evidence of neurotoxicity was first described as debilitating peripheral neuropathy in patients on long-term perhexiline treatment (Bourrat et al., 1975; Bousser et al., 1976; Nicolas et al., 1976; Bady et al., 1978; Laplane and Bousser, 1981; Goble and Horowitz, 1984). Further symptoms included proximal myopathy (Tomlinson and Rosenthal, 1977), delayed motor nerve conduction velocity and paraesthesia (indicative of peripheral nerve damage) (Fraser et al., 1977; Fraser and Miller, 1978; Bouche et al., 1979), and also sensory neuropathy (Lorentz and Shortall, 1983). Morphological analysis using light microscopy on fibre preparations from different patients revealed neurogenic atrophy, severe loss of

myelinated fibres and evidence of Wallerian degeneration (Lhermitte et al., 1976; Said, 1978) and this was experimentally replicated in mice (Fardeau et al., 1979). Moreover, Bouche and colleagues (1979) provided evidence that the neuropathy was related to lipid storage in the Schwann cells. Importantly, the symptoms of neurotoxicosis were improved or abolished on cessation of perhexiline treatment (Said, 1978; Bouche et al., 1979; Wijesekera et al., 1980; Gordon and Gordon, 1981).

Several patient case studies also reported evidence of hepatotoxicity and detrimental changes to liver function and morphology following long-term perhexiline therapy (Igishu, 1976; McDonald, 1977; Kopelman and Morgan, 1977; Long et al., 1980; Poupon et al., 1980; Horowitz et al., 1982). This toxicity included the development of liver cirrhosis (Bonnet et al., 1978; Crinquette et al., 1981; Hamichi et al., 1982; Hay and Gwynne, 1983; Pieterse et al., 1983; Robson and Wing, 1983), hepatitis (Beaugrand et al., 1977; Lenoir and Blanchon, 1978; Dawes and Moulder, 1982; Valmalle et al., 1989; Satz et al., 1991) and acute hepatic failure (Roche et al., 1979; Roberts et al., 1981).

Moreover, many patients exhibited liver damage resembling alcohol-induced hepatitis (Paliard et al., 1978; Forbes et al., 1979; Pessayre et al., 1979). Further histological analyses revealed evidence of hepatic lesions (Beaugrand et al., 1978), liver parenchymal changes indicative of drug-induced hepatitis (Lageron, 1979), focal liver cell necrosis, micronodular cirrhosis, portal tract fibrosis and numerous inflammatory infiltrates/inflammation (Forbes et al., 1979; Morgan et al., 1984). More detailed histological analyses revealed abnormalities such as enlarged hepatocytes (Lewis et al., 1979) and increased hepatic phospholipid

content indicative of phospholipidosis (Pessayre et al., 1979). Alanine transaminase (ALT), routinely used clinically as a diagnostic measure of liver disease (Kim et al., 2008), was also markedly raised in several patients described in these case studies (McDonald et al., 1977; Lewis et al., 1979; Morgan et al., 1984). Indeed, Atkinson and co-workers (1980) observed a ~46-fold increase in serum ALT levels in an angina patient put on perhexiline medication, serum levels returning to normal 6 weeks after discontinuing its use. Moreover, in an *in vitro* study on human liver cell lines, exposure to perhexiline maleate led to rapid and direct cellular toxicity within a few days (Le Gall et al., 1980). A further study on cultured hepatocytes demonstrated phospholipid accumulation following perhexiline treatment (Lageron et al., 1981).

By August 1983, approximately 131 cases of neuropathy and 80 cases of hepatotoxicity had been reported within the UK alone (Shah, 2006). Other prevalent symptoms included marked weight loss (Myers and Ronthal, 1978; Pessayre et al., 1979), papilloedema (Atkinson et al., 1980), hypoglycaemia (Dally et al., 1977; Paliard et al., 1978) and renal failure (Paliard et al., 1978). Consequently, more detailed investigations were performed to determine the exact cause of perhexiline-mediated toxicity.

1.10.2. Association of perhexiline toxicity with its pharmacokinetics and pharmacogenetics

Historically important observations made by Singlas and colleagues (1978a and 1978b) revealed that patients who experienced severe neuro- and/or hepatotoxicity had significantly elevated perhexiline plasma levels compared to those who did not experience adverse effects. This led to the hypothesis that perhexiline toxicity was related to excessive

drug accumulation that could be attributed to its metabolism. To assess drug metabolism, these patients were given debrisoquine which was known to be hydroxylated by the hepatic enzyme cytochrome P450 2D6 (CYP2D6) (Shah et al., 1982; Shah et al., 1983). Using this substitute, it was established that patients with perhexiline-induced neuropathy (Shah et al., 1982) and/or perhexiline-mediated liver injury (Morgan et al., 1984) had impaired debrisoquine metabolism, indicative of impaired CYP2D6 activity. In contrast, patients who did not experience toxicity had a normal debrisoquine hydroxylation ratio. Clearly, these experiments suggested that perhexiline metabolism is achieved via hydroxylation by CYP2D6.

Subsequently, the heterogenic metabolism of perhexiline between different patient cohorts was found to be attributable to genetic polymorphisms of the CYP2D6 enzyme such that the population can be broadly divided into 'poor metabolisers/hydroxylators (PM)' and 'extensive metabolisers/hydroxylators' (Cooper et al., 1984; Barclay et al., 2003), although intra-group variations do exist (Sørensen et al., 2003). Patients treated with perhexiline who were PMs were therefore more susceptible to attaining high drug plasma levels and thus adverse effects. Approximately 10% of US and European Caucasians harbour a CYP2D6 mutation rendering them PMs (Evans et al., 1993). Moreover, metabolism of perhexiline by CYP2D6 may be saturable (Horowitz et al., 1981) raising the possibility that any patient is potentially at risk if the dose of perhexiline is too high.

As discussed in section 1.9.1, later studies revealed that at high concentrations perhexiline produced a major reduction in FA β-oxidation in the cardiac and hepatic mitochondria

(Deschampes et al., 1994; Fromenty and Pessayre, 1995). Excessive inhibition of β-oxidation cannot be compensated by carbohydrate metabolism and thus is detrimental (Ashrafian et al., 2007b). Furthermore, Meier and colleagues (1986) demonstrated that perhexiline treatment in rats that were PMs led to systemic lipidosis. With the identification by Kennedy and colleagues (1996) that the inhibition of β-oxidation was achieved through CPT1 targeting, and given that brain and liver isoforms of this enzyme existed, perhexiline-mediated CPT1 inhibition was implicated in the observed adverse effects. This explained the phospholipidosis and FA accumulation observed in histological studies on patients with perhexiline-induced neurotoxicity (Bouche et al., 1979) and liver toxicity (Pessayre et al., 1979; Lageron et al., 1981; Fromenty and Pessayre, 1995). Essentially, high plasma concentrations of perhexiline caused systemic CPT1 inhibition which was no longer cardiac-specific, leading to lipidosis and thus neuro- and hepatotoxicity (Ashrafian et al., 2007b).

1.10.3. The establishment of a therapeutic dose of perhexiline

Following the revelation of how perhexiline causes severe adverse effects, it was recognised that perhexiline plasma levels would need to be carefully regulated and monitored if it were to be used for therapeutic reasons in patients, particularly in those categorised as PMs (Ashrafian et al., 2007b). Horowitz and colleagues (1986) adjusted the perhexiline dose over a 9 month period in a group of 19 patients with angina according to the clinical emergence of toxicity. The authors reported that patients who developed neurological and/or hepatic side effects had a perhexiline plasma concentration between 0.72 – 2.86 mg/L. Thereafter, in another group of similar patients, they adjusted the drug dose to maintain a steady concentration of <0.6 mg/L. With this dose adjustment, almost all patients showed

improvements in their symptoms of angina and this was not accompanied by any significant adverse effect. It was therefore concluded that providing perhexiline plasma levels were closely maintained between 0.15 – 0.6 mg/L (0.5 – 2.2 µM), the drug could be safely used clinically (Horowitz et al., 1986). This was supported by a series of clinical studies in patients with angina, as long-term treatment with therapeutic monitoring of perhexiline plasma levels reduced the severity and frequency of attack without incidence of severe toxicity (Pilcher et al., 1985; Cole et al., 1990; Horowitz et al., 1995). Indeed, a recent audit of 170 patients who had been on perhexiline therapy for up to 50 months confirmed the absence of severe adverse effects (Phuong et al., 2016). In light of these findings, experimental and clinical investigations into the therapeutic potential of perhexiline have regained prominence.

1.11. Experimental and clinical investigations of perhexiline

Perhexiline has continued to demonstrate significant promise since the establishment of a therapeutic dosing regimen. Furthermore, as the early clinical studies on patients with angina demonstrated that perhexiline improved coronary flow, LV function and metabolic efficiency without causing symptomatic hypotension, it was again considered for therapeutic use in other conditions characterised by cardiac oxygen deficiency (e.g. ischaemic heart disease, aortic stenosis) or cardiac energy deficiency (e.g. HCM, HF) (Ashrafian et al., 2007b).

1.11.1 The therapeutic efficacy of perhexiline

In the isolated rat heart Langendorff model of low-flow ischaemia (95% flow reduction), the effective *ex vivo* dose of perhexiline was found to be 2 µM (equivalent to ~0.6 mg/L

therapeutic dose). In this study the authors observed a significant improvement in diastolic tension during 60 min ischaemia in hearts perfused pre-ischaemia with 2 µM, but not 0.5 µM perhexiline (Kennedy et al., 2000). However, neither perhexiline nor oxfenicine had any effect on systolic function (assessed as heart rate x developed tension) during ischaemia or on cardiac function during the 30 min reperfusion period. Nonetheless, perhexiline enhanced coronary flow under normoxic conditions as assessed by a reduction in perfusion pressure in the Langendorff isolated rat heart preparation and a reduction in perfusion tension during myography in isolated rat coronary artery vessels (Kennedy et al., 1999). In addition, Unger and colleagues (2005) also reported that although acute 60 min normoxic perfusion with 2 µM perhexiline had no effect on cardiac efficiency, longer transdermal pre-treatment for 24 h induced a 29% increase in cardiac work and 30% increase in cardiac efficiency in the non-ischaemic working rat heart.

This therapeutic efficacy was demonstrated clinically: in a small study on 15 elderly patients with severe inoperable aortic stenosis, which can often lead to HF, perhexiline therapy for 3 months improved symptoms and NYHA functional class, when maintained within the therapeutic plasma range (Unger et al., 1997). Additionally, in a systematic review conducted on 26 RCTS which included 700 angina patients, perhexiline was revealed as extremely potent in improving symptoms when maintained within the therapeutic plasma range (Killalea and Krum, 2001). In contrast, 12 months perhexiline treatment did not improve myocardial deformation in a study on 36 patients with ischaemic LV dysfunction as a result of MI, despite drug dosing having been adjusted to maintain steady therapeutic plasma

levels (Bansal et al., 2010). The extent of metabolic impairment was not pre-determined in this cohort so the results are difficult to fully assess.

On the other hand, in the more recent CASPER and HYPER clinical trials, which were run in parallel, perhexiline therapy was not protective against ischaemia/reperfusion injury in patients undergoing coronary artery bypass graft (CABG) surgery. To elaborate, in the CASPER trial, an RCT on 286 patients with ischaemic heart disease but normal LV function and no hypertrophy, pre-operative perhexiline treatment did not improve myocardial protection following CABG as cardiac index during reperfusion was not improved relative to the placebo group (Drury et al., 2015). The HYPER trial, which demonstrated similar results, was an RCT conducted on 112 with LV hypertrophy secondary to aortic stenosis, undergoing CABG (Senanayake et al., 2015). In the latter study, despite the presence of hypertrophy in these patients, a pathological state characterised by disturbed metabolism and a critical step to HF development (Berenji et al., 2005), myocardial injury (e.g. post-operative troponin release) was not attenuated following perhexiline therapy.

In combination, these trials suggested that the use of perhexiline in cardiac surgery is limited. However, despite both trials utilising a dosing regimen apparently adequate to achieve therapeutic drug levels, 27% of patients in the CASPER trial in fact had plasma levels below the therapeutic range (<0.15 mg/L), whilst only 47% in the HYPER trial had plasma levels within the therapeutic range. Such studies demonstrate the difficulties in using perhexiline therapy due to inter-individual variations of drug metabolism. Given this limitation, it can be argued that studies should be performed to investigate the effect of

perhexiline in ischaemia/reperfusion in a setting in which perhexiline administration at an effective dose is ensured, such as in an experimental Langendorff model.

In studies to date, perhexiline therapy has proved more successful in ischaemic conditions characterised by impaired cardiac energetics such as cardiomyopathy and more importantly HF (Steggal et al., 2017). For example, in mice with isoproterenol-induced irreversible HF, ATP depletion and oxidative stress culminated in cardiac dysfunction (i.e. decreased fractional shortening) which was attenuated following oral administration of perhexiline (Stapel et al., 2017). Furthermore, in a genetic knock-in mouse model of HCM, twice-daily intraperitoneal injection of perhexiline attenuated cardiac hypertrophy and remodelling, decreased mRNA expression of the fibrotic marker collagen type 1 and reduced oxidative stress, although the HCM hypertrophic phenotype was not completely reversed (Gehmlich et al., 2015). These results are consistent with the small clinical study on 46 patients with symptomatic non-obstructive HCM, in which perhexiline treatment corrected diastolic function (improved diastolic filling), improved exercise capacity (increased peak oxygen consumption), improved symptomatic status (reduced NYHA functional class) and increased the myocardial PCr/ATP ratio by 36% (Abozguia et al., 2010). Furthermore, in an RCT on 50 patients with HFrEF secondary to DCM, short-term perhexiline treatment increased the PCr/ATP ratio by 30% and improved the NYHA functional class (17% reduction) despite no change in LVEF (Beadle et al., 2015).

Perhexiline also provided symptomatic relief with minimal side effects in a study on 151 patients with CHF and/or refractory angina and demonstrated that those with angina were

more likely to respond positively to treatment (Phan et al., 2009b). Moreover in a double-blind RCT on 56 patients with HFrEF, Lee and colleagues (2005) reported a 10% improvement in LVEF, 21% reduction in NYHA functional class, 17% increase in peak oxygen consumption (important prognostic marker), and improved resting and peak stress myocardial function following 2 months perhexiline treatment. These therapeutic effects were accompanied by improvements in skeletal muscle energetics (PCr recovery post-exercise). Only one phase II clinical trial on patients with HFpEF undergoing perhexiline therapy has been completed (Singh et al., 2014) but the results are not yet disclosed.

In view of the available evidence, perhexiline is currently widely used for the management and treatment of refractory and unstable angina in Australia and New Zealand and was recently awarded orphan drug status by the Food and Drug Administration. However, it is only available off licence in the UK, on a named patient and consultant cardiologist basis (Phan et al., 2009b). Importantly, in the context of this thesis, the precise mechanism of perhexiline-induced protection remains to be fully elucidated; many groups questioning the role of CPT1 inhibition in the observed therapeutic effects as discussed below (section 1.11.2).

1.11.2 Potential cardioprotective mechanisms of perhexiline

To date, various proteins have been hypothesised to be involved in the cardioprotective mechanism(s) of perhexiline **[Figure 1.11]**

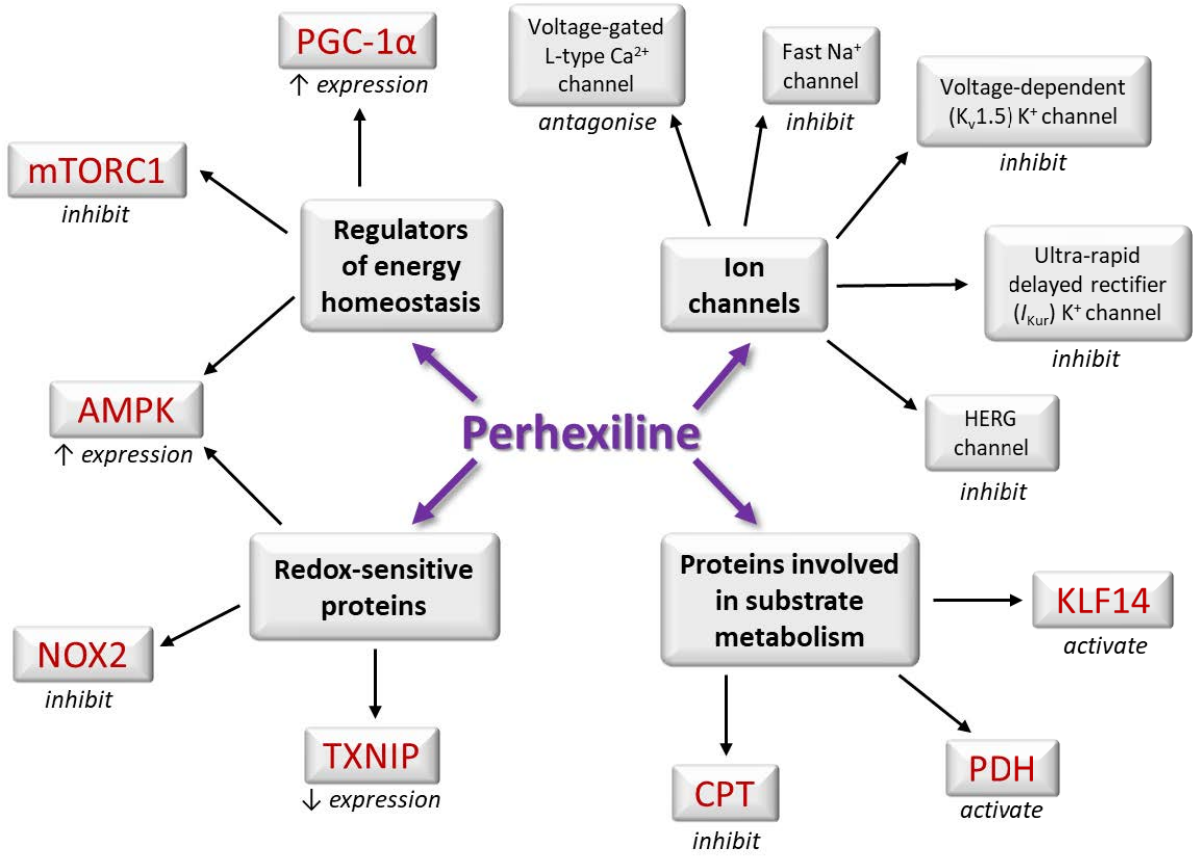

Figure 1.11. The potential cardioprotective mechanisms of perhexiline

An overview of the current mechanisms of action of perhexiline is shown. Early studies identified that perhexiline inhibited the activity of several ion channels. Various proteins have now been considered to be involved in the cardioprotective mechanism of perhexiline (in red text), many of which have a role in cardiac metabolism and energetic status. A greater emphasis has also been placed on the upregulation of glucose oxidation over the decrease in fatty acid oxidation, achieved through CPT1 inhibition.

AMPK, 5' adenosine monophosphate-activated protein kinase; Ca^{2+}, calcium ion; CPT, carnitine palmitoyltransferase; HERG, human ether-ago-go-related gene; K^{+}, potassium ion; KLF14, Krüppel-like factor 14, KLF14; mTORC1, mammalian target of rapamycin complex 1; Na^{+}, sodium ion; NOX2, nicotinamide adenine dinucleotide phosphate oxidase 2; PGC-1α, peroxisome proliferator activated receptor-γ coactivator-1α; PDH, pyruvate dehydrogenase; TXNIP, thioredoxin-interacting protein.

On the basis of early studies it was suggested that perhexiline modulated ion channel activity, and that this explained the observed vasodilatory effects (Hudak et al., 1973; Cappola, 2015). No studies seem to have been performed on the action of perhexiline on the

vascular smooth muscle. However, at high intracellular concentrations, perhexiline inhibited voltage-gated L-type Ca^{2+} ion channels in cultured chick embryo ventricular cells, and produced negative inotropic effects (Barry et al., 1985). In skinned muscle fibres from the rabbit psoas muscle, perhexiline increased troponin-C Ca^{2+} affinity thereby increasing contractility (Morano et al., 1989), but whether it has similar effects in cardiac muscle seems not to have been tested. Perhexiline also inhibited the fast Na^{+} ion channels in rat brain, rat heart and guinea pig atria preparations (Grima et al., 1988). Moreover, perhexiline inhibited the voltage-dependent $K_v1.5$ K^{+} ion channel in human embryonic kidneys and the ultra-rapid delayed rectifier (I_{Kur}) K^{+} ion channel in cultured human atrial myocytes (Rampe et al., 1995). In cultured cell lines, perhexiline also achieved voltage- and frequency-dependent inhibition of the human ether-ago-go-related gene (HERG) channel, which contributes to the heart's electrical activity (Walker et al., 1999). However, perhexiline's electrophysiological effects are minimal and unlikely to improve cardiac work and efficiency (Ashrafian et al., 2007b).

Following the revelation that perhexiline inhibited CPT1B activity (Kennedy et al., 1996) this became the favoured mechanism of action. However, subsequent studies by Kennedy and colleagues (1999 and 2000) revealed that CPT1B inhibition may not be the therapeutic mechanism of perhexiline. The improvements in rat coronary artery flow following perhexiline treatment were not affected by addition of CPT1B inhibitor etomoxir (Kennedy et al., 1999), whilst the attenuation in diastolic tension in rat hearts subjected to low-flow ischaemia was not accompanied by a decrease in long chain acyl-carnitines (a product of CPT1 activity) (Kennedy et al., 2000). Moreover, Unger and co-workers (2005) reported improvements in cardiac work and efficiency in the absence of changes in palmitate FA

oxidation in the Langendorff rat heart model. It was therefore proposed that CPT1-independent mechanisms of perhexiline may be more important (George et al., 2016), such as a shift towards carbohydrate metabolism. However, in a clinical study on HCM patients, Abozguia and co-workers (2010) reported decreases in both FA and glucose serum levels suggesting an increase in cellular uptake of *both* cardiac substrates. Nonetheless, in *ex vivo* H9c2 myocytes, perhexiline treatment promoted glucose uptake alone, and the authors suggested that this was mediated by an increase in GLUT4 recruitment to the plasma membrane (Nobuhara et al., 2013).

The mechanisms were explored further in a metabolomics and proteomics study performed by Yin and colleagues (2013) which showed an increase in PDH complex activation in mice treated orally for 4 weeks with perhexiline, providing evidence that an upregulation of PDH and thus glucose oxidation may be a therapeutically relevant mechanism. These authors also reported an increase in lactate and amino acid uptake which would re-balance flux through the TCA cycle, and proton donation within the mitochondria which would serve to alter the intracellular redox environment. Furthermore, in a genetic HCM mouse model, metabolomics revealed that perhexiline-induced changes involved around 272 unique metabolites within the myocardium, including a reduction of those involved in FA β-oxidation, changes in the glycolytic, glycerol, pentose phosphate and TCA pathway – all indicative of an upregulation of glucose oxidation (Gehmlich et al., 2015).

Perhexiline was also shown to activate the Krüppel-like factor 14 (KLF14), a regulator of lipid metabolism, thereby reducing atherosclerotic lesion development in apolipoprotein E-

deficient mice (Guo et al., 2015). Surprisingly, such results have not been demonstrated clinically as both Drury et al. (2015) and Beadle et al. (2015) reported no change in cardiac substrate utilisation in CABG and HFrEF patients respectively. However, Beadle and colleagues (2015) still observed improvements in myocardial energetics with perhexiline, suggesting that it may not only modulate cardiac substrate utilisation. In support of this, in LV biopsies taken from CABG patients, perhexiline administration was associated with a significant reduction in TXNIP expression in parallel to significant increases in AMPK and PGC-1α expression (Ngo et al., 2011). Moreover, superoxide formation by NADPH oxidase 2 (NOX2) was reduced by 44% in intact neutrophils following 2 μM perhexiline pre-treatment and NOX2 activity was directly inhibited in pig valve interstitial cells and cardiac fibroblasts (Kennedy et al., 2006). Such results of NOX2 inhibition were reflected by Liberts and colleagues (2007) in patients with angina and by Gatto and colleagues (2013) in a cell-based assay. These studies therefore suggest the ability of perhexiline to attenuate oxidative stress by modulating redox pathways. This idea was supported by a study in patients with stable angina or acute coronary syndrome; perhexiline therapy for 3 days inhibited superoxide release from neutrophils *in vitro* (Willoughby et al., 2002). Furthermore, in an automated cell-based assay, perhexiline inhibited the activity of mammalian target of rapamycin complex 1 (mTORC1), a regulator of cellular metabolism and autophagy (Balgi et al., 2009). During ischaemia, mTOR activation was shown to upregulate HIF-1α which in turn increased PDK activity, thereby decreasing glucose metabolism (Cairns et al., 2011).

Despite this wide array of clinical and experimental observations, the cardioprotective mechanisms of perhexiline are still not fully understood, thus requiring further investigation.

1.11.3. The existing challenges with perhexiline therapy

It remains evident that the full therapeutic potential of perhexiline and its underlying mechanism of action have yet to be fully explored. It is also apparent that despite the establishment of a therapeutic drug range (Horowitz et al., 1986) and a validated protocol for loading perhexiline gradually in patients (Philpott et al., 2004), maintaining constant therapeutic perhexiline serum levels remains a problem. Such challenges were highlighted in clinical trials (Senanayake et al., 2015; Drury et al., 2015) which concluded that perhexiline may be more useful when therapy is prolonged, monitored and optimised, but limited in the setting of cardiac surgery when this is not feasible. Furthermore, whilst it is possible to deduce the patient populations most at risk to adverse effects e.g. by determining the metabolic ratio of perhexiline's metabolite cis-hydroxy-perhexiline (OH-perhexiline) over perhexiline (the parent drug) (Sallustio et al., 2002), drug metabolism remains highly polymorphic and variable even within PMs (Chong et al., 2016). Moreover, extra caution is required when treating patients already faced with liver impairment of other origins and for those on additional medications which require CYP2D6 metabolism which could cause contraindication (Davies et al., 2004; Davies et al., 2006). In view of all these problems, Signal Pharma aimed to design and develop a perhexiline analogue which could retain the same therapeutic profile and efficacy without the metabolic liability related to CYP2D6 metabolism.

1.12. Fluoroperhexiline-1 (FPER-1): a novel derivative of perhexiline

The chemical structure of perhexiline consists of a carbon chain –CH–CH_2 backbone with two saturated cyclohexane rings and one pyridine ring **[Figure 1.10 and 1.12]** (Ashrafian et al.,

2007b). To date, relatively few attempts to modify the structure of perhexiline have been made (Leclerc et al., 1982; Tassoni et al., 2007; Schou, 2010). Perhexiline hydroxylation by CYP2D6 can take place on one or both cyclohexyl rings and as such, modification of this part of the drug structure was trialled first by Signal Pharma and are now published (Tseng et al., 2017).

The concept of developing and synthesising a new analogue was based on altering the site of drug metabolism in the hopes that the absence of complex and variable pharmacokinetics would remove the current challenges faced with using perhexiline clinically. Cycloalkyl perhexiline analogues, in which the cyclohexyl rings were substituted with cycloalkyl rings, retained an almost identical pharmacokinetic and stability profile to perhexiline and proved disappointing (Tseng et al., 2017). Subsequently, the incorporation of fluorine atoms onto one or more of the cyclohexyl rings, generating a range of fluoroperhexiline (FPER) derivatives, was trialled.

Of these FPER derivatives, 4,4-*gem*-difluoro-perhexiline or 'FPER-1' **[Figure 1.12]** was highly stable, with a great reduction in susceptibility to CYP2D6 metabolism, when tested in the presence of CYP2D6-expressing Bactosomes prepared from rat liver microsomes (Tseng et al., 2017). Importantly, *in vitro* assays demonstrated that FPER-1 remained potent at inhibiting mitochondrial CPT1 (IC_{50} = 45 μM) isolated from rats when compared to perhexiline (IC_{50} = 11 μM) (Tseng et al., 2017).

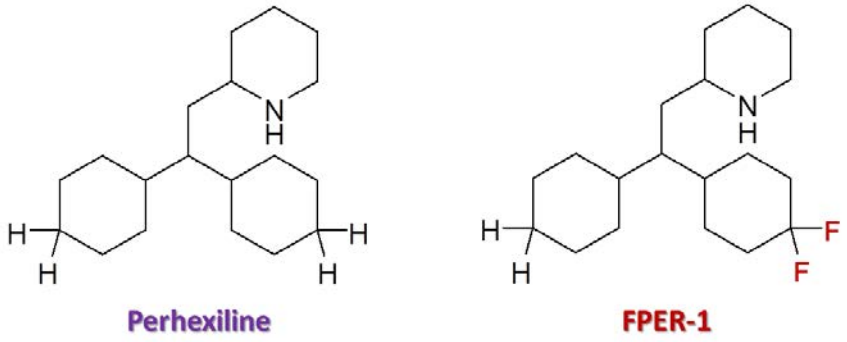

Figure 1.12. The chemical structure of FPER-1 compared to perhexiline

FPER-1 contains the addition of two fluorine atoms to one cyclohexane ring, thus modifying its pharmacokinetics compared to perhexiline.

FPER-1, fluoroperhexiline-1.

Moreover, perhexiline is known to accumulate selectively within the myocardium *in vivo* and this property was also replicated by FPER-1 following oral gavage in mice and rats as reported in our recent study (Tseng et al., 2017). In BALB/c mice oral gavage with 10 mg/kg perhexiline led to a 5.7-fold drug accumulation in the myocardium over plasma at 1 h, and 4.8-fold at 8 h. FPER-1 at 10 mg/kg showed an even greater selectively for the myocardium, with a 10.7-fold accumulation at 1 h and 9.5-fold at 8 h. In addition, for the same oral dose, at 1 h FPER-1 was present at a plasma concentration ~3-fold greater than perhexiline (0.35 mg/L vs 0.12 mg/L) and a myocardial concentration ~5.6-fold greater than perhexiline (3.73 mg/L *vs* 0.66 mg/L). Similar results with regards to drug stability and distribution were also observed following 10 mg/kg oral gavage of perhexiline or FPER-1 in Sprague Dawley rats (Tseng et al., 2017).

Thus, the available evidence suggests that FPER-1 is an optimal match as an orally bioavailable perhexiline analogue. What remains to be tested is whether FPER-1 retains the therapeutic efficacy of perhexiline and whether the mechanisms of action are the same.

1.13. Summary

As discussed above, increasing experimental and clinical evidence has demonstrated that impaired cardiac metabolism and energetics are key characteristics of both HFrEF and HFpEF. Consequently, metabolic modulators capable of correcting this metabolic disturbance have been highly considered as pharmacotherapeutic agents for this malignant disease. Perhexiline is one such metabolic drug, specifically a CPT1 and FA oxidation inhibitor, with a long history of potent efficacy in the treatment and management of angina. Despite perhexiline's withdrawal from clinical use in the 1980s due to the emergence of severe neuro- and hepatotoxicity, the establishment of a therapeutic dose in 1986 and a clearer understanding of its pharmacokinetics and pharmacogenetics have brought perhexiline back to the forefront of cardiovascular research. Perhexiline has since been demonstrated to be a valuable agent in aortic stenosis, HCM and in HFrEF. However, the role of CPT1 inhibition in these effects is controversial and despite a wide range of proteins such as PDH and TXNIP being considered, the precise cardioprotective mechanism(s) have not been fully elucidated. Of greater importance, the clinical use of perhexiline remains challenging because of the requirement for individualised dosing and dose titration, resulting from the highly polymorphic and unpredictable CYP2D6 drug metabolism within the population, a characteristic which has limited the use of perhexiline.

Consequently, Signal Pharma have designed and synthesised FPER-1, a perhexiline analogue, with a similar chemical structure but an altered site of CYP2D6 metabolism. So far, FPER-1 has shown promise *in vitro* and *in vivo* in animal studies, demonstrating a stable and predictable metabolism without compromised drug potency. These findings suggest that

FPER-1 may be a useful replacement agent for use in a broader spectrum of patients. What remains to be defined is whether this new derivative retains the same therapeutic efficacy as its parent drug.

1.14. Thesis aims

With this background, the aims of the work in this PhD thesis were:

1) To determine whether both perhexiline and FPER-1 can improve *ex vivo* cardiac haemodynamics pre- and post-ischaemia.

2) To determine whether perhexiline and FPER-1 can delay the progression from LV hypertrophy to HF *in vivo*.

3) To determine the cardioprotective molecular mechanism(s) of perhexiline and FPER-1 *ex vivo* and *in vivo*.

To fulfil these aims, both perhexiline and FPER-1 were assessed *ex vivo,* in an isolated murine heart Langendorff model and *in vivo,* in an abdominal aortic constriction murine model of cardiac hypertrophy and HF.

Chapter 2:
Materials and Methods

Chapter 2: Materials and Methods

2.1. Animals

Male C57Bl/6 mice aged 8-10 weeks (25 – 30 g) were used for *ex vivo* experiments (Langendorff model; Chapter 3 and 4), whilst 6-8 week old male C57Bl/6 mice (18 – 23 g) were used for *in vivo* experiments (acute toxicity model; Chapter 5 and abdominal aortic constriction model; Chapter 6). Mice were supplied by Charles Rivers, housed 4-5 per cage, on a 12-12 h light-dark cycle with food and water available *ad libitum.* All animal procedures and experiments were conducted in accordance with the Animals Scientific Procedures Act (ASPA) 1986 following ethical approval.

2.2. Chemicals and reagents

All chemicals and reagents used in this thesis are presented within tables throughout the text or otherwise stated within text.

2.3. *Ex vivo* Langendorff isolated perfusion of the mouse heart model

2.3.1. Perfusate preparation

For *ex vivo* Langendorff experiments, murine hearts were cannulated and perfused with either a standard Krebs-Henseleit buffer (KHB) (Tanno et al., 2003) or a high-fat KHB containing free fatty acid palmitate (Kennedy et al., 2000), prepared one day prior to experiment **[Table 2.1]**. The high-fat KHB buffer consisted of 3% bovine serum albumin (BSA) pre-conjugated to 1.2 mM palmitate as previously described (Belke et al., 1999) and was prepared as outlined in **Figure 2.1**. Briefly, BSA was dissolved in 250 ml of standard KHB

(without glucose and sodium bicarbonate ($NaHCO_3$)) under constant stirring at 37 °C to form a concentrated 12% BSA solution. In parallel, palmitate was dissolved into a distilled water:ethanol solution (60:40 ratio) containing sodium carbonate (Na_2CO_3) (1:1.2 molar ratio of Na_2CO_3 to palmitate). Next, the palmitate solution was mixed at 100 °C until fully dissolved, with heating continued until all ethanol was evaporated and only the water volume remained. The dissolved palmitate was then quickly mixed with the 12% BSA solution at 37 °C to initiate conjugation. After thorough mixing, the BSA-palmitate conjugate was dialysed overnight, at room temperature, against 16 volumes of standard KHB (without glucose and $NaHCO_3$) using a 10 kDa molecular weight cut-off Slide-A-lyzer dialysis flask (Thermo Scientific) under constant stirring. The following day, the dialysed conjugate was made up to 1 L KHB with the addition of glucose, $NaHCO_3$, lactate and insulin.

Once prepared, both standard and high-fat KHB were filtered through a glass microfiber membrane of pore size 1.6 µm (Whatman) using a vacuum pump (KNF Lab VP series) and stored at 4 °C until use.

2.3.2. Preparation of perhexiline and fluoroperhexiline-1

Perhexiline and fluoroperhexiline-1 (FPER-1) were supplied by Signal Pharma and stored at 4 °C until use. Stock solutions were pre-prepared in dimethyl sulfoxide (DMSO; Sigma) and stored in aliquots at -20 °C. Drug aliquots were thawed on the day of use and diluted into the appropriate KHB at a final DMSO concentration of 0.2%. Perhexiline was used at 2 µM and FPER-1 at either 2 or 10 µM.

Table 2.1. Krebs-Henseleit buffers (KHB)

Standard KHB	High-fat KHB	Chemical Formula	Concentration	Company
Sodium chloride		NaCl	118.5 mM	Sigma
Sodium bicarbonate		$NaHCO_3$	25 mM	Fisher Scientific
Potassium chloride		KCl	4.7 mM	VWR International
Magnesium sulfate		$MgSO_4.7H_2O$	1.2 mM	VWR International
Potassium phosphate		KH_2PO_4	1.2 mM	VWR International
Glucose		$C_6H_{12}O_6$	11 mM	Fisher Scientific
Calcium chloride		$CaCl_2.2H_2O$	1.4 mM	VWR International
-	Sodium L-lactate	$C_3H_5NaO_3$	1.1 mM	Sigma
-	Sodium palmitate	$CH_3(CH_2)_{14}COONa$	1.2 mM	Sigma
-	Bovine serum albumin	-	0.45 M (3%)	Europa Bioproducts
-	Insulin	-	100 µU/ml	Actrapid

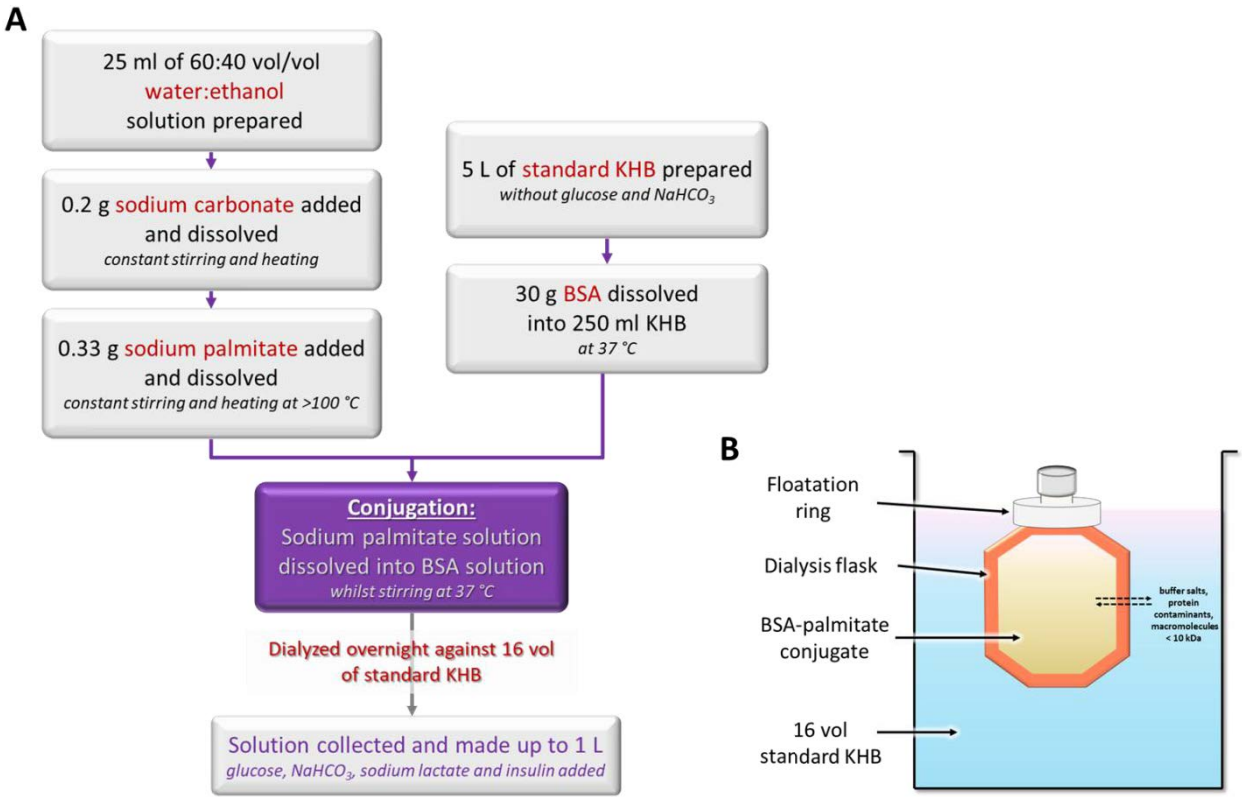

Figure 2.1. BSA-palmitate conjugation protocol

A modified high-fat KHB was used to perfuse isolated murine hearts. **A:** A flowchart outlining the optimised protocol according to Belke et al. (1999), in which sodium palmitate was pre-conjugated to BSA to enable the fatty acid to dissolve in the KHB. **B:** Schematic of the BSA-palmitate conjugate dialysis set-up.

BSA, bovine serum albumin; KHB, Krebs-Henseleit buffer; $NaHCO_3$, sodium bicarbonate.

2.3.3. Langendorff set-up

Terminal anaesthesia was induced in mice by intraperitoneally (i.p) injecting a 50:50 co-administration of the anaesthetic sodium pentobarbital (300 mg/Kg; Euthatal) and the anti-coagulant heparin (150 units; Wockhardt). Once unconscious, as assessed by instigation of the pedal reflex, a thoracotomy was performed to isolate the heart. The heart was quickly excised by the lungs to minimise cardiac damage and placed into ice-cold KHB to arrest beating. The heart was then cannulated via the aorta on a 21-gauge blunted needle and mounted onto the Langendorff apparatus within a 5 min window to preserve cardiac function **[Figure 2.2a and 2.2b]**. Once mounted, the heart was retrogradely perfused at a constant perfusion pressure using an STH pump controller (ADInstruments, Peristaltic pump; Gilson) at 80 mmHg with KHB, gassed with 95% O_2/5% CO_2 at a constant temperature of 37 °C (Digital flow heater; Grant Instruments) and pH of 7.0. At the onset of perfusion the left ventricle chamber was carefully exposed and a polyvinyl-chloride (cling-film) balloon gently inserted and inflated with distilled water. This balloon was connected to a pressure transducer which measured the changes in left ventricular pressure (LVP). Pacing was also initiated by positioning a 25 µm tungsten wire (ADInstruments) onto the apex of the heart and switching on a pacing stimulator (6002 Stimulator; Harvard apparatus).

To maintain consistent, physiological conditions, the following cardiac parameters – left ventricular developed pressure (LVDP), left ventricular end-diastolic pressure (LVEDP), coronary flow rate (CFR) and heart rate – were kept within specific inclusion criteria appropriate for murine hearts during the first 10 min of stabilisation as previously described (Sutherland et al., 2003) **[Table 2.2]**. All parameters were continuously monitored and

recorded throughout the experiments using Powerlab 4/35 (ADInstruments). The perfused heart was also immersed in KHB at 37 °C throughout each protocol.

Table 2.2. Inclusion criteria

Cardiac Parameter	Inclusion Criteria
Perfusion pressure	80 mmHg
Left ventricular developed pressure	>50 mmHg
Left ventricular end-diastolic pressure	6-10 mmHg
Coronary flow rate	2-5 ml/min
Heart rate	500-600 bpm

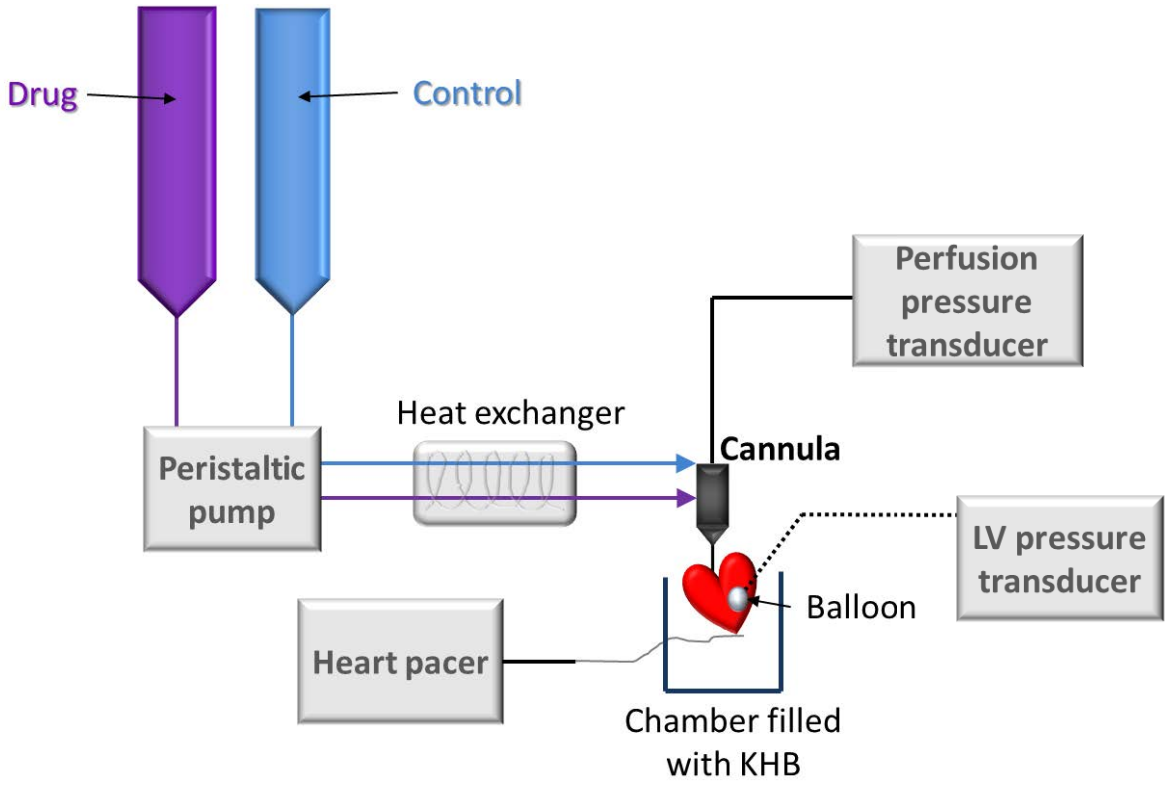

Figure 2.2a. Simplified schematic of the Langendorff set-up

The murine heart was immersed in a chamber filled with KHB at 37 °C and perfused with either a control or drug solution at 37 ˚C via the peristaltic pump. The peristaltic pump was switched off to establish global ischaemia, and switched on to commence reperfusion. A pressure transducer connected to a fluid-filled balloon, which was inserted into the left ventricle, recorded pressure changes throughout the experiment. The heart was continuously paced during perfusion.

KHB, Krebs-Henseleit buffer; LV, left ventricle.
Adapted from Sutherland et al. (2003).

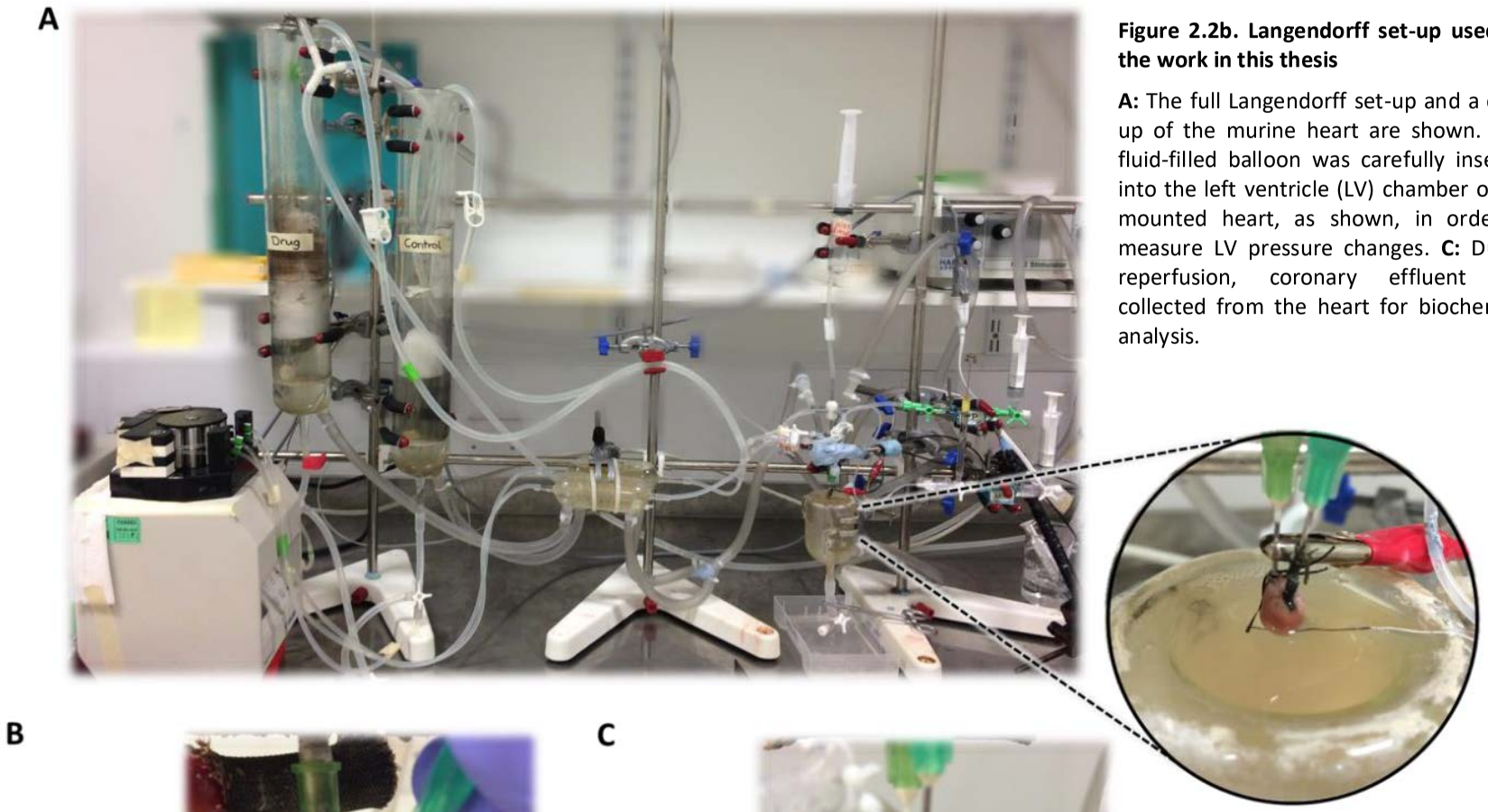

Figure 2.2b. Langendorff set-up used for the work in this thesis

A: The full Langendorff set-up and a close up of the murine heart are shown. **B:** A fluid-filled balloon was carefully inserted into the left ventricle (LV) chamber of the mounted heart, as shown, in order to measure LV pressure changes. **C:** During reperfusion, coronary effluent was collected from the heart for biochemical analysis.

2.3.4. Experimental protocols

In all experimental protocols (A to E; **[Figure 2.3]**) hearts were stabilised for an initial 10 min, to allow cardiac parameters to be adjusted within inclusion criteria. When required, global no-flow ischaemia was established by manually switching off the peristaltic pump (Gilson); the pacing was turned off 2 min into ischaemia. Similarly, when required, reperfusion was commenced by manually switching the peristaltic pump back on; pacing was re-started 5 min into reperfusion.

Protocol A: Assessing the effects of high-fat buffer on cardiac haemodynamics

To determine the effects of high-fat buffer (BSA-palmitate in KHB) on cardiac function, hearts were perfused for 40 min in either standard or high-fat KHB and cardiac haemodynamics (LVP, LVDP, LVEDP and CFR) recorded throughout and compared.

Protocol B: Assessing the effects of high-fat buffer on infarct size

To assess the effect of high-fat buffer on infarct size, a separate batch of hearts were subjected to ischaemia/reperfusion as previously described (Tanno et al., 2003). Hearts were perfused for 40 min stabilisation in either standard or high-fat KHB, followed by 30 min global ischaemia and 120 min reperfusion in the same KHB as used for stabilisation. At the end of reperfusion hearts were stained with 1% triphenyltetrazolium chloride (TTC; Sigma) for subsequent measurement of infarct size (see section 2.4).

Protocol C: Assessing the anti-ischaemic effects of perhexiline and FPER-1

Hearts were stabilised for 10 min in control high-fat KHB then perfused for a further 30 min with either 1) control (high-fat KHB), 2) 2 µM perhexiline, 3) 2 µM FPER-1 or 4) 10 µM FPER-

1. Hearts were then subjected to 30 min global ischaemia and 60 min reperfusion in control (high-fat KHB). Hypercontracture magnitude and time to hypercontracture were assessed at the onset of reperfusion (section 2.3.5). Coronary effluent was collected 5 min into reperfusion and stored at -80 ˚C for lactate biochemical analysis (see section 2.5). Cardiac haemodynamics (LVP, LVDP, LVEDP and CFR) were recorded throughout the 40 min stabilisation and 60 min reperfusion.

Protocol D: Collection of cardiac samples for molecular analysis 1

To assess potential molecular mechanisms of perhexiline and FPER-1, hearts were stabilised for 10 min in control (high-fat KHB) and then perfused for a further 30 min with either 1) control (high-fat KHB), 2) 2 µM perhexiline, 3) 2 µM FPER-1 or 4) 10 µM FPER-1. Hearts from each treatment group were then either snap-frozen in liquid nitrogen at the end of 40 min stabilisation (T1) or following 30 min global ischaemia (T2) and stored at -80 °C for Western blotting (see section 2.6).

Protocol E: Collection of cardiac samples for molecular analysis 2

To further determine molecular mechanisms of perhexiline and FPER-1, hearts were stabilised for 10 min in control high-fat KHB and then perfused for a further 60 min with either 1) control (high-fat KHB), 2) 2 µM perhexiline, 3) 2 µM FPER-1 or 4) 10 µM FPER-1. Following this extended 70 min stabilisation, hearts were snap-frozen in liquid nitrogen (T3) and stored at -80 °C for Western blotting (see section 2.6).

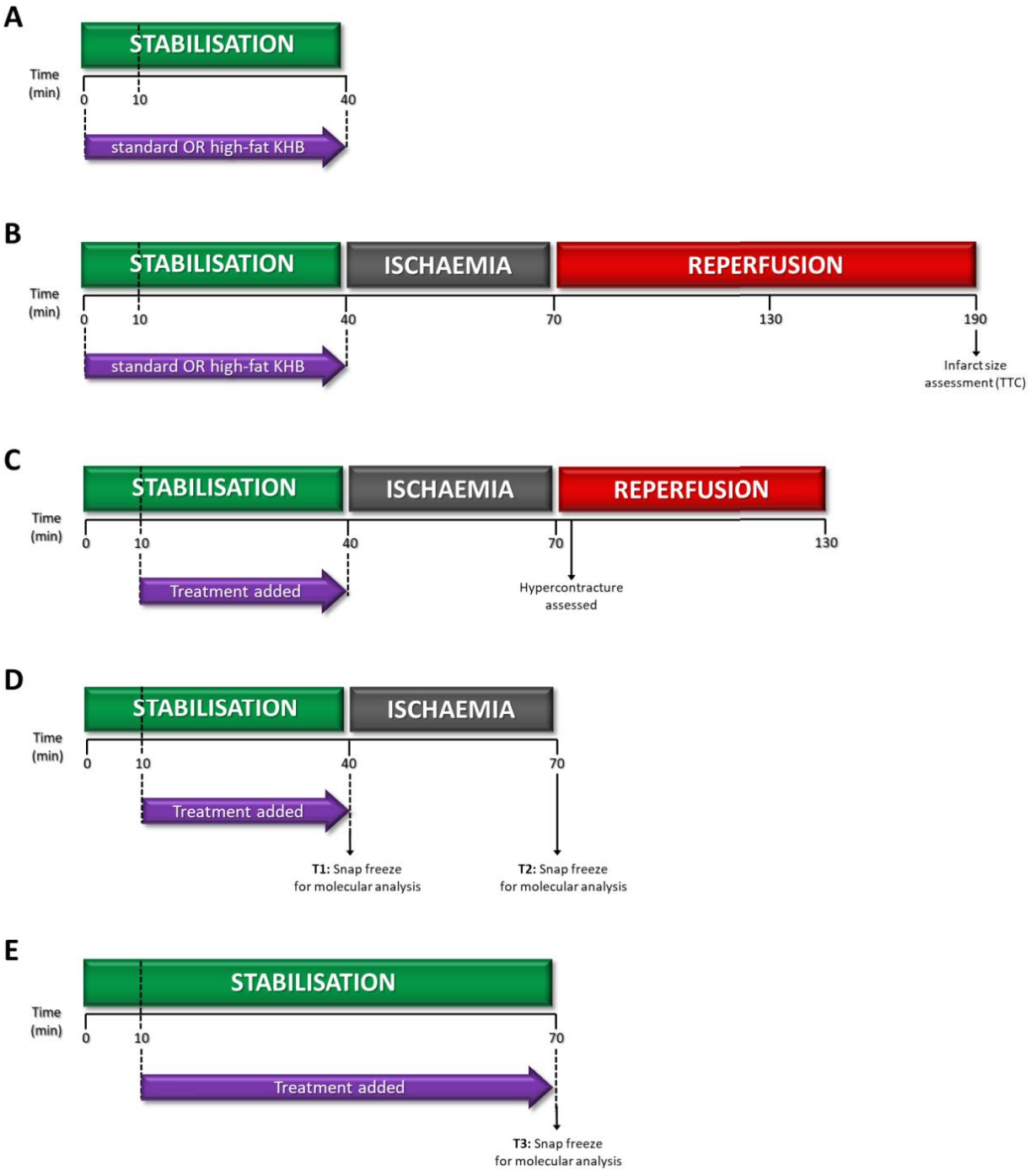

Figure 2.3. Langendorff experimental protocols

Experimental protocols **A** to **E** implemented for *ex vivo* Langendorffs are shown. For details, refer to text in section 2.3.4.

KHB, Krebs-Henseleit buffer; TTC, triphenyltetrazolium chloride.

2.3.5. Langendorff data acquisition

The cardiac parameters (LVDP, LVEDP and CFR) recorded during stabilisation and/or reperfusion were collected and analysed post-experiment using Labchart Version 7 (ADInstruments), by highlighting and selecting 5 sec of the recorded trace every 10 min for stabilisation and reperfusion **[Figure 2.4]**. Using the Labchart software, LVdP/dt, which describes the change in left ventricular pressure (LVP) over time, was also measured throughout stabilisation by selecting LVdP/dt max and LVdP/dt min on the Labchart data pad and highlighting the LVP trace from 9 to 10 min, 9 to 20 min, 9 to 30 min and 9 to 40 min **[Figure 2.5]**. The maximal rate of pressure increase; LVdP/dt max, is an indicator of cardiac contractility whilst the maximal rate of pressure reduction; LVdP/dt min, is an indicator of cardiac relaxation.

The restoration of coronary flow and perfusion pressure at reperfusion were accompanied by a spike in LVP, known as hypercontracture. Hypercontracture magnitude and time to hypercontracture were extracted at the onset of reperfusion as shown in **Figure 2.6**. At the start of reperfusion, the maximal peak in LVP was taken as the hypercontracture, as previously described (Varnavas et al., 2011). This was achieved by selecting 'maximum' value on the Labchart data pad and highlighting the peak of the LVP trace, while time to hypercontracture was determined by calculating the difference (in seconds) between the time at reperfusion and the time of peak LVP (hypercontracture). Time points of reperfusion and peak LVP were identified by selecting 'time' on the Labchart data pad and highlighting the corresponding part of the LVP trace.

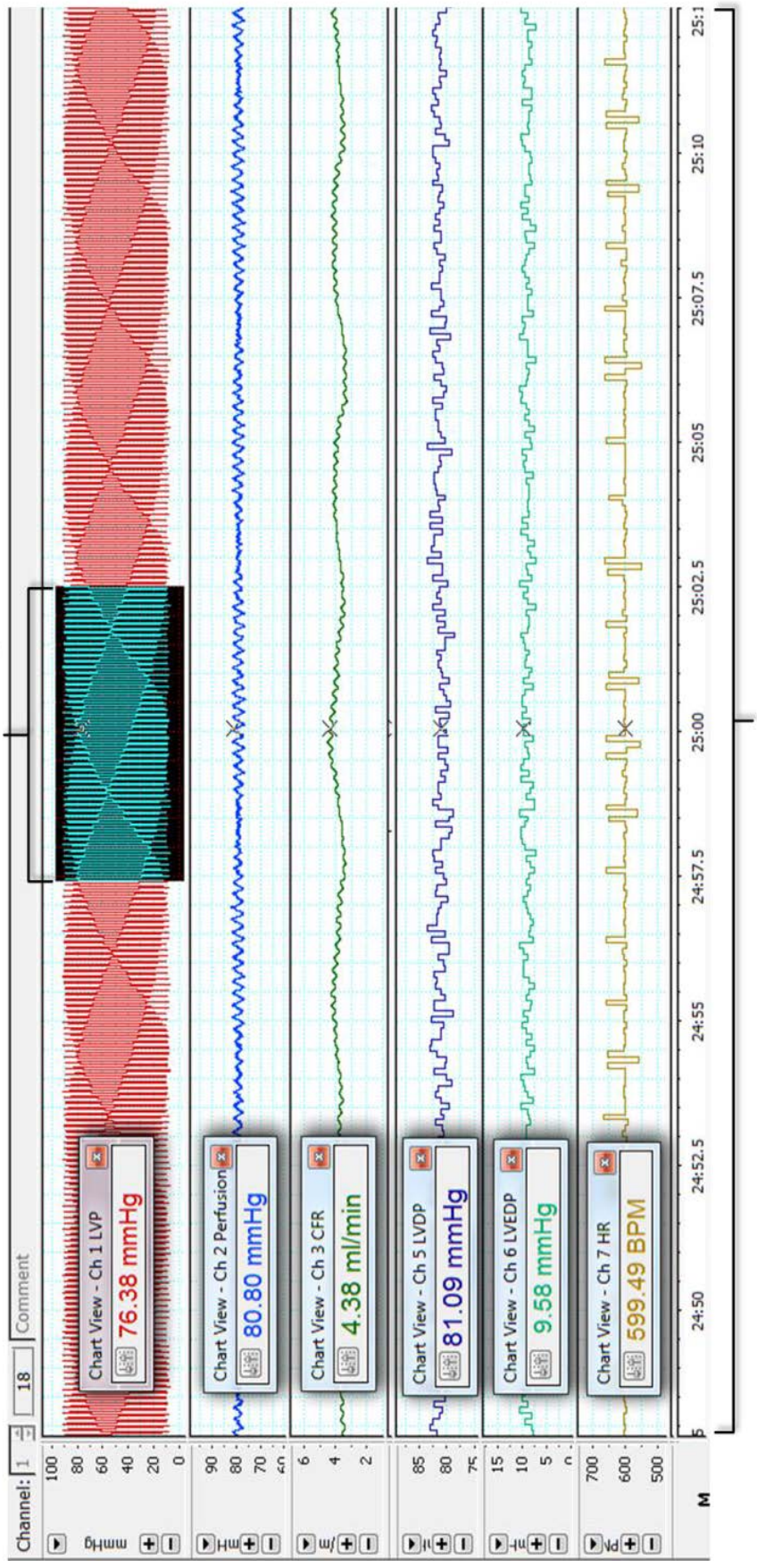

Figure 2.4. Example of a haemodynamics trace recorded from the Langendorff

Immediately after hearts were mounted onto the Langendorff system, a fluid-filled balloon was inserted into the left ventricle to measure LVP, LVDP and LVEDP. The CFR was also recorded during perfusion. The perfusion pressure was maintained at ~80 mmHg and HR between 500-600 beats per minute. For cardiac function analysis, 5 sec of the trace at incremental time points were selected and analysed using the data analysis tool on the Labchart software for both stabilisation and reperfusion.

CFR, coronary flow rate; HR, heart rate; LVDP, left ventricular developed pressure; LVEDP, left ventricular end-diastolic pressure; LVP, left ventricular pressure.

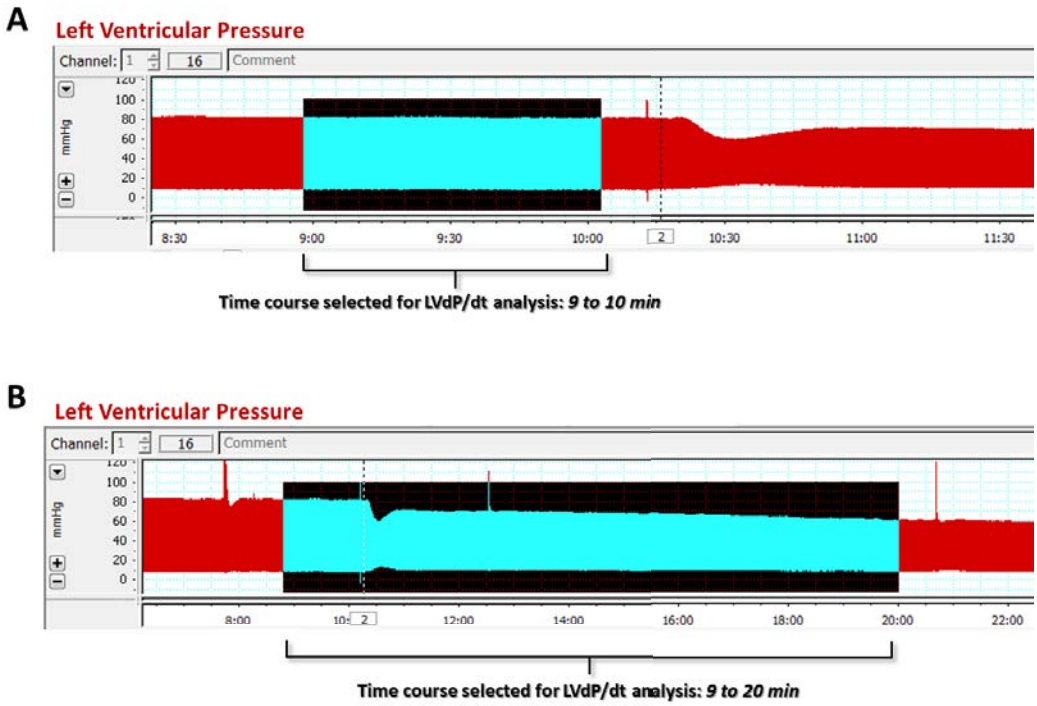

Figure 2.5. Change in left ventricular pressure over time analysis

The change in left ventricular pressure (LVP) over time (LVdP/dt) was assessed during stabilisation in hearts subjected to Langendorff protocol C, by selecting the desired part of the LVP trace and using the data analysis Labchart software. **A:** LVP from 9 to 10 min was selected to measure baseline LVdP/dt prior to the addition of perhexiline or FPER-1. **B**: LVP from 9 to 20 min was selected to measure change in pressure over the first 20 min of stabilisation. This was also carried out from 9 to 30 min and 9 to 40 min.

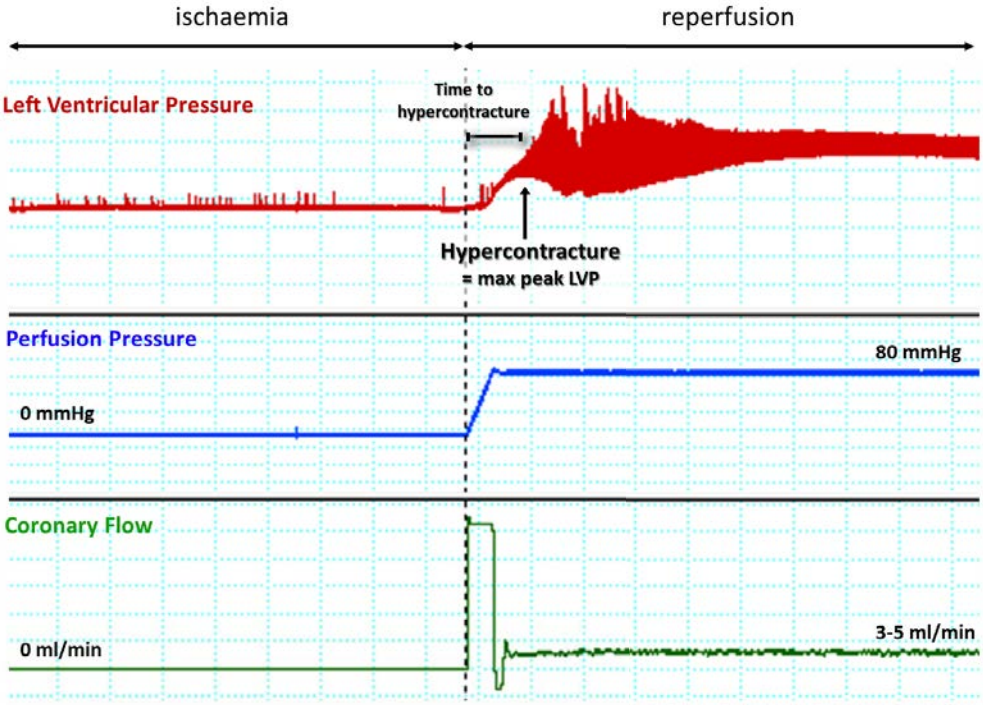

Figure 2.6. Hypercontracture analysis

Hypercontracture magnitude was assessed by measuring the maximum peak in left ventricular pressure (LVP) at the onset of reperfusion and the time to hypercontracture assessed by measuring the length of time between restoration of perfusion and the peak in LVP, in hearts from Langendorff protocol C.

2.4. Cardiac infarct size analysis

To determine the effects of a high-fat buffer on cardiac cell death post-ischaemia, infarction analysis was conducted on hearts from Langendorff protocol B.

2.4.1. Triphenyltetrazolium chloride staining

TTC staining distinguishes between metabolically active, viable cells and metabolically inactive, non-viable cells. This differentiation is achieved as the white TTC powder is reduced into a red compound (1, 3, 5-triphenylformazan) by various dehydrogenase enzymes active only in living cells (Benedek et al., 2006). Therefore, viable tissue is stained red whereas non-viable dead or 'infarcted' tissue is stained white **[Figure 2.7]**. Following 120 min reperfusion in control KHB, the heart was removed from the Langendorff apparatus, and gently perfused with 5 ml of freshly made 1% TTC in phosphate buffered saline (PBS; Sigma) at 37 °C. The TTC solution was manually infused at a rate of ~1 ml/min. Next, the heart was incubated for 10 min at 37 °C in ~2 ml of 1% TTC. After incubation, the atria were dissected; the heart blot dried and stored at -20 °C for up to 1 week.

2.4.2. Heart preparation for infarction analysis

Hearts were prepared for infarction analysis as previously described (Tanno et al., 2003) **[Figure 2.7]**. Briefly, the frozen heart was fixed in ice-cold 2.5% glutaraldehyde (Merck) for 2 min followed by embedding in 5% agarose (Bioline) in a vertical orientation, apex down, using a 27-gauge needle to hold in place whilst the agarose set. The needle was then removed and the agarose heart block sectioned into 0.7 mm thick slices using a Vibratome (Agar scientific), from the top of the ventricles to the apex. Immediately after being

sectioned, each heart slice was individually fixed in 10% formaldehyde (Merck) for 24 h overnight at room temperature. The following day, the formaldehyde solution was replaced with PBS and the heart incubated for 24 h overnight at 4 °C. The next day, heart slices were separated from the surrounding agarose and scanned between two glass plates using a CanoScan 5600F scanner (Canon).

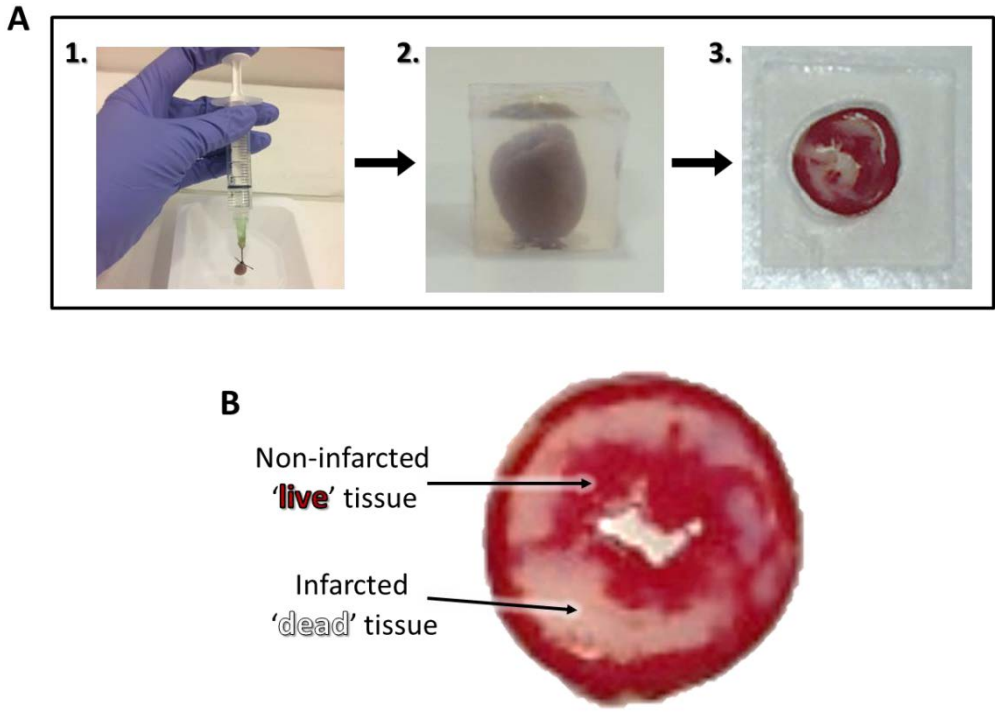

Figure 2.7. Heart preparation for infarction size analysis

A: An overview of the heart preparation required for infarct size analysis following Langendorff protocol B. 1. 1% triphenyltetrazolium chloride (TTC) heart perfusion. 2. Embedding the heart into an agarose block. 3. 0.7 mm heart sections made using a Vibratome **B:** A representative image of a scanned heart slice following 1% TTC staining, to be used for Image J infarction size analysis.

2.4.3. Image J infarction size analysis

Scanned hearts were independently coded and blindly analysed by two independent investigators using Image J software as previously described (Tanno et al., 2003) **[Figure 2.8]**.

In brief, the saturation and brightness of each slice was manually altered using a red colour threshold selector on Image J to select the total area of the slice (area at risk), the infarcted area and the non-infarcted area of the slice. Percentage infarct size was defined as area of infarction over total area at risk. This was carried out for each heart section and an average calculated for each heart.

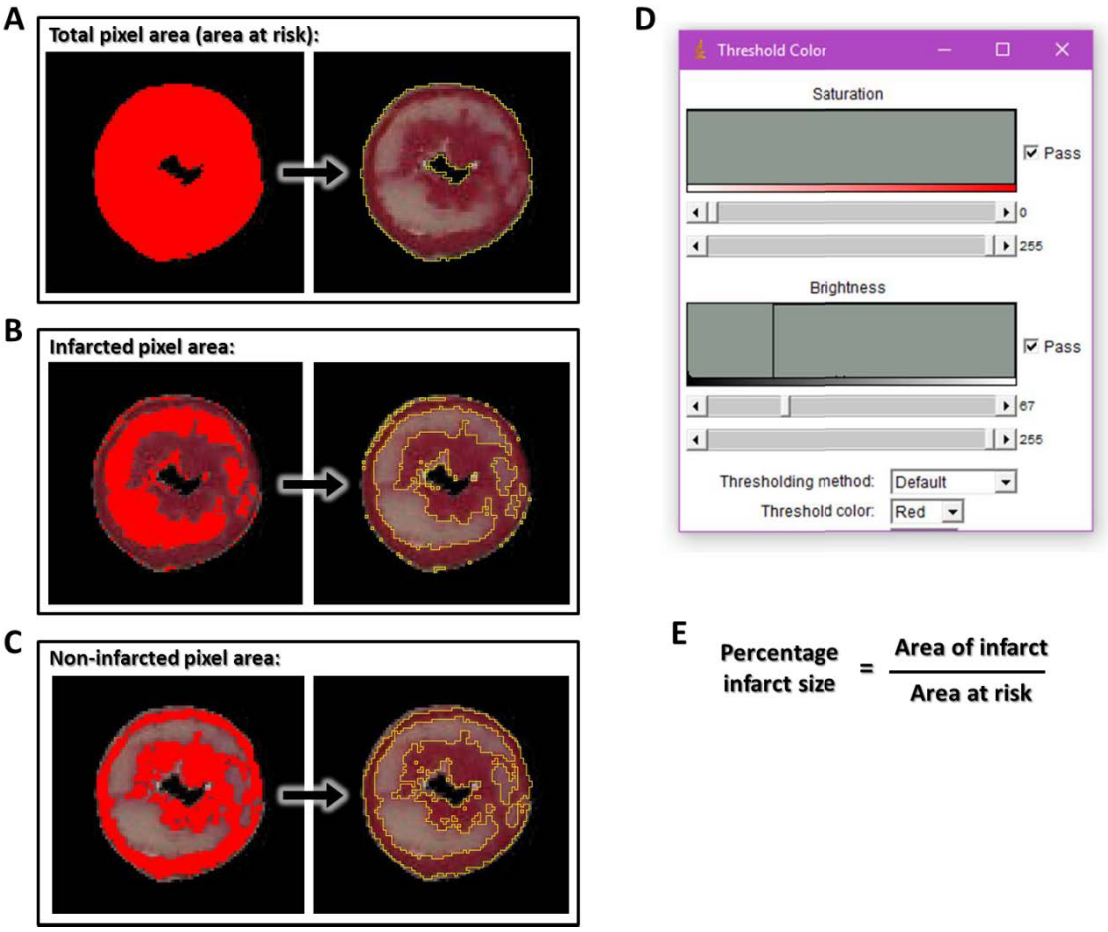

Figure 2.8. Image J infarction size analysis

Image J software was used to blindly analyse heart slices obtained by sectioning hearts subjected to Langendorff protocol B on a Vibratome. **A:** Selection of total pixel area of heart section. **B:** Selection of infarcted pixel area. **C:** Selection of non-infarcted pixel area. **D:** Threshold colour window on Image J used for separating infarcted and non-infarcted areas of heart section by altering the saturation and brightness of the image followed by area selection and pixel measuring. **E:** Equation used for calculating percentage infarct size.

2.5. Biochemical analysis of lactate content

To assess whether perhexiline or FPER-1 altered lactate release (a readout of glycolysis) post-ischaemia, lactate content in effluent samples collected from Langendorff protocol C were colorimetrically determined using a BioVision kit (#K607-100), as previously described (Wu et al., 2013).

2.5.1. Sample deproteinisation

Frozen cardiac effluent samples were thawed on ice at room temperature then individually deproteinised using a commercial kit (BioVision; #K808-200). Deproteinisation was necessary to remove enzymes such as lactate dehydrogenase which would otherwise cause rapid lactate degradation. Briefly, effluent samples were mixed with ice-cold perchloric acid (supplied ready to use in the kit) in a 5:1 ratio, vortexed, and placed on ice for 5 min. Next, samples were centrifuged at 13 000 x*g* for 2 min at 4 °C before being transferred into fresh eppendorfs. Following deproteinisation, samples were neutralised by addition of 6.4 µl ice-cold neutralisation buffer (supplied ready to use in kit) and vigorously vortexed, allowing the excess acid to precipitate. Samples were subsequently placed on ice for 5 min, centrifuged at 13 000 x*g* for 2 min at 4 °C and the resulting neutralised effluent extracted. Neutralised cardiac effluent samples were then assayed for lactate content (section 2.5.2).

2.5.2. Lactate colorimetric assay and analysis

The BioVision lactate assay kit was used to determine the lactate content of each cardiac effluent sample, with all reagents kept on ice. For this particular kit, lactate detection

involves lactate (present in the tested samples) being oxidised by lactate oxidase (present in supplied enzyme mix) in the following enzymatic reaction:

Lactate + oxygen → pyruvate + hydrogen peroxide

The hydrogen peroxide product is detected by reacting and binding with a probe (supplied in kit) to generate a colour at an optical density of 570 nm.

Lactate assay reagents were prepared and used as per the manufacturer's guidelines. Briefly, to a 96-well plate, effluent samples were added in duplicates at a 1/20 dilution with lactate assay buffer. Lactate standards were freshly prepared and added in duplicates at: 0, 2, 4, 6, 8 and 1 nmol/well. Next, a reaction mix was prepared, consisting of 46 µl lactate assay buffer, 2 µl lactate enzyme mix and 2 µl lactate probe (provided in DMSO and warmed to room temperature), and added to each standard and sample. The plate was then covered in aluminium foil and incubated on a shaker for 30 min at room temperature. Following incubation, the absorbance was read at 570 nm using a colorimetric plate reader (KC4; Biotek). The absorbance values were then used to plot a lactate standard curve **[Figure 2.9]** and to calculate the lactate content of each effluent sample.

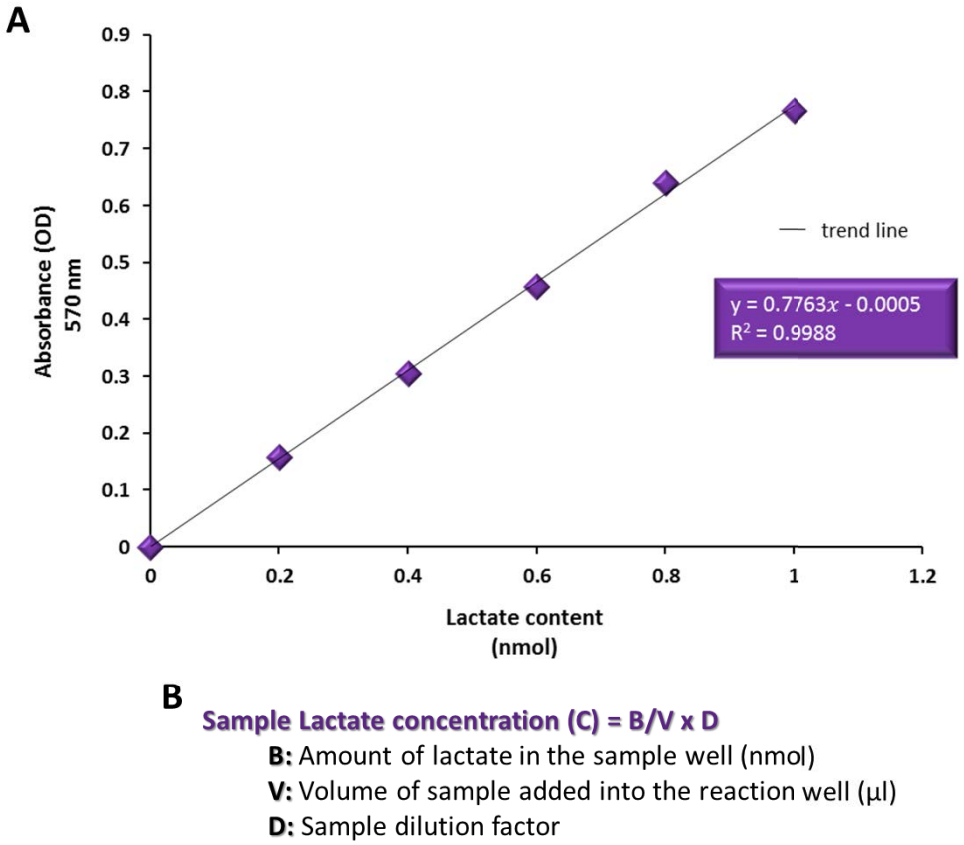

Figure 2.9. Lactate assay standard curve and calculation

Cardiac effluent samples collected 5 min into reperfusion from Langendorff protocol C were subjected to a lactate assay. **A:** An example of the lactate standard curve generated from the colorimetric BioVision lactate assay kit. **B:** The equation used to determine the lactate concentration in cardiac effluent samples.

OD, optical density.

2.6. Western blot analysis of *ex vivo* drug mechanisms

To investigate the molecular mechanism(s) of perhexiline-mediated protection and whether FPER-1 replicated these, the expression or phosphorylation of various proteins involved in cardiac function, cardiac metabolism and cell survival were assessed by Western blotting in whole mouse hearts. All antibodies (primary and secondary) used throughout this thesis are shown in **Table 2.3**.

Table 2.3. Primary and secondary antibodies (Ab)

Protein	1° Ab dilution	1° Ab species; company	2° Ab dilution	2° Ab species; company
Phospho-PLB Ser16	1:5000 5% milk	Rabbit; Badrilla	1:2000 NO milk	Goat; Cell signalling
Phospho-PLB Thr17	1:2000 5% milk	Rabbit; Badrilla	1:2000 NO milk	Goat; Cell signalling
Total PLB	1:20 000 5% milk	Mouse; Abcam	1:10 000 1% milk	Goat; Dako
CPT1B	1:1000 5% milk	Rabbit; Origene	1:5000 5% milk	Goat; Cell signalling
Phospho-PDH Ser232	1:5000 5% milk	Rabbit; Milipore	1:10 000 1% milk	Donkey; Amersham
Phospho-PDH Ser293	1:5000 5% milk	Rabbit; Abcam	1:10 000 1% milk	Donkey; Amersham
Phospho-PDH Ser300	1:5000 5% milk	Rabbit; Millipore	1:5000 1% milk	Donkey; Amersham
Total PDH	1:5000 5% BSA	Rabbit; Cell signalling	1:5000 1% milk	Donkey; Amersham
Phospho-GSK3αβ Ser21/9	1:1000 5% BSA	Rabbit; Cell signalling	1:2000 1% milk	Donkey; Amersham
Total GSK3αβ	1:2000 3% milk	Mouse; Milipore	1:10 000 1% milk	Goat; Dako
Phospho-Akt Ser473	1:1000 5% BSA	Rabbit; Cell signalling	1:5000 1% milk	Donkey; Amersham
Total Akt	1:1000 5% BSA	Rabbit; Cell signalling	1:1000 1% milk	Donkey; Amersham
Phospho-ERK1/2 Thr202/Tyr204	1:1000 5% BSA	Rabbit; Cell signalling	1:5000 1% milk	Donkey; Amersham
Total ERK1/2	1:1000 5% BSA	Rabbit; Cell signalling	1:1000 1% milk	Donkey; Amersham
TXNIP	1:1000 5% milk	Rabbit; Abcam	1:1000 1% milk	Donkey; Amersham
UCP3	1:1000 5% milk	Rabbit; Abcam	1:5000 1% milk	Donkey; Amersham
ANT	1:1000 5% milk	Santa Cruz; Abcam	1:5000 1% milk	Donkey; Amersham
Actin (Loading control)	1:2000 0.5% milk	Mouse; Sigma	1:5000 1% milk	Goat; Dako

Akt, protein kinase B; ANT, adenine nucleotide translocase; CPT1B, carnitine palmitoyltransferase 1B; ERK1/2, extracellular signal-regulated kinase 1/2; GSK3αβ, glycogen synthase kinase 3αβ; PDH, pyruvate dehydrogenase; PLB, phospholamban; TXNIP, thioredoxin-interacting protein; UCP3, uncoupling protein 3.

2.6.1. Cardiac lysate preparation and protein content determination

Snap-frozen hearts collected from Langendorff protocols D and E were mechanically homogenised in liquid nitrogen using a pestle and mortar with the addition of 500 µl ice-cold homogenisation buffer, prepared freshly on the day **[Table 2.4]**. Cardiac homogenate was then collected and freeze-thawed twice by placing the sample into liquid nitrogen until frozen then removing and placing on ice until thawed, in order to facilitate protein extraction. After the final freeze-thaw, the homogenate was centrifuged at 13 000 rpm at 4 °C for 15 min and the resulting supernatant extracted. The protein content of each supernatant was then analysed using a Bio-Rad D_c kit and freshly prepared BSA standards in homogenisation buffer (standard concentrations: 0, 0.2, 0.4, 0.6, 0.8, 1.0 mM).

Table 2.4. Western blot buffer components

Buffer	Buffer component	Concentration	Company
Homogenisation buffer	Tris-HCl pH 7.4	10 mM	Trisma-base: Sigma HCl: VWR
	Sodium fluoride	5 mM	Sigma
	Sodium orthovanadate	2 mM	Sigma
	Protease inhibitor	1 Tablet	Roche
1x Resolving buffer	Tris base	25 µM	Sigma
	Glycine	192 µM	Sigma
	Sodium dodecyl sulphate	0.1%	Sigma
	Distilled water	Made to 1 L	/
Wet transfer buffer (stored at 4 °C)	Methanol	100 mM	VWR
	Tris base	25 µM	Sigma
	Glycine	192 µM	Sigma
	Distilled water	Made to 1 L	/

HCl, hydrochloric acid.

First, the cardiac lysate was diluted 1/20 in homogenisation buffer and 5 µl added in triplicates into a 96-well plate alongside 5 µl of each BSA standard also pipetted in triplicates.

Next, the Bio-Rad kit solutions were added to the cardiac lysates, starting with 25 µl working solution A (a 1:40 combination of reagent A and S) followed by 200 µl reagent B. Finally, the plate was covered in aluminium foil, placed on a shaker for 15 min at room temperature, and absorbance values read at 750 nm using a colorimetric plate reader (KC4; Biotek). The absorbance values for the BSA standards were used to produce a protein standard curve **[Figure 2.10]** and to calculate the protein content of each cardiac sample. The resulting values were used to prepare the cardiac samples in homogenisation buffer at a final concentration of 1.25 M with the addition of an equal volume of 2x laemmli buffer (Bio-Rad) containing 5% β-mercaptoethanol (Sigma) to reduce protein disulphide bonds, and stored at -20 °C for Western blotting (section 2.6.2)

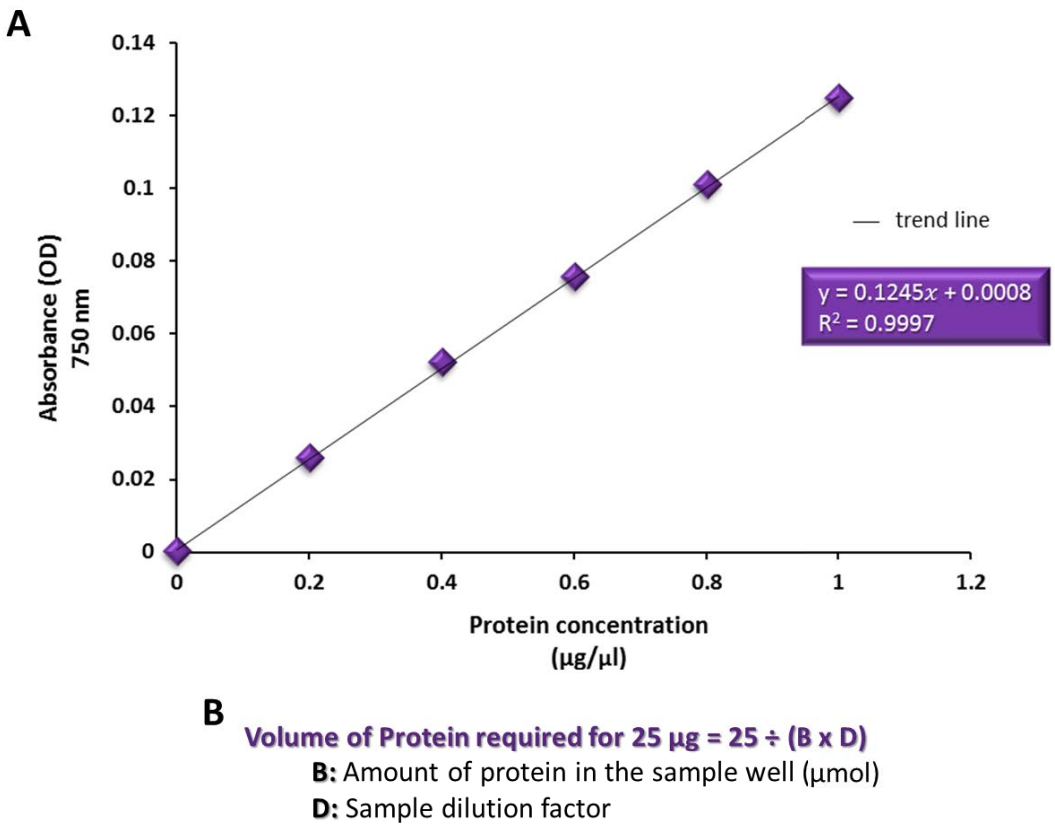

Figure 2.10. Protein assay standard curve and calculation

Murine hearts collected from Langendorff protocol D and E were subjected to protein assay. **A:** An example of the protein standard curve generated using the Bio-Rad protein assay kit. **B:** Equation used to calculate volume of cardiac supernatant required to prepare 25 µg protein in 2x laemmli buffer for Western blotting.

OD, optical density.

2.6.2. Western blotting and analysis

In preparation for Western blotting, each cardiac lysate sample was boiled at 95 °C for 5 min to denature the proteins and centrifuged at 1000 rpm at 4 °C for 5 min. Twenty-five micrograms (in 20 µl) of cardiac protein were loaded per well onto either 10% (for all protein detection except phospholamban (PLB)) or 15% (for PLB detection) sodium dodecyl sulphate (SDS) polyacrylamide gels **[Table 2.5]**, next to a protein ladder (Bio-Rad). Gels were prepared using the Bio-Rad gel casting system, 1.0 mm glass spacer plate and glass short plates (Bio-Rad). First, the resolving gel components were mixed and pipetted into the gel casting plates and set using a thin layer of butan-1-ol (Sigma). Once the resolving gel had set, the butan-1-ol was rinsed using distilled water and the stacking gel mixed and pipetted directly on top. Ten well combs (Bio-Rad) were then inserted into the stacking gel and allowed to set. Gels were either used immediately after setting or stored at 4 °C for up to 2 days, wrapped in damp paper towels and foil.

Proteins were separated at 150 volts for up to 90 min in freshly made 1x resolving buffer **[Table 2.4]** in an electrophoresis tank (Mini-PROTEAN Tetra Cell; Bio-Rad). Following gel electrophoresis, proteins were wet transferred onto polyvinylidene fluoride (PVDF) membranes (Amersham) which were pre-activated by soaking in methanol (VWR) for 15 min. The wet transfer sandwich was prepared by placing the PVDF atop the gel, with a blotting paper (Bio-Rad) and fibre pad (Bio-Rad) on either side **[Figure 2.11]**. The sandwich was then held within a cassette and placed in a wet transfer tank (Mini Trans-Blot cell; Bio-Rad) where proteins were transferred at 100 volts for 90 min in ice-cold wet transfer buffer **[Table 2.4]**. Membranes were then blocked at room temperature for 2 h with 5% non-fat milk (Bio-

Rad)/PBS 0.1% Tween (PBST), with the exception of membranes ran for PLB which were blocked for only 30 min under the same conditions.

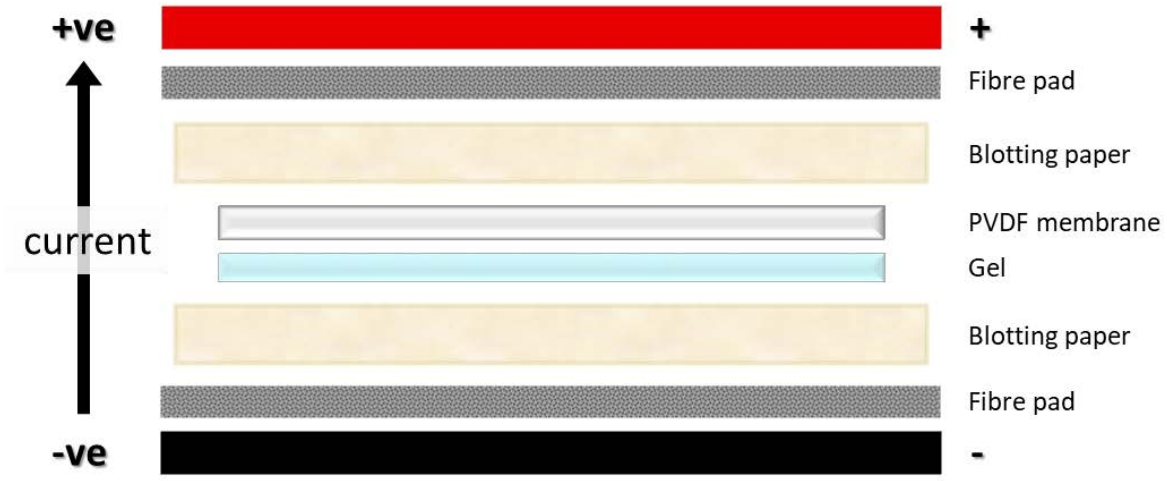

Figure 2.11. Simplified schematic of the Western blot wet transfer cassette set-up

The PVDF membrane and electrophoresis gel were sandwiched between blotting paper and fibres pads for wet transfer at 100 volts.

PVDF, polyvinylidine.

Table 2.5. Stacking and resolving gel components

Gel component	Concentration			Company
	Stacking gel	10% Resolving gel	15% Resolving gel	
Bis-Acrylamide	4.67%	10%	15%	National diagnostics
Tris-HCl pH 6.8	13.97 µM	-	-	Trisma-base: Sigma HCl: VWR
Tris-HCl pH 8.8	-	2.65 µM		
Sodium dodecyl sulphate	0.1%	0.1%		Sigma
Tetramethylethyl-enediamine	0.58 mM	1 mM		Sigma
Ammonium persulfate	0.17%	0.1%		Sigma
Distilled water	/	/	/	/

HCl, hydrochloric acid.

Blocked PVDF membranes were incubated with primary antibodies **[Table 2.3]** at 4 °C overnight on a shaker. The following day, membranes were washed with PBST 4x 15 min before incubation in the appropriate secondary antibody **[Table 2.3]**, which was conjugated to the horseradish peroxidase (HRP) detection enzyme, for 1 h at room temperature. Next, membranes were washed 4x 15 min in PBST and finally, incubated in enhanced chemiluminescence solution (Thermo Fisher Scientific) for 3 min prior to developing. Western blots were subsequently developed on hyperfilm (Amersham) using the Compact x4 processor (Xograph), scanned using the CanoScan 5600F (Conon) and analysed densitometrically on Adobe CS Photoshop.

For loading control detection (actin) and where PVDF membranes were re-used, membranes were blocked in 5% non-fat milk/PBST for 1 h followed by incubation in 0.05% sodium azide (Sigma)/5% non-fat milk/PBST solution for 1 h, at room temperature. Sodium azide inhibits the HRP enzyme bound to the secondary antibody, thereby preventing chemiluminescence detection at previously probed sites.

2.7. *In vivo* acute toxicity model: 1-week dosing study

To identify the optimum route of administration and drug dose for *in vivo* studies, a series of 1-week acute toxicity studies were conducted on 6-8 week old male C57Bl/6 mice **[Figure 2.12]**.

2.7.1. Drug preparation

Perhexiline and FPER-1 were supplied by Signal Pharma and stored at 4 °C until use. A drug suspension was first made by weighing and mixing the required amount of drug with Tween 80 (Sigma) in a 1.5 ml centrifuge tube at room temperature. The drug-Tween 80 suspension was then gradually dissolved into 0.5% sodium carboxymethyl cellulose (NaCMC; Sigma)/distilled water solution to gain a final concentration of 0.1% Tween 80 followed by thorough vortexing. Prepared drug formulations were stored at 4 °C until use and freshly prepared every 2-3 days throughout the study to maintain drug stability. A vehicle solution of 0.5% NaCMC/0.1% Tween 80 in distilled water was also prepared and stored at 4 °C. The preparation protocol used was as per Tseng et al. (2017).

2.7.2. Experimental design and treatment regimen

C57Bl/6 mice were used in one of four protocols (A to D) listed below based on two key objectives.

Objective 1: Assess the route of administration.

Objective 2: Assess the optimum drug dose.

Vehicle, perhexiline or FPER-1 were administered either by i.p injection (protocol A), or oral gavage (protocol B-D) for objective 1 whereas four separate drug doses (10, 20, 50 and 70 mg/kg) were tested for objective 2. Vehicle or drug was administered according to mouse body weight (e.g. 250 µl vehicle/drug for a 25 g mouse) for i.p and gavage.

Protocol A (pilot study)

A pilot study was conducted in mice subjected to abdominal aortic constriction, carried out by Dr James Clark at King's College London as previously described (Boguslavskyi et al., 2014). Mice were administered either 1) vehicle, 2) 30 mg/kg perhexiline, or 3) 30 mg/kg FPER-1 via daily i.p injection 1 week post-surgery, prior to the onset of hypertrophy, for an intended 4 weeks.

Protocol B

Mice were administered either 1) vehicle, 2) 10 mg/kg perhexiline, 3) 20 mg/kg perhexiline, 4) 10 mg/kg FPER-1, or 5) 20 mg/kg FPER-1 via oral gavage once daily for 7 days. On day 8, organs were harvested (24 h post-feed) as detailed in section 2.7.3.

Protocol C

Mice were administered either 1) vehicle, 2) 50 mg/kg perhexiline or 3) 50 mg/kg FPER-1 via oral gavage twice daily for 7 days. Organs were then harvested on day 7 at either 1 or 8 h post-feed, or on day 8, 24 h post-feed (section 2.7.3).

Protocol D

Mice were administered either 1) 70 mg/kg perhexiline or 2) 70 mg/kg perhexiline via oral gavage once daily for 7 days. Organs were harvested on day 7 at either 1 or 8 h post-feed, or on day 8, 24 h post-feed (section 2.7.3).

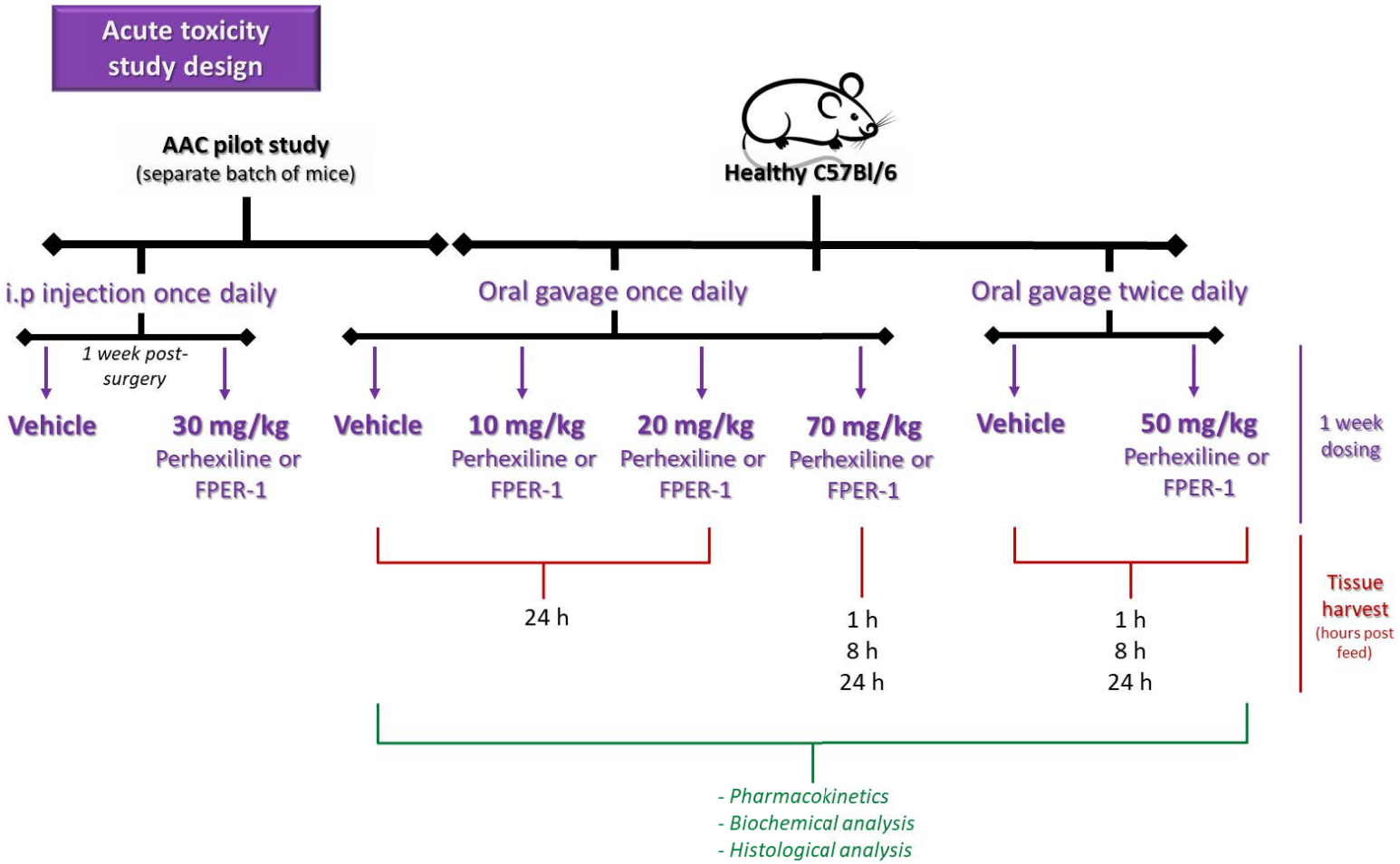

Figure 2.12. Acute toxicity study experimental design

Schematic outlining the experimental design used for assessing the *in vivo* acute toxicity of perhexiline and FPER-1. In a pilot study on mice subjected to AAC, i.p injection of vehicle, 30 mg/kg perhexiline or FPER-1 once daily for an intended 4 weeks was conducted by Dr James Clark at King's College London. Acute toxicity was then assessed in mice orally gavaged with vehicle, 10 mg/kg, 20 mg/kg or 70 mg/kg drug once daily and in mice orally gavaged with vehicle or 50 mg/kg drug twice daily. After 1 week, orally gavaged mice were sacrificed then plasma and organs harvested for pharmacokinetics, biochemical and histological assessment.

AAC, abdominal aortic constriction; i.p, intraperitoneally.

2.7.3. Tissue and plasma harvest

At the end of the 1-week dosing study, orally gavaged mice were sacrificed as described in section 2.3.2. A thoracotomy was carried out and the heart excised. The heart was then dissected from the lungs, quickly perfused with 1 ml cold standard KHB to remove all blood, blot dried, snap-frozen in liquid nitrogen and stored at -80 °C for future work. Next, a 1 ml syringe pre-coated in 0.5 M ethylenediaminetetraacetic acid (EDTA; VWR) was used to slowly collect blood from the thoracic cavity. EDTA was used to prevent coagulation and haemolysis. Collected blood was immediately centrifuged at 1000 x*g* for 10 min at room temperature and the plasma extracted and stored at -80 °C for drug pharmacokinetics (section 2.8) and biochemical alanine transaminase (ALT) (section 2.10) analysis. The right liver lobe was also isolated, rinsed in standard KHB, blot dried and fixed in 4% formaldehyde (Ferndale pharmaceuticals) for histopathology (section 2.9). Plasma was also collected from control non-gavaged mice (housed for 1 week), and subjected to ALT analysis.

2.8. Drug pharmacokinetics analysis

High performance liquid chromatography-tandem mass spectrometry (HPLC-MS/MS) was used to assess drug pharmacokinetics in plasma collected from *in vivo* mice studies (acute toxicity model; section 2.7 and abdominal aortic constriction model; section 2.12). Plasma samples were prepared and analysed by Professor Benedetta Sallustio's group at The Queen Elizabeth Hospital, Adelaide, Australia using a method adapted from Westley and co-workers (2015).

2.8.1. Sample preparation and separation

Briefly, 150 µl of acetonitrile containing 1 mg/L internal standards, D11-perhexiline and D11-hydroxy (OH)-perhexiline (TRC) was added to 50 µl of plasma sample. The sample was then mixed followed by centrifugation for 5 min at 16,000 x*g*. The supernatant was transferred into a fresh 1.5 ml centrifuge tube and mixed with 100 µl of 0.05% formic acid followed by transferring into HPLC vials. The Agilent 1100 series HPLC apparatus (Agilent Technologies) which consisted of a degasser, an injector and column oven was used to carry out HPLC analysis. Of the sample preparation, 25 µl was injected into a Luna Phenyl-hexyl HPLC column (5 µm; 2.1 mm x 50 mm; Phenomonex Inc) which was used to carry out chromatographic separation of the analytes at 50 °C. In this set up, the mobile phases consisted of solution A: 100% methanol (Scharlau), 2 mM ammonium acetate (VWR), 0.1% formic acid (Merck), and solution B: 100% water, 2 mM ammonium acetate, 0.1% formic acid. Initially, a gradient consisting of 60% solution A:40% solution B, pumped at 500 µl/min flow rate was used, and the percentage of solution A increased over 0.7 min to 90%. Using the 90% solution A, analytes were eluted between 0.7 and 2.8 min followed by returning the solution A to 60%. Total run time per sample equated to 3.5 min.

2.8.2. Mass spectrometry

Prior to assessment of drug concentrations, the pure perhexiline, OH-perhexiline and FPER-1 were used to make plasma calibration standards and plasma quality controls, to validate the calibration curve generated. Control samples from vehicle-treated mice were also used to check for interferes. An API2000 mass spectrometer (AB SCIEX Pty LtD) was used to detect analytes by multiple reaction monitoring using positive ionization mode. The mass

spectrometer parameters set for perhexiline m/z 278.3 > 81.1, D11-perhexiline m/z 289.4 > 83.2, OH-perhexiline m/z 294.3 > 81.1, D11-OH-perhexiline 305.3 > 81.2 and FPER-1 m/z 314.1 > 294.4 are displayed in **Table 2.6**. The valco valve was placed in position to send the first 0 – 0.7 min of eluent to waste, the next 0.7 – 3.0 min of eluent to the mass spectrometer and the final 2.8 – 4 min to waste again. Assay validation was carried out as detailed in Westley et al. (2015).

Table 2.6. Mass spectrometer parameters

Compound	Dwell time (ms)	Declustering potential (V)	Entrance potential (V)	Collision entrance potential (V)	Collision energies (V)	Collision exit potential (V)
Perhexiline	180	40	9	15	40	5
Hydroxy (OH)-perhexiline	420	25	20	16	47	0
FPER-1	300	71	11.5	11.5	27	6

2.9. Histological analysis of liver toxicity

Histological staining was used to assess whether perhexiline and FPER-1 caused hepatotoxicity **[Figure 2.13]**.

2.9.1. Sample dehydration and embedding

Following fixation in 4% formaldehyde for up to 1 week, liver lobes were removed from the fixative and placed into histological cassettes then processed by dehydration in a series of ethanol dilutions (70%, 95% and 100%; VWR). Liver lobes were then placed into Histo-Clear solution (National diagnostics) and cleared, a process which replaces the dehydrant with a reagent that is miscible with the embedding medium. After processing, the liver lobes were

immersed in paraffin wax at 65 °C for 2 h, embedded into paraffin blocks and then allowed to cool until solid.

2.9.2. Sample sectioning and rehydration

Paraffin wax blocks were sectioned at 6 µm using a microtome (Bright Instruments) and placed into a tissue floatation water bath (Medizintechnik) at 37 °C before transferring onto microscope slides (Klinipath). Microscope slides were then placed into a mini-oven (CellPath) for 2 h at 60 °C to enhance tissue adhesion and remove excess paraffin. Lastly, the liver sections were rehydrated by immersing the slides into the clearing agent xylene and re-hydrator alcohol. Liver sections were then ready for staining.

2.9.3. Histological staining and analysis

Liver sections were histologically stained with haematoxylin and eosin (H&E) to assess tissue integrity/damage, whilst Van Gieson staining was used to assess fibrosis following drug treatment. For both stains, in-house protocols were used which consisted of immersing the microscope slides in various solutions, followed by mounting in DPX (CellPath) **[Table 2.6]**. Stained sections were imaged under a bright-field microscope (Zeiss Axioscan.Z1) with a x20 objective lens. Images were then randomly selected and qualitatively assessed for markers of necrosis, inflammation and fibrosis.

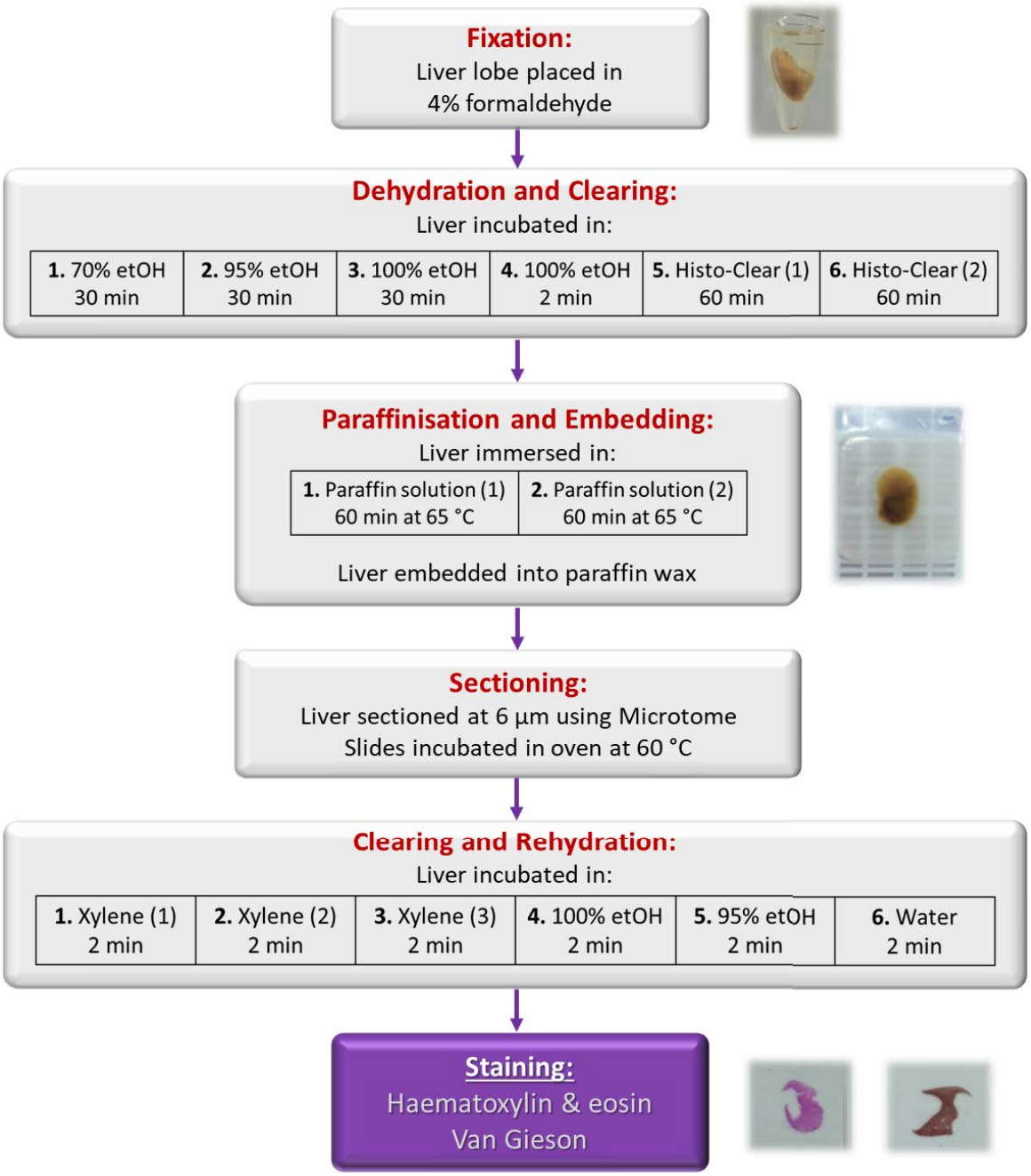

Figure 2.13. Histological analysis of liver toxicity

Liver samples collected from *in vivo* mice experiments were histologically assessed for drug-induced liver toxicity using haematoxylin & eosin and Van Gieson staining. Histology was carried out using the protocol shown.

etOH, ethanol.

Table 2.7. Histological staining protocol

Solution	Immersion time for each stain		Company
	Haematoxylin & eosin	Van Gieson	
Water	-	5 min	/
Celestine blue	-	5 min	Propath
Water	2x 2 min	2x 2min	/
Haematoxylin Harris	4 min	4 min	Propath
Water	2 min	2 min	/
Acid Alcohol	30 sec	30 sec	Propath
Water	2 min	2 min	/
Scott's tap water substitute	30 sec	30 sec	Propath
Water	2min	2 min	/
Van Gieson	-	3 min	Propath
Eosin	1 min	-	Propath
Water	2x 2 min	-	/
Alcohol	4x 2 min	2x 3 min	Propath
Xylene	3x 2 min	3x 2 min	Propath

2.10. Biochemical analysis of liver toxicity: alanine transaminase content

Alanine transaminase is routinely used clinically as a biomarker of liver health and hepatocellular injury (Kim et al., 2008). To assess ALT content, frozen plasma samples collected from *in vivo* experiments (section 2.7 and 2.12) were thawed at room temperature then subjected to an ALT activity assay using a colorimetric kit (Sigma; #MAK052). This assay involves ALT (present in the tested samples) catalysing the following reversible reaction:

Alanine + α-ketoglutarate ↔ pyruvate + glutamate

The pyruvate produced is detected by a subsequent reaction which turns an almost colourless probe into a colour at an optical density of 570 nm.

The ALT content is then determined based on the following principle:

One milliunit of ALT = amount of enzyme that generates 1.0 µmole of pyruvate per min

2.10.1. Alanine transaminase colorimetric assay and analysis

The ALT assay kit reagents were prepared/reconstituted as per the manufacturer's guidelines on the day of use. In brief, pyruvate standards were prepared at the following concentrations: 0, 0.2, 0.4, 0.6, 0.8 and 1 nmol/well and 20 µl added to a 96-well plate in duplicates. Twenty microlitres of undiluted plasma were then added in duplicates to the plate. A master reaction mix consisting of 86 µl ALT assay buffer, 2 µl ALT enzyme mix, 10 µl ice-cold ALT substrate and 2 µl fluorescent peroxidase substrate (provided in DMSO and warmed to room temperature) was then added to each well, and the plate covered in aluminium foil and incubated at room temperature on a shaker for 3 min. The plate was read at 570 nm using a colorimetric plate reader (KC4; Biotek) and the measured values taken as the 'initial' reading. The plate was then immediately incubated at 37 °C for 2 h and re-read at 570 nm. This 'final' reading was the time point at which ALT activity began to plateau and was used to plot a standard curve with the difference between the 'final' and 'initial' reading of each plasma sample calculated and compared to the standard curve to determine the ALT content **[Figure 2.14]**.

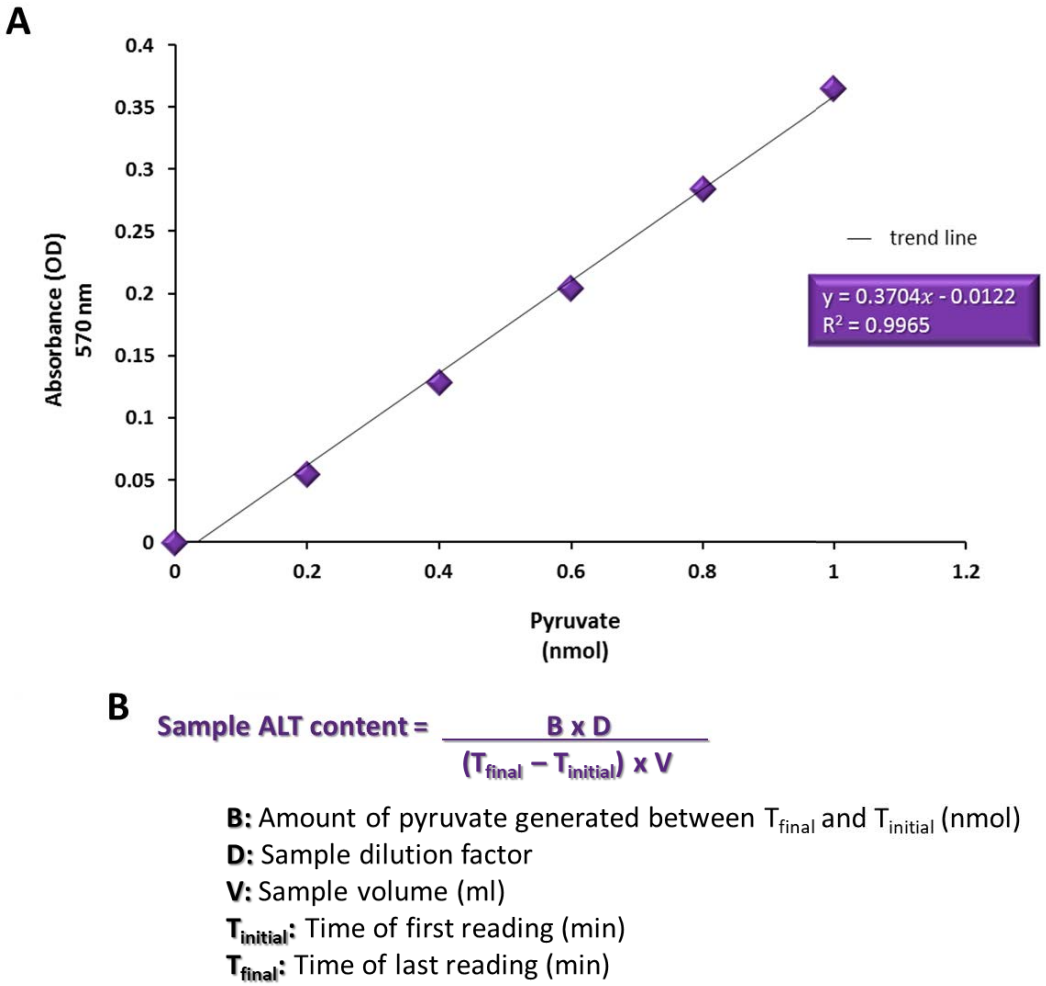

Figure 2.14. Alanine transaminase assay standard curve and calculations

Plasma samples collected from *in vivo* mice experiments were biochemically assessed for drug-induced liver toxicity by measuring ALT content. **A:** An example of the pyruvate standard curve generated using the colorimetric Sigma ALT assay kit. **B:** Equation used to calculate plasma ALT content.

ALT, alanine transaminase; OD, optical density.

2.11. Non-invasive *in vivo* imaging: echocardiography

Using echocardiography *in vivo* imaging was conducted to measure cardiac dimensions and function at baseline and following abdominal aortic constriction in male C57Bl/6 mice (see section 2.12).

2.11.1. Echocardiography set-up

Mice were first placed under general anaesthesia using an induction chamber (VetTech solutions Ltd) with 5% isoflurane/95% oxygen before being transferred to an anaesthetic nose cone, located on a platform heated to 37 °C, under 2% isoflurane/98% oxygen at a flow rate of 1 ml/min. Once under light sedation, all fur was removed from the chest and abdomen (in preparation for surgery) using a shaver (Contura trimmer; Wella) and hair removal cream (Veet) applied for ~30 sec before being gently wiped clear using a damp medical swab. Mice were immobilised onto the heated platform in the supine position, with each limb secured onto electrocardiography electrode pads to continuously monitor breathing pattern and heart rate. Warmed ultrasonic gel (37 °C; Henleys Medical) was applied onto the cardiac region of the closed-chest and transthoracic 2D echocardiographic imaging performed using Vevo 2100 (VisualSonics) and a 30-MHz linear signal transducer. Mice were continuously monitored during the 15 – 30 min procedure, ensuring a core body temperature of ~37 °C and heart rate of 400-500 bpm.

2.11.2. Long and short axis imaging

The mouse heart was visualised in the parasternal long-axis (LA) view and parasternal short-axis (SA) view **[Figure 2.15]** first in bright (B) mode and then in movie/motion (M) mode. B-mode was used to position the transducer at the correct angle of the heart at a 12.7 mm focus depth, at the level of the papillary muscle and to locate the areas of interest. The area of interest was then marked using a single scan line and the echocardiographic image transitioned into M-mode. From the M-mode, movement of the cardiac wall and chambers were visualised during end-diastole and end-systole and all measurements of cardiac

dimensions and function taken in this setting. To expand, in M-mode LA view the interventricular septal wall (IVS) thickness was measured at end-diastole and end-systole whilst in the M-mode SA view the left ventricular anterior wall (LVAW) thickness, the left ventricular posterior wall (LVPW) thickness and left ventricular internal diameter (LVID) at end-diastole and end-systole were measured.

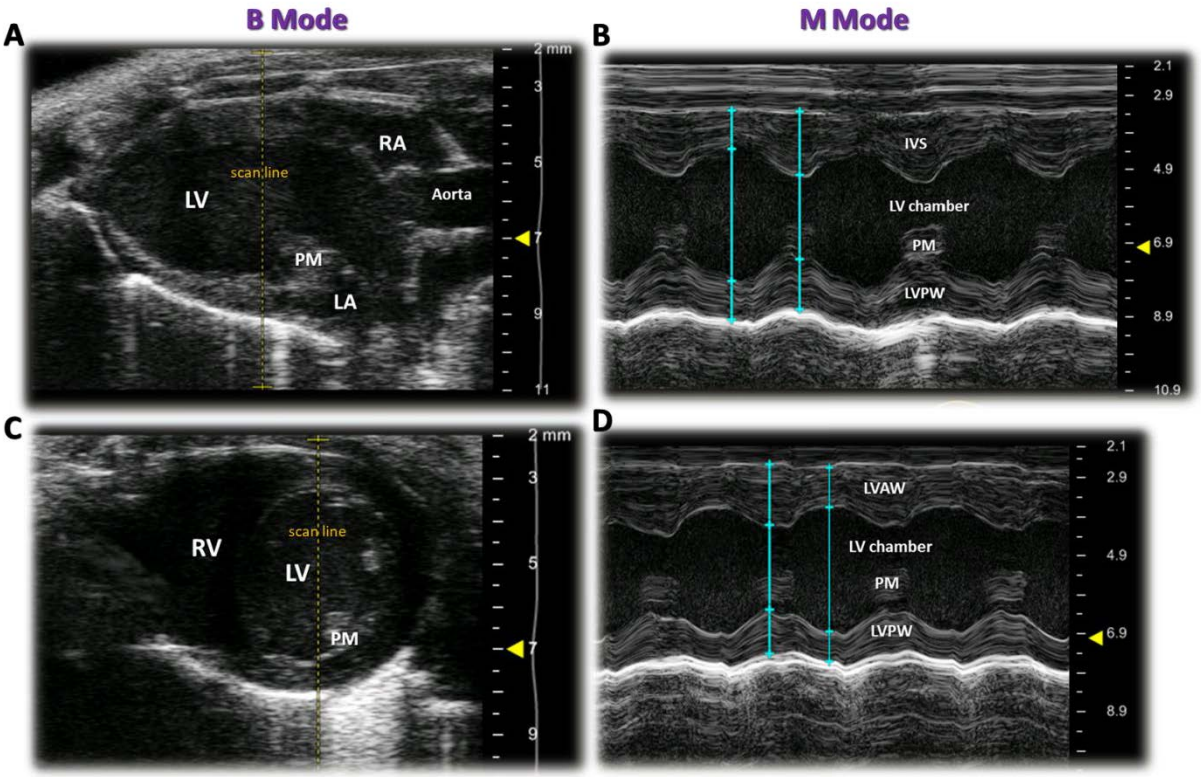

Figure 2.15. Echocardiography imaging in long and short axis view

Cardiac dimensions were measured in M-mode and then used by Vevo 2100 software to calculate cardiac function such as ejection fraction and fractional shortening. **A:** B-mode parasternal long-axis view of the left ventricle. **B:** M-mode image from parasternal long-axis view, with analysis traces in blue. **C:** B-mode short-axis view of right and left ventricle. **D:** M-mode image from short-axis view, with analysis traces in blue.

IVS, interventricular septal wall; LA, left atria; LV, left ventricle; LVAW, left ventricular anterior wall, LVPW, left ventricular posterior wall; PM, papillary muscle; RA, right atria; RV, right ventricle.

2.11.3. Doppler flow measurements

To measure aortic and mitral valve flow, colour Doppler imaging was used in the B-mode to visualise and position the sample volume over the correct location and then pulse-wave (PW) Doppler imaging in M-mode used to take readings at a 10˚ beam-to-flow angle **[Figure 2.16]**. For the aortic valve, the sample volume was taken at the root of the aortic arch whilst mitral valve images were taken at the site of mitral valve opening.

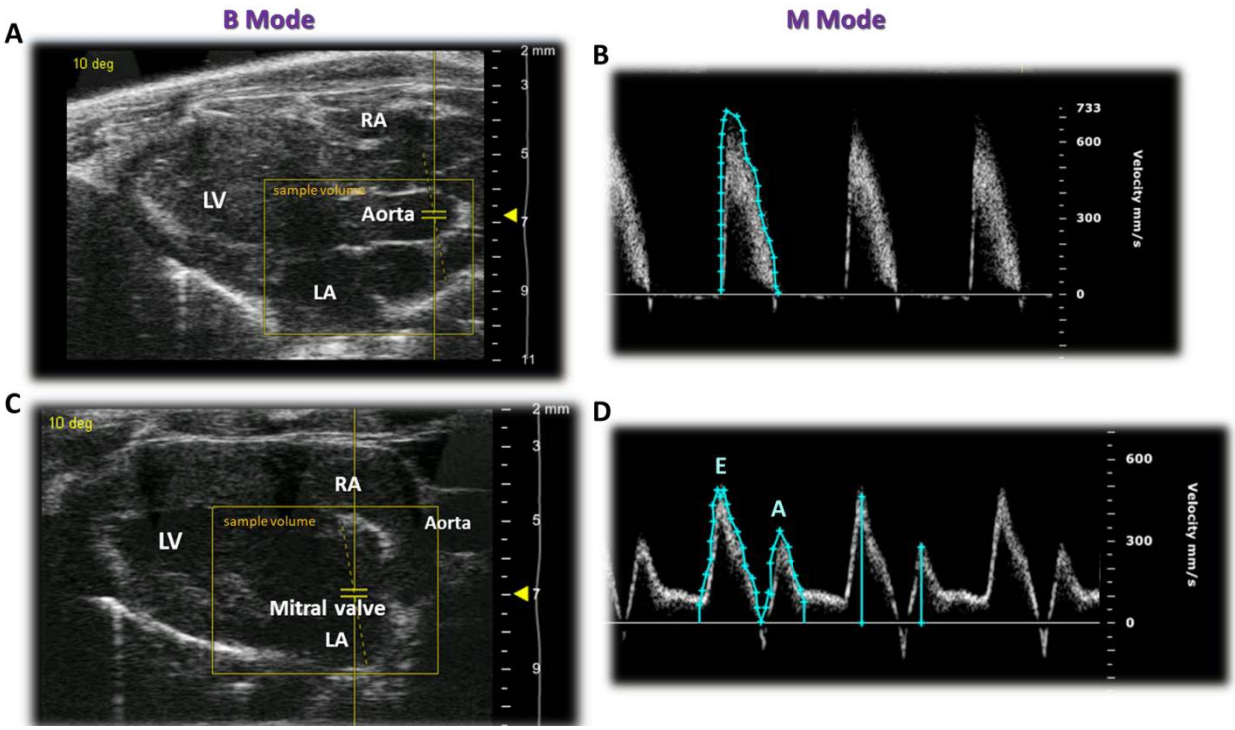

Figure 2.16. Echocardiography Doppler flow of aortic and mitral valve flow

Aortic and mitral valve flow were first imaged using colour Doppler imaging, then readings taken using pulse-wave Doppler. **A:** B-mode parasternal long-axis view of the left ventricle following colour Doppler detection of aortic valve flow. **B:** M-mode image of aortic valve flow in pulse-wave Doppler mode, with analysis traces in blue. **C:** B-mode parasternal long-axis view of the left ventricle following colour Doppler detection of mitral valve flow. **D:** M-mode image of mitral valve flow (with E and A wave) in pulse-wave Doppler mode, with analysis traces in blue.

LA, left atria; LV, left ventricle; RA, right atria.

2.11.4. Analysis of cardiac dimensions, function and flow

Analyses of all measurements taken from echocardiographic imaging were carried out using the cardiac package of the Vevo 2100 software. Mouse ID, treatment (if any) and echocardiography time points (baseline, week 1, 3 or 5) were coded independently to ensure blinding where possible during analysis. Using the software tracing tool, the cardiac dimensions in LA and SA view for both end-diastole and end-systole were determined by free-hand tracing of the left ventricle structural parameters (chamber size, wall thickness) of the M-mode images **[Figure 2.15]**. Cardiac function i.e. ejection fraction (EF) and fractional shortening (FS) and morphometric marker LV mass were calculated automatically by the Vevo software from the dimension measurements taken in the SA view (d: end-diastole, s: end-systole):

$$\%EF = ((LVIDd^3 – LVIDs^3)/LVIDd^3) \times 100$$

$$\%FS = ((LVIDd – LVIDs)/LVIDd) \times 100$$

$$LV\ mass = (IVSd + LVIDd + LVPWd)^3 – (LVIDd)^3$$

Lastly, PW Doppler flow images of aortic and mitral valve flow from both LA and SA views were analysed by free-hand tracing of individual wave pulses **[Figure 2.16]**. From these traces the Vevo software automatically calculated the velocity time integral (VTI), peak velocity and peak flow gradient. A line was also drawn across the mitral E and A wave (from peak to base), and from this an E/A ratio (marker of diastolic function) was calculated by the Vevo software.

2.12. *In vivo* model of hypertrophy and failure: abdominal aortic constriction

The well-established pressure overload model of abdominal aortic constriction (AAC) was used as previously described (Moyes et al., 2015) to induce LV hypertrophy and progression to heart failure (HF), and subsequently assess the effects of perhexiline and FPER-1 on delaying disease progression.

2.12.1. Surgical abdominal aortic constriction

Approximately 30 min prior to surgery, 6-8 week old C57Bl/6 mice were subcutaneously injected with the analgesic buprenorphine (3 ml/mg; Vetergesic). Mice were then anaesthetised with 5% isoflurane/95% oxygen at a flow rate of 1 ml/min in an induction chamber. Once under general anaesthesia, mice were transferred to a nose cone, restrained in supine position and the anaesthetic dose lowered to 3% isoflurane/97% oxygen to maintain a steady respiratory rate and breathing pattern. The respiratory rate and depth of sedation were continuously monitored throughout the surgery with the anaesthetic dose adjusted if required. As noted in section 2.11.1, the surgical site was pre-cleared of fur on the day of baseline echocardiographic measurements. Following confirmation of absent pedal reflex the operation site was cleaned using chlorhexidine gluconate (Hibitane) and AAC surgery commenced under sterile and aseptic conditions **[Figure 2.17]**. All surgical tools were sterilised in an autoclave at 121 °C prior to surgery.

First, a linear midline incision was made in the abdomen, caudal to the ribcage. A second median incision was then made through the linea alba, between the rectus abdominus muscles to expose the abdominal cavity. Using a SZX10 Olympus microscope, organs within

the retroperitoneal space (i.e. the stomach, intestines, spleen and liver) were carefully dissected and retracted, and the abdominal aorta located at a position superior to the renal arteries. Exposed organs were kept moist throughout the procedure using sterile saline warmed to 37 °C (Aqupharm). Next, a pair of fine-nosed forceps was used for blunt dissection, to clean and expose the abdominal aorta, in between the celiac artery and superior mesenteric artery, by separating it from the surrounding adventitial adipose tissue. Suprarenal aortic constriction was then performed by passing an 8-0 non-absorbable nylon suture (Ethicon) under the abdominal aorta and using this to tie the aorta against a 27-gauge blunted needle to produce a 30% ligation. The needle was subsequently removed, the 8-0 suture trimmed, all organs replaced into the abdominal cavity, the abdominal wall closed using a 6-0 absorbable vicryl suture (Ethicon) and the skin closed using 9 mm autoclips (Kent Scientific) and an Autoclip Applier (Kent Scientific). For sham-operated mice, an identical surgical procedure was conducted with the exception of AAC; instead the 8-0 suture was passed under the aorta and then pulled out. Following surgery, each mouse was given 0.5 ml glucose-saline (Aqupharm) subcutaneously, monitored regularly and provided post-operative analgesia as often as required. Any mouse that experienced excessive blood loss due to internal organ bleeding/vessel rupture during surgery was perioperatively euthanised according to ASPA guidelines.

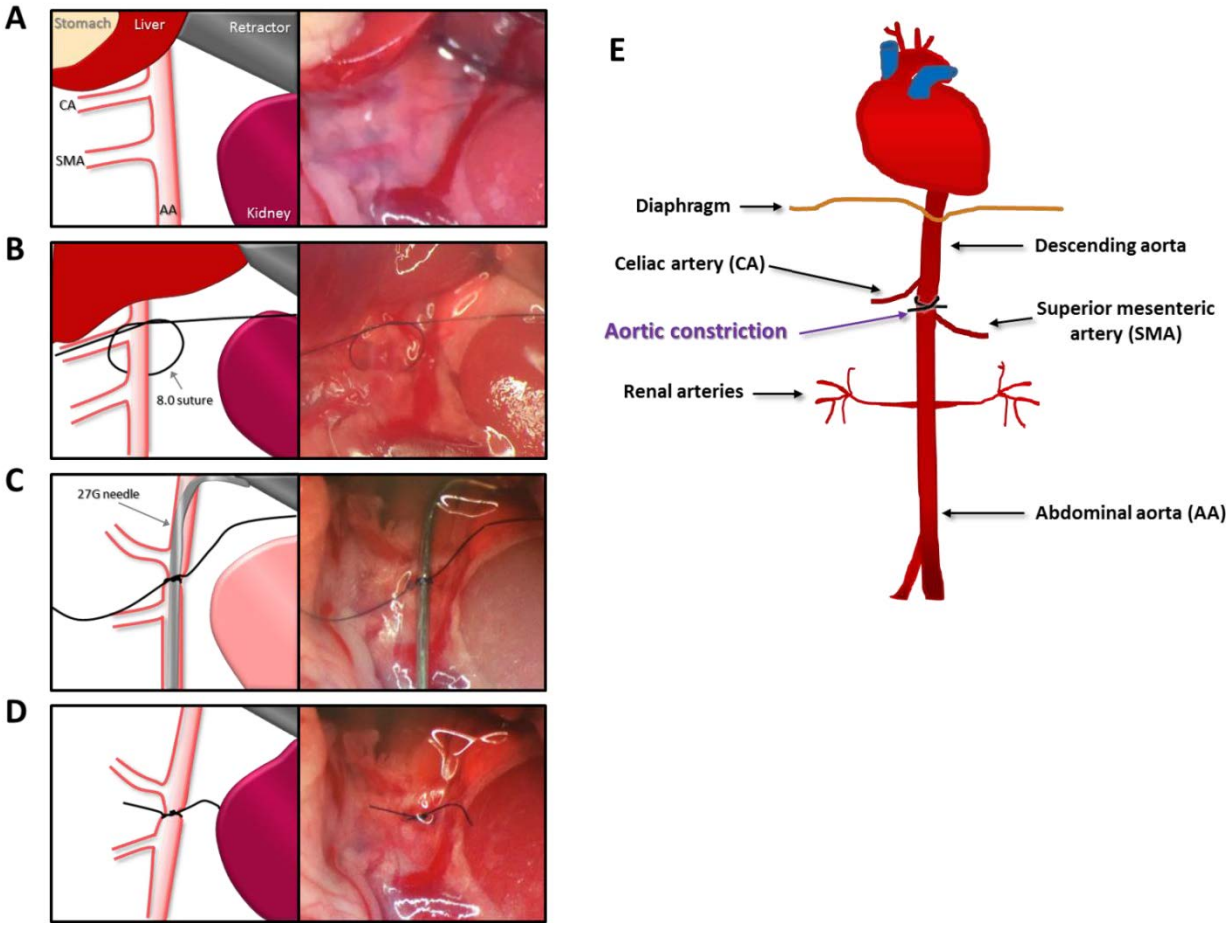

Figure 2.17. Abdominal aortic constriction surgery

Panel A to D displays the AAC procedure step by step, with a 2D schematic on the left-hand side and real-time photo on the right-hand side. **A:** Organs are retracted to expose the suprarenal abdominal aorta**. B:** After dissecting the aorta, an 8.0 suture is passed underneath and an open knot made. **C**: A 27G needle is placed on top of the aorta and the suture tied securely. **D:** The needle is carefully removed and the suture trimmed. **E:** Labelled diagram of the abdominal aorta and the site of constriction.

AA, abdominal aorta; AAC, abdominal aortic constriction; CA, celiac artery; G, Gauge; SMA, superior mesenteric artery.

2.12.2. Experimental design and timescale

One day prior to AAC surgery, echocardiography (section 2.11) was carried out to gain baseline cardiac dimensions and functional data. Following AAC, each mouse was kept for 5 weeks with follow-up echocardiography measurements taken at week 1, 3 and 5 **[Figure**

2.18]. An autoclip removing forcep (Kent Scientific) was used to remove surgical staples from each AAC mouse at week 1 under general anaesthesia (2% isoflurane/98% oxygen), prior to echocardiography.

In a preliminary set of experiments, mice were subjected to AAC and echocardiography without vehicle or drug treatment so as to establish the viability of the HF model, whereas sham-operated mice were treated with vehicle only. Following confirmation of hypertrophy and progression to HF induced by AAC, all AAC mice thereafter were randomly assigned to vehicle or drug, and treatment commenced at week 1 until the end of the study via once-daily oral gavage of either 1) vehicle (0.5% NaCMC/0.1% Tween 80), 2) 70 mg/kg perhexiline or 3) 70 mg/kg FPER-1. The vehicle and drugs were prepared every 2-3 days as described in section 2.7.1. Mice that showed signs of illness (including >15% body weight loss, reduced mobility and rapid breathing) post-surgery or during the 5 week study were euthanised according to ASPA guidelines.

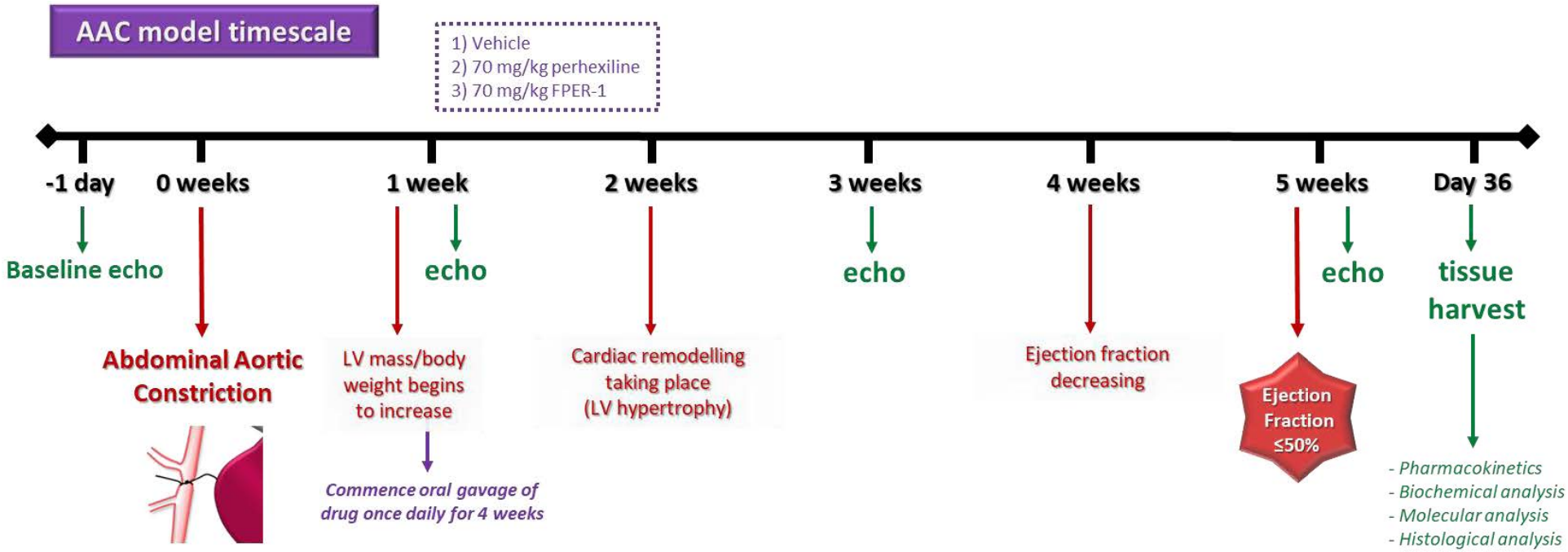

Figure 2.18. Abdominal aortic constriction experimental design and timescale

Schematic outlining the experimental timescale used for the heart failure model of AAC. Following aortic constriction, mice were kept for 5 weeks with drug treatment commencing at week 1. Echocardiography was carried out at baseline (pre-AAC), week 1, week 3 and week 5. At the end of week 5 mice were sacrificed and plasma and organs harvested for pharmacokinetics, biochemical, molecular and histological assessment.

AAC, abdominal aortic constriction; LV, left ventricular.

2.12.3. Tissue and plasma harvest

Each mouse was sacrificed as described in section 2.3.2; the heart was excised, dissected from the lungs and quickly perfused with 1 ml cold standard KHB to remove all blood. The ventricles were then isolated, blot dried, snap-frozen in liquid nitrogen and stored at -80 °C for Western blotting (see section 2.6 and 2.15). Blood was collected using a 1 ml 0.5 M EDTA-coated syringe from the thoracic cavity, centrifuged at 1000 x*g* for 10 min then plasma extracted and stored at -80 °C for drug pharmacokinetics analysis (see section 2.8), biochemical ALT analysis (see section 2.10) and brain natriuretic peptide (BNP) analysis (see section 2.13). Following blood collection, the right liver lobe was isolated, rinsed in standard KHB and fixed in 4% formaldehyde for histopathology (see section 2.9).

2.13. Biochemical analysis of cardiac failure: brain natriuretic peptide release

To further assess the extent of HF in AAC mice (section 2.12), circulating plasma levels of the clinical biochemical marker of HF, BNP, was quantified using an enzyme immunoassay (EIA) kit (Phoenix pharmaceuticals, #EK-011-23). The BNP EIA works on the basic principle of enzyme competition as outlined below:

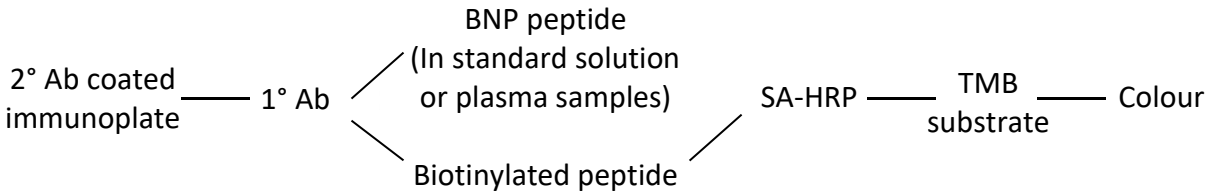

The intensity of yellow colour generated is detected at an optical density of 450 nm and is inversely proportional to the amount of BNP peptide in the tested sample.

2.13.1. Brain natriuretic peptide colorimetric assay and analysis

The BNP assay reagents and accompanying immunoplate were brought to room temperature prior to opening and then prepared/reconstituted as described in the kit protocol on the day of experiment. Briefly, peptide standards of 0.01, 0.1, 1, 10 and 100 ng/ml were prepared, and to the 96-well immunoplate 50 µl of the prepared peptide standards were added in duplicates, along with two wells left blank for the 0 ng/ml standard and an additional two wells loaded with 50 µl 1x assay buffer alone to calculate total binding. Plasma samples from each mouse were thawed on ice then loaded in duplicates at a 1/2 dilution (25 µl plasma sample:25 µl assay buffer). Twenty-five microlitres of rehydrated primary antibody and 25 µl of biotinylated peptide were then added to each well except the two blanks and the plate sealed with acetate plate sealer (APS) and placed on an orbital shaker at 350 rpm for 2 h at room temperature. Next, the contents of the wells were discarded and the plate washed 4x with assay buffer and 12 µl of Streptavidin-horseradish peroxidase (SA-HRP) added into each well. The plate was then resealed with APS and incubated for 1 h at room temperature, shaking at 350 rpm. The contents of the plate was discarded and washed 4x again followed by the addition of 100 µl tetramethylbenzidine (TMB) substrate solution to each well, resealed with APS, covered in aluminium foil and incubated for 1 h at room temperature, shaking at 350 rpm. The reaction was terminated by addition of 100 µl 2N hydrochloric acid and the immunoplate immediately read at 450 nm using a colorimetric plate reader (KC4; Biotek). A sigmoidal standard curve was then generated on a semi-log scale **[Figure 2.19]** and the equation of the curve determined. The concentration of BNP peptide in the sample was then extrapolated from the curve using this equation and multiplied by the dilution factor used.

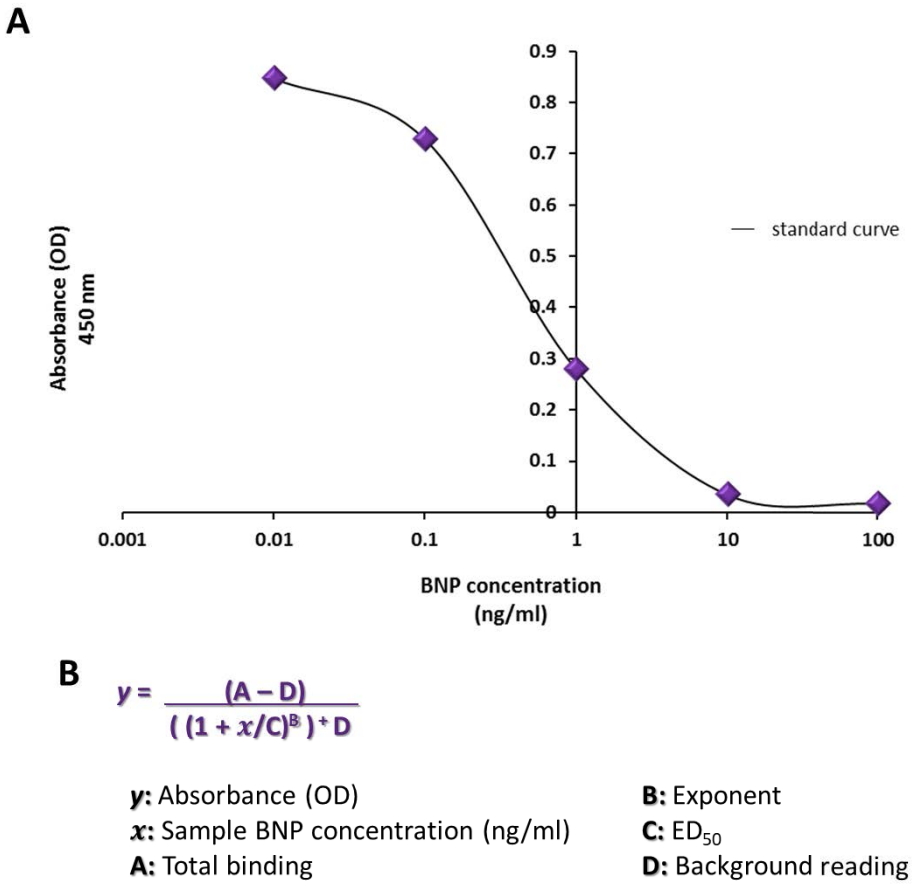

Figure 2.19. Brain natriuretic peptide assay standard curve and calculations

Plasma samples collected from *in vivo* sham-operated and abdominal aortic constricted vehicle-treated mice were biochemically assessed for BNP levels, a marker of heart failure. **A:** An example of the BNP sigmoidal standard curve generated using the colorimetric Phoenix pharmaceuticals BNP assay kit. **B:** Equation used to calculate plasma BNP concentration.

BNP, brain natriuretic peptide; OD, optical density.

2.14. Western blot analysis of *in vivo* drug mechanisms

To determine the molecular mechanism(s) of perhexiline and FPER-1 in the *in vivo* AAC model, the expression and/or phosphorylation of proteins involved in cardiac function, cardiac metabolism and cell survival were assessed by Western blotting in harvested mouse ventricles (section 2.12.3). All antibodies (primary and secondary) used are shown in **Table 2.3**. Ventricle lysate preparation, protein assay and Western blotting were conducted as outlined in section 2.6, with frozen ventricles homogenised in 300 µl homogenisation buffer.

Chapter 3:
Investigating the effects of perhexiline and FPER-1 in the *ex vivo* Langendorff model

Chapter 3: Investigating the effects of perhexiline and FPER-1 in the *ex vivo* Langendorff model

3.1. Introduction

Perhexiline is an anti-ischaemic agent (Ashraf ian et al., 2007b), originally used clinically for treating angina due its ability to successfully reduce incidence of angina, severity of attack and improve cardiac function (Horowitz et al., 1896; Cole et al., 1990). Following the discovery that perhexiline inhibited carnitine palmitoyltransferase 1B (CPT1B), and thus was a metabolic modulator (Kennedy et al., 1996), this mechanism was implicated in perhexiline's anti-ischaemic effects.

Based on this metabolic-modulating property, perhexiline was expected to be therapeutic in cardiovascular disorders characterised by low oxygen or ischaemia and metabolic disturbances such as aortic stenosis (Unger et al., 1997), cardiomyopathy (Abozguia et al., 2010; Beadle et al., 2015) and heart failure (HF) (Lee et al., 2005; Phan et al., 2009b). As discussed in Chapter 1 (section 1.7) HF involves detrimental changes in cardiac metabolism, including a shift away from glucose metabolism towards the less efficient fatty acid (FA) metabolism, uncoupling of glycolysis from glucose oxidation (Sorokina et al., 2007; Dai et al., 2012) and oxidative stress (Tsutsui et al., 2011). In combination, these metabolic changes lead to impaired adenosine triphosphate (ATP) production and decreased cardiac efficiency and function (Loudon et al., 2016). Furthermore, FA overload within the cardiomyocyte cytosol and mitochondria is a common feature of cardiovascular diseases associated with low oxygen levels and/or ischaemia because such conditions lead to downregulation of the

β-oxidation pathway enzymes involved in FA metabolism (Sack et al., 1996; Pellieux et al., 2006). When investigated in such settings, perhexiline improved symptoms, exercise capacity and/or cardiac function, and increased cardiac energetics in patients with hypertrophic cardiomyopathy (HCM) (Abozguia et al., 2010) or HF (Lee et al., 2005).

Unfortunately perhexiline's beneficial effects have been overshadowed by its associated neuro- and hepatotoxicity, which ultimately led to its withdrawal from use in the 1980s (Shah et al., 1982). Perhexiline-induced toxicity resulted from high plasma levels in patients who were poor metabolisers of the drug; this caused excessive, sustained CPT1 inhibition and thus systemic phospholipidosis (discussed in Chapter 1, section 1.10.2) (Morgan et al., 1984; Barclay et al., 2003). Following these findings, it was established that perhexiline plasma levels should be maintained between 0.5 – 2.2 μM to avoid toxicity (Horowitz et al., 1986).

Nonetheless, constant monitoring of perhexiline plasma levels in patients remains clinically unattractive. As such, Signal Pharma have designed, developed and synthesised a novel perhexiline analogue, fluoroperhexiline-1 (FPER-1), which does not have the unfavourable metabolic liability of perhexiline (Tseng et al., 2017). However, FPER-1 has yet to be tested for therapeutic efficacy and it remains to be elucidated whether FPER-1 can retain/replicate perhexiline's therapeutic effects. Furthermore the effective dose of FPER-1 needs to be determined. The Langendorff model has been used previously to investigate the cardioprotective potential of perhexiline; 2 μM perhexiline was identified as the effective dose (Kennedy et al., 1999; Kennedy et al., 2000; Unger et al., 2005). Therefore, the main

objective of the work in this chapter was to evaluate FPER-1 and compare it to the parent drug perhexiline, using the well-established *ex vivo* isolated murine heart model.

Aims:

1. To determine whether perhexiline and FPER-1 can improve cardiac haemodynamics in hearts perfused with a high-fat buffer pre- and post-ischaemia.
2. To determine whether FPER-1 can replicate the observed protective effects of perhexiline and, if so, establish to what extent.

3.2. Methodology

An expanded methodology is presented in Chapter 2, sections 2.3 and 2.4, with Langendorff protocols A, B and C outlined in **Figure 2.3**.

In brief, male C57Bl/6 mice (25 – 30 g) were placed under terminal anaesthesia, hearts rapidly isolated, mounted onto the Langendorff system, and retrogradely perfused with either standard Krebs-Henseleit buffer (KHB) (Tanno et al., 2003) or a high-fat KHB consisting of bovine serum albumin (BSA) pre-conjugated to 1.2 mM palmitate (Belke et al., 1999), depending on the protocol. In protocol A and C, the following haemodynamics: left ventricular developed pressure (LVDP), left ventricular end-diastolic pressure (LVEDP), the maximum rate of left ventricular pressure (LVP) increase and reduction over time (LVdP/dt max and min; calculated from LVP) and coronary flow rate (CFR), were measured during stabilisation and/or reperfusion by inserting a water-filled balloon into the left ventricle.

Protocol A: To determine the effects of a high-fat buffer on cardiac function hearts were perfused with either standard or high-fat KHB for 40 min stabilisation.

Protocol B: To assess the effects of a high-fat buffer on infarct size a separate batch of hearts were stabilised for 40 min with either standard or high-fat KHB, followed by 30 min global ischaemia, 120 min reperfusion and 1% triphenyltetrazolium chloride (TTC) staining (section 2.4).

Protocol C: To investigate whether perhexiline or FPER-1 improved function post-ischaemia, hearts were stabilised for 10 min in control high-fat KHB, followed by 30 min perfusion with either 1) control (high-fat KHB), 2) 2 µM perhexiline, 3) 2 µM FPER-1 or 4) 10 µM FPER-1. Hearts were then subjected to 30 min global ischaemia and 60 min reperfusion.

3.2.1. Statistical analysis

All data in this chapter are expressed as means ±standard error of the mean (SEM). Two-way analysis of variance (ANOVA) with Bonferroni post-hoc test was used to compare the effects of standard KHB on normoxic cardiac function over time (LVDP, LVEDP, LVdP/dt and CFR) and to the effect of high-fat KHB on the same parameters over time. An unpaired t-test was used to compare the effect of standard KHB and high-fat KHB on infarct size. Two-way ANOVA with Bonferroni post-hoc test was also used to compare the effects of drug treatment (2 µM perhexiline, 2 or 10 µM FPER-1) versus the control (high-fat KHB) on pre-ischaemic cardiac function over time and a one-way ANOVA with Bonferroni post-hoc test used to compare the effect of each treatment versus control on function post-ischaemia. Graphpad Prism version 6.0 was used to carry out all analysis. $p<0.05$ was considered statistically significant. Number of mice used is indicated in the figure legends.

3.3. Results

3.3.1. Effects of high-fat KHB on cardiac function during stabilisation, compared to standard KHB

Using standard KHB to perfuse the hearts, LVDP significantly decreased over time (1.4-fold at 40 min; *p<0.0001*) whilst there was no significant effect on LVEDP (*p>0.99*) **[Figure 3.1A+B]**. CFR also significantly decreased relative to the initial reading in standard KHB-perfused hearts during stabilisation (1.4-fold at 40 min; *p<0.0001*) **[Figure 3.1C]**. Perfusion with high-fat KHB did not significantly alter any parameter tested in comparison to standard KHB perfusion (*p=0.21, 0.78* and *0.45* respectively) **[Figure 3.1]**.

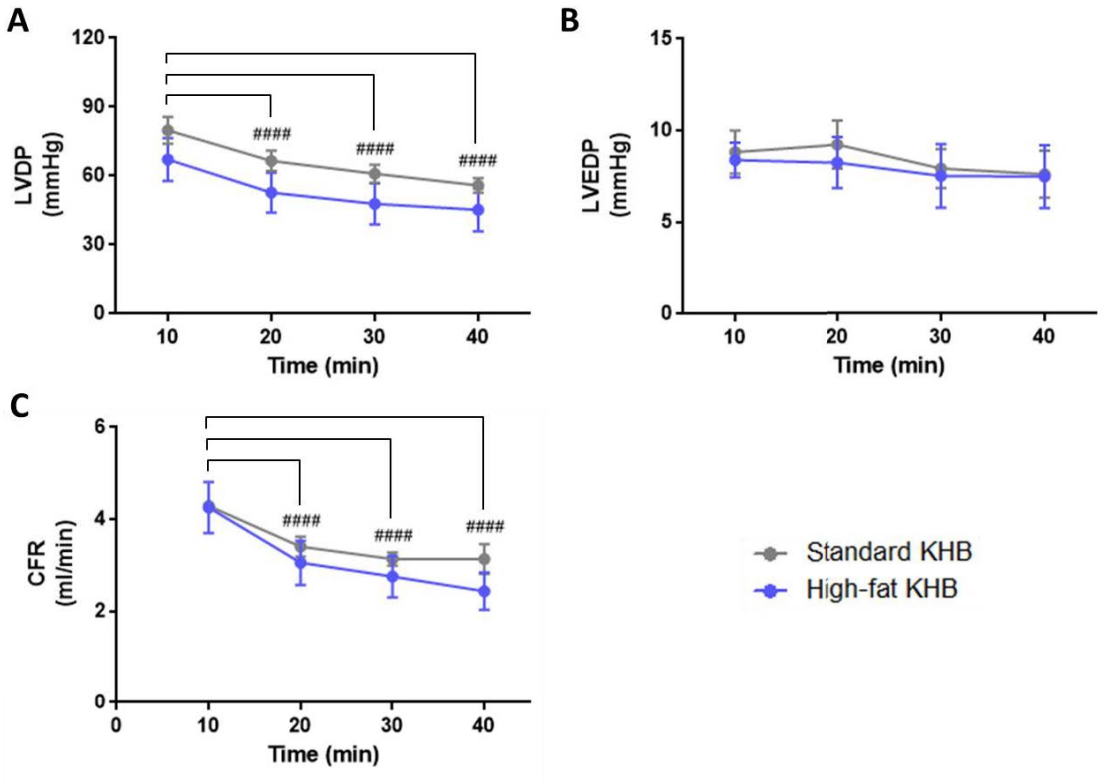

Figure 3.1. Effects of high-fat KHB on cardiac function during stabilisation, compared to standard KHB

A: Left ventricular developed pressure (LVDP), **B:** Left ventricular end-diastolic pressure (LVEDP) & **C:** Coronary flow rate (CFR) from mouse hearts perfused for 40 min with either standard KHB or high-fat KHB. Data are presented as mean ±SEM; n = 5-6 mice. ####*p<0.0001* Standard KHB vs Baseline (Two-way ANOVA followed by Bonferroni post-hoc test).

3.3.2. Effects of high-fat KHB on infarct size following ischaemia/reperfusion compared to standard KHB

Hearts perfused with high-fat KHB demonstrated a significantly lower infarct size following ischaemia/reperfusion compared to those perfused with standard KHB (49.8 ±1.3% versus 13.6 ±3.6%; *p<0.001*) **[Figure 3.2]**.

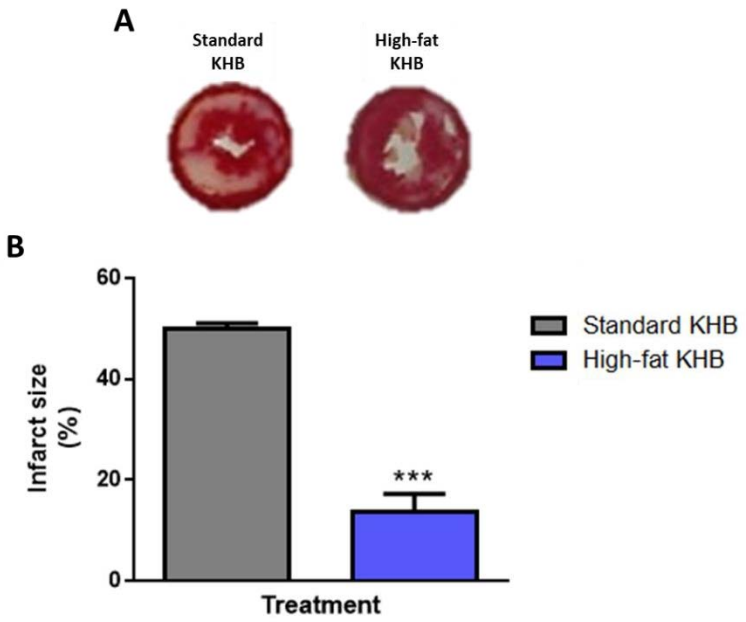

Figure 3.2. Effects of high-fat KHB on infarct size following ischaemia/reperfusion, compared to standard KHB

A: Representative heart slices & **B:** Percentage infarct size from mouse hearts perfused for 40 min with either standard KHB or high-fat KHB, which had been subjected to ischaemia/reperfusion. Data are presented as mean ±SEM; n = 4-5 mice. ****p<0.001* vs Standard KHB (Unpaired t-test).

3.3.3. Effects of perhexiline and FPER-1 on cardiac function pre-ischaemia

Pre-ischaemia, perfusion with high-fat KHB alone (control solution) led to a significant decrease in LVDP (1.2-fold at 40 min; *p<0.05*), LVEDP (1.7-fold at 40 min; *p<0.0001*) and CFR (1.5-fold at 40 min; *p<0.0001*) over time when compared to the initial reading. By contrast, neither LVDP nor CFR changed when 2 µM perhexiline or FPER-1 (2 or 10 µM) were used during the 40 min stabilisation relative to control (*p=0.97*) **[Figure 3.3A+C]**. However, LVEDP

significantly increased following perfusion with 10 µM FPER-1 (1.1-fold increase at 40 min; *p<0.0001*) compared to control (1.6-fold decrease at 40 min), whereas no change was observed with 2 µM perhexiline or 2 µM FPER-1 (*p>0.99* for both) **[Figure 3.3B]**.

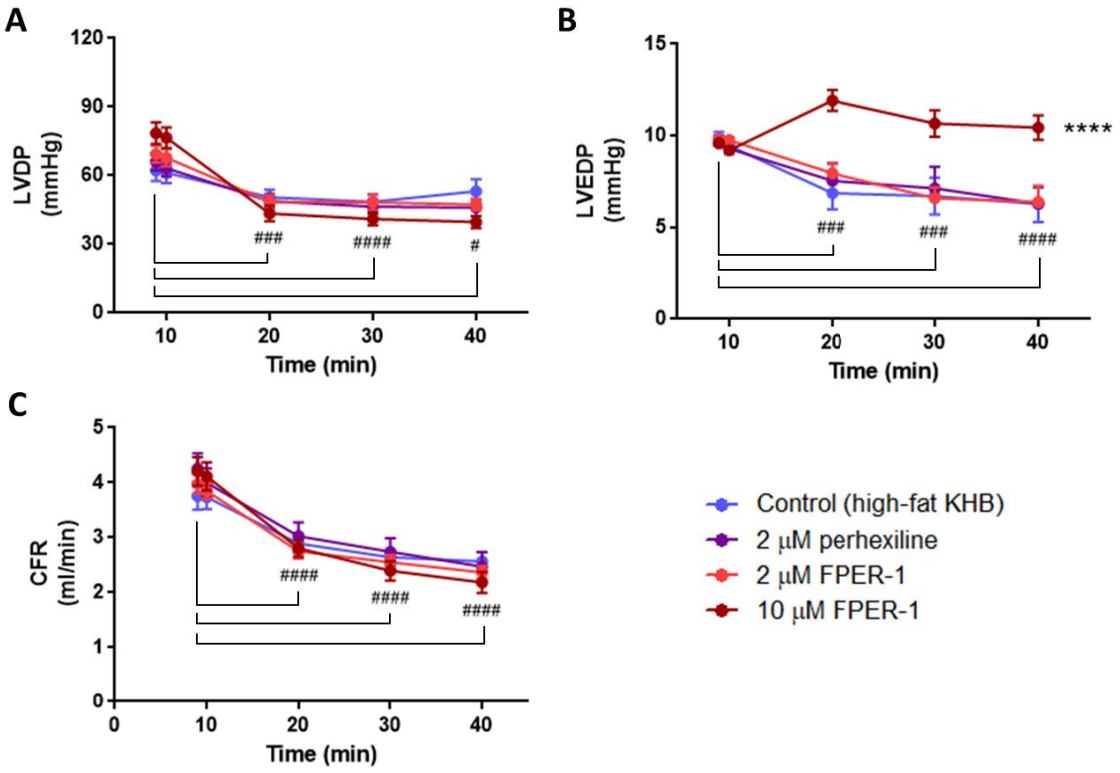

Figure 3.3. Effects of perhexiline and FPER-1 on cardiac function pre-ischaemia

A: Left ventricular developed pressure (LVDP), **B:** Left ventricular end-diastolic pressure (LVEDP) & **C:** Coronary flow rate (CFR) from mouse hearts perfused for 30 min with either control (high-fat KHB), 2 µM perhexiline, 2 µM FPER-1 or 10 µM FPER-1. Data are presented as mean ±SEM; n = 12-19 mice. #*p<0.05* Control (high-fat KHB) vs Baseline; ###*p<0.001* Control (high-fat KHB) vs Baseline; ####*p<0.0001* Control (high-fat KHB) vs Baseline; ****p<0.0001* vs Control (high-fat KHB) (Two-way ANOVA followed by Bonferroni post-hoc test).

3.3.4. Effects of perhexiline and FPER-1 on contractility and relaxation pre-ischaemia

In control (high-fat KHB) perfused hearts, LVdP/dt max (marker of cardiac contractility) was significantly increased at 40 min stabilisation (1.6-fold; *p<0.05*) **[Figure 3.4A]**. Perfusion with either 2 µM perhexiline or 10 µM FPER-1 further increased LVdP/dt max relative to the control (3.1-fold; *p<0.001* and 2.3-fold; *p<0.01* respectively); any effect achieved with 2 µM

FPER-1 perfusion was not significant (2.2-fold increase; *p=0.15*). In control (high-fat KHB) perfused hearts, LVdP/dt min (marker of cardiac relaxation) did not change during stabilisation **[Figure 3.4B]**. In contrast, during 2 µM perhexiline or 10 µM FPER-1 perfusion LVdP/dt min significantly increased relative to the control (5.3-fold; *p<0.0001* and 3.8-fold; *p<0.001*), whilst a trend of an increase was present with 2 µM FPER-1 perfusion (2.9-fold; *p=0.09*).

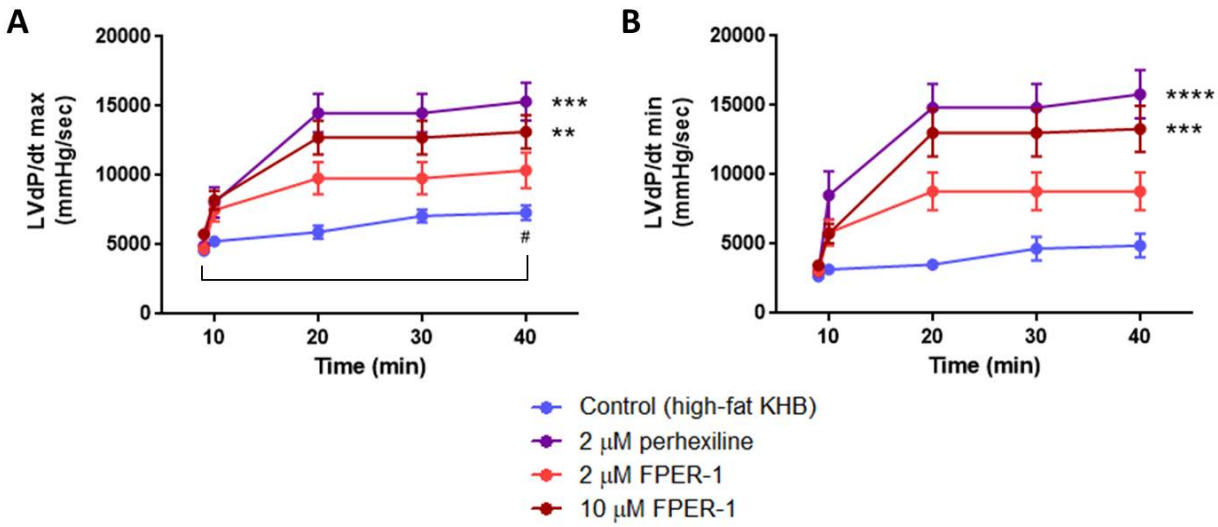

Figure 3.4. Effects of perhexiline and FPER-1 on cardiac contractility and relaxation pre-ischaemia

A: Maximum rate of left ventricular pressure increase (LVdP/dt max) & **B:** Maximum rate of left ventricular pressure reduction (LVdP/dt min) from mouse hearts perfused for 30 min with either control (high-fat KHB), 2 µM perhexiline, 2 µM FPER-1 or 10 µM FPER-1. Data are presented as mean ±SEM; n = 12-19 mice. #*p<0.05* Control (high-fat KHB) vs Baseline; ***p<0.01,* ****p<0.001* (high-fat KHB); *****p<0.0001* vs Control (high-fat KHB) (Two-way ANOVA followed by Bonferroni post-hoc test).

3.3.5. Effects of perhexiline and FPER-1 on cardiac function post-ischaemia

Following ischaemia, both 2 and 10 µM FPER-1 significantly improved LVDP (mean of 29 ±1.3 mmHg and 29 ±2.1 mmHg post-ischaemia respectively; *p<0.01* for both) relative to the control (mean of 21.6 ±0.7 mmHg post-ischaemia) but it was unchanged by 2 µM perhexiline

perfusion (*p>0.99*) **[Figure 3.5A]**. In contrast, LVEDP was improved with 2 µM perhexiline perfusion (mean of 33.5 ±3.1 mmHg post-ischaemia; *p<0.001*) relative to the control (mean of 55.4 ±3.8 mmHg post-ischaemia) and a similar improvement was also achieved with 2 µM FPER-1 (mean of 40.8 ±3.4 mmHg post-ischaemia; *p<0.05*) and 10 µM FPER-1 (mean of 24.9 ±2.3 mmHg post-ischaemia; *p<0.001*) perfusion **[Figure 3.5B]**. Furthermore, CFR was improved by perfusion with 2 µM perhexiline (mean of 1.7 ±0.1 ml/min post-ischaemia; *p<0.001*), 2 µM FPER-1 (mean of 1.8 ±0.1 ml/min post-ischaemia; *p<0.01*) and 10 µM FPER-1 (mean of 1.7 ±0.1 ml/min post-ischaemia; *p<0.001*) relative to the control (mean of 1.2 ±0.1 ml/min post-ischaemia) **[Figure 3.5C]**.

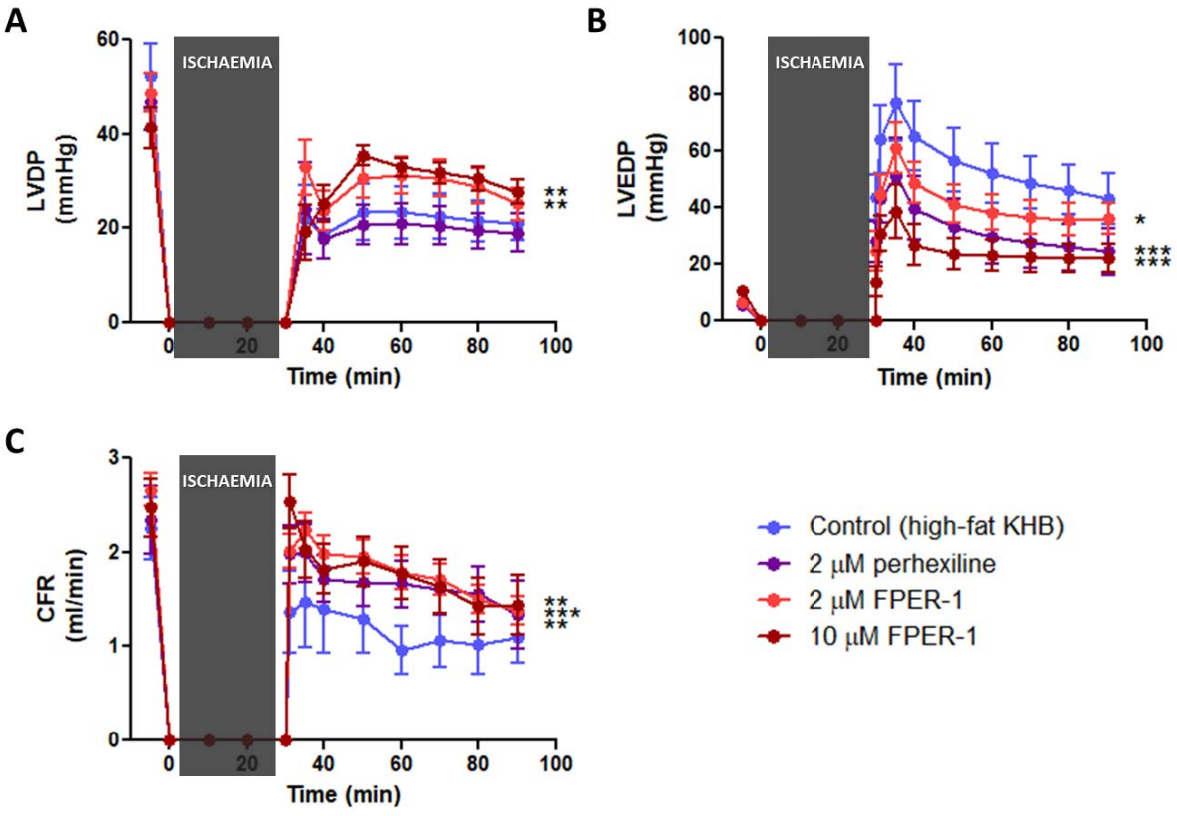

Figure 3.5. Effects of perhexiline and FPER-1 on cardiac function post-ischaemia

A: Left ventricular developed pressure (LVDP), **B:** Left ventricular end-diastolic pressure (LVEDP) & **C:** Coronary flow rate (CFR) from mouse hearts perfused for 30 min pre-ischaemia with either control (high-fat KHB), 2 µM perhexiline, 2 µM FPER-1 or 10 µM FPER-1, which had been subjected to ischaemia/reperfusion (all hearts reperfused in control high-fat KHB). Data are presented as mean ±SEM; n = 9-10 mice. **p<0.05* vs Control (high-fat KHB); ***p<0.01* vs Control (high-fat KHB); ****p<0.001* vs Control (high-fat KHB) (One-way ANOVA followed by Bonferroni post-hoc test).

3.3.6. Effects of perhexiline and FPER-1 on hypercontracture post-ischaemia

Post-ischaemia, hypercontracture magnitude (Chapter 2, section 2.3.5) was significantly reduced by both 2 µM perhexiline (31% decrease) and 10 µM FPER-1 (33.9% decrease) relative to the control (*p<0.05* for both groups) but unchanged by 2 µM FPER-1 (*p=0.83*) **[Figure 3.6A]**. In contrast, the time to hypercontracture was not altered by drug treatment relative to the control (*p=0.77*) **[Figure 3.6C]**.

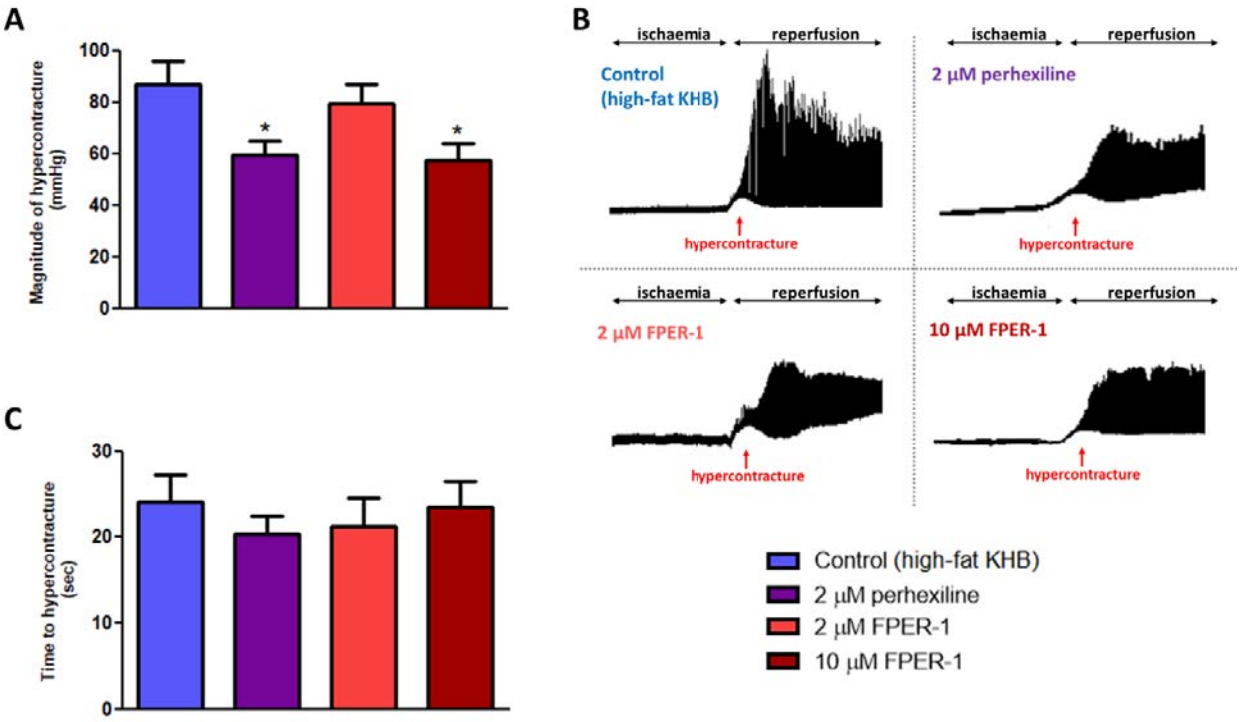

Figure 3.6. Effects of perhexiline and FPER-1 on hypercontracture post-ischaemia

A: Magnitude of hypercontracture at reperfusion, **B:** Representative hypercontracture traces & **C:** Time to hypercontracture from mouse hearts perfused for 30 min pre-ischaemia with either control (high-fat KHB), 2 µM perhexiline, 2 µM FPER-1 or 10 µM FPER-1, which had been subjected to ischaemia/reperfusion (all hearts reperfused in control high-fat KHB). Data are presented as mean ±SEM; n = 9-10 mice. *$p<0.05$ vs Control (high-fat KHB) (One-way ANOVA followed by Bonferroni post-hoc test).

3.4. Discussion

Disturbances in FA metabolism, and FA overload within the cardiomyocytes are well-characterised features of many cardiovascular diseases and related to the metabolic

alterations that occur during ischaemia (Fillmore et al., 2014). In the present study, the primary aim was to evaluate whether the metabolic agents perhexiline and FPER-1 could improve cardiac function/haemodynamics during high-fat perfusion and following an ischaemic stress in the *ex vivo* Langendorff model. However, it was first essential to identify the effect of a high-fat buffer on cardiac function under normoxic conditions, and whether the high fat would alter normal function even in the absence of an ischaemic insult. As such, isolated murine hearts were perfused with a modified KHB that contained 1.2 mM palmitate (Kennedy et al., 2000) and compared to a standard KHB (Tanno et al., 2003). In the present study, the change in function (i.e. slight decrease in LVDP and CFR) observed during stabilisation following standard KHB perfusion corresponded to the standard KHB results from other studies (Gao et al., 2013; Baumgardt et al., 2016).

The concentration of 1.2 mM palmitate has been reported in plasma from patients following ischaemic events i.e. post-myocardial infarction (Allison et al., 1969; Mueller and Ayres, 1978). Furthermore, Kuzmicic and colleagues (2014) reported that high palmitate promoted mitochondrial fission in cultured rat cardiomyocytes and decreased oxygen consumption rate. However, the present results demonstrated that perfusion with a high-fat buffer (1.2 mM palmitate) did not reduce cardiac function (LVDP or LVEDP) relative to perfusion with a standard buffer, during normoxia. These results resemble those of Gmeiner et al. (1975) who observed no change in cardiac function in isolated rat hearts exposed to 0.4 mM palmitate. Furthermore, in the present study, CFR was similar between hearts perfused with either standard KHB or high-fat KHB. Nonetheless, it is possible that although function remained relatively unchanged following high-fat perfusion, cardiac mechanical efficiency was

reduced. High fat levels can dramatically decrease mechanical efficiency, as demonstrated *in vivo* in pigs, in which intralipid and heparin (fat activator) infusion increased myocardial oxygen consumption by 48% compared to glucose infusion for the same level of cardiac work done (Korvald et al., 2000). However, under normoxic conditions, sufficient oxygen levels exist to maintain cardiac function despite the increased oxygen consumption. Therefore ischaemic conditions/an ischaemic event, in which oxygen levels become insufficient and limited, may be required for a decrease in mechanical efficiency to transpire into reduced function.

Aasum and colleagues (2003) demonstrated, in a working mouse heart model, that high-fat KHB (1.2 mM palmitate) perfusion was associated with decreased cardiac efficiency and function during reperfusion, post-ischaemia. Thus, the assessment was made in the present study of whether perfusion with a high-fat buffer would increase cell death (assessed by infarction size) following ischaemia/reperfusion, relative to perfusion with a standard KHB. Interestingly, the high-fat KHB significantly *reduced* infarct size following ischaemia/reperfusion relative to standard KHB. Previous studies showed that 0.5 mM palmitate induced apoptosis in neonatal rat cardiomyocytes (Sparagna et al., 2000), adult rat cardiomyocytes (Spillman et al., 2015) and in H9c2 cells (Wei et al., 2013). However, the present results cannot be directly compared with these *in vitro* studies given that the perfusate used in the present study contained another metabolic substrate: 11 mM glucose. In closer similarity with the present study, Löster and Punzel (1998) demonstrated that, following 20 min no-flow ischaemia, rat hearts that were perfused with both glucose and high fat (1.2 mM palmitate) had improved LV function at reperfusion relative to hearts

perfused with glucose and low fat (0.4 mM palmitate). Therefore, it is reasonable to argue that the presence of two metabolic substrates (glucose and high fat) provided the isolated heart with a greater energy source prior to ischaemia, thereby protecting against cell death during reperfusion, and explaining why infarct size was reduced.

Having assessed the effects of high-fat KHB on cardiac function during normoxia and infarct size following ischaemia/reperfusion, the protective potential of perhexiline and its novel derivative FPER-1 were investigated. Both drugs were prepared in DMSO (final concentration of 0.2% in KHB) and the same percentage of DMSO was added to the control (high-fat KHB) solution to ensure that any observed effects were solely due to drug perfusion and not DMSO. This precaution was important as DMSO was reported to have cardioprotective properties by reducing post-ischaemic LV dysfunction in rat hearts subjected to global ischaemia/reperfusion (Dmitriev et al., 2012). In that study DMSO was administered intraperitoneally to rats for 3 days prior to Langendorff experimentation. DMSO pre-treatment in cardiomyocytes subjected to hydrogen peroxide-induced injury was also demonstrated to be cytoprotective by reducing oxidative damage and apoptotic rate (Man et al., 2014).

With these measures in place, the drug concentration used in the present study was based on work by Kennedy and colleagues (2000), who investigated the anti-ischaemic properties of perhexiline in a low-flow rat heart Langendorff model. They evaluated 0.5 and 2 µM perhexiline, doses which fall at either end of the established therapeutic range in patients (0.5 – 2.2 µM) (Horowitz et al., 1986). Their results revealed that perfusion with 2 µM

perhexiline was effective at improving LV function during ischaemia, but 0.5 μM perhexiline had no effect. Therefore, in the present study 2 μM perhexiline was used for assessing cardiac function/haemodynamics in the murine Langendorff model. To investigate the effects of FPER-1, and whether it would replicate perhexiline's beneficial effects, FPER-1 was initially used at 2 μM. Signal Pharma found that FPER-1 is 25% less potent than perhexiline in inhibiting CPT1B activity, as the IC_{50} for FPER-1 was 4-fold higher than the IC_{50} for perhexiline (Tseng et al., 2017). However, when mice were orally treated with 10 mg/kg perhexiline or FPER-1, FPER-1 accumulated approximately 5½ times greater in the myocardium when compared to perhexiline at 1 h post-treatment (3726.8 ng/ml with FPER-1 versus 664.5 ng/ml with perhexiline). Therefore the effects of 10 μM FPER-1, a dose 5-fold greater than the effective dose of 2 μM perhexiline, were also tested.

The results during stabilisation revealed that 2 μM perhexiline did not alter cardiac haemodynamics (LVDP, LVEDP or CFR) in hearts perfused with a high-fat KHB. These results were not surprising as the 40 min stabilisation period was under normoxic conditions and previous work by Unger and colleagues (2005) revealed that short-term perfusion with 2 μM perhexiline had no effect on cardiac efficiency in the non-ischaemic working rat heart. The 2 μM FPER-1 dose also had no effect on cardiac function during normoxia whilst the higher 10 μM dose had no effect on LVDP or CFR, suggesting that perhexiline and FPER-1 are very similar in normoxia. However, in hearts perfused with 10 μM FPER-1, LVEDP initially increased and then was maintained around ~10 mmHg during stabilisation. These findings suggest that, at a higher dose, FPER-1 has the unfavourable effect of increasing LVEDP pre-ischaemia, an effect which was not observed with control and was not induced by the

therapeutic dose of perhexiline or the lower dose of FPER-1. It is important to note that, as discussed above, the present data showed that perfusion with high-fat buffer did not impair cardiac function or coronary flow pre-ischaemia. Therefore, rather than the pre-ischaemic data suggesting a lack of protection, these results showed that perhexiline and FPER-1 did not enhance normal cardiac function.

During stabilisation markers of cardiac contractility (LVdP/dt max) and relaxation (LVdP/dt min) were also assessed. Previous studies have shown that palmitate impairs excitation-contraction coupling in cultured mouse ventricular myocytes (Haim et al., 2009) and impairs contractility in cultured rat cardiomyocytes (Spillman et al., 2015). The present results demonstrated that 2 µM perhexiline was effective in enhancing contractility and, although not replicated by the corresponding dose of FPER-1, these effects were achieved with 10 µM FPER-1. More importantly, both 2 µM perhexiline and 10 µM FPER-1 were extremely effective in enhancing cardiac relaxation during stabilisation. This suggests that these metabolic agents have a greater influence on the diastolic function of the heart and have significant lusitropic effects. However, for both contractility and relaxation there were clear dose-dependent effects between 2 and 10 µM FPER-1 showing that a higher dose of FPER-1 is essential to replicate perhexiline's beneficial effects. These findings corroborate other studies that showed perhexiline can enhance muscle contractility in the rabbit psoas muscle (Morano et al., 1989) and contractile function of dog hearts in an open-chest model (Ono et al., 1982).

Interestingly, the detrimental effects of 1.2 mM palmitate perfusion in a working rat heart Langendorff model were associated with distorted Ca^{2+} handling which coincided with the detrimental effects of palmitate on contractile function (Steigen et al., 1994). Moreover, Morano et al. (1989) demonstrated that perhexiline enhanced contractility by sensitising the muscle fibres for Ca^{2+} binding thus increasing the Ca^{2+} responsiveness of the contractile apparatus. These results may explain the ability of perhexiline and its derivative to enhance the Ca^{2+}-regulated functions of cardiac contractility and relaxation in the present study.

In contrast to the present findings, several studies have suggested perhexiline to be a negative inotropic agent. A study in cultured chick embryo ventricular cells demonstrated that 0.83 µM perhexiline was required for 50% inhibition of contractile amplitude (Barry et al., 1985). Another study showed that 10 µM perhexiline had both negative chronotropic and inotropic effects on isolated guinea pig atria when tested using myography (Pérez et al., 1982). However, both of these studies were conducted on isolated cardiac cells or dissected cardiac tissue rather than whole heart muscle, which may alter the normal physiological muscular response to drug stimulation.

Having assessed the effects of perhexiline and FPER-1 during normoxia in the presence of high-fat, the effects of these agents were assessed following an ischaemic insult, by using a well-established Langendorff protocol (Tanno et al., 2003) in which the hearts were subjected to global no-flow ischaemia and reperfusion. Global ischaemia causes detrimental effects on cardiac function in reperfused hearts (Apstein et al., 1977). The present post-ischaemic data revealed that both perhexiline and FPER-1 improved cardiac haemodynamics

following ischaemia, when perfused pre-ischaemia with high-fat buffer. High-fat buffer alone (1.2 mM palmitate) was found to suppress the recovery of cardiac function in a working rat heart Langendorff model of hypothermic arrest (Mjøs et al., 1991). Moreover, 1.2 mM palmitate increased ischaemic and reperfusion damage (contracture magnitude, creatine phosphokinase release), including a 25% reduction in LVDP recovery, and increased diastolic pressure in isolated rabbit hearts (Pasini et al., 1991). Therefore, it was anticipated that high fat in combination with ischaemia would lead to deleterious effects on heart function during reperfusion. LVEDP, which describes the pressure at the end of cardiac relaxation/diastole, is highlighted as an important marker of ventricular performance and as a diagnostic measure for identifying patients with increased risk for developing late symptoms of HF (Mielniczuk et al., 2007). Indeed, that study showed that a high LVEDP (>30 mmHg) correlated with a higher risk of death or of HF. Consistent with this, LVEDP was impaired post-ischaemia in the present study in the high-fat group and these effects were abrogated by both 2 µM perhexiline and 10 µM FPER-1. Perfusion with 2 µM FPER-1 also improved LVEDP with a clear dose-dependent effect. The present results therefore support those of Kennedy and colleagues (2000) in that 2 µM perhexiline attenuated the increase in diastolic tension during ischaemia in a low-flow ischaemia rat heart model. In contrast, their study did not show any protective effects of perhexiline on diastolic function during reperfusion. However, it is important to note that the ischaemic insult (of 95% flow reduction and continued pacing) used in their model was not as extensive as the 100% global ischaemia and no pacing used in the present study. Similar to the results presented here, perhexiline did improve LV diastolic function in patients with HCM (Abozguia et al., 2010). In addition, the present results complement other studies that showcased the ability of FA oxidation inhibitors such as

etomoxir (Lopaschuk et al., 1990) and oxfenicine (Ikizler et al., 2003) to improve LV function post-ischaemia. The present results now demonstrate that the FA oxidation inhibitor FPER-1 has a similar ability, like perhexiline, to improve LV function post-ischaemia.

Interestingly, LVDP, which describes the pressure generated between systole and diastole, was only improved post-ischaemia by FPER-1 and not perhexiline, with both derivative concentrations (2 and 10 μM) having similar efficacy. This data suggests that unlike perhexiline, FPER-1 may have the capacity to improve systolic function thereby improving LVDP. Unfortunately, measuring systolic function (as a product of heart rate and developed pressure) was not possible in the present model given that hearts were paced at a constant rate. However, it may be noted that Kennedy and colleagues (2000) did measure systolic function (as a product of heart rate and developed tension) and observed no improvement with 0.5 or 2 μM perhexiline during low-flow ischaemia or reperfusion.

In parallel with ventricular function, the present study also assessed coronary flow post-ischaemia. CFR was improved by 2 μM perhexiline and both doses of FPER-1 with near identical efficacy. Perhexiline was previously classed as a vasodilating agent (Barry et al., 1985) and observed to have beneficial vasodilator properties in Langendorff-perfused rat hearts and coronary artery ligated rat hearts (Kennedy et al., 1999). The present findings also corroborate those of Ono and colleagues (1982) who demonstrated in an open-chest canine model that intravenous administration of perhexiline increased coronary flow, in addition to reducing aortic and systemic blood pressure. Furthermore, Klassen and colleagues (1976) observed improvements in coronary diastolic pressure and preserved endocardial flow in the

ischaemic canine myocardium when perhexiline was given intravenously. In some contrast, in a small study on patients with coronary heart disease, perhexiline administration during tachycardia-induced angina did not alter coronary sinus blow flow (Pepine et al., 1974), but this might be explained if the coronary vessels capacity to dilate was compromised by ischaemic heart disease. Herein, the present results clearly demonstrate that FPER-1 can have beneficial effects on coronary flow suggesting it has vasodilating properties similar to perhexiline.

In addition to cardiac function assessment, the effects of perhexiline and FPER-1 on post-ischaemic hypercontracture magnitude were evaluated. Hypercontracture is a well-established marker of ischaemic injury and myocardial cell death and is exacerbated by reoxygenation that takes place at reperfusion (Ruiz-Meana and García-Dorado, 2009). It describes the abrupt and excessive shortening of myocytes, which leads to sarcolemmal rupture and apoptosis and is highly correlated with the extent of ATP depletion prior to reperfusion (Ruiz-Meana et al., 1995). Moreover, hypercontracture is associated with causing elevated LVEDP following an ischaemic event, when assessed in isolated feline hearts (Schaff et al., 1981). The present results provided the promising novel finding that 2 µM perhexiline reduced hypercontracture magnitude post-ischaemia and this was replicated by 10 µM FPER-1. These findings reflect the effects of FA oxidation inhibitor trimetazidine, which reduced hypercontracture size following ischaemia in rat cardiomyocytes (Ruiz-Meana et al., 1996) and in ventricular myocytes from rabbits subjected to pressure overload (Dedkova et al., 2013). Delaying the time to hypercontracture development is also considered protective by allowing the cardiomyocytes more time to readjust pH, ion and ATP

levels following ischaemia, which subsequently reduces the probability for cell shortening and cell death (Inserte et al., 2008). However, neither perhexiline nor FPER-1 increased the time to hypercontracture during reperfusion.

3.4.1. Study limitations

In the present study 1.2 mM palmitate (high fat) was used to perfuse mouse hearts and assess haemodynamics, with and without drug perfusion. Despite using a well-established protocol of BSA-palmitate pre-conjugation (Belke et al., 1999) to prepare the high-fat buffer, it is possible that not all the weighed palmitate was successfully conjugated and dissolved in the KHB. As such, on reflection, it would have been useful to measure the final palmitate concentration for each batch of BSA-palmitate KHB made and this could have been assessed spectrophotometrically using a free FA quantification commercial kit. However, the use of suitable percentage of BSA (3%) for conjugation should avoid this problem and Oliveira and co-workers (2015) have demonstrated that conjugation of 0.5 mM palmitate to 1% BSA led to only 0.02 mM of unbound palmitate. Moreover, given that BSA contains Ca^{2+} binding sites, the level of free Ca^{2+} ions present in the high-fat KHB buffer may have been reduced which could have had an impact on cardiac function. Therefore, in future it would be useful to measure the levels of free Ca^{2+} in the KHB buffer throughout the experimental protocol.

Another limitation of the present study was that a model of global ischaemia was used as opposed to low-flow ischaemia in order to subject hearts to a more severe ischaemic stressor. This in turn meant that cardiac function during ischaemia itself could not be recorded. It would have been interesting to investigate whether FPER-1 can also protect diastolic function during ischaemia as Kennedy and colleagues (2000) observed with 2 µM

perhexiline. Moreover, in order to assess whether perhexiline and/or FPER-1 provided protection against ischaemia, post-ischaemic function was measured in reperfused hearts. It is well known that restoration of blood flow after an ischaemic insult results in another form of myocardial injury; reperfusion injury, which takes place in parallel to ischaemic injury (Kalogeris et al., 2012). It is therefore inevitable that the post-ischaemic data included the effects of reperfusion injury on cardiac function, which may have detracted from the potential anti-ischaemic effects of perhexiline and FPER-1. It should be noted that a clinical trial on patients with ischaemic heart disease undergoing coronary artery bypass graft (CABG) surgery revealed that 3-day pre-operative treatment with perhexiline did not protect against reperfusion injury (Drury et al., 2015). Similar observations were made in patients with LV hypertrophy given perhexiline for a minimum of 5 days pre-surgery (Senanayake et al., 2015). However, these ischaemia/reperfusion injury trials were conducted on patients with diseased hearts and thus already compromised cardiac function whereas in the present study, healthy mice were subjected to ischaemia/reperfusion. Additionally, as outlined in Chapter 1, section 1.11.1 a therapeutic dose of perhexiline was not maintained in all patients. As such, the post-ischaemic data for LVEDP and CFR obtained in the present study are still promising for both perhexiline and FPER-1, despite the presence of reperfusion injury. Nonetheless, it is recognised that these agents, in particular the novel derivative FPER-1, should be investigated during ischaemia alone.

3.4.2. Future considerations

As discussed above (section 3.4.1), the Langendorff model implemented in the present study involved global no-flow ischaemia. Therefore to complement these data it would be

beneficial to assess the effects of perhexiline on the same parameters (LVDP, LVEDP and CFR) but using low-flow ischaemia, and determine whether the effects are replicated by FPER-1. This would aid in identifying the anti-ischaemic properties of both agents. Markers of systolic function i.e. the rate pressure product which is equivalent to heart rate multiplied by the systolic pressure (Herr et al., 2015), would also be useful to measure in the Langendorff-perfused hearts.

Furthermore, the present results showed that high-fat buffer perfusion reduced infarct size. Therefore it was not possible to use infarction to measure cell death/injury. Perhexiline has already been demonstrated to reduce infarct size in open-chest canine models (Daniell et al., 1977; Ono et al., 1982) and this was in the absence of high fat. As such, it would be useful to perfuse mouse hearts with perhexiline or FPER-1 in standard KHB, and investigate the effects on infarct size in the absence of high fat. Furthermore, additional markers of muscle cell death could also be tested such as creatine kinase and lactate dehydrogenase release (Brancaccio et al., 2010).

Importantly the present study showed that 10 µM FPER-1 successfully replicated both the normoxic and post-ischaemic effects of perhexiline. However, for completeness it would be imperative to assess a range of FPER-1 concentrations, as due to time constraints it was only possible to test one additional dose alongside 2 µM, the established working dose of perhexiline. It is possible that an FPER-1 concentration between 2 – 10 µM may still provide the beneficial effects observed with 10 µM. When tested *in vitro* Signal Pharma demonstrated that FPER-1 inhibits CPT1B activity with 25% less potency than perhexiline

(Tseng et al., 2017). It can therefore be speculated that perhaps a 4-fold higher dose of FPER-1 (8 µM) may be sufficient to replicate perhexiline's beneficial effects on function. Assessing different concentrations of FPER-1 in the Langendorff model would also be important for identifying a range of effective doses for FPER-1. Lastly, it would also be useful to use prolonged perhexiline/FPER-1 therapy in mice *in vivo* followed by heart isolation and functional assessment on the Langendorff system in a similar manner as to Unger and colleagues (2005), to determine whether the results following prolonged treatment reflect that of the acute treatment used in the studies described in this chapter.

3.4.3. Conclusion

Using isolated mouse hearts in the Langendorff global ischaemia/reperfusion model, the present data demonstrate that 2 µM perhexiline improves LV function and flow post-ischaemia in hearts perfused with high-fat KHB, thus protecting the hearts from ischaemic injury, corroborating published studies. The present results also show that, whilst perhexiline had no normoxic effects on cardiac function even during high fat perfusion, it had both positive inotropic and lusitropic effects during pre-ischaemia. More importantly, the results of this study provide the novel findings that FPER-1, a newly developed analogue of perhexiline, also has positive inotropic and lusitropic properties and provides protection to LV function and coronary flow following ischaemia. Therefore, despite the altered chemical structure, FPER-1 has promising beneficial effects that replicate its parent drug perhexiline. In the present study 10 µM FPER-1, a concentration 5-fold higher than the effective dose of perhexiline, had similar therapeutic efficacy, however, whether a lower dose would also achieve such effects requires investigation.

Chapter 4:
Investigating the molecular mechanism(s) of perhexiline and FPER-1 treatment *ex vivo*

Chapter 4: Investigating the molecular mechanism(s) of perhexiline and FPER-1 treatment *ex vivo*

4.1. Introduction

The results of Chapter 3 demonstrated that 2 µM perhexiline enhanced markers of cardiac contractility and relaxation during normoxia and improved cardiac functional recovery (pressure and flow) post-ischaemia. These beneficial effects were replicated by 10 µM of the novel derivative fluoroperhexiline-1 (FPER-1).

As indicated in Chapter 1 (section 1.9.1) perhexiline was first described as a metabolic modulator when it was shown to decrease myocardial lactate extraction in coronary artery disease patients (Pepine et al., 1974). In 1996, perhexiline was then revealed to be an inhibitor of carnitine palmitoyltransferase 1B (CPT1B) (Kennedy et al., 1996). Initially, this mechanism was believed to underlie the therapeutic effects of perhexiline, by CPT1B inhibition resulting in a shift from FA metabolism towards the more efficient, oxygen sparing, glucose metabolism (Faadiel Essop and Opie, 2004). However, later studies in the isolated rat heart revealed that perhexiline-induced protection occurred despite a lack of change in FA oxidation or CPT1B activity (Kennedy et al., 2000; Unger et al., 2005). Similar results were obtained in patients with dilated cardiomyopathy; short-term perhexiline treatment improved cardiac energetics without altering substrate utilisation (Beadle et al., 2015). These studies led to speculations that, although perhexiline inhibits CPT1B, other mechanisms are primarily involved in rendering protection, in particular an increase in glucose oxidation. Experimental murine studies have supported this, demonstrating that perhexiline increases

pyruvate dehydrogenase (PDH) activity (Yin et al., 2013) and upregulates the carbohydrate pathway (Gehmlich et al., 2015). As described in Chapter 1 (section 1.11.2), modulation of other metabolic proteins have also been reported, including reduced thioredoxin-interacting protein (TXNIP) expression (Ngo et al., 2011). Nonetheless, the exact cardioprotective mechanism of perhexiline is not fully elucidated and it remains unknown whether the molecular targets are restricted to metabolic pathways.

Therefore, the aim of the work in this chapter was to gain insights into the potential mechanism(s) underlying the protection induced by acute perhexiline and FPER-1 treatment in the isolated mouse heart, by investigating the expression/phosphorylation of multiple signalling pathways. The secondary aim was to discern whether the perhexiline- and FPER-1-mediated protection were due to activation/inhibition of the same or different proteins.

Aims:

1. To investigate the molecular mechanism(s) underlying perhexiline- and FPER-1-induced protection *ex vivo*.
2. To determine whether FPER-1 targets the same molecular pathways as perhexiline and if so, to what extent.

4.2. Methodology

A detailed methodology is presented in Chapter 2, with section 2.3 outlining the Langendorff protocols (C, D and E; **Figure 2.3**) and section 2.5 and 2.6 describing the molecular analysis. In brief, isolated hearts from male C57Bl/6 mice (25 – 30 g) were retrogradely perfused on

the Langendorff system and, following 10 min stabilisation, were perfused with either 1) control (high-fat Krebs-Henseleit buffer (KHB)), 2) 2 µM perhexiline, 3) 2 µM FPER-1 or 4) 10 µM FPER-1 for 30 min in protocol C and D, or for 60 min in protocol E, under normoxic conditions.

Protocol C: Following stabilisation, hearts were subjected to 30 min global ischaemia and 60 min reperfusion. Coronary effluent was collected at 5 min reperfusion and colorimetrically assayed for lactate content (section 2.5).

Protocol D: Hearts were snap-frozen in liquid nitrogen either straight after the 40 min stabilisation (T1; "pre-ischaemia") or following 30 min global ischaemia (T2; "ischaemia") for Western blotting.

Protocol E: Hearts were snap-frozen in liquid nitrogen immediately after the extended 70 min stabilisation for Western blotting (T3; "extended normoxia").

Collected hearts were then prepared for Western blotting and subjected to a Western blotting protocol which included gel electrophoresis, wet transfer, membrane incubation with the desired antibodies and developing (detailed in section 2.6). Developed hyperfilms were scanned and densitometrically analysed on Adobe CS Photoshop.

4.2.1. Statistical analysis

All data within this chapter are expressed as means ±standard error of the mean (SEM). The effect of each treatment (2 µM perhexiline, 2 or 10 µM FPER-1) on protein expression or phosphorylation and on lactate content were compared to control (high-fat KHB) using a

one-way analysis of variance (ANOVA) with Bonferroni post-hoc test. Graphpad Prism version 6.0 was used for all analysis. *p<0.05* was considered statistically significant. Number of mice used is indicated in the figure legends.

4.3. Results

4.3.1. Effects of perhexiline and FPER-1 on PLB phosphorylation

As discussed in Chapter 1 (section 1.3.2), phospholamban (PLB) is involved in the highly energetic processes of cardiac contractility and relaxation (Kranias and Hajjar, 2012). PLB phosphorylation at Ser16 and/or Thr17 reduces its activity which increases Ca^{2+} cycling, thus increasing inotropy and lusitropy (Colyer, 1998).

PLB can be present as a pentamer or dissociated into different sized monomers (Kirchberger and Antonetz, 1982). By using blocking peptides specially supplied by Professor John Colyer (of Badrilla), raised against the phosphorylated PLB antibodies at Ser16 **[Figure 4.1A]** and Thr17 **[Figure 4.1B]**, the molecular weight of PLB was approximately 12 kDa in the cardiac samples as the bands present at this weight, for PLB phosphorylated at Ser16 (p-PLB^{Ser16}) and Thr17 (p-PLB^{Thr17}), were absent when the membranes were probed with the antibody and corresponding blocking peptide together.

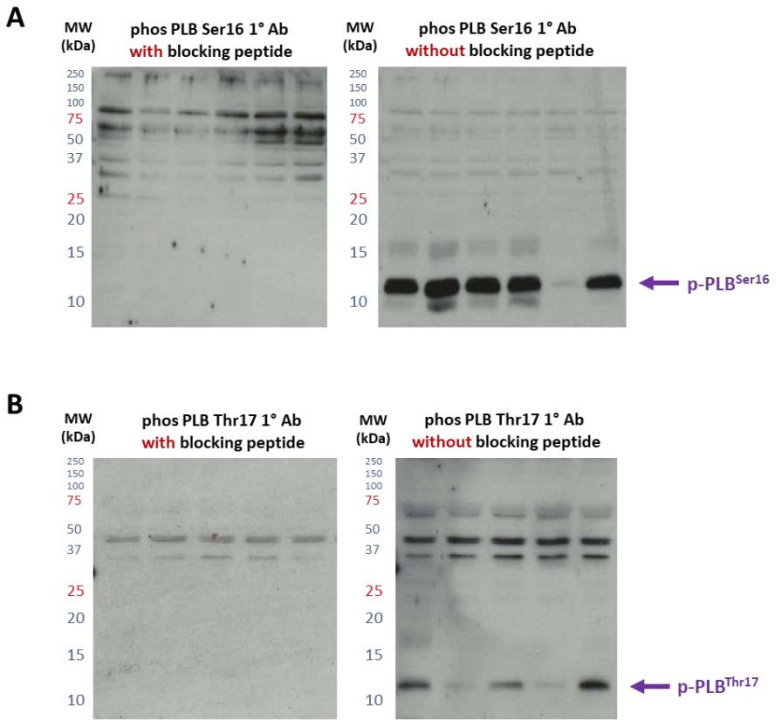

Figure 4.1. Identification of phosphorylated PLB molecular weight in Western blot

A: Two membranes containing identical cardiac samples probed with phosphorylated PLB Ser16 (p-PLB^{Ser16}) primary antibody with blocking peptide (left-hand side) and without blocking peptide (right-hand side). **B:** Two membranes containing identical cardiac samples probed with phosphorylated PLB Thr17 (p-PLB^{Thr17}) primary antibody with blocking peptide (left-hand side) and without blocking peptide (right-hand side).

Pre-ischaemia, PLB phosphorylation at Ser16 was significantly increased by 2 µM perhexiline (3.5-fold; *p<0.01*), 2 µM FPER-1 (3.0-fold; *p<0.05*) and 10 µM FPER-1 (3.1-fold; *p<0.05*) compared to the control **[Figure 4.2A+B]**. Concomitantly, PLB phosphorylation at Thr17 was significantly increased pre-ischaemia but only by 2 µM perhexiline (2.8-fold; *p<0.05*) and 10 µM FPER-1 (2.9-fold; *p<0.01*) relative to the control, whilst any effect of 2 µM FPER-1 treatment was not significant (1.6-fold increase; *p>0.99*) **[Figure 4.2A+C]**. In contrast, in ischaemia, p-PLB^{Ser16} and p-PLB^{Thr17} were not altered in any of the treatment groups (*p=0.99* for both sites) **[Figure 4.2D-F]**.

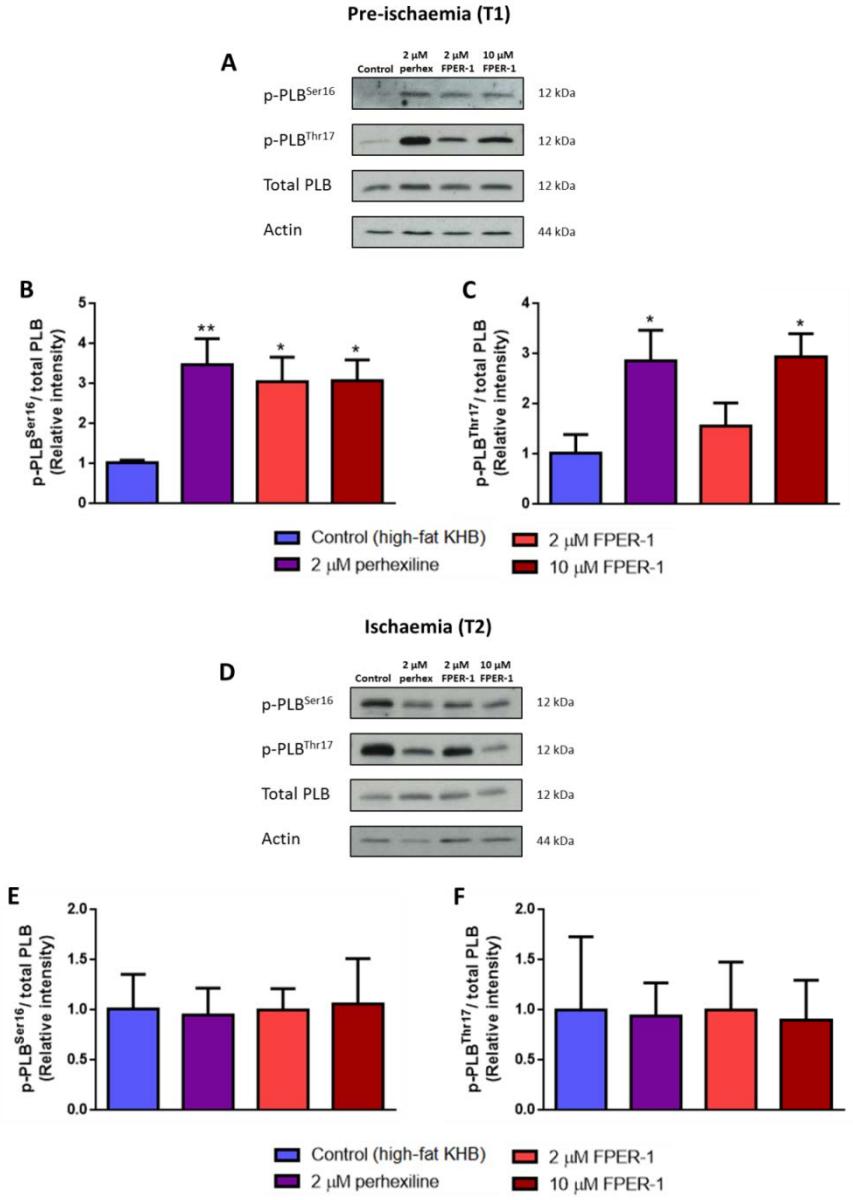

Figure 4.2. Effects of perhexiline and FPER-1 on PLB phosphorylation following pre-ischaemic perfusion (T1), and after subsequent ischaemia (T2)

Hearts were perfused for 30 min pre-ischaemia with either 1) control (high-fat KHB), 2) 2 µM perhexiline, 3) 2 µM FPER-1 or 4) 10 µM FPER-1. **A:** Representative Western blots for phosphorylated PLB Ser16, Thr17, total PLB and loading control actin at T1. **B:** Normalised mean phosphorylated PLB^{Ser16} over total PLB at T1. **C**: Normalised mean phosphorylated PLB^{Thr17} over total PLB at T1. **D:** Representative Western blots for phosphorylated PLB Ser16, Thr17, total PLB and loading control actin at T2. **E:** Normalised mean phosphorylated PLB^{Ser16} over total PLB at T2. **F:** Normalised mean phosphorylated PLB^{Thr17} over total PLB at T2. Data are presented as mean ±SEM; n = 6-8 mice. *$p<0.05$ vs Control (high-fat KHB); **$p<0.01$ vs Control (high-fat KHB) (One-way ANOVA followed by Bonferroni post-hoc test).

4.3.2. Effects of perhexiline and FPER-1 on CPT1B expression

To investigate whether the perhexiline- and FPER-1-induced protection involved changes in cardiac FA metabolism, the expression of the rate-limiting enzyme CPT1B (discussed in Chapter 1, section 1.7.2) was assessed.

Pre-ischaemia, CPT1B expression was not significantly changed by 2 µM perhexiline or FPER-1 (2 or 10 µM) relative to the control (*p=0.81*) **[Figure 4.3A+B]**. In contrast, in ischaemia, CPT1B expression was significantly reduced in hearts perfused with 10 µM FPER-1 (2.5-fold, *p<0.05*). However, any effect of 2 µM perhexiline treatment was not significant (1.6-fold decrease, *p=0.42*) and 2 µM FPER-1 perfusion had no effect (*p>0.99*) **[Figure 4.2C+D]**.

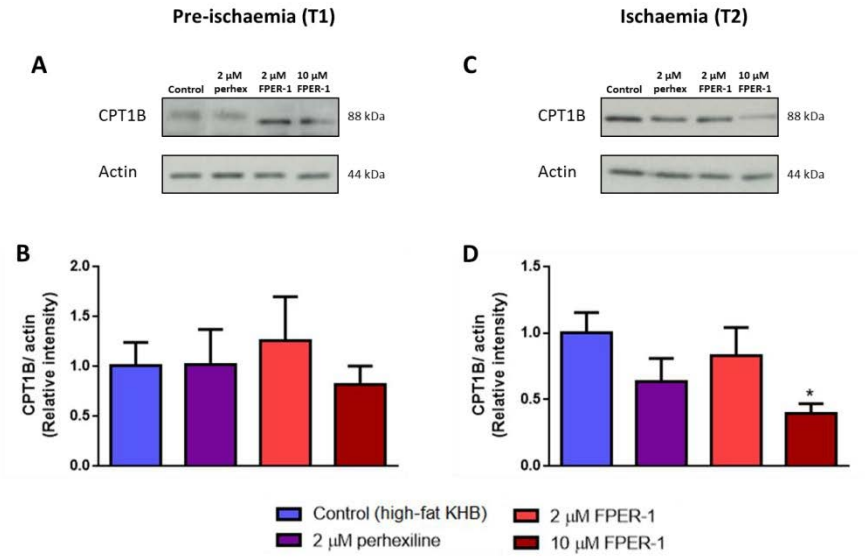

Figure 4.3. Effects of perhexiline and FPER-1 on CPT1B expression following pre-ischaemic perfusion (T1), and after subsequent ischaemia (T2)

Hearts were perfused for 30 min pre-ischaemia with either 1) control (high-fat KHB), 2) 2 µM perhexiline, 3) 2 µM FPER-1 or 4) 10 µM FPER-1. **A:** Representative Western blots for total CPT1B and loading control actin at T1. **B:** Normalised mean CPT1B over actin at T1. **C:** Representative Western blots for total CPT1B and loading control actin at T2. **D:** Normalised mean CPT1B over actin at T2. Data are presented as mean ±SEM; n = 6-8 mice. **p<0.05* vs Control (high-fat KHB) (One-way ANOVA followed by Bonferroni post-hoc test).

4.3.3. Effects of perhexiline and FPER-1 on PDH phosphorylation

To determine whether the perhexiline- and FPER-1-induced protection were associated with changes in glucose metabolism, the activity of the rate limiting enzyme PDH (discussed in Chapter 1, section 1.7.5) was assessed by measuring phosphorylation at Ser232 (p-PDH^{Ser232}), Ser293 (p-PDH^{Ser293}) and Ser300 (p-PDH^{Ser300}). Dephosphorylation indicates increased activity.

Consistent with the CPT1B data, pre-ischaemia, there was no significant change in PDH phosphorylation at any of the three sites, in hearts perfused with 2 µM perhexiline or FPER-1 (2 or 10 µM) relative to the control (*p=0.79*, *0.97* and *0.98* respectively) **[Figure 4.4A-D]**. In ischaemia, there was also no significant change in p-PDH^{Ser232} following perfusion with 2 µM perhexiline (*p=0.77*) or either concentration of FPER-1 (*p>0.99* for both) relative to the control **[Figure 4.4E+F]**. In contrast, p-PDH^{Ser293} was significantly reduced by 2 µM perhexiline (2.3-fold, *p<0.05*) and 10 µM FPER-1 (2.6-fold, *p<0.01*) relative to the control **[Figure 4.4E+G]**. A similar effect was observed with 2 µM FPER-1, but this was not significant (1.8-fold decrease; *p=0.06*). Phosphorylation of PDH at Ser300 was significantly reduced by 2 µM FPER-1 (2.5-fold; *p<0.01*) and 10 µM FPER-1 perfusion (2.3-fold; *p<0.05*), but any effect of 2 µM perhexiline was not significant (1.6-fold decrease; *p=0.17*) **[Figure 4.4E+H]**.

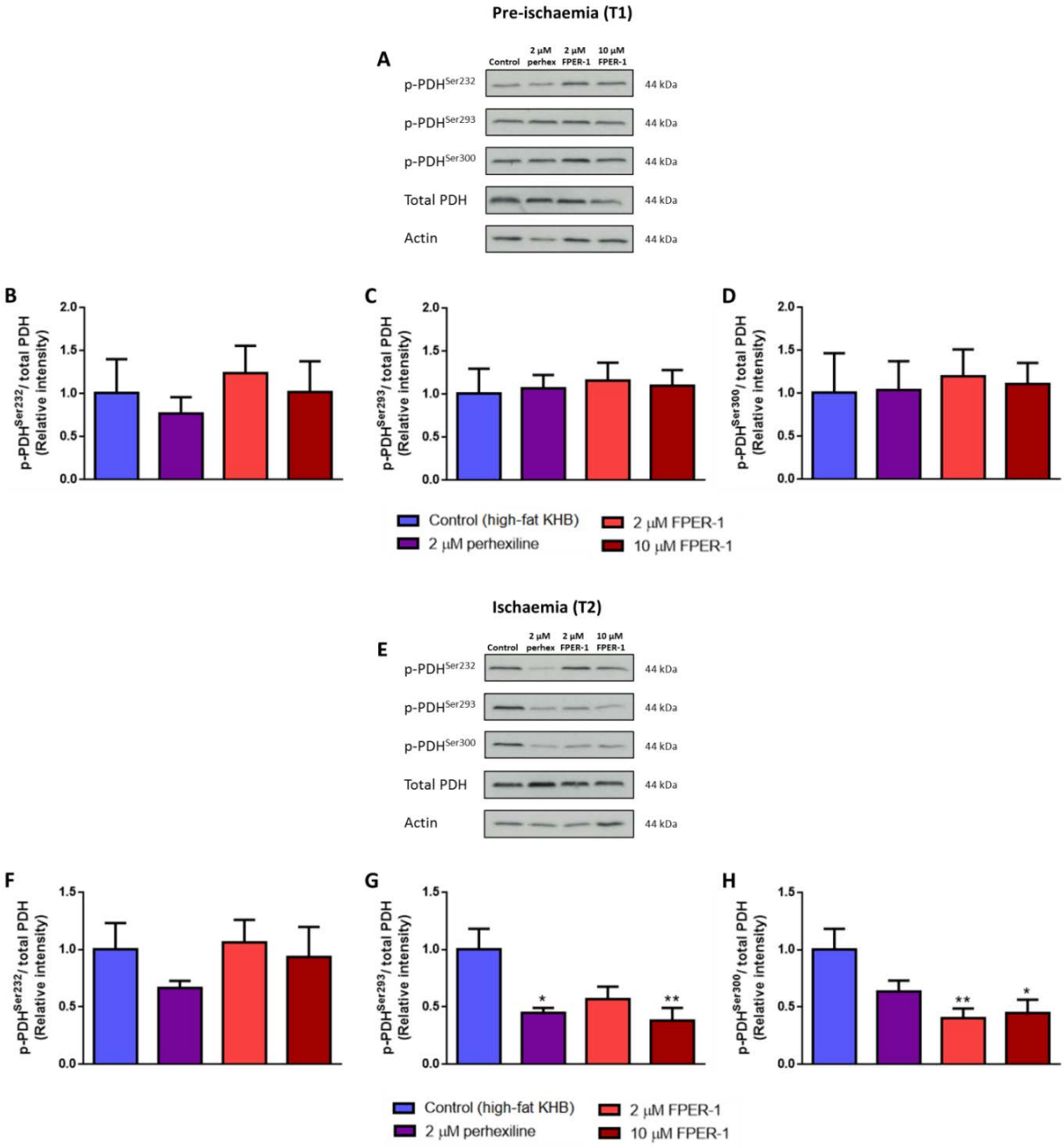

Figure 4.4. Effects of perhexiline and FPER-1 on PDH phosphorylation following pre-ischaemic perfusion (T1), and after subsequent ischaemia (T2)

Hearts were perfused for 30 min pre-ischaemia with either 1) control (high-fat KHB), 2) 2 µM perhexiline, 3) 2 µM FPER-1 or 4) 10 µM FPER-1. **A:** Representative Western blots for phosphorylated PDH Ser232, Ser293, Ser300, total PDH and loading control actin at T1. **B:** Normalised mean phosphorylated PDH^{Ser232} over total PDH at T1. **C:** Normalised mean phosphorylated PDH^{Ser293} over total PDH at T1. **D:** Normalised mean phosphorylated PDH^{Ser300} over total PDH at T1. **E:** Representative Western blots for phosphorylated PDH Ser232, Ser293, Ser300, total PDH and loading control actin at T2. **F:** Normalised mean phosphorylated PDH^{Ser232} over total PDH at T2. **G:** Normalised mean phosphorylated PDH^{Ser293} over total PDH at T2. **H:** Normalised mean phosphorylated PDH^{Ser300} over total PDH at T2. Data are presented as mean ±SEM; n = 6-8 mice. *$p<0.05$ vs Control (high-fat KHB); **$p<0.01$ vs Control (high-fat KHB) (One-way ANOVA followed by Bonferroni post-hoc test).

Based on the lack of PDH dephosphorylation pre-ischaemia, these results suggested that perhexiline and FPER-1 only activate PDH when metabolism is disrupted, such as during ischaemia. Since Patel and Olson (1984) showed a significant decrease in PDH activity in rat hearts subjected to 95% low-flow ischaemia and Vary and Randle (1984) observed a reduced concentration of active PDH in rat hearts submitted to global ischaemia, it was likely that perhexiline and FPER-1 upregulated glucose metabolism during ischaemia, thereby correcting the metabolic impairment.

As 30 min pre-ischaemic perfusion with perhexiline or FPER-1 was sufficient to cause effects in ischaemia it was possible that 30 min perfusion was not sufficient to cause effects in normoxia. Consequently, in an additional set of experiments the drug perfusion time in normoxia was doubled from 30 to 60 min and PDH phosphorylation assessed.

Following extended normoxic perfusion, PDH phosphorylation at Ser232, 293 and 300 were unchanged by any treatment compared to the controls (*p=0.79*, *0.95* and *0.99* respectively) **[Figure 4.5]**.

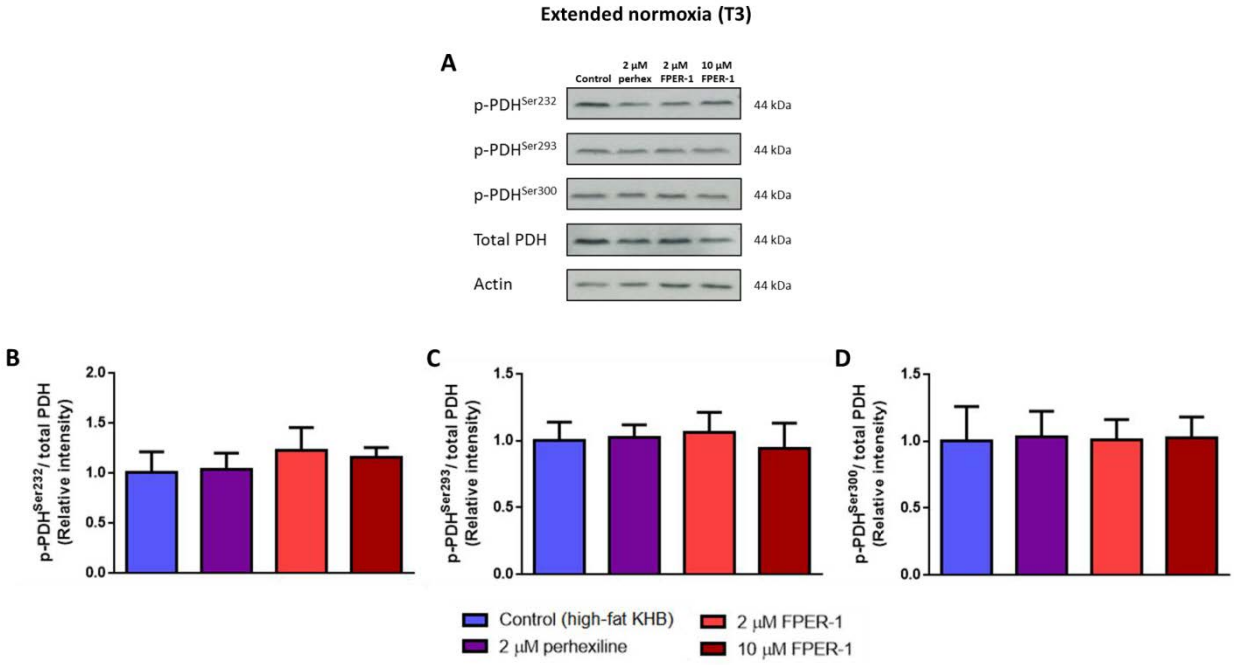

Figure 4.5. Effects of perhexiline and FPER-1 on PDH phosphorylation following extended normoxic perfusion (T3)

Hearts were perfused for an extended 60 min with either 1) control (high-fat KHB), 2) 2 µM perhexiline, 3) 2 µM FPER-1 or 4) 10 µM FPER-1. **A:** Representative Western blots for phosphorylated PDH Ser232, Ser293, Ser300, total PDH and loading control actin at T3. **B:** Normalised mean phosphorylated PDH^{Ser232} over total PDH at T3. **C:** Normalised mean phosphorylated PDH^{Ser293} over total PDH at T3. **D:** Normalised mean phosphorylated PDH^{Ser300} over total PDH at T3. Data are presented as mean ±SEM; n = 4 mice.

4.3.4. Effects of perhexiline and FPER-1 on GSK3αβ phosphorylation

Following the observation that perhexiline or FPER-1 treatment supposedly increased PDH activity, the activity of glycogen synthase kinase 3 (GSK3), a protein upstream of PDH, was assessed. GSK3 inhibits glycogen synthesis through glycogen synthase phosphorylation (Embi et al., 1980), is involved with negative feedback regulation of insulin signalling (Liberman and Eldar-Finkelman, 2005) and forms part of the cardioprotective 'Reperfusion Injury Salvage Kinase (RISK)' pathway (Hausenloy and Yellon, 2007). Phosphorylation at Ser21/9 and subsequent inactivation of GSK3αβ is cardioprotective against ischaemia/reperfusion injury by preventing apoptosis and necrosis (Juhaszova et al., 2004).

Pre-ischaemia, phosphorylation of GSK3αβ at Ser21/9 (p-GSK3αβ$^{Ser21/9}$) was not altered by 2 µM perhexiline or FPER-1 (2 or 10 µM) perfusion relative to the control (*p=0.87*) **[Figure 4.6A+B]**. However, in ischaemia, p-GSK3αβ$^{Ser21/9}$ was significantly increased by 2 µM perhexiline (2.1-fold; *p<0.05*) and 10 µM FPER-1 (2.3-fold; *p<0.*05), when compared to the control; any effect of 2 µM FPER-1 was not significant (1.7-fold increase, *p=0.38*) **[Figure 4.6C+D]**.

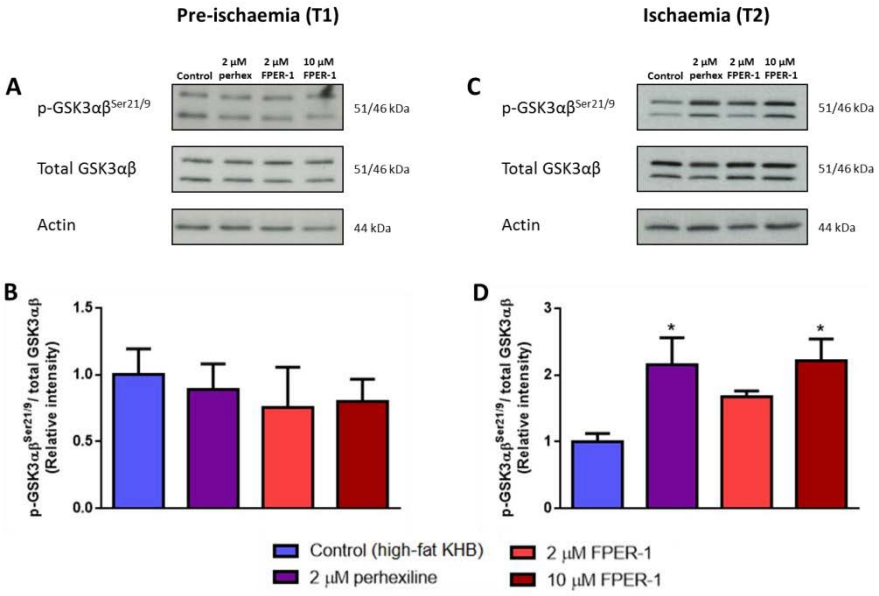

Figure 4.6. Effects of perhexiline and FPER-1 on GSK3αβ phosphorylation following pre-ischaemic perfusion (T1) and after subsequent ischaemia (T2)

Hearts were perfused for 30 min pre-ischaemia with either 1) control (high-fat), 2) 2 µM perhexiline, 3) 2 µM FPER-1 or 4) 10 µM FPER-1. **A:** Representative Western blots for phosphorylated GSK3αβ Ser21/9, total GSK3αβ and loading control actin at T1. **B:** Normalised mean phosphorylated GSK3αβ$^{Ser21/9}$ over total GSK3αβ at T1. **C:** Representative Western blots for phosphorylated GSK3αβ Ser21/9, total GSK3αβ and loading control actin at T2. **D:** Normalised mean phosphorylated GSK3αβ$^{Ser21/9}$ over total GSK3αβ at T2. Data are presented as mean ±SEM; n = 7-10 mice. **p<0.05* vs Control (high-fat KHB) (One-way ANOVA followed by Bonferroni post-hoc test).

4.3.5. Effects of perhexiline and FPER-1 on Akt and ERK1/2 phosphorylation

Assuming that GSK3αβ activity was decreased in ischaemia following perhexiline or FPER-1 perfusion, the upstream proteins of GSK3 were of interest. GSK3αβ is regulated by several proteins including protein kinase C and p70S6 kinase (Beurel et al., 2015) as well as members

of the cardioprotective RISK pathway: protein kinase B (Akt) and extracellular signal-regulated kinase 1/2 (ERK1/2) (Hausenloy and Yellon, 2007). Phosphorylation of Akt at Ser473 (p-Akt^{Ser473}) and ERK1/2 at Thr202/Tyr204 (p-ERK1/2$^{Thr202/Tyr204}$) leads to their activation and in turn, phosphorylation and inhibition of GSK3αβ (Miura and Miki, 2009).

Pre-ischaemia, Akt phosphorylation at Ser473 was not altered by perfusion with 2 µM perhexiline or FPER-1 (2 or 10 µM) (*p=0.58*) **[Figure 4.7A+B]**. In ischaemia, any effect of 2 µM perhexiline (1.4-fold increase, *p=0.52*) or 10 µM FPER-1 (1.2-fold increase; *p>0.99*) was not significant, and 2 µM FPER-1 had no effect (*p>0.99*) relative to the control **[Figure 4.7C+D]**. Similarly, p-Akt^{Ser473} was not changed by any treatment following the extended 70 min normoxic perfusion in comparison to the control (*p=0.52*) **[Figure 4.7E+F]**.

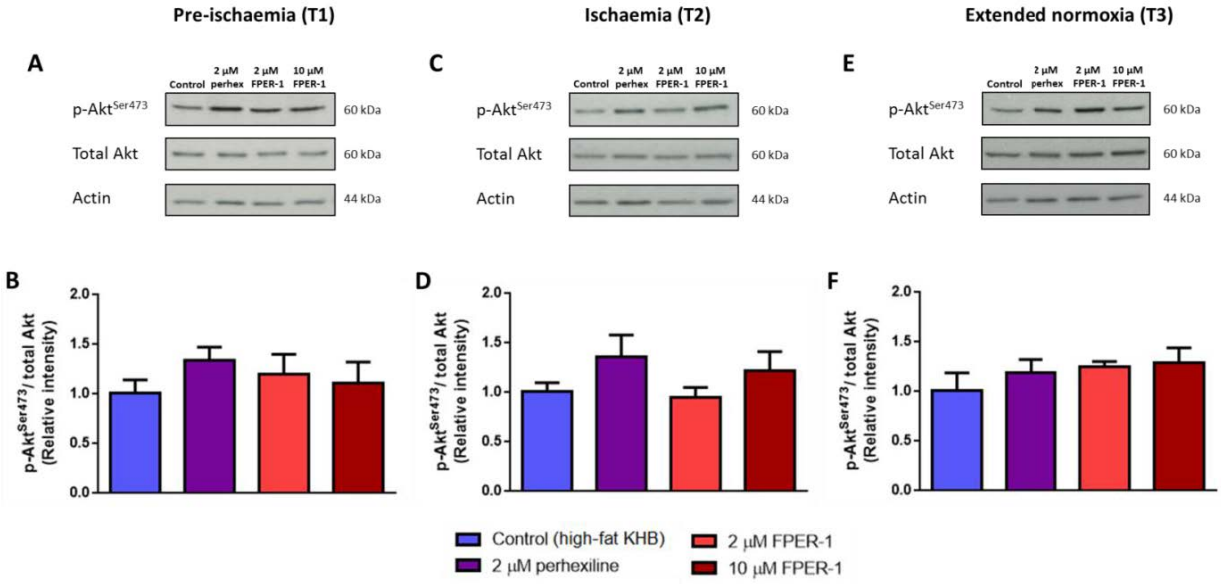

Figure 4.7. Effects of perhexiline and FPER-1 on Akt phosphorylation following pre-ischaemic perfusion (T1), after subsequent ischaemia (T2) and following extended normoxic perfusion (T3)

Hearts were perfused for 30 min pre-ischaemia or for an extended 60 min normoxia with either 1) control (high-fat KHB), 2) 2 µM perhexiline, 3) 2 µM FPER-1 or 4) 10 µM FPER-1. **A:** Representative Western blots for phosphorylated Akt Ser473, total Akt and loading control actin at T1. **B:** Normalised mean phosphorylated Akt^{Ser473} over total Akt at T1. **C:** Representative Western blots for phosphorylated Akt Ser473, total Akt and loading control actin at T2. **D:** Normalised mean phosphorylated Akt^{Ser473} over total Akt at T2. **E:** Representative Western blots for phosphorylated Akt Ser473, total Akt and loading control actin at T3. **F:** Normalised mean phosphorylated Akt^{Ser473} over total Akt at T3. Data are presented as mean ±SEM; n = 6-8 mice.

There was also no significant effect on p-ERK1/2$^{Thr202/Tyr204}$ with 2 µM perhexiline or FPER-1 (2 or 10 µM), pre-ischaemia or during ischaemia compared to the controls (*p=0.9 and 0.99* respectively) **[Figure 4.8]**.

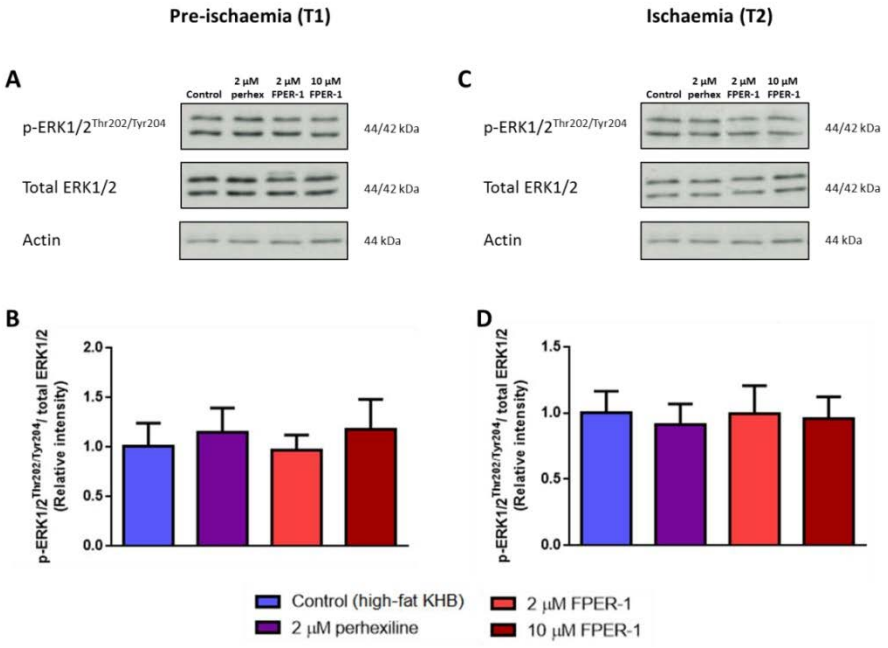

Figure 4.8. Effects of perhexiline and FPER-1 on ERK1/2 phosphorylation following pre-ischaemic perfusion (T1), and after subsequent ischaemia (T2)

Hearts were perfused for 30 min pre-ischaemia with either 1) control (high-fat KHB), 2) 2 µM perhexiline, 3) 2 µM FPER-1 or 4) 10 µM FPER-1. **A:** Representative Western blots for phosphorylated ERK1/2 Thr202/Tyr204, total ERK1/2 and loading control actin at T1. **B:** Normalised mean phosphorylated ERK1/2$^{Thr202/Tyr204}$ over total ERK1/2 at T1. **C:** Representative Western blots for phosphorylated ERK1/2 Thr202/Tyr204, total ERK1/2 and loading control actin at T2. **D:** Normalised mean phosphorylated ERK1/2$^{Thr202/Tyr204}$ over total ERK1/2 at T2. Data are presented as mean ±SEM; n = 7-10 mice.

4.3.6. Effects of perhexiline and FPER-1 on TXNIP, UCP3 and ANT expression

The expression of thioredoxin-interacting protein (TXNIP), a metabolic regulator and a redox-sensitive protein (Tsutsui et al., 2011), was also assessed. TXNIP expression was not altered

by any of the drug treatments pre-ischaemia or during ischaemia relative to the controls (*p=0.26 and 0.94* respectively) **[Figure 4.9]**.

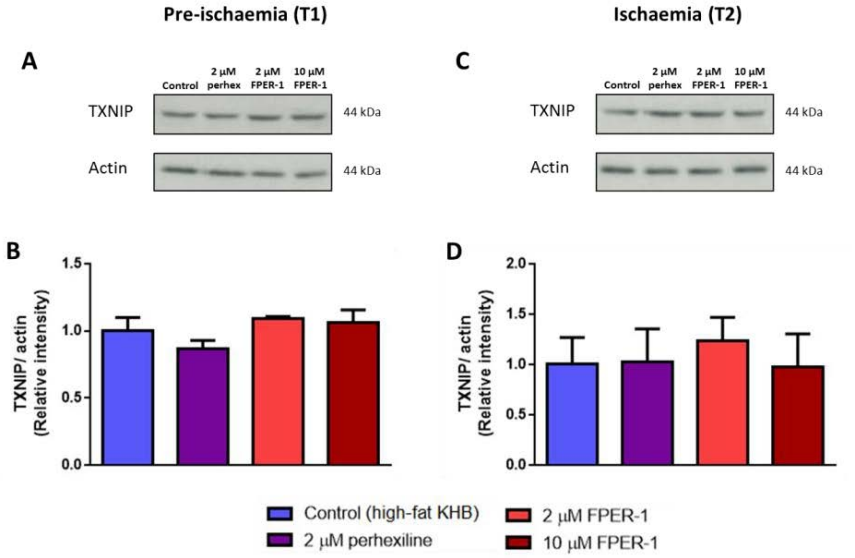

Figure 4.9. Effects of perhexiline and FPER-1 on TXNIP expression following pre-ischaemic perfusion (T1), and after subsequent ischaemia (T2)

Hearts were perfused for 30 min pre-ischaemia with either 1) control (high-fat KHB), 2) 2 µM perhexiline, 3) 2 µM FPER-1 or 4) 10 µM FPER-1. **A:** Representative Western blots for total TXNIP and loading control actin at T1. **B:** Normalised mean TXNIP over actin at T1. **C:** Representative Western blots for total TXNIP and loading control actin at T2. **D:** Normalised mean TXNIP over actin at T2. Data are presented as mean ±SEM; n = 6-8 mice.

Similarly, expression of the mitochondrial uncoupling proteins UCP3 and adenine nucleotide translocase (ANT), which are involved in the response to oxidative stress (Tsutsui et al., 2011), were not changed by 2 µM perhexiline or FPER-1 (2 or 10 µM) perfusion pre-ischaemia (*p=0.96* and *0.75* respectively) **[Figure 4.10A-D]** or in ischaemia (*p=0.99* and *0.96* respectively) relative to the controls **[Figure 4.10E-H]**.

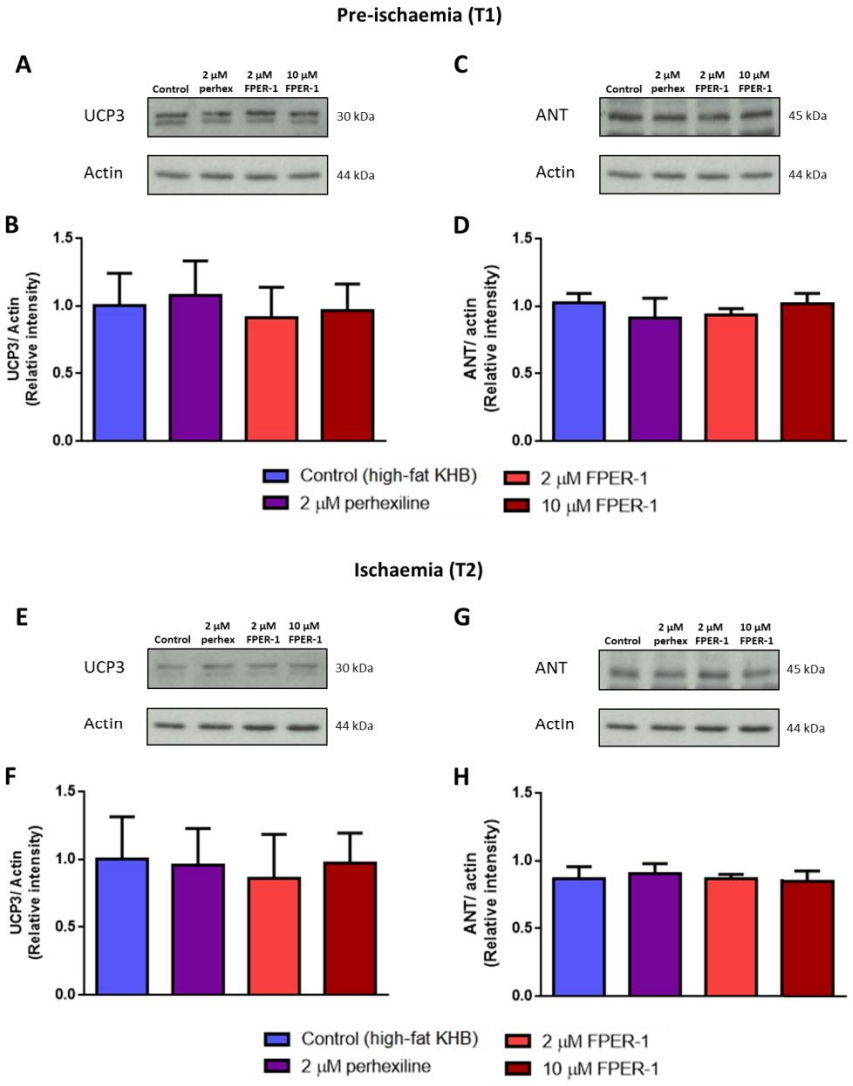

Figure 4.10. Effects of perhexiline and FPER-1 on UCP3 and ANT expression following pre-ischaemic perfusion (T1), and after subsequent ischaemia (T2)

Hearts were perfused for 30 min pre-ischaemia with either 1) control (high-fat KHB), 2) 2 µM perhexiline, 3) 2 µM FPER-1 or 4) 10 µM FPER-1. **A:** Representative Western blots for total UCP3 and loading control actin at T1. **B:** Normalised mean UCP3 over actin at T1. **C:** Representative Western blots for total ANT and loading control actin at T1. **D:** Normalised mean ANT over actin at T1. **E:** Representative Western blots for total UCP3 and loading control actin at T2. **F:** Normalised mean UCP3 over actin at T2. **G:** Representative Western blots for total ANT and loading control actin at T2. **H:** Normalised mean ANT over actin at T2. Data are presented as mean ±SEM; n = 6-8 mice.

4.3.7. Effects of perhexiline and FPER-1 on lactate release post-ischaemia

Finally, post-ischaemic lactate release in coronary effluent was not altered by pre-ischaemic perfusion of 2 µM perhexiline or FPER-1 (2 or 10 µM) relative to the control (*p>0.*99) **[Figure 4.11]**.

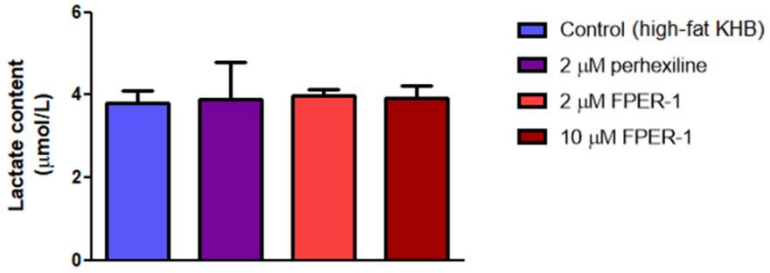

Figure 4.11. Effects of perhexiline and FPER-1 on lactate release post-ischaemia

Lactate content in coronary effluent collected at 5 min reperfusion, from hearts perfused for 30 min pre-ischaemia with either control (high-fat KHB), 2 µM perhexiline, 2 µM FPER-1 or 10 µM FPER-1, which had been subjected to ischaemia/reperfusion (hearts reperfused in control high-fat KHB). Data are presented as mean ±SEM; n = 3 mice.

4.4. Discussion

Perhexiline is a known CPT1B inhibitor (Kennedy et al., 1996), however, it is now believed that this mechanism may not underlie its therapeutic effects (George et al., 2016), and additional proteins may instead be involved in perhexiline-mediated protection (Balgi et al., 2009; Gatto et al., 2013; Ngo et al., 2011). As such, the main aim of the studies described in this chapter was to gain insights into the mechanism(s) behind the perhexiline-induced protection observed in Chapter 3 by assessing metabolic and pro-survival proteins. The secondary aim was to assess whether the novel derivative FPER-1 targets the same proteins.

4.4.1. Effects of perhexiline and FPER-1 on the cardiac contractility-relaxation pathway

The results of Chapter 3 (section 3.3.4) provided evidence that 2 µM perhexiline and 10 µM FPER-1 enhance cardiac contractility and relaxation during normoxia in the isolated heart.

The results of the present chapter provide novel evidence that both perhexiline and FPER-1 decrease PLB activity, judged by increased phosphorylation, during normoxic high-fat perfusion. This is consistent with evidence that high-fat increases PLB activity, as demonstrated in isolated rat ventricular myocytes (Relling et al., 2006). The level of phosphorylation observed in the present study at Ser16 was similar in all three treatment groups, but a clear dose-dependent effect was present with the two concentrations of FPER-1 for phosphorylation at Thr17. A previous study in rat hearts subjected to ischaemia/reperfusion revealed that an increase in p-PLB^{Thr17} played a greater role in post-ischaemic mechanical recovery than p-PLB^{Ser16} (Said et al., 2003). The authors used transgenic mice to replace either the Ser16 or Thr17 site with an alanine residue and found that mutant mice with Thr17 replaced showed substantially impaired post-ischaemic contractile and relaxation recovery, whereas contractile recovery was only marginally depressed and relaxation recovery unchanged with Ser16 replaced. The increased phosphorylation at Thr17 in the present study mirrored the increases in the markers of cardiac contractility and relaxation in Chapter 3 (section 3.3.4). Taken together these data suggest that PLB phosphorylation at Thr17 plays a greater role in enhancing cardiac contractility/relaxation during normoxic perfusion with perhexiline or FPER-1.

The present results also demonstrated that PLB phosphorylation during ischaemia was not altered at either site with perhexiline or FPER-1 relative to the control and thus not involved with the drug-induced protection observed post-ischaemia in Chapter 3. However, it should be noted that PLB phosphorylation at both residues was increased in Langendorff-perfused rat hearts when assessed at the end of global ischaemia (Mattiazzi et al., 2004) and this

increase was greater and more sustained in paced hearts (Mundiña-Weilenmann et al., 2003). Therefore if PLB phosphorylation were increased by ischaemia in the control group of the present study, any changes in phosphorylation induced by perhexiline or FPER-1 may have been masked and difficult to separate from the ischaemia-induced changes.

4.4.2. Effects of perhexiline and FPER-1 on fatty acid metabolism

The results of Chapter 3 (section 3.3.5 and 3.3.6) also demonstrated that perhexiline and FPER-1 improved cardiac function post-ischaemia. As perhexiline is a CPT1B inhibitor, an obvious question was whether these effects were associated with CPT1B modulation.

To date, studies have shown somewhat surprisingly, that CPT1 may not be a key mechanism for perhexiline-induced anti-ischaemic protection. Kennedy and colleagues (2000) demonstrated that despite improvements in diastolic function, perhexiline-treated rat hearts subjected to low-flow ischaemia had no change in long chain acyl-carnitine levels (the product of CPT1 activity) whilst Unger and colleagues (2005) observed no change in palmitate oxidation following perhexiline pre-treatment in the working rat heart model, even though cardiac mechanical efficiency was improved. However, neither of these studies investigated the effect of perhexiline on CPT1 expression. In the present study, CPT1B expression was not significantly altered by perhexiline or FPER-1 at 2 µM in hearts subjected to ischaemia, but *was* reduced by 10 µM FPER-1. Recent work from Signal Pharma demonstrated using an *in vitro* spectrophotometric assay that FPER-1 at four times the concentration of perhexiline was required to inhibit rat CPT1 activity by 50% (Tseng et al., 2017). These findings may explain why the effects on CPT1B expression were more

pronounced with 10 µM FPER-1, as a 5-fold greater dose than perhexiline was used. Irrespective, the present results suggest that FPER-1 at a concentration that produced similar improvements in cardiac function post-ischaemia to 2 µM perhexiline had the additional effect of decreasing CPT1B expression.

4.4.3. Effects of perhexiline and FPER-1 on glucose metabolism

In light of the CPT1B results it is reasonable to hypothesise that the anti-ischaemic effects observed with perhexiline and FPER-1 were, at least in part, due to the upregulation of glucose metabolism (i.e. PDH activation) rather than CPT1 inhibition. Targeting these two metabolic pathways together would allow myocardial energetics and thus efficiency to be improved to a greater extent.

As expected, in normoxia, PDH phosphorylation was not altered with either perhexiline or FPER-1, mirroring the lack of change in cardiac function under this condition, despite the presence of high fat (Chapter 3, section 3.3.3). However, in ischaemia all three treatment groups elicited significant decreases in PDH phosphorylation (indicative of PDH activation), suggesting improved glycolysis-glucose oxidation coupling and glucose metabolism during ischaemia. These results are consistent with those of Yin and co-workers (2013) who were the first to show through proteomics and immunoblotting that perhexiline given orally, induced PDH activation in the mouse heart. The present results extended these findings by providing evidence that under ischaemic conditions, PDH Ser293 and Ser300 are the target isoforms for these metabolic agents. In addition, the present results confirmed that at both doses, FPER-1 works in a similar manner to perhexiline.

The increased PDH activity during ischaemia provides insights into the mechanisms behind the post-ischaemic protection observed to some extent in all three treatment groups in the functional data of Chapter 3. These data also agree with studies on other FA oxidation inhibitors such as oxfenicine (Higgins et al., 1980) and trimetazidine (Kantor et al., 2000), which increased PDH activation during ischaemic conditions in the isolated rat heart. In addition, PDH activation (by dichloroacetate) protected against ischaemia/reperfusion injury in Langendorff mouse hearts (Ussher et al., 2012). Further complementing the present data, Gehmlich et al. (2015) observed changes in the glycolytic, glycerol and pentose pathways when mice with hypertrophic cardiomyopathy were injected with perhexiline, indicating increased glucose utilisation and thus carbohydrate metabolism. Therefore, in combination, the present results and those of previous studies suggest that perhexiline's anti-ischaemic properties are in part mediated by the oxygen sparing effect of upregulated glucose metabolism. Importantly, the present results indicate that this is replicated by FPER-1.

Finally, the present results showed no change in PDH phosphorylation status with any of the treatments during the extended normoxic perfusion (70 min). These data confirm that, in the present model, perhexiline and FPER-1 only upregulated PDH in the presence of ischaemia and metabolic dysfunction, but not under normoxic, albeit high fat, conditions. Nonetheless, it is important to note that Yin and colleagues (2013) did observe an increase in PDH activation in healthy non-ischaemic mice following 4-week oral perhexiline treatment. This suggests that chronic drug exposure may be required to activate PDH in the absence of an ischaemic insult; even rat cardiomyocytes exposed to 2 µM perhexiline for 48 h had no change in glucose oxidation (Unger et al., 2005). However, the absence of drug-induced PDH

activation in normoxia in the present study may also be due to the 1.2 mM palmitate FA concentration used. High fat levels can antagonise PDH activity through the Randle cycle as discussed in Chapter 1 (section 1.7.6). Furthermore, in Langendorff rat hearts perfused with only 0.5 mM palmitate, PDH was mostly inactivated during both normoxia and ischaemia (Veitch et al., 1995). In support of this concept, ranolazine increased PDH activity in normoxic rat hearts perfused for 30 min with 0.4 or 0.8 mM palmitate but not with 1.2 mM palmitate (Clarke et al., 1996). With this in mind, it would be interesting to see whether perhexiline and FPER-1 can upregulate PDH in hearts perfused with a palmitate concentration lower than 1.2 mM.

Regarding GSK3αβ, whilst there was no change in pre-ischaemic phosphorylation, both perhexiline and FPER-1 increased GSK3αβ phosphorylation at Ser21/9 in ischaemia, suggestive of GSK3αβ inactivation. It may be that this ischaemic inhibition contributed to the metabolic mechanisms by which perhexiline and FPER-1 induced the anti-ischaemic effects on LV function described in Chapter 3 (section 3.3.5 and 3.3.6). In support of this, in working rat hearts subjected to global ischaemia, perfusion with GSK3 inhibitor SB-216763 improved post-ischaemic LV function and this was associated with a decrease in glycolysis and H^+ ion production but an increase in glucose oxidation (Omar et al., 2010). The results of that study therefore suggested that GSK3αβ inhibition during ischaemia improves glycolysis-glucose oxidation coupling, which is normally dysregulated during low oxygen conditions. Moreover, in the present study, the fact that perhexiline and FPER-1 inhibited GSK3αβ in ischaemia alone complements the finding that these drugs also activated PDH in ischaemia only. It may be that GSK3αβ is involved in PDH regulation as suggested by Hoshi and colleagues (1996)

who showed that GSK3 activity led to PDH phosphorylation and inactivation both *in vitro* and in hippocampal cultures, resulting in mitochondrial dysfunction. Similarly, Keung and colleagues (2013) showed that oxfenicine also inhibited GSK3 activity in hearts from obese mice whilst also increasing PDH activity.

4.4.4. Effects of perhexiline and FPER-1 on proteins upstream of GSK3αβ

The activity of GSK3αβ is inhibited via phosphorylation at Ser21/9 by Akt and ERK1/2 (Beurel et al., 2015), with this inhibition demonstrated as cardioprotective in ischaemia (Hausenloy and Yellon, 2007). Moreover, Akt and/or ERK1/2 activation is implicated as a possible cardioprotective mechanism of the metabolic drug HO-3089, a poly (ADP-ribose) polymerase (PARP) inhibitor (Kovacs et al., 2009). Following 25 min global ischaemia in isolated rat Langendorff hearts, HO-3089 improved cardiac recovery and energetic status, reduced oxidative damage and these changes were accompanied by an upregulation of Akt and ERK1/2 and downregulation of GSK3 (Kovacs et al., 2009). This study suggests that Akt and ERK activation may have a role in improving cardiac metabolism.

In the present study Akt phosphorylation was not changed during normoxia, even when drug perfusion was extended from 30 to 60 min, whilst the changes observed with 2 µM perhexiline and 10 µM FPER-1 during ischaemia were not statistically significant. By contrast, Andreadou and co-workers (2013) found that ranolazine induced Akt activation-GSK inhibition in rabbit hearts submitted to 30 min global ischaemia and this was associated with reduced infarct size. On the other hand, Ileana and colleagues (2017) observed no change in Akt phosphorylation in ranolazine-treated skeletal muscle cells exposed to oxidative stress.

These studies suggest that the model used may influence which pathways are upregulated by metabolic agents. In the global ischaemia model used in the present study, activation of Akt does not appear to be a key mechanism of perhexiline- or FPER-1-induced GSK3αβ inhibition although it may play a minor role given the non-significant increase in Akt phosphorylation in ischaemia complemented that of GSK3αβ inhibition and PDH activation achieved during ischaemia.

The activity of ERK1/2, involved in cell survival and proliferation (Hausenloy and Yellon, 2007), and the subsequent inhibition of GSK3 has been identified as cardioprotective during ischaemia in isolated Langendorff rat hearts (Lin et al., 2011) and isolated Langendorff mouse hearts (Kabir et al., 2015). Grassian and colleagues (2011) also demonstrated in extracellular matrix attached cells that ERK is involved in regulating and promoting PDH flux. However, in the present study, perhexiline or FPER-1 did not alter ERK1/2 phosphorylation during normoxia or in ischaemia. These results contrast with the findings that trimetazidine upregulates ERK1/2 activity during normoxia in mice *in vivo* (Z. Liu et al., 2016) and that ranolazine activates ERK1/2 in isolated rabbit hearts subjected to ischaemic injury (Efentakis et al., 2016). Conversely, ranolazine did not upregulate ERK1/2 in healthy rat hearts (Fu et al., 2013). The present findings thereby suggest that like Akt, ERK1/2 is not a key molecular target of perhexiline or FPER-1.

4.4.5. Effects of perhexiline and FPER-1 on redox-sensitive proteins

Cardiac metabolism and reactive oxygen species (ROS) production are interrelated processes that take place within the mitochondria. As discussed in Chapter 1 (section 1.7.8), TXNIP is

involved in decreasing glucose metabolism and increasing oxidative stress (Wang and Yoshioka, 2017). As such, downregulation of TXNIP is considered therapeutic in cardiovascular diseases characterised by ischaemia. Furthermore, perhexiline itself decreased TXNIP expression in ischaemia/reperfusion LV biopsies from patients undergoing coronary artery bypass surgery (Ngo et al., 2011). However, in the present study, perhexiline did not alter TXNIP expression in normoxic or ischaemic hearts and neither did FPER-1. Other proteins involved in regulating oxidative stress alone in the settings of dysregulated cardiac metabolism, are the uncoupling proteins UCP3 and ANT (Loudon et al., 2016), however it is unclear whether they are protective or harmful during ischaemia (Murray et al., 2008). Herein, neither perhexiline nor FPER-1 altered UCP3 or ANT expression during normoxia or in ischaemia relative to that seen in control hearts under the same conditions. Therefore this suggests that, as with TXNIP, these redox-sensitive proteins are not involved in the anti-ischaemic mechanisms of perhexiline or FPER-1 *ex vivo*.

However, it should be acknowledged that due to the study design it was not possible to determine the effects of ischaemia alone on protein expression. Thus, it is possible that there was no change in TXNIP, UCP3 or ANT expression during ischaemia for the drugs to modulate. The evidence in the literature on these three proteins is actually confused. To expand, Yoshioka and colleagues (2012) demonstrated that TXNIP deletion in mice improved post-ischaemic cardiac function, but induced mitochondrial impairment and PDH inactivation. TXNIP deletion in fact increased oxidative phosphorylation uncoupling and decreased glycolysis-glucose oxidation coupling. Regarding UCP3, in left ventricles from rat hearts subjected to global ischaemia, mitochondrial UCP3 levels were considerably increased

(Safari et al., 2014) whereas UCP3 expression was unchanged in ischaemic pig hearts (McFalls et al., 2006). Concerning ANT, mitochondrial expression was surprisingly decreased after only 5 min of global ischaemia in the isolated rat heart (Duan and Karmazyn, 1989) and reduced by 20% compared to the control value in another similar study (Asimakis and Conti, 1984). This reduction in ANT expression (and activity) during low-flow ischaemia was correlated to reduced oxidative phosphorylation (Lochner et al., 1981). Thus, in light of the literature it is difficult to deduce how TXNIP, UCP3 or ANT may have been affected by ischaemia in the present study. Nevertheless, it can be argued that neither perhexiline, nor FPER-1 altered their levels, relative to control, during ischaemia.

4.4.6 Effects of perhexiline and FPER-1 on lactate release

Lactate levels are elevated in the heart during ischaemia due to an increase in anaerobic glycolysis, and this was associated with PDH inactivation when measured in the isolated rat heart (Patel and Olson, 1984), thus suggesting glycolysis-glucose oxidation uncoupling. Clarke and co-workers (1993) also observed significant elevations in lactate release in guinea pig hearts subjected to low-flow ischaemia, accompanied by reduced tissue adenosine triphosphate (ATP) content. This raised the possibility that a decrease in lactate content with perhexiline or FPER-1 treatment would indicate improved glycolysis-glucose oxidation coupling, complementing the increase in PDH activity. However, pre-ischaemic perhexiline or FPER-1 perfusion did not alter lactate content in the post-ischaemic cardiac effluent samples, relative to the control. These results corroborate those of Kennedy and colleagues (2000) who observed no change in perfusate lactate release during ischaemia or reperfusion in rat hearts treated with 2 µM perhexiline or 0.5 mM oxfenicine. Interestingly, perhexiline did

inhibit lactate release from rat hearts during normal flow (Kennedy et al., 2000) and a perhexiline-induced increase in lactate utilisation was identified in the normoxic working rat heart model (Jeffrey et al., 1995). These studies suggest that perhexiline alters lactate release/utilisation in normoxia, a condition that was not assessed in the present study. Conversely ranolazine did reduce lactate release during low-flow ischaemia in the guinea pig heart (Clarke et al., 1993) and trimetazidine treatment supressed lactate plasma levels during cardiac ischaemia in the anaesthetised rat (Kara et al., 2006). This suggests that there may be mechanistic differences between these FA oxidation inhibitors and perhexiline/FPER-1.

4.4.7. Study limitations

To assess the molecular mechanism(s) of perhexiline and FPER-1, Western blotting was used in the present study. This technique allows protein detection, without directly assessing activation, and thus can only indicate phosphorylation status from which changes in activation can be suggested. Therefore, it will be important in future studies, where possible, to use colorimetric or fluorometric assays which directly measure protein activity to fully interpret the present data. Importantly, as discussed in section 4.4.5, the effect of ischaemia alone on protein expression/phosphorylation was not measured therefore making it difficult to fully interpret the effects of drug treatment under this condition, but this could be resolved by carrying out gel electrophoresis with a mix of normoxic and ischaemic samples. Moreover, the n values used in the studies described in this chapter were based on power calculations from previous molecular work. In light of the trends observed with CPT1B, PDH

and Akt, retrospective power calculations revealed that group sizes of 9 to 15 would be required to fully interpret these results.

Furthermore, although lactate content was not changed in the effluent samples from treated hearts, the number of samples used was low at only three per group. In addition, lactate was only measured post-ischaemia at one time point. As indicated above, lactate content may have been altered by the drugs during normoxia as previously observed (Kennedy et al., 2000), and lactate content may have been reduced post-ischaemia relative to normoxic levels by the drugs used. In future studies, it would be helpful to take several samples for lactate assay at different time points pre- and post-ischaemia. It would also be useful to consider lactate levels within the cardiac tissue itself. Lastly, although key metabolic proteins such as PDH were investigated, it cannot be confirmed that changes in these proteins were associated with increases in cardiac energetics and ATP production as these parameters were not directly assessed.

4.4.8. Future considerations

With regards to the points discussed in section 4.4.7, it would be important to consider using activity assays i.e. for PDH and GSK3αβ to further validate the findings of this chapter. The use of metabolomic and proteomic screening on Langendorff cardiac samples perfused with perhexiline or FPER-1 would also be useful to further identify proteins and metabolites, in a less biased fashion, which are altered in this model and may be connected to the changes observed in the present study. It would also be useful to assess the effect of pre-ischaemic drug treatment on the expression/phosphorylation of the discussed proteins post-ischaemia

(during reperfusion), as previous studies have demonstrated changes in these proteins at this timepoint (Hausenloy and Yellon, 2007; Ngo et al., 2011; Liu et al., 2014). Additionally, measuring palmitate and glucose oxidation and/or uptake would be useful to fully determine the metabolic effects of these drugs.

Importantly, a direct assessment of ATP production and/or mitochondrial respiration would be necessary to confirm that the drug-induced protection and protein changes observed were associated with improvements in cardiac energetics. Such assessments can be carried out by measuring ATP production either with colorimetric assay kits or bioluminescent assays following mitochondria isolation (Drew and Leeuwenburgh, 2003). Furthermore, energy sensing proteins such as 5' adenosine monophosphate-activated protein kinase (AMPK) would be useful markers of cardiac energetic status and can easily be assessed by Western blotting (Hardie et al., 2012). Another approach would be to measure oxygen consumption rate (OCR) as a marker of mitochondrial respiration (and thus ATP production) in cultured mouse cardiomyocytes treated with perhexiline or FPER-1 in combination with the highly sensitive Seahorse technique. The Seahorse assay was previously used to measure mitochondrial bioenergetics in rat cardiomyocytes following *in vivo* treatment with ranolazine or trimetazidine (Fang et al., 2012). In addition, the use of cultured cardiomyocytes would allow for various doses of the novel drug FPER-1 to be tested as well as various drug incubation times.

Lastly, it would be important to consider the effects of these drugs following chronic treatment either *ex vivo* or *in vivo* to allow comparison with the results obtained in the isolated heart model reported here, in which drug treatment was acute.

4.4.9. Conclusion

The aim of the studies described in this chapter was to identify possible mechanisms behind the protective effects induced in mouse hearts by perhexiline and its analogue FPER-1. Herein novel evidence is provided that both agents upregulate the cardiac contractility-relaxation pathway by increasing PLB phosphorylation. This would be expected to decrease PLB inhibition over the sarco-endoplasmic reticulum Ca^{2+}-ATPase (SERCA) pump involved in Ca^{2+} cycling. Whether this effect was direct or secondary to increases in cardiac energetics remains to be elucidated. Novel evidence is also provided that perhexiline increases glucose metabolism by upregulating PDH activity through dephosphorylation of Ser293 and Ser300. These effects were complemented by a decrease in GSK3αβ activity as judged by Ser21/9 phosphorylation, a change that has been shown to inhibit PDH activity in neuronal cells. Importantly, these proteins were similarly targeted by FPER-1, the 10 μM dose having a greater effect on GSK3αβ, mirroring the functional results of Chapter 3. The present data also indicated that the pro-survival pathways Akt and ERK1/2, and the redox-sensitive proteins TXNIP, UCP3 and ANT, are not targets of perhexiline or FPER-1 in this model.

Taken together, these results confirm the potential of both perhexiline and FPER-1 to correct metabolic dysfunction following ischaemia and importantly, provide evidence that these drugs target the same non-metabolic protein during normoxia.

Chapter 5: Investigating perhexiline and FPER-1 acute toxicity and pharmacokinetics *in vivo*

Chapter 5: Investigating perhexiline and FPER-1 acute toxicity and pharmacokinetics *in vivo*

5.1. Introduction

The results of the previous two chapters demonstrated the cardioprotective potential and mechanisms of perhexiline and the novel derivative fluoroperhexiline-1 (FPER-1), in the isolated mouse heart. Following these findings, these agents were assessed *in vivo*.

As outlined in Chapter 1 (section 1.9), perhexiline was considered useful against angina, having minimal effects on the neurohormonal system (Ashrafian et al., 2007b) and being effective in patients who were non-responders of conventional treatments (White and Lowe, 1983). Unfortunately, perhexiline's therapeutic use was curtailed in the 1980s, following the emergence of severe neuro- and hepatotoxicity in several patient case studies (discussed in Chapter 1, section 1.10.1), which caused the rapid withdrawal of perhexiline from clinical use (Shah et al., 1982).

Following investigations undertaken to identify the cause of perhexiline-induced toxicity, it was discovered that those suffering from severe toxicity had significantly higher drug plasma levels compared to those experiencing no symptoms (Singlas et al., 1978a). It was later established that the high drug plasma levels in subsets of patients were related to the heterogeneity of perhexiline metabolism by cytochrome P450 2D6 (CYP2D6) (detailed in Chapter 1, section 1.10.2). Genetic polymorphisms in CYP2D6 caused some patients to be 'poor metabolisers' culminating in high and toxic drug plasma levels, resulting in sustained

systemic carnitine palmitoyltransferase 1 (CPT1) inhibition and thus systemic lipidosis (Meier et al., 1986). Due to this excessive CPT1 inhibition, isoforms in the liver (CPT1A) and brain (CPT1C) were undesirably targeted alongside the cardiac isoform (CPT1B), resulting in neuro- and hepatotoxicity. To avoid these effects, but remain therapeutic clinically, Horowitz and colleagues (1986) showed that plasma perhexiline concentrations should be maintained between 0.15 – 0.6 mg/L (0.5 – 2.2 μM). However, the necessity for constant plasma level monitoring proved unacceptably arduous. Furthermore, in patients with existing liver impairment or those on other CYP2D6-metabolised drugs, extra care would be required with perhexiline therapy, thereby reinforcing the need for a new drug.

FPER-1 is hypothesised to retain similar efficacy as perhexiline without the metabolic liability or toxicity (Tseng et al., 2017). In fact, the results of the previous chapters indicated that FPER-1 *does* retain perhexiline's efficacy *ex vivo* and therefore it was important to test both agents *in vivo*. However, prior to this it was essential to first assess potential toxicity and to identify optimal drug doses.

Aims:

1. To determine a safe and optimal route of drug administration *in vivo* in mice.

2. To determine a safe, non-toxic and optimal dose of perhexiline and FPER-1 *in vivo*.

5.2. Methodology

A detailed method is presented in Chapter 2, sections 2.7 to 2.10. Briefly, male C57Bl/6 mice (18 – 23 g) were used in one of four protocols (A to D) **[Figure 2.12]** with drugs prepared in 0.5% sodium carboxymethyl cellulose (NaCMC)/0.1% vehicle solution.

Protocol A (pilot study): Intraperitoneal injection (i.p) of vehicle, 30 mg/kg perhexiline or FPER-1 once daily for an intended 4 weeks (see Results, section 5.3.1) in mice 1 week post-abdominal aortic constriction (AAC), conducted by Dr James Clark, London. Post-mortems were conducted on mice found dead.

Protocol B: Oral gavage of 10 or 20 mg/kg perhexiline or FPER-1 once daily for 7 days in healthy mice, organs being harvested 24 h post-final dose.

Protocol C: Oral gavage of 50 mg/kg perhexiline or FPER-1 twice daily for 7 days in healthy mice, organs being harvested 1, 8 or 24 h post-final dose.

Protocol D: Oral gavage of 70 mg/kg perhexiline or FPER-1 once daily for 7 days in healthy mice, organs being harvested 1, 8 or 24 h post-final dose.

At the point of harvest, blood was collected, plasma extracted and subjected to drug pharmacokinetics assessment by Professor Benedetta Sallustio's group, Australia (section 2.8) and colorimetrically assayed for alanine transaminase (ALT) content (hepatotoxicity marker; section 2.10). The right liver lobe was also isolated and fixed in 4% formaldehyde for histological analysis of liver damage, inflammation and fibrosis by staining sections with haematoxylin and eosin (H&E) or Van Gieson (section 2.9).

5.2.1. Statistical analysis

All data in this chapter are expressed as means ±standard error of the mean (SEM). Drug plasma levels following 50 or 70 mg/kg perhexiline or FPER-1 dosing were statistically compared using two-way analysis of variance (ANOVA) with Bonferroni post-hoc test. One-way ANOVA with Bonferroni post-hoc test was used to statistically compare ALT plasma levels between untreated controls and the vehicle-treated group as well as between drug-treated groups and the vehicle-treated group at 1, 8 and 24 h. Graphpad Prism version 6.0 was used for analysis. $p<0.05$ was considered statistically significant. Number of mice used is indicated in the figure legends.

5.3. Results

5.3.1. Survival and body weight of mice following perhexiline or FPER-1 administration

In protocol A, daily i.p injection of 30 mg/kg perhexiline or FPER-1 in AAC mice proved lethal with 100% mortality in both drug groups by day 7 **[Figure 5.1]**. Mortality occurred as early as day 2 with 50% of injected mice dead by day 5 with perhexiline and day 6 with FPER-1. Furthermore, all perhexiline-injected mice and 5 out of 6 FPER-1-injected mice experienced weight loss >10% during the 7-day treatment **[Table 5.1]**. Drug-treated mice also appeared bloated with swollen abdomens and experienced reduced mobility prior to death. All vehicle-injected mice survived to day 7 although 4 out of 6 showed >10% weight loss suggesting intolerance to the injections and/or vehicle solution used.

In contrast, in healthy mice, daily oral gavage of perhexiline or FPER-1 at 10, 20 or 70 mg/kg induced no mortality **[Figure 5.1]**. Additionally, weight loss >10% did not occur with the low

doses (10 or 20 mg/kg), and only 1 out of 9 mice showed >10% weight loss with 70 mg/kg perhexiline or FPER-1 gavage **[Table 5.1]**. In vehicle-gavaged mice, no weight loss >10% was observed and 100% survival achieved. However, twice-daily oral gavage with 50 mg/kg perhexiline or FPER-1 led to mortality (2 out of 9 mice) by day 7, the first death occurring at day 3 with FPER-1 and day 4 with perhexiline **[Figure 5.1]**. Moreover, 4 out of 9 mice gavaged twice daily with 50 mg/kg perhexiline and 3 out 9 mice given FPER-1 had weight loss >10% during the 1-week study **[Table 5.1]**.

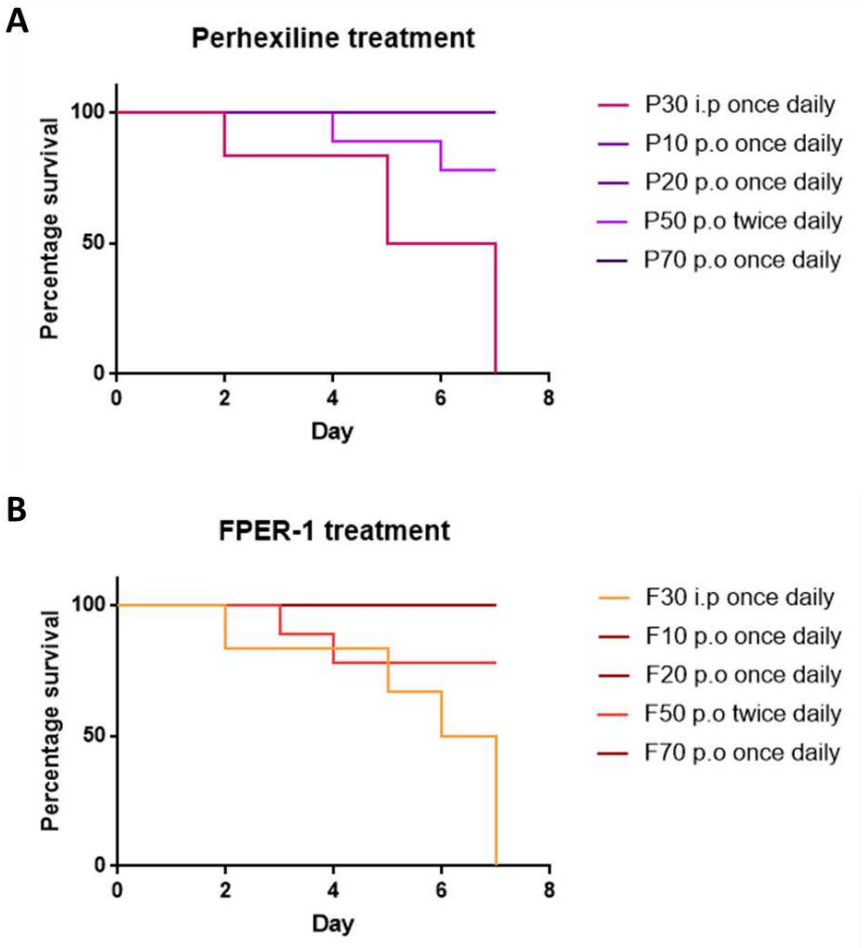

Figure 5.1. Survival of mice following daily administration of perhexiline or FPER-1

Kaplan-Meier graphs showing percentage survival for **A:** perhexiline-treated mice & **B:** FPER-1-treated mice.

i.p, intraperitoneally; p.o, orally. n = 6 mice for i.p; n = 2 mice for 10 and 20 mg/kg p.o and n = 9 mice for 50 and 70 mg/kg p.o.

Table 5.1. Weight loss and survival of mice following daily administration of perhexiline or FPER-1

Route of administration	Treatment dose (mg/kg)		% mice with >10% weight loss	% survival at Day 7
i.p once daily	Vehicle		66.7	100
p.o once daily			0	100
p.o twice daily			0	100
i.p once daily	Perhexiline	30	100	0
p.o once daily		10	0	100
p.o once daily		20	0	100
p.o twice daily		50	44.4	78
p.o once daily		70	11.1	100
i.p once daily	FPER-1	30	83.3	0
p.o once daily		10	0	100
p.o once daily		20	0	100
p.o twice daily		50	33.3	78
p.o once daily		70	11.1	100

i.p, intraperitoneally; p.o, orally. n = 6 mice for i.p; n = 2 mice for 10 and 20 mg/kg p.o and n = 9 mice for 50 and 70 mg/kg p.o.

5.3.2. Plasma levels following oral gavage of perhexiline or FPER-1

In protocol B, once-daily oral gavage of 10 mg/kg perhexiline or FPER-1 for 7 days, resulted in undetectable drug plasma levels at 24 h post-final administration. An increase to 20 mg/kg perhexiline only increased the plasma levels to 0.02 ±0.01 mg/L at 24 h post-treatment (n=2) and dosing of 20 mg/kg FPER-1 resulted in 0.1 mg/L FPER-1 (n=2). The perhexiline metabolite hydroxy (OH)-perhexiline was also undetectable with either 10 or 20 mg/kg perhexiline (n=2).

In protocol C, oral gavage of 50 mg/kg perhexiline, given twice daily, achieved perhexiline plasma levels of 0.15 ±0.03 mg/L at 1 h post-final dose (within the therapeutic range: 0.15 – 0.6 mg/L), but was not maintained at 8 or 24 h **[Figure 5.2A]**. In contrast, in protocol D, once-daily dosing of 70 mg/kg perhexiline achieved significantly higher plasma levels at 1 h (0.63

±0.08 mg/L; *p<0.0001*) which remained in the therapeutic range at 8 h (0.22 ±0.07 mg/L), however this was not significantly different from the 50 mg/kg dose (*p=0.05*). Plasma levels of OH-perhexiline following 50 mg/kg perhexiline twice-daily gavage reached 0.09 ±0.03 mg/L at 1 h, and fell at a similar rate as the parent drug over 24 h **[Figure 5.2B]**. However, metabolite levels following 70 mg/kg perhexiline once-daily gavage were significantly higher at 1 h (0.38 ±0.03 mg/L; *p<0.001*) and 8 h post-final dose (0.28 ±0.03 mg/L; *p<0.001*) than those achieved with 50 mg/kg perhexiline.

Twice-daily gavage of 50 mg/kg FPER-1 achieved plasma levels of 3.27 ±0.36 mg/L at 1 h post-final dose and were above perhexilines' therapeutic range at 24 h (1.46 ±0.18 mg/L) **[Figure 5.2C]**. Plasma levels following 70 mg/kg FPER-1 once-daily gavage were not significantly different from those achieved with 50 mg/kg FPER-1 (*p=0.42*), being 3.94 ±0.44 mg/L at 1 h post-final gavage, falling to 1.19 ±0.05 mg/L at 24 h. For both 50 and 70 mg/kg FPER-1, plasma levels were significantly higher than those achieved for perhexiline at the same given dose (*p<0.0001*). In addition, with 50 or 70 mg/kg perhexiline, plasma levels fell to IC_{50} by ~6.5 or 6.2 h respectively, whereas 50 or 70 mg/kg FPER-1 reached IC_{50} at ~19.2 or 18.2 h respectively.

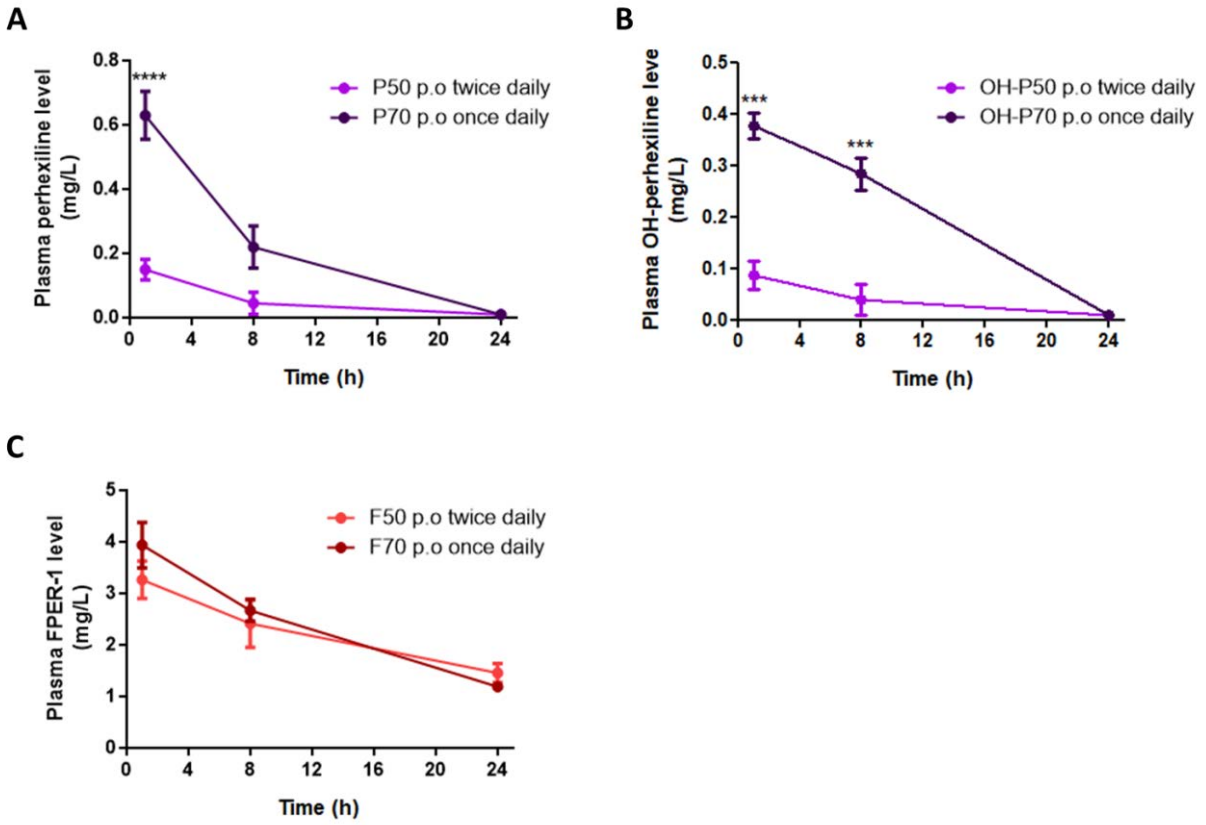

Figure 5.2. Plasma levels of perhexiline, its metabolite and FPER-1 following 50 or 70 mg/kg oral gavage

Plasma levels of **A:** perhexiline & **B:** perhexiline metabolite hydroxy (OH)-perhexiline over 24 h, following oral gavage (p.o) with 50 (P50) or 70 mg/kg perhexiline (P70). **C:** Plasma levels of FPER-1 over 24 h following oral gavage with 50 (F50) or 70 mg/kg FPER-1 (F70). Data are presented as mean ±SEM; n = 3 mice. ****p<0.001* vs 50 mg/kg dose; *****p<0.0001* vs 50 mg/kg dose (Two-way ANOVA followed by Bonferroni post-hoc test).

5.3.3. Liver integrity, fibrosis and function following oral gavage of perhexiline or FPER-1

To assess liver integrity, sections were stained with H&E **[Figure 5.3]**. For reference purposes, a liver section with severe necrosis and loss of integrity is shown by black arrows in **Figure 5.3A** and a section with severe inflammation is shown in **Figure 5.3B** (inflammatory cells stained blue and boxed in red) (Sjölin et al., 2002). Livers harvested from mice gavaged with either perhexiline or FPER-1, irrespective of dose, demonstrated no signs of necrosis,

loss of integrity or severe inflammation compared to livers from vehicle-treated mice; hepatocytes were intact and the hepatic vasculature appeared healthy **[Figure 5.3]**. However, minute clusters of inflammatory cells were present, albeit rarely, in some liver sections from mice treated with 70 mg/kg drug, 24 h post-final gavage (boxed in red) **[Figure 5.3N+V]**.

To assess fibrosis, additional liver sections were stained with Van Gieson, which stains collagen in red (black arrows) **[Figure 5.4]** (Soldatow et al., 2013). As a reference, a liver section with severe pericellular fibrosis and perisinusoidal collagen deposition is shown in **Figure 5.4A** (Tomita et al., 2013), whilst a liver section with thick bundles of proliferous collagen fibres and pseudo-lobules is shown in **Figure 5.4B** (Li et al., 2015). There was no evidence of fibrosis or increased collagen deposition around individual hepatocytes or hepatic vessels in any liver examined from drug-treated mice; they resembled the vehicle-treated livers **[Figure 5.4]**.

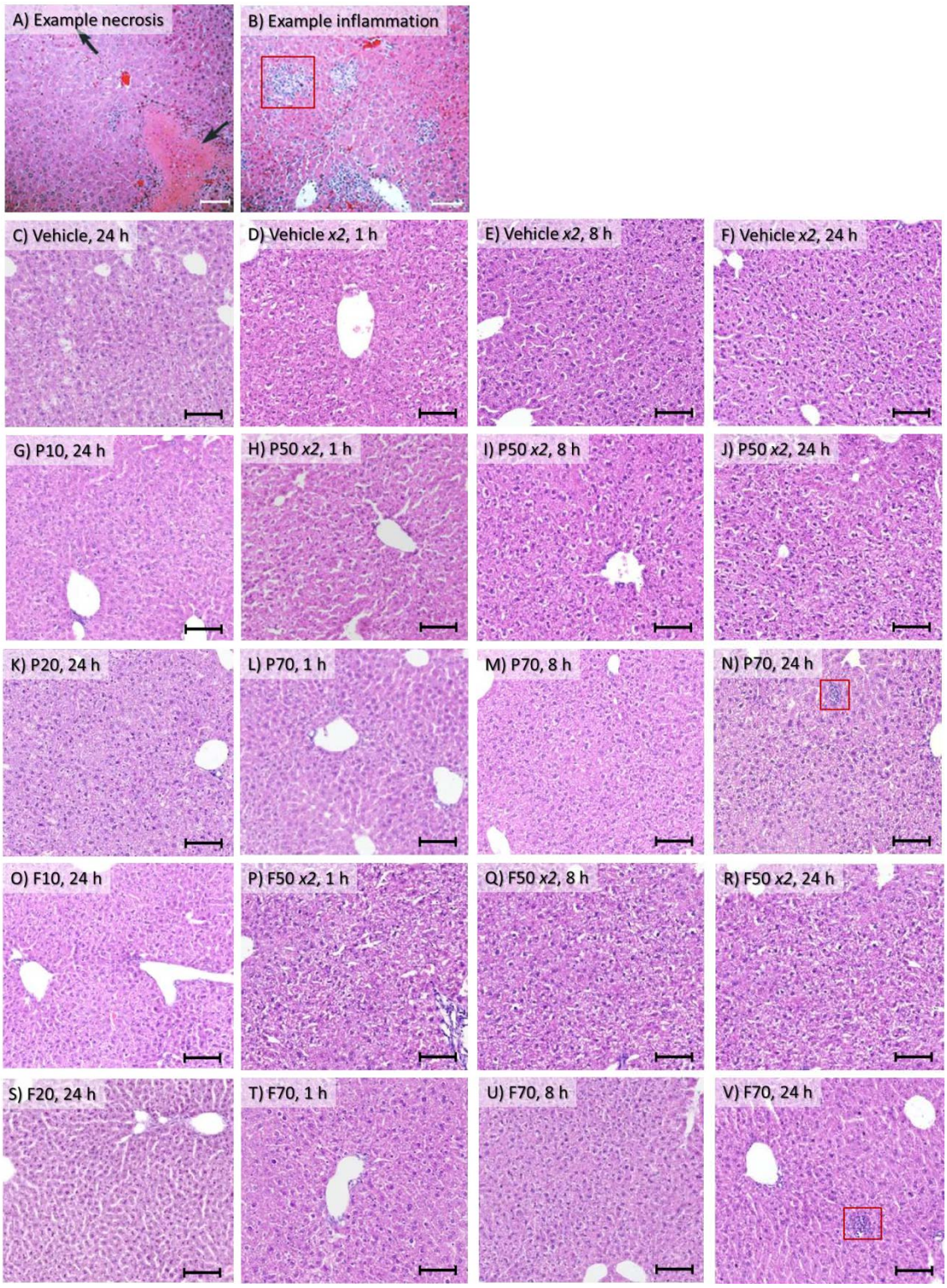

Figure 5.3. Photomicrographs of liver sections stained to assess liver integrity and inflammation following 1-week oral gavage with perhexiline or FPER-1

A+B: For reference, sections showing liver necrosis and inflammatory foci respectively from Sjölin et al. (2002).

Representative liver sections from **C-F:** vehicle-treated mice, **G-N:** perhexiline-treated mice & **O-V:** FPER-1-treated mice. Doses are indicated on sections as: perhexiline (P) or FPER-1 (F) at 10, 20, 50 or 70 mg/kg, given once daily or twice daily (*x2*), harvested at 1, 8 or 24 h post-final gavage. All sections were stained with haematoxylin and eosin and scanned with x20 objective. Scale bar = 100 µm. Black arrow = necrosis. Red box = inflammation. n = 2-3 mice

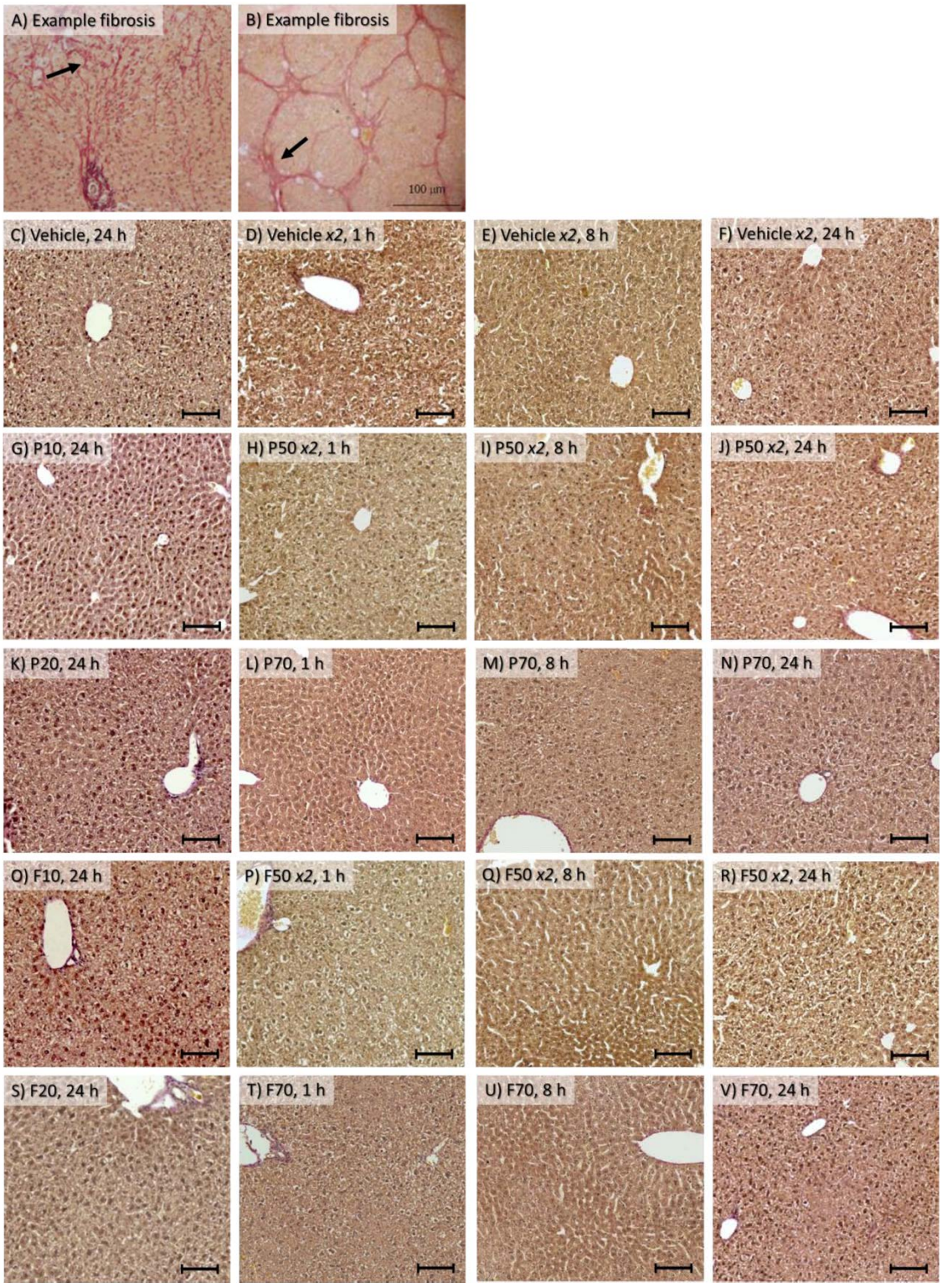

Figure 5.4. Photomicrographs of liver sections stained to assess liver fibrosis following 1-week oral gavage with perhexiline or FPER-1

A+B: For reference, a section showing pericellular liver fibrosis from Tomita et al. (2013) and a section showing fibrosis and pseudo-lobules from Li et al. (2015) respectively.

Representative liver sections from **C-F:** vehicle-treated mice, **G-N:** perhexiline-treated mice & **O-V:** FPER-1-treated mice. Doses are indicated on sections as: perhexiline (P) or FPER-1 (F) at 10, 20, 50 or 70 mg/kg, given once daily or twice daily (*x2*), harvested at 1, 8 or 24 h post-final gavage. All sections were stained with Van Gieson and scanned with x20 objective. Scale bar = 100 µm. Black arrow = fibrosis. n = 2-3 mice.

Liver toxicity was also assessed by measuring plasma ALT levels in mice gavaged with perhexiline or FPER-1 at 50 or 70 mg/kg, doses which achieved detectable drug plasma levels **[Figure 5.5]**.

Plasma ALT levels were not significantly altered following vehicle treatment compared to non-gavaged control mice (*p=0.2*), and were comparable at 1, 8 and 24 h post-final gavage **[Figure 5.5]**. In addition, ALT levels in mice treated with 50 or 70 mg/kg perhexiline or FPER-1 were not significantly different from vehicle-treated mice at 1, 8 or 24 h post-gavage (*p=0.24*, *0.13* and *0.25* respectively).

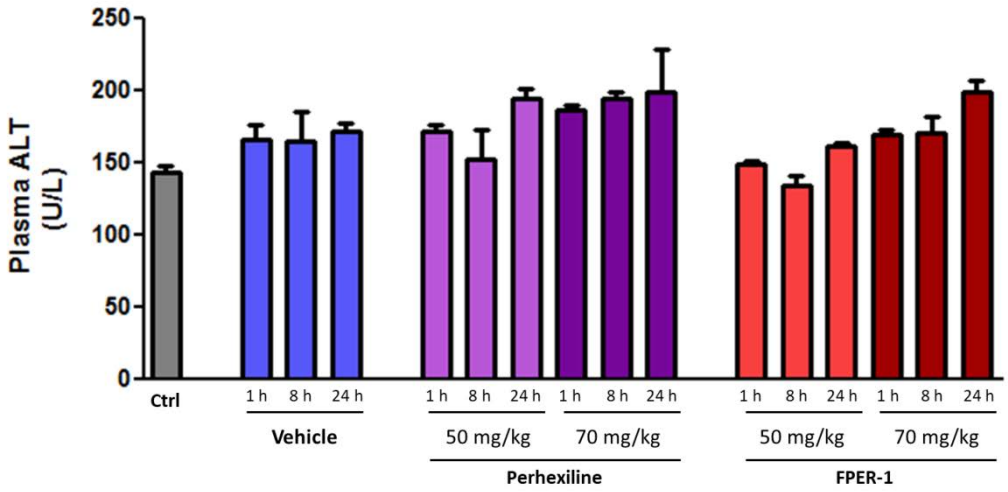

Figure 5.5. Plasma ALT levels following 1-week oral gavage with perhexiline or FPER-1

Plasma ALT levels measured in control (Ctrl) non-gavaged mice, and in mice gavaged with vehicle, 50 mg/kg perhexiline or FPER-1 twice daily, or 70 mg/kg perhexiline or FPER-1 once daily for 1 week, at 1, 8 or 24 h post-final treatment. Data are presented as mean ±SEM; n = 3-6 mice.

5.4. Discussion

In previous cardiovascular animal studies, perhexiline has been given transdermally (Unger et al., 1997), orally using food pellets (Meier et al., 1986; Yin et al., 2013), orally by manual restraint and gavage (Guo et al., 2015; Esposito et al., 2016) or i.p through manual restraint

and injection (Gehmlich et al., 2015). Of these studies, Gehmlich and colleagues (2015) were the only group to use prolonged perhexiline treatment; in their mouse model of hypertrophic cardiomyopathy (HCM), perhexiline injected twice daily at 30 mg/kg for 6 weeks induced improvements in hypertrophy. Therefore, in the present study pilot experiments were first performed on AAC mice (a heart failure model) in collaboration with King's College London, 30 mg/kg perhexiline or FPER-1 being given once daily by i.p injection, 1 week post-surgery. The intention was that mice would be treated for 4 weeks since hypertrophy commences approximately 2 weeks post-surgery (Boguslavskyi et al., 2014). Unfortunately, i.p drug injection proved fatal with significant weight loss and mortality in both drug groups. The vehicle group also showed weight loss. It is known that introducing irritable substances into the peritoneum can lead to peritonitis or painful ileus, which can affect feeding (Turner et al., 2011). Indeed, the mice of the present study showed no obvious signs of inflammation or infection, but had empty bowels suggesting reduced feeding – a possible reason for the weight loss. Therefore, it seems likely the injected drugs accumulated within the abdomen, and were poorly absorbed due to the nature of the vehicle solution used.

The protocol/solution used to prepare FPER-1 in the present study was trialled and tested by Signal Pharma and compatible with this new drug (Tseng et al., 2017). For consistency, perhexiline was prepared in the same manner, which involved dissolving into a starch based solution (0.5% NaCMC in sterile water). NaCMC at concentrations of 10% have been established as non-toxic to the lung, heart, kidney and liver when given orally for 3 months in mice (Mondal and Yeasmin, 2016), but its safety when given i.p is unknown. Gehmlich and

colleagues (2015) who purified perhexiline from perhexiline maleate tablets, dissolved it in 1.8% hydroxylpropyl-beta-cyclodextrin in sterile saline and administered by i.p, reported no severe changes in body weight. This suggests that the present vehicle solution was not appropriate for i.p administration. P.P. Liu and co-workers (2016) also used i.p perhexiline injections in mice with chronic lymphocytic leukaemia without adverse effects, but the nature of the vehicle solution used was not provided.

Having found that i.p injection was not a viable option for these studies alternative routes of administration were considered. In a study on heterotopic ossification in mice, perhexiline was mixed with food powder and given orally for 30 days, with mice fed *ad libitum* (R. Yamamoto et al., 2013). Perhexiline was also added to food pellets in the studies by Meier et al. (1986) and Yin et al. (2013). This method was not attractive because accurate dosing could not be ensured. The alternative, more consistent method of oral treatment is oral gavage: Guo and colleagues (2015) gave perhexiline three times a week for 6 weeks at 10 mg/kg, without side effects, in atherosclerotic mice. Oral gavage of perhexiline is also used in oncology research (Ren et al., 2015; Vella et al., 2015). Moreover, perhexiline was given orally in a 0.5% methylcellulose solution to Sprague-Dawley rats in a toxicology study (Yudate et al., 2012) and orally in 1% methylcellulose in a mouse model of peripartum cardiomyopathy (Stapel et al., 2017) indicating that NaCMC would be appropriate for oral treatment. Therefore, oral gavage was chosen as the route of administration for subsequent experiments, and drug pharmacokinetics conducted on all gavaged mice to determine which perhexiline dose would achieve therapeutic plasma levels (0.15 – 0.6 mg/L) and whether this would be maintained over 24 h.

Oral gavage was commenced at 10 mg/kg as this had been deemed safe by Guo and co-workers (2015) and by preliminary studies with both perhexiline and FPER-1 conducted by Signal Pharma (Tseng et al., 2017). Consistent with these studies, 10 mg/kg perhexiline or FPER-1 led to no fatalities or obvious adverse effects in the present study. Unfortunately, 10 mg/kg perhexiline or FPER-1 did not achieve detectable plasma levels 24 h post-treatment. This was consistent with unpublished work by Signal Pharma in which BALB/c mice were gavaged daily with 10 mg/kg perhexiline or FPER-1 (personal communication). In that study, plasma levels were detectable 1 h post-gavage (0.12 mg/L perhexiline and 0.66 mg/L FPER-1), 4 h post-gavage (0.03 mg/L perhexiline and 0.13 mg/L FPER-1) but fell to near 0 at 8 h. Similarly, in recent work on Sprague-Dawley rats, Signal Pharma showed that gavage with 10 mg/kg perhexiline or FPER-1 led to low drug plasma levels at 1 h (0.1 mg/L perhexiline and 0.39 mg/L FPER-1) and at 8 h post-gavage (0.03 mg/L perhexiline and 0.18 mg/L FPER-1) (Tseng et al., 2017). Based on these studies a dose of 10 mg/kg by gavage was considered too low to achieve drug plasma levels within the therapeutic range in mice.

Increasing the dose to 20 mg/kg perhexiline or FPER-1 daily gavage proved unsuccessful, plasma levels at 24 h post-treatment being only 0.02 and 0.01 mg/L respectively. Gehmlich et al. (2015) reported perhexiline plasma levels of 0.59 ±0.16 mg/L following twice-daily i.p injections at 30 mg/kg, but the time point at which plasma was taken was not reported. Therefore, it seemed prudent to test higher drug doses for gavage in the present study. In a recent leukaemia study, C57Bl/6 mice were treated for 5 days with perhexiline at 53.68 mg/kg (route of administration and doses per day not stated) with no reported side effects (Schnell et al., 2015). In a pharmacokinetics study, Esposito and colleagues (2016) reported

that one oral gavage dose of 70 mg/kg perhexiline in C57Bl/6 mice achieved drug plasma levels of 1 – 2 mg/L at 1 h and was still detectable at 24 h. Moreover, higher perhexiline doses of 100 mg/kg (R.Yamamoto et al., 2013) and 400 mg/kg (Ren et al., 2015) have been given orally in mice, without toxicity or adverse effects. Therefore, the present study was continued with 50 mg/kg gavage for 7 days conducted twice daily and finally, a single dose of 70 mg/kg daily for 7 days in line with the study by Esposito et al. (2016).

The present results revealed that twice-daily gavage of 50 mg/kg perhexiline reached therapeutic plasma levels (0.15 ±0.03 mg/L; therapeutic range: 0.15 – 0.6 mg/L) at 1 h post-final treatment but fell below this by 8 h. Conversley, mice receiving the once-daily 70 mg/kg perhexiline demonstrated perhexiline levels within the therapeutic range at 1 h post-gavage (0.63 ±0.08 mg/L), and remained within the therapeutic range at 8 h (0.22 ±0.07 mg/L). Moreover, twice-daily dosing with perhexiline was accompanied by increased side effects as assessed by increased weight loss and death of 2 out of 9 mice tested, even though histopathology and plasma ALT assessment indicated that 50 mg/kg perhexiline was not hepatotoxic. This suggested that the two gavages per day were causing adverse effects. Rather, it seems likely that the deaths were caused by drug-induced irritation of the oesophagus which had a negative impact on feeding when they were gavaged twice daily. In contrast, the single 70 mg/kg dose was not accompanied by severe weight loss or mortality; it achieved a therapeutic level of the drug systemically for 8 h and was therefore a dose that could be used in functional studies (see Chapter 6). As expected, perhexiline metabolite (OH-perhexiline) was present at lower levels than perhexiline itself, falling at a similar rate over the 24 h period with both 50 and 70 mg/kg doses, indicating normal perhexiline metabolism.

Regarding FPER-1, plasma levels achieved with both 50 and 70 mg/kg were significantly higher than perhexiline, remained high 8 h later, with detectable levels at 24 h post-final gavage that were above perhexiline's therapeutic range. These high levels corroborate the stability and altered metabolism of this new derivative achieved by the addition of a 4,4-difluoro group to one of the cyclohexyl rings i.e. the site of drug metabolism. Importantly, the two FPER-1 dosing regimens achieved similar plasma levels at each time point. FPER-1 stability was also highlighted by the time taken to fall to IC_{50} following FPER-1 treatment, which was greater than that for perhexiline at both the 50 and 70 mg/kg doses. These findings were consistent with our pharmacokinetics results (Tseng et al., 2017): FPER-1 was present at higher plasma levels than perhexiline for the same given dose in mice and rats.

As observed with perhexiline, mice subjected to twice-daily gavage of FPER-1 showed significant weight loss, with 2 out of 9 mice dead by day 7, but liver histology and plasma ALT levels indicated this was not due to liver toxicity, again suggesting the adverse effects were related to the additional gavage. By contrast, survival following single dosing with 70 mg/kg demonstrated that high FPER-1 plasma levels are tolerable and safe. Interestingly, the drug plasma levels achieved 1 h post-gavage with 70 mg/kg FPER-1 (3.94 mg/L or 12.6 μM) were ~5.5 fold greater than that achieved with 70 mg/kg perhexiline (0.63 mg/L or 2.3 μM). The results of Chapters 3 and 4 showed that 10 μM FPER-1, a dose 5-fold greater than the therapeutic 2 μM dose of perhexiline, was required to induce the same protection and molecular effects in isolated mouse hearts. Therefore, these data are internally consistent. Taking all of this into consideration, once-daily doses of 70 mg/kg perhexiline or FPER-1 were

regarded as optimal for achieving perhexiline plasma levels within the therapeutic range and appropriate to use in the *in vivo* model of cardiac hypertrophy and failure (Chapter 6).

Following pharmacokinetics assessment, the next priority was to assess whether acute administration of perhexiline or FPER-1 at the doses measured were hepatotoxic or safe *in vivo*, given that perhexiline has a long history of hepatotoxicity (Shah, 2006). Using the well-established technique of liver histology (Soldatow et al., 2013), it was confirmed that perhexiline maintained within the therapeutic range was safe following 1-week oral administration and that the new derivative was safe when given at the same dose. Consistent with this, plasma ALT, which is released from hepatocytes into the blood following injury (Gowda et al., 2009), was not altered following drug treatment, falling within the normal ALT range (66.5 ±184.9 U/L) for C57Bl/6 mice (Charles River, 2011) at all doses and time points.

5.4.1. Study limitations

To assess perhexiline and FPER-1 toxicity *in vivo* and to determine a safe and optimal dose mice were treated with various drug doses. However, only two routes of administration were assessed, i.p and oral gavage, of which gavage was optimal, based on fewer adverse effects. For future studies, especially if longer treatment windows are required, slow drug infusion by osmotic minipumps may be considered as this is less stressful to the animal and more convenient (Doucette et al., 2000). Use of this implanted device would avoid adverse effects in heart rate and body temperature, which daily restraint induces in mice (Meijer et al., 2006). Osmotic pumps may also enable the drug doses to remain constant and within the

therapeutic range throughout the day rather than falling by 8 h post-gavage. In addition, only four oral doses were assessed and therefore, it is possible that a dose between 50 and 70 mg/kg would have achieved therapeutic and non-toxic plasma levels. Moreover, only acute drug toxicity was assessed as mice were treated with perhexiline/FPER-1 for just 1 week, whereas serious perhexiline-induced toxicity takes around 3 months to develop in patients (Killalea and Krum, 2001). Thus, the present data do not guarantee that prolonged/chronic drug treatment would be non-toxic.

5.4.2. Future considerations

Having established that 70 mg/kg perhexiline provides plasma levels within the therapeutic range at 1 and 8 h post-treatment, a comprehensive time course would be useful to not only determine peak plasma levels prior to 1 h but also the rate of decay between 1 and 8 h and 8 and 24 h. The period of time over which perhexiline is likely to remain therapeutic could then be assessed. Furthermore, it would be important to measure drug levels within the myocardium itself and in at risk organs such as the liver. Licari and colleagues (2015) had discovered that perhexiline accumulates ~16.6-fold more in the plasma than liver in Sprague Dawley rats and ~20.4-fold greater in the plasma than liver in Dark Agouti rats. Such information would be useful for establishing a safe dose in mice.

As perhexiline-induced toxicity involves non-specific CPT1 inhibition resulting in systemic phospholipidosis, measuring fatty infiltration in liver sections would be useful as microvesicular steatosis was previously observed in patients on long-term perhexiline medication (Pessayre et al., 1979; Forbes et al., 1979; Lewis et al., 1979; Le Gall et al., 1980).

Importantly, future studies should assess peripheral neurotoxicity in perhexiline- and FPER-1-treated mice as this adverse effect was present in many patients (Fraser et al., 1977; Singlas et al., 1978b; Shah et al., 1982). Experimental assessment of peripheral neurotoxicity could include Von Frey hair mechanical stimulation to determine peripheral neural function, although this may not be as sensitive in mice (Hogan et al., 2004), or alternatively nerve velocity conductance measurements (Renn et al., 2011).

5.4.3. Conclusion

The present 1-week dosing study established that daily gavage of perhexiline or FPER-1 at 70 mg/kg is a suitable route of drug administration and dose when prepared in a starch-based solution. On the other hand, although 50 mg/kg perhexiline given twice daily achieved plasma levels within the therapeutic range at 1 h, this was accompanied by significant adverse effects probably attributable to the twice-daily gavage. Importantly, the present pharmacokinetics assessment demonstrated that FPER-1 is metabolised at a slower rate than perhexiline, plasma levels being much greater for the same dose, therefore highlighting the differences in their pharmacokinetics. Despite the higher drug plasma levels in FPER-1-treated mice, there was no evident difference in weight or survival relative to perhexiline-treated mice, indicating that high FPER-1 plasma levels are well-tolerated. Liver histopathology and plasma ALT also confirmed that when given acutely, perhexiline and FPER-1 are not hepatotoxic. With this background, a safe methodology and optimal dosing regimen for drug treatment had now been achieved to determine the therapeutic efficacy of perhexiline and FPER-1 *in vivo.*

Chapter 6: Investigating the effects of perhexiline and FPER-1 in an *in vivo* model of cardiac hypertrophy and failure

Chapter 6: Investigating the effects of perhexiline and FPER-1 in an *in vivo* model of cardiac hypertrophy and failure

6.1. Introduction

In Chapter 3 and 4 perhexiline and fluoroperhexiline-1 (FPER-1) were demonstrated as protective *ex vivo* in the isolated mouse heart, by targeting metabolic and non-metabolic proteins. In Chapter 5, a safe *in vivo* dose of both drugs was identified, which achieved perhexiline plasma levels within the therapeutic range. With this foundation, these drugs could now be tested for therapeutic efficacy in a model of cardiac hypertrophy and progression to failure.

As discussed in Chapter 1 (section 1.7), metabolic dysfunction occurs in both heart failure with reduced ejection fraction (HFrEF) and heart failure with preserved ejection fraction (HFpEF) (Neubauer et al., 2007; Hunter et al., 2016) and thus perhexiline, a metabolic modulator, is considered an alternative therapeutic agent (Owan et al., 2006). The metabolic disturbances of HF include decreased fatty acid (FA) oxidation (Sack et al., 1996; Pellieux et al., 2006), decreased glucose oxidation (Doenst et al., 2010; Zhabyeyev et al., 2013), uncoupling of glycolysis from glucose oxidation with incomplete compensation via anaplerotic pathways (Sorokina et al., 2007) and oxidative stress (Tsutsui et al., 2011). In combination these lead to detrimental changes in mitochondrial morphology (Dai et al., 2012) and impaired cardiac energetics (Neubauer et al., 1992). This in turn causes an imbalance between energy demand and supply, culminating in cardiac dysfunction and remodelling (Tuomainen and Tavi, 2017).

As outlined in Chapter 1 (section 1.11.1), so far perhexiline therapy has been promising in patients with HFrEF (Lee et al., 2005; Beadle et al., 2015) or hypertrophic cardiomyopathy (HCM) (Abozguia et al., 2010), by improving symptoms and attenuating cardiac dysfunction in parallel to improving muscle energetics. *In vivo*, perhexiline has had similar benefits by improving cardiac function and metabolism in mice with HF (Stapel et al., 2017) or HCM (Gehmlich et al., 2015).

However, perhexiline has yet to be tested in a pressure overload model of cardiac hypertrophy progressing to HF. In addition, discrepancies exist with regards to perhexiline's therapeutic benefits and cardioprotective mechanism, despite therapeutic plasma levels being used; in patients with left ventricular (LV) hypertrophy undergoing coronary artery bypass graft (CABG) surgery, perhexiline treatment did not provide myocardial protection (Senanayake et al., 2015), whilst Beadle and colleagues (2015) observed improvements in function but no change in cardiac substrate utilisation. Furthermore, due to the highly variable metabolism of perhexiline, constant plasma level monitoring and dose titration is required to avoid toxicity (Lee et al., 2005; Phan et al., 2009b). Lastly, the novel derivative, FPER-1, has not been tested in an *in vivo* model of cardiac disease. Therefore the key objective of the work in this chapter was to determine whether perhexiline and FPER-1 could delay HF progression, and if so, by which molecular mechanism(s).

Aims:

1. To establish an *in vivo* murine model of cardiac hypertrophy and progression to HF.

2. To determine whether perhexiline and FPER-1 delay the progression from cardiac hypertrophy to HF.

3. To determine potential cardioprotective molecular mechanism(s) of perhexiline and FPER-1 *in vivo*, in a model of cardiac hypertrophy and progression to HF.

6.2. Methodology

A detailed methodology is presented in Chapter 2, sections 2.8 to 2.14. Briefly, male C57Bl/6 mice (18 – 23 g) were subjected to pressure overload following abdominal aortic constriction (AAC) for 5 weeks, to induce hypertrophy and HF **[Figure 2.18]**. AAC was conducted under general anaesthesia; the abdominal aorta constricted at a suprarenal level against a 27-gauge needle, by careful placement of a ligature. Sham-operated mice were subjected to a similar surgical procedure with the exception of AAC. Cardiac function and dimensions were measured pre-surgery (baseline) and post-surgery (week 1, 3 and 5) using echocardiography (section 2.11). Thus, parasternal images of the left side of the heart were taken to measure LV ejection fraction (EF), fractional shortening (FS) (markers of cardiac function; primary end-points) and the following parameters at end-diastole and end-systole: LV volume, LV internal diameter (LVID), interventricular septal wall (IVS) thickness, LV posterior wall (LVPW) thickness and LV anterior wall (LVAW) thickness (all markers of cardiac remodelling; secondary end-points). Aortic and mitral valve variables were also measured using pulse-wave Doppler imaging. The LV mass-to-body weight (BW) ratio (LV mass/BW) at each time point and heart weight-to-BW ratio (HW/BW) at week 5 were also calculated as morphometric markers.

To establish the model, mice were first subjected to AAC without treatment, and then randomised to one of four groups: 1) sham-operated vehicle-treated, 2) AAC vehicle-treated, 3) AAC 70 mg/kg perhexiline-treated and 4) AAC 70 mg/kg FPER-1-treated. Treated mice were orally gavaged once daily, from 1 week post-surgery, until week 5 when mice were sacrificed. Blood was collected, plasma extracted and subjected to drug pharmacokinetics assessment by Professor Benedetta Sallustio's group, Australia (section 2.8), and colorimetrically assayed for the hepatotoxicity marker alanine transaminase (ALT) (section 2.10) and immunoassayed for the HF marker brain natriuretic peptide (BNP) (section 2.13). Hearts from sham-operated and AAC-treated mice were isolated, cannulated, perfused with standard Krebs-Henseleit buffer (KHB) and snap-frozen for Western blotting (section 2.6 and 2.14). Additionally, the right liver lobe was harvested and fixed in 4% formaldehyde for histological assessment of liver damage and fibrosis by staining sections with haematoxylin and eosin (H&E) or Van Gieson (section 2.9).

6.2.1. Statistical analysis

Data within this chapter are expressed as means ±standard error of the mean (SEM). Two-way analysis of variance (ANOVA) with Bonferroni post-hoc test was used to compare echocardiographic data between untreated AAC mice and sham-operated mice and the week post-AAC (week 1, 3 and 5) to baseline, as well as between vehicle-treated AAC mice to drug-treated AAC mice (70 mg/kg perhexiline or FPER-1). The HW/BW ratio between sham and AAC untreated mice and BNP plasma levels between sham and vehicle-treated AAC mice were compared using an unpaired t-test. Differences in body weight at week 5, ALT plasma levels and protein expression and/or phosphorylation between each group was determined

using a one-way ANOVA with Bonferroni post-hoc test. Graphpad Prism version 6.0 was used for all analysis. *p<0.05* was considered statistically significant. Number of mice used is indicated in the figure legends.

6.3. Results

6.3.1. Establishing the model of abdominal aortic constriction in mice

To establish the *in vivo* model, multiple parameters of cardiac function and dimension were compared in AAC and sham-operated mice.

6.3.1.1. Cardiac function and hypertrophy following AAC

As expected, the echocardiographic data demonstrated that EF and FS remained unchanged over the 5-week protocol in sham-operated mice (*p>0.99* for both) **[Figure 6.1B+C**, open bars**]**. By contrast, EF in AAC mice was significantly reduced from 71.8 ±1.3% to 61.3 ±0.7% 3 weeks post-surgery (*p<0.0001*), with a further significant reduction to 51.9 ±1.5% 5 weeks post-surgery (*p<0.0001*) **[Figure 6.1B**, grey bars**]**. In addition, FS decreased significantly by week 3 (*p<0.0001*), with a further decrease by week 5 post-constriction relative to baseline (*p<0.0001*) **[Figure 6.1C]**, these reductions were significant compared to the sham controls (*p<0.0001* for all). Similarly, sham-operated mice showed no change in LV mass/BW ratio (*p>0.99*), whereas AAC mice showed a significant increase in LV mass/BW by week 3 (1.3-fold; *p<0.05*) and a further increase at week 5 relative to baseline (1.4-fold; *p<0.001*) and sham controls (1.5-fold; *p<0.001*) **[Figure 6.1D]**. Furthermore, the HW/BW ratio was also significantly greater in the AAC mice 5 weeks post-surgery than in the sham group (1.4-fold; *p<0.001*) **[Figure 6.1E]**. Heart weight was significantly lower in AAC mice relative to the sham

controls (1.5-fold; *p<0.01*) **[Figure 6.10F]** whilst body weight was not different **[Figure 6.10G]**.

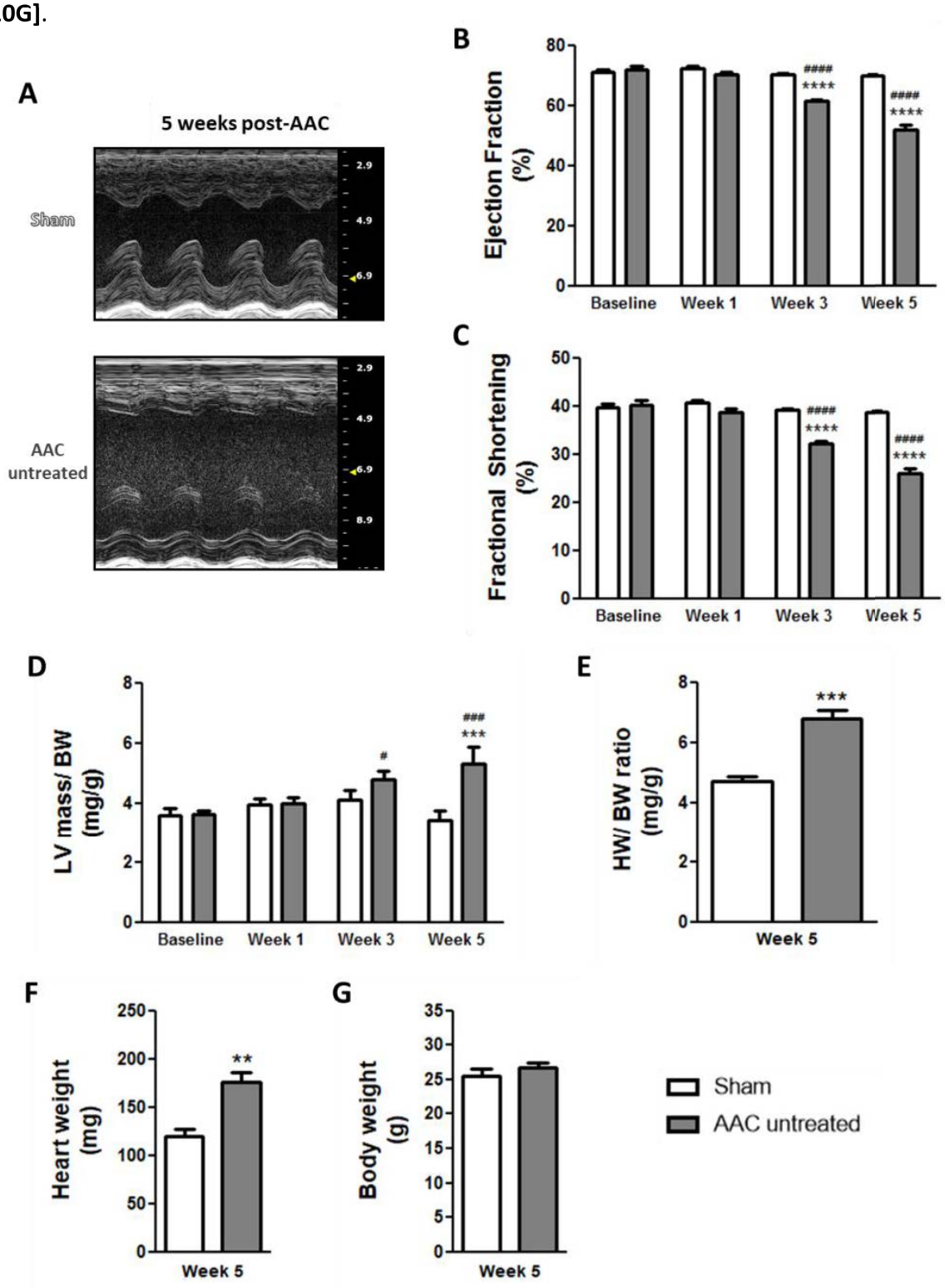

Figure 6.1. Cardiac function and hypertrophy following 5 weeks of AAC

Values measured in sham and AAC untreated mice, pre-surgery (baseline) and post-surgery (week 1, 3 and 5). **A:** Representative echocardiographic M-mode images 5 weeks post-constriction. **B:** Percentage ejection fraction (EF). **C:** Percentage fractional shortening (FS). **D:** Left ventricular (LV) mass-to-body weight (BW) ratio. **E:** Heart weight (HW)-to-body weight (BW) ratio. **F:** Heart weight. **G:** Body weight. Data are presented as mean ±SEM; n = 6-10 mice. *#p<0.05* vs Baseline; *###p<0.001* vs Baseline; *####p<0.0001* vs Baseline; ***p<0.01* vs Sham; ****p<0.001* vs Sham; *****p<0.0001* vs Sham (Two-way ANOVA followed by Bonferroni post-hoc test).

6.3.1.2. Cardiac remodelling at end-diastole and end-systole following AAC

Again, as expected LV end-diastolic volumes and dimensions in sham-operated mice, remained unchanged during the 5-week protocol (*p>0.99* for all) **[Figure 6.2]**. Furthermore, the LV volume and LVID at diastole were not significantly altered in AAC mice relative to baseline (*p=0.05* and *>0.99* respectively) or sham controls (*p=0.06* and *>0.99* respectively) **[Figure 6.2A+B]**. In contrast, IVS and LVAW thickness significantly increased by week 3 (1.2-fold; *p<0.01* and 1.2-fold; *p<0.05* respectively) in AAC mice, with a further increase 5 weeks post-constriction relative to baseline (1.3-fold; *p<0.0001* and 1.3-fold; *p<0.01* respectively) and sham controls (1.3-fold; *p<0.01* and 1.3-fold; *p<0.05* respectively) **[Figure 6.2C+D]**. In addition, the LVPW thickness was significantly increased in AAC mice by week 3 and 5 when compared to baseline (1.3-fold; *p<0.001* and 1.4-fold; *p<0.0001* respectively) and sham controls (1.4-fold; *p<0.001* and 1.5-fold; *p<0.0001* respectively) **[Figure 6.2E]**.

Similarly, LV end-systolic volumes and dimensions remained unchanged in sham-operated mice during the protocol (*p>0.99* for all) **[Figure 6.3]**. In contrast, there was a significant increase in LV end-systolic volume and LVID in AAC mice at week 3 (1.5-fold; *p<0.01* and 1.2-fold; *p<0.01* respectively), with a further increase at week 5 relative to baseline (2.1-fold; *p<0.0001* and 1.3-fold; *p<0.0001* respectively) and sham-operated mice (1.5-fold; *p<0.01* and 1.2-fold; *p<0.01* respectively) **[Figure 6.3A+B]**. However, IVS, LVAW and LVPW thickness were not significantly altered following AAC during the 5-week study (*p=0.98*, *>0.99* and *0.06* respectively) **[Figure 6.3C-E]**.

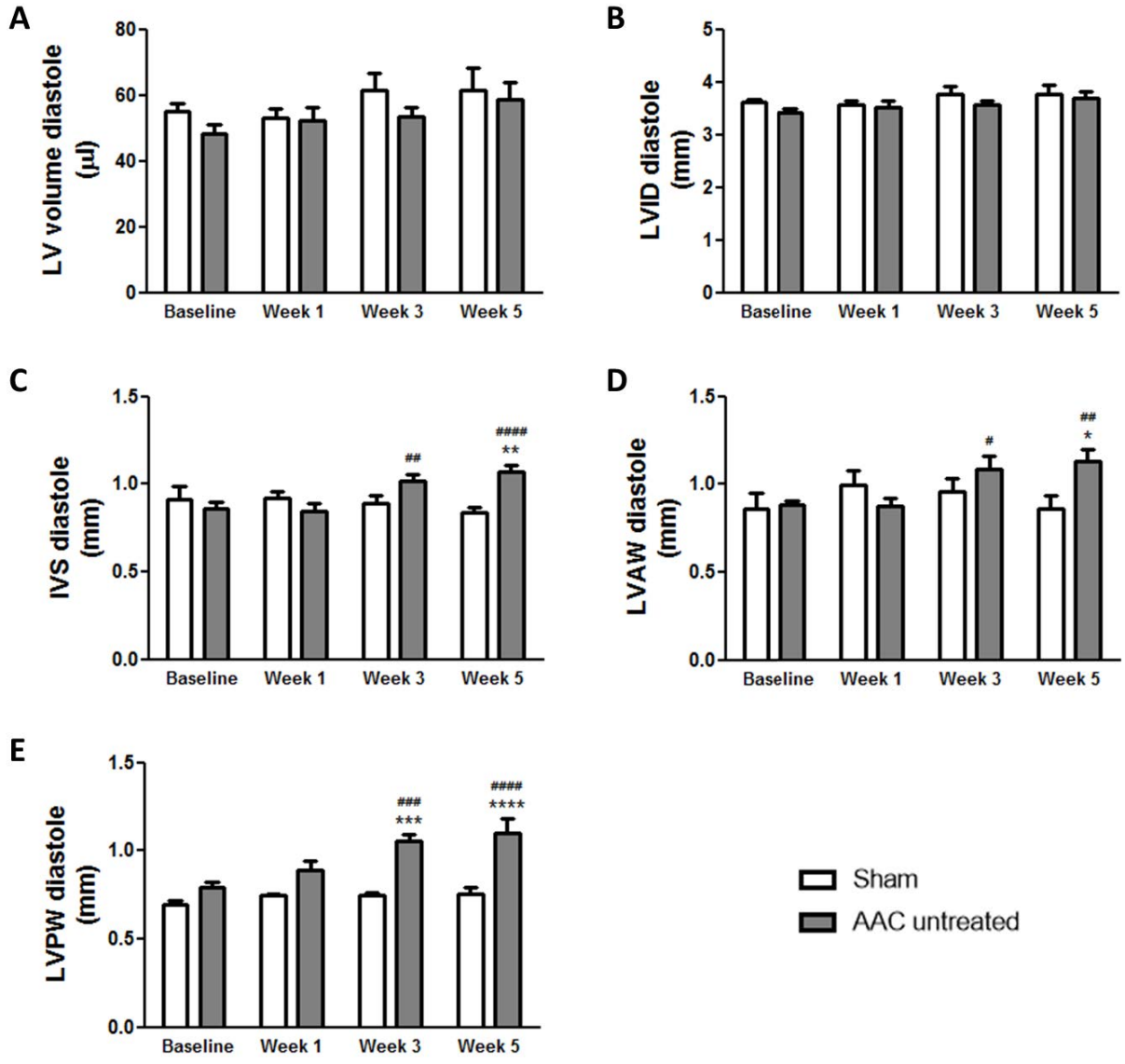

Figure 6.2. Cardiac volumes and dimensions at end-diastole following 5 weeks of AAC

Values measured in sham and AAC untreated mice, pre-surgery (baseline) and post-surgery (week 1, 3 and 5) at end-diastole. **A:** Left ventricular (LV) volume. **B:** Left ventricular internal diameter (LVID). **C:** Interventricular septal wall (IVS) thickness. **D:** Left ventricular anterior wall (LVAW) thickness. **E:** Left ventricular posterior wall (LVPW) thickness. Data are presented as mean ±SEM; n = 6-10 mice. #*p<0.05* vs Baseline; ##*p<0.01* vs Baseline; ###*p<0.001* vs Baseline; ####*p<0.0001* vs Baseline; **p<0.05* vs Sham; ***p<0.01* vs Sham; ****p<0.001* vs Sham; *****p<0.0001* vs Sham (Two-way ANOVA followed by Bonferroni post-hoc test).

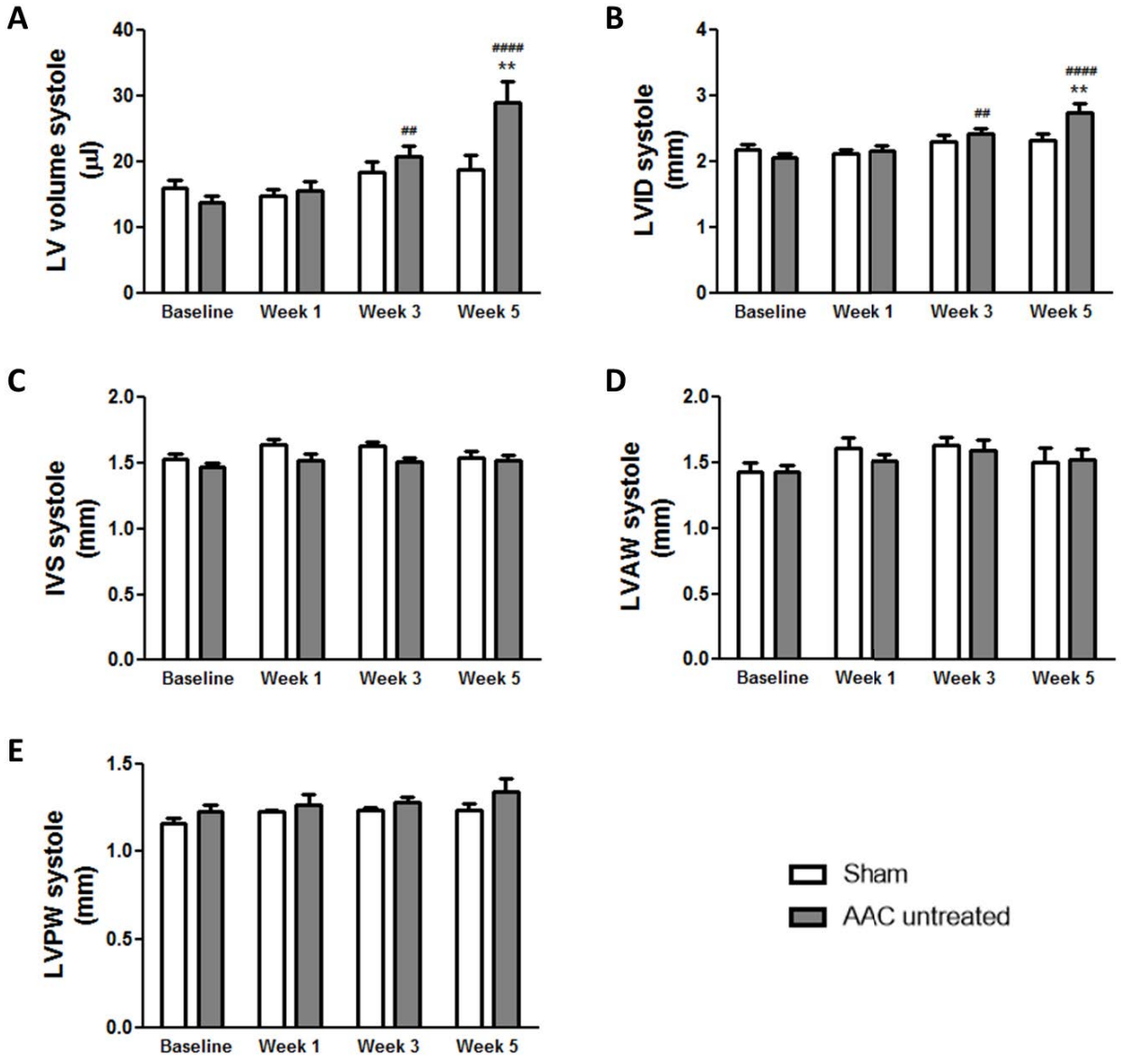

Figure 6.3. Cardiac volumes and dimensions at end-systole following 5 weeks of AAC

Values measured in sham and AAC untreated mice, pre-surgery (baseline) and post-surgery (week 1, 3 and 5) at end-systole. **A:** Left ventricular (LV) volume. **B:** Left ventricular internal diameter (LVID). **C:** Interventricular septal wall (IVS) thickness. **D:** Left ventricular anterior wall (LVAW) thickness. **E:** Left ventricular posterior wall (LVPW) thickness. Data are presented as mean ±SEM; n = 6-10 mice. *##p<0.01* vs Baseline; *####p<0.0001* vs Baseline; ***p<0.01* vs Sham (Two-way ANOVA followed by Bonferroni post-hoc test).

6.3.1.3. Aortic and mitral valve variables following AAC

Aortic and mitral valve Doppler measurements did not change in sham-operated mice during the 5-week study (*p>0.99* for all) **[Figure 6.4]**. In contrast, in AAC mice, both aortic peak velocity and peak gradient increased significantly at week 3 (1.2-fold; *p<0.01* and 1.5-fold; *p<0.01* respectively), with a further increase at week 5 relative to baseline (1.4-fold; *p<0.0001* and 1.2-fold; *p<0.0001* respectively) and sham controls (1.5-fold; *p<0.0001* and 2.1-fold; *p<0.001* respectively) **[Figure 6.4A+B]**. In addition, aortic VTI significantly increased in AAC mice at week 3 (1.3-fold; *p<0.01*) and week 5 when compared to baseline (1.2-fold; *p<0.05*) and sham controls (1.4-fold; *p<0.05* and 1.5-fold; *p<0.01* respectively) **[Figure 6.4C]**. However, all mitral valve variables (VTI, peak velocity, peak gradient and E/A ratio) remained unaltered during the 5-week study in AAC mice (*p>0.99* for all) **[Figure 6.4D-G]**.

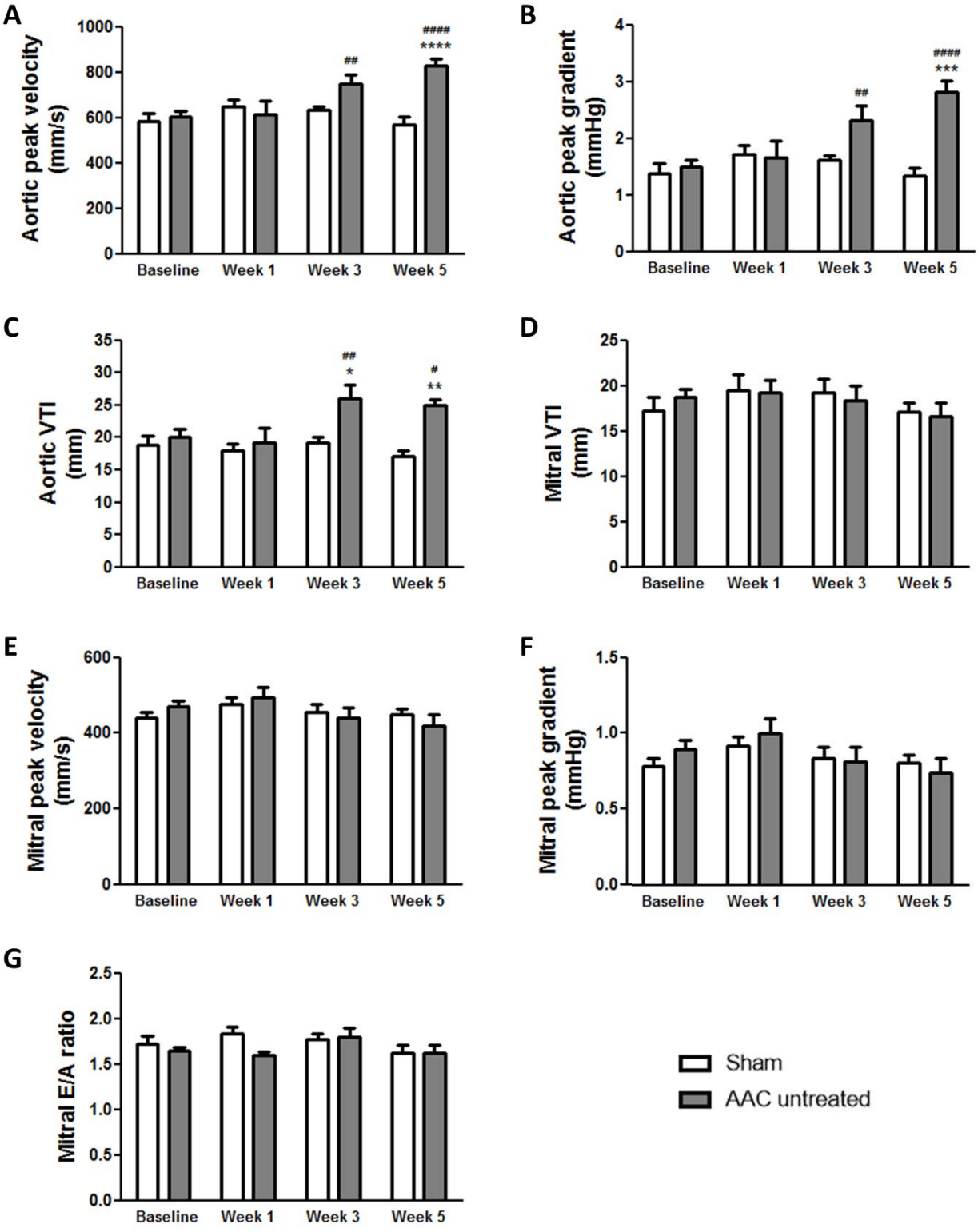

Figure 6.4. Aortic and mitral valve variables following 5 weeks of AAC

Values measured in sham and AAC untreated mice, pre-surgery (baseline) and post-surgery (week 1, 3 and 5). **A:** Aortic peak velocity. **B:** Aortic peak gradient. **C:** Aortic velocity time integral (VTI). **D:** Mitral velocity time integral (VTI). **E:** Mitral peak velocity. **F:** Mitral peak gradient. **G:** Mitral E/A ratio. Data are presented as mean ±SEM; n = 6-10 mice. *#p<0.05* vs Baseline; *##p<0.01* vs Baseline; *####p<0.0001* vs Baseline; **p<0.05* vs Sham; ***p<0.01* vs Sham; ****p<0.001* vs Sham; *****p<0.0001* vs Sham (Two-way ANOVA followed by Bonferroni post-hoc test).

6.3.1.4. Plasma BNP levels following AAC

Mean BNP plasma levels remained unaltered at week 5 in AAC mice receiving vehicle-treatment, relative to sham controls (*p=0.17*) **[Figure 6.5]**. This data indicated that although AAC induced hypertrophy and remodelling, it did not cause significant HF.

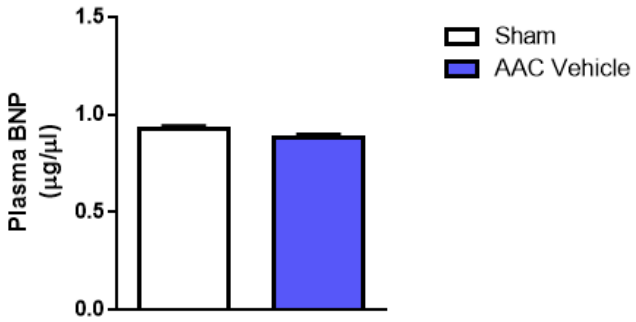

Figure 6.5. Plasma BNP levels following 5 weeks of AAC

Plasma brain natriuretic peptide (BNP) levels measured in sham and vehicle-treated AAC mice at the end of 5 weeks. Data are presented as mean ±SEM; n = 6-7 mice.

6.3.2. Survival, drug toxicity and drug pharmacokinetics in AAC mice

6.3.2.1. Survival and body weight of mice following 5 weeks of AAC

Survival following AAC was high at 90.2%, most fatalities occurred perioperatively (7 out of 48 AAC mice) due to surgical complications (i.e. ruptured vena cava or spleen bleed) and later mortalities typically occurring during the first week post-surgery (3 out of 48 AAC mice) prior to the commencement of vehicle/drug treatment **[Figure 6.6A]**. Only 1 death took place on day 14, due to accidental administration of liquid into the lungs following gavage. Body weight between all groups: sham, AAC untreated, AAC treated (vehicle, 70 mg/kg perhexiline or FPER-1) were similar at baseline and remained comparable to each other at the end of the 5-week protocol (*p=0.96*) **[Figure 6.6B]**.

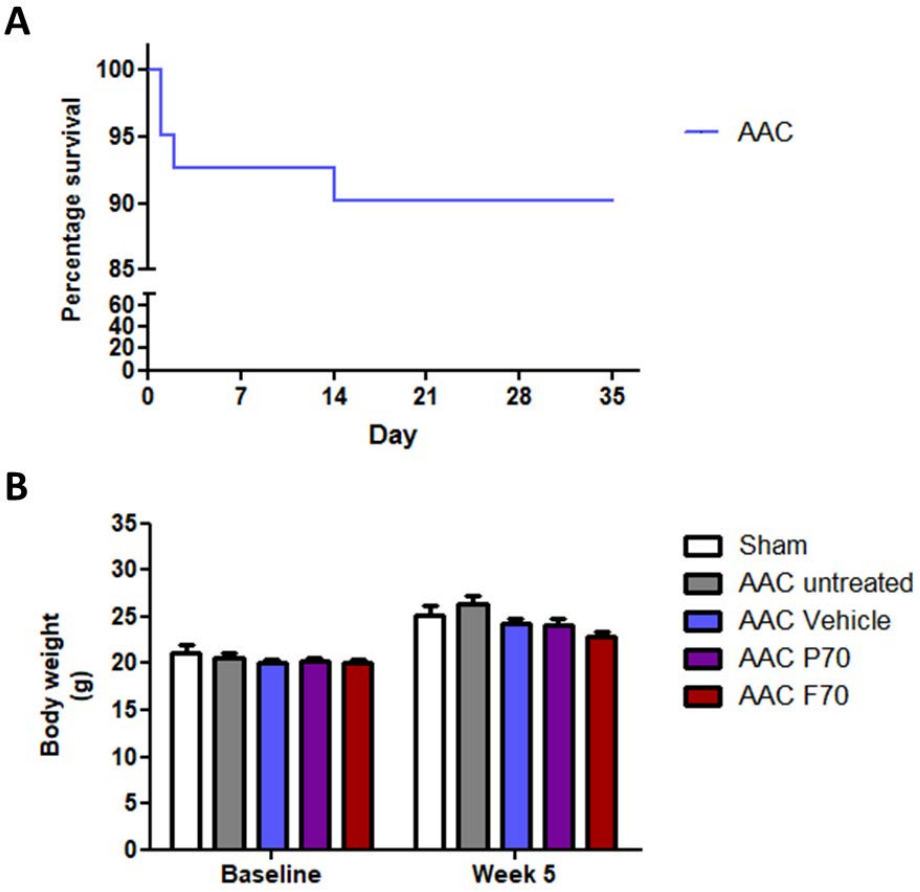

Figure 6.6. Survival and body weight of mice following 5 weeks of AAC

A: Kaplan-Meier graph showing percentage survival for AAC mice. n = 48 mice. **B:** Body weight of sham-operated and AAC untreated mice, and of AAC mice treated with either vehicle, 70 mg/kg perhexiline (P70) or 70 mg/kg FPER-1 (F70), measured pre-surgery (baseline) and at the end of the study (week 5). Data are presented as mean ±SEM; n = 6-10 mice.

6.3.2.2. Perhexiline and FPER-1 plasma levels following 4-week treatment in AAC mice

Plasma levels of the two drugs measured at 1 h post-final gavage in AAC mice were as expected based on the results from Chapter 5 (section 5.3.2) **[Figure 6.7]**. Perhexiline plasma levels achieved following 4-week daily gavage at a dose of 70 mg/kg was 0.88 ±0.09 mg/L. Hydroxy (OH)-perhexiline plasma levels were 3-fold less than perhexiline, at 0.29 ±0.02 mg/L.

In contrast, daily gavage with 70 mg/kg FPER-1 achieved much greater plasma levels of 3.23 ±0.19 mg/L.

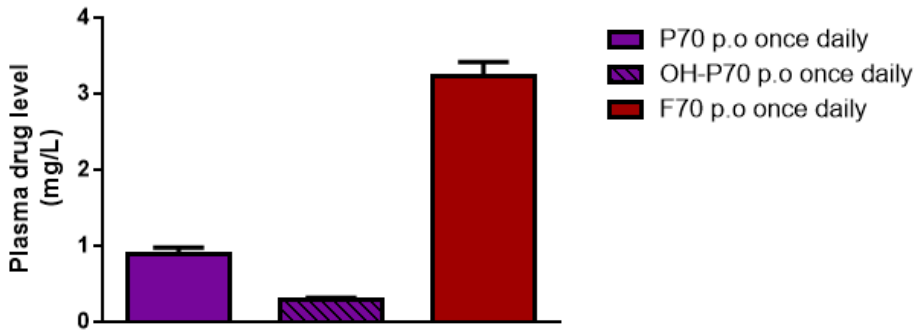

Figure 6.7. Plasma levels of perhexiline, its metabolite and FPER-1 following 4-week treatment in AAC mice

Plasma levels of perhexiline, its metabolite (hydroxy (OH)-perhexiline) and FPER-1, measured at 1 h post-final treatment in AAC mice orally gavaged (p.o) with 70 mg/kg perhexiline (P70) or 70 mg/kg FPER-1 (F70) for 4 weeks. Data are presented as mean ±SEM; n = 9 mice.

6.3.2.3. Liver integrity, fibrosis and function following 4-week treatment with perhexiline or FPER-1 in AAC mice

Livers from AAC mice did not appear morphologically different from sham-operated mice; hepatocytes and hepatic vessels appeared regular and intact **[Figure 6.8]**. Furthermore, 4-week daily gavage with vehicle, 70 mg/kg perhexiline or FPER-1 did not cause liver damage, or induce inflammation or fibrosis.

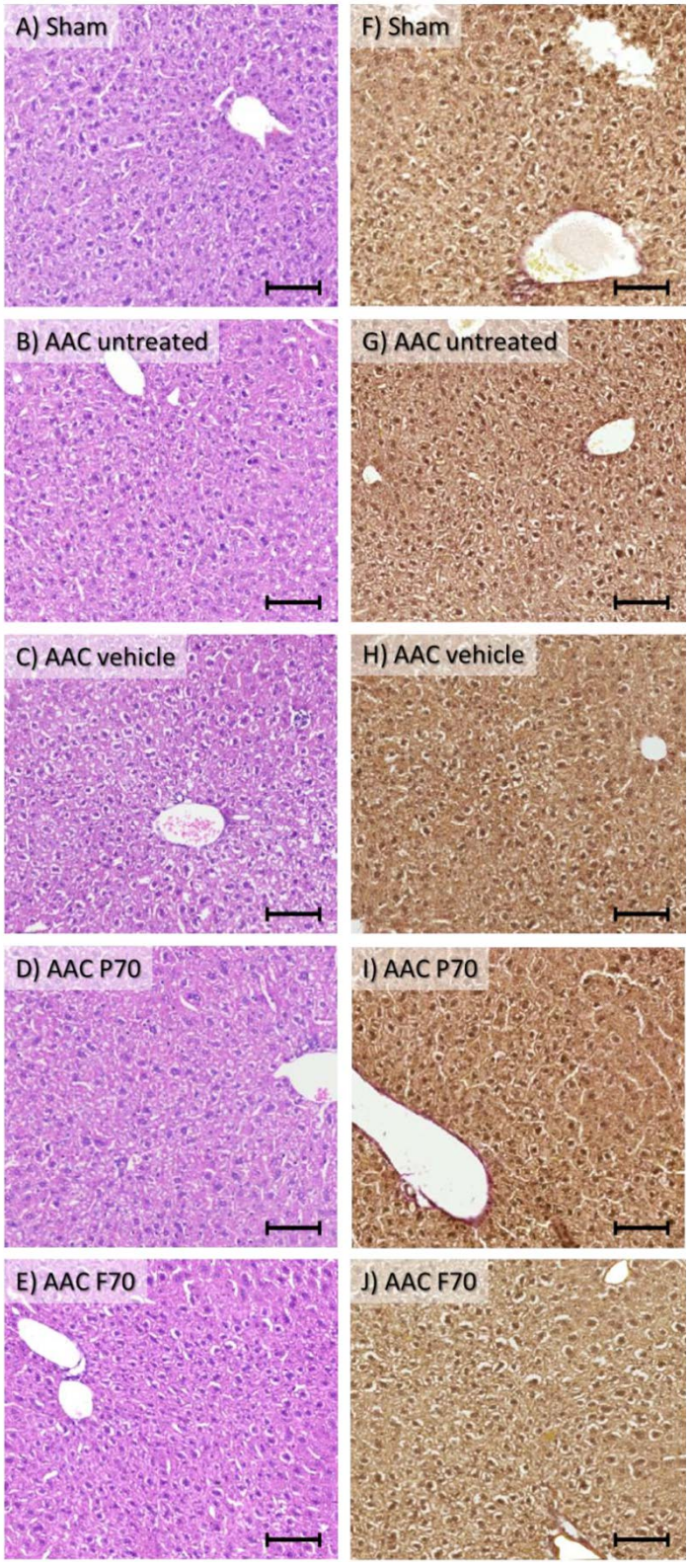

Figure 6.8. Photomicrographs of liver sections stained to assess liver integrity, inflammation or fibrosis following 4-week treatment with perhexiline or FPER-1 in AAC mice

Representative liver sections from **A+F:** sham mice, **B+G:** AAC untreated mice, **C+H:** AAC vehicle-treated mice, **D+I:** AAC 70 mg/kg perhexiline-treated mice (P70) & **E+J:** AAC 70 mg/kg FPER-1-treated mice (F70).

Sections were stained with either haematoxylin and eosin **(A-E)** or Van Gieson **(F-J)**, and scanned with x20 objective. Scale bar = 100 µm. n = 6-10 mice.

Plasma ALT levels were not significantly different between sham, AAC-untreated or AAC-treated (vehicle, 70 mg/kg perhexiline or FPER-1) mice (*p=0.63*) **[Figure 6.9]**.

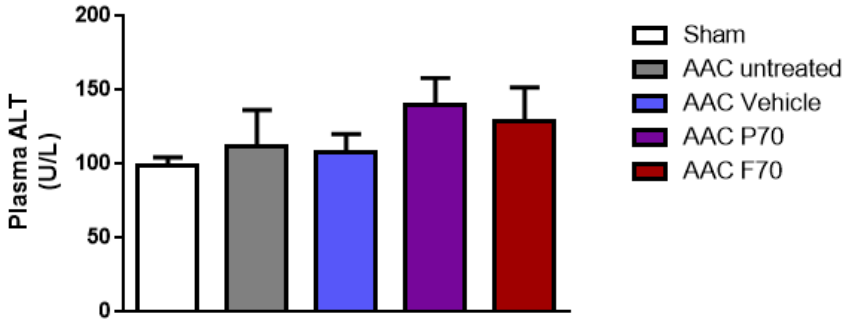

Figure 6.9. Plasma ALT levels following 4-week treatment with perhexiline or FPER-1 in AAC mice

Plasma alanine transaminase (ALT) levels measured in sham-operated and AAC untreated mice, and in AAC mice treated with either vehicle, 70 mg/kg perhexiline (P70) or 70 mg/kg FPER-1 (F70), 1 h post-final treatment. Data are presented as mean ±SEM; n = 6-10 mice.

6.3.3. Investigating the effects of perhexiline and FPER-1 treatment in AAC mice

6.3.3.1. Effects of perhexiline and FPER-1 on cardiac function and hypertrophy in AAC mice

Echocardiographic data measured in vehicle-treated AAC mice confirmed a decrease in LV function with significant reductions in EF and FS at week 3 and 5 post-surgery (*p<0.0001* for all) **[Figure 6.10B+C**, blue bars**]**. Treatment with 70 mg/kg perhexiline significantly improved EF at week 5 (*p<0.001*) as well as FS at week 3 (*p<0.05*) and 5 relative to the vehicle group (*p<0.001*) **[Figure 6.10B+C**, purple bars**]**. In contrast, AAC mice treated with 70 mg/kg FPER-1 showed similar EF and FS to vehicle controls (*p>0.99* for all) **[Figure 6.10B+C**, red bars**]**.

Furthermore, the increase in LV mass/BW ratio observed in vehicle-treated AAC mice (1.3-fold; *p<0.01* and 1.3-fold; *p<0.001* at week 3 and 5 respectively) was not significantly attenuated by perhexiline or FPER-1 (1.2-fold decrease for both at week 5; *p=0.11* and *0.06* respectively) **[Figure 6.10D]**. However, the HW/BW ratio at week 5 was significantly lower in AAC mice treated with perhexiline (1.4-fold; *p<0.001*) or FPER-1 (1.3-fold; *p<0.01*) relative to vehicle-treated AAC mice **[Figure 6.10E]**. Heart weight was significantly lower in perhexiline-treated and FPER-1-treated AAC mice (1.4-fold; *p<0.01* for both) relative to vehicle-treated AAC mice **[Figure 6.10F]** whilst body weight remained similar between all three AAC-treated groups **[Figure 6.10G]**.

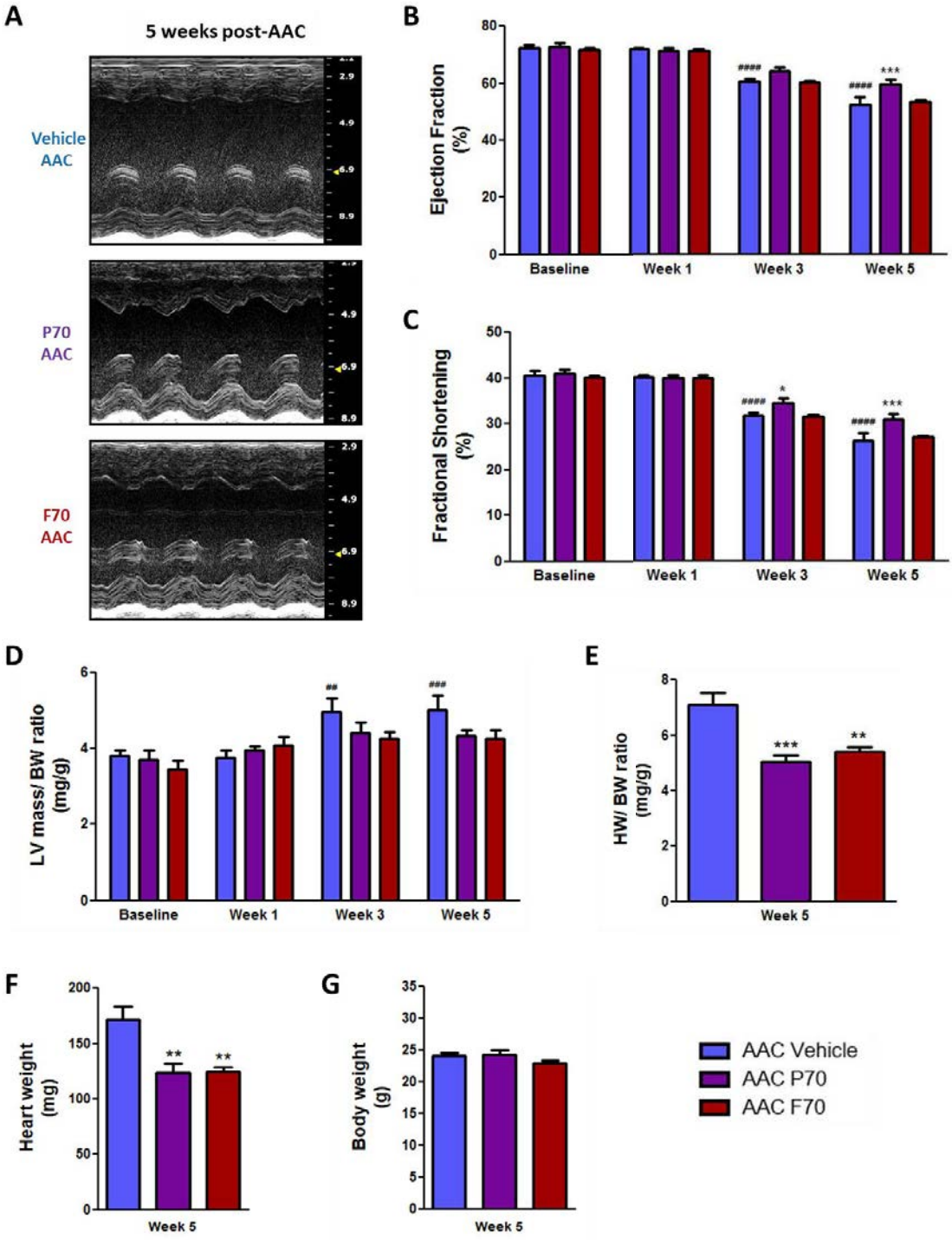

Figure 6.10. Effects of perhexiline and FPER-1 on cardiac function and hypertrophy in AAC mice

Values measured in AAC mice treated with either vehicle, 70 mg/kg perhexiline (P70), or 70 mg/kg FPER-1 (F70), pre-surgery (baseline) and post-surgery (at week 1, 3 and 5). **A:** Representative echocardiographic M-mode images 5 weeks post-constriction. **B:** Percentage ejection fraction (EF). **C:** Percentage fractional shortening (FS). **D:** Left ventricular (LV) mass-to-body weight (BW) ratio. **E:** Heart weight (HW)-to-body weight (BW) ratio. **F:** Heart weight. **G:** Body weight. Data are presented as mean ±SEM; n = 9 mice. ##*p<0.01* vs Baseline; ###*p<0.001* vs Baseline; ####*p<0.0001* vs Baseline; **p<0.05* vs AAC Vehicle; ***p<0.01* vs AAC Vehicle; ****p<0.001* vs AAC Vehicle (Two-way ANOVA followed by Bonferroni post-hoc test).

6.3.3.2. Effects of perhexiline and FPER-1 on cardiac remodelling at end-diastole and end-systole in AAC mice

Measurements of LV volume and LVID at end-diastole were unchanged in vehicle-treated AAC mice (*p>0.99* for both) or drug-treated AAC mice (*p=0.38* and *0.34* respectively) **[Figure 6.11A+B]**. In contrast, in vehicle-treated AAC mice, IVS thickness was significantly increased at week 3 and 5 relative to baseline (1.3-fold; *p<0.0001* for both), and this was not significantly altered by perhexiline or FPER-1 treatment (*p=0.25*) **[Figure 6.11C]**. The LVAW thickness also increased in vehicle-treated AAC mice (1.2-fold; *p<0.001* and 1.4-fold; *p<0.0001* at week 3 and 5 respectively), and this was not different in perhexiline-treated AAC mice **[Figure 6.11D]**. However, the increase in LWAW was significantly attenuated in FPER-1-treated AAC mice at both week 3 and 5 (1.2-fold; *p<0.01* for both) relative to the vehicle group. Finally, LVPW was also significantly increased in vehicle-treated AAC mice at week 3 (1.2-fold; *p<0.0001*) and week 5 (1.3-fold; *p<0.0001*) and treatment with perhexiline or FPER-1 significantly reduced this increase at week 3 (1.1-fold; *p<0.05* and 1.2-fold; *p<0.0001* respectively) and week 5 (1.2-fold; *p<0.001* and 1.2-fold; *p<0.0001* respectively) **[Figure 6.11E]**.

In contrast, at end-systole, LV volume increased significantly by week 5 in AAC mice (1.9-fold; *p<0.001*) **[Figure 6.12A]**. Any effect of perhexiline treatment on LV volume was not significant (1.3-fold decrease; *p=0.14*) and FPER-1 had no effect (*p>0.99*). In the vehicle-treated AAC group, LVID was also significantly increased at week 3 and 5 (1.2-fold; *p<0.01* and 1.3-fold; *p<0.0001* respectively), and this was comparable in the drug-treated AAC

groups (*p=0.27*) **[Figure 6.12B]**. In contrast, IVS, LVAW and LVPW remained unchanged in the vehicle-treated and drug-treated AAC groups **[Figure 6.12C-E]**.

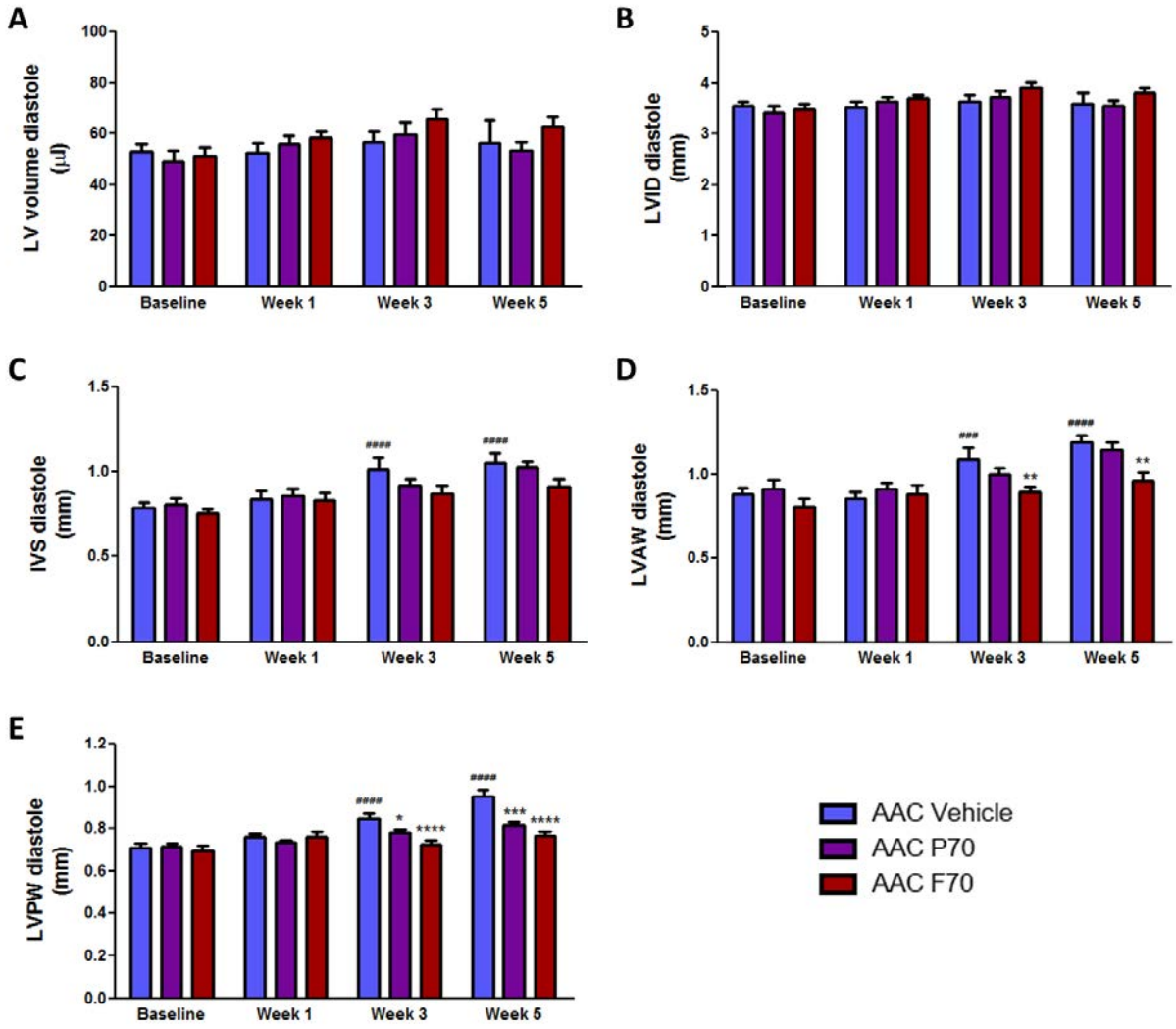

Figure 6.11. Effects of perhexiline and FPER-1 on cardiac volumes and dimensions at end-diastole in AAC mice

Values measured in AAC mice treated with either vehicle, 70 mg/kg perhexiline (P70), or 70 mg/kg FPER-1 (F70), pre-surgery (baseline) and post-surgery (at week 1, 3 and 5). **A:** Left ventricular (LV) volume. **B:** Left ventricular internal diameter (LVID). **C:** Interventricular septal wall (IVS) thickness. **D:** Left ventricular anterior wall (LVAW) thickness. **E:** Left ventricular posterior wall (LVPW) thickness. Data are presented as mean ±SEM; n = 9 mice. *###p<0.001* vs Baseline; *####p<0.0001* vs Baseline; **p<0.05* vs AAC Vehicle; ***p<0.01* vs AAC Vehicle; ****p<0.001* vs AAC Vehicle; *****p<0.0001* vs AAC Vehicle (Two-way ANOVA followed by Bonferroni post-hoc test).

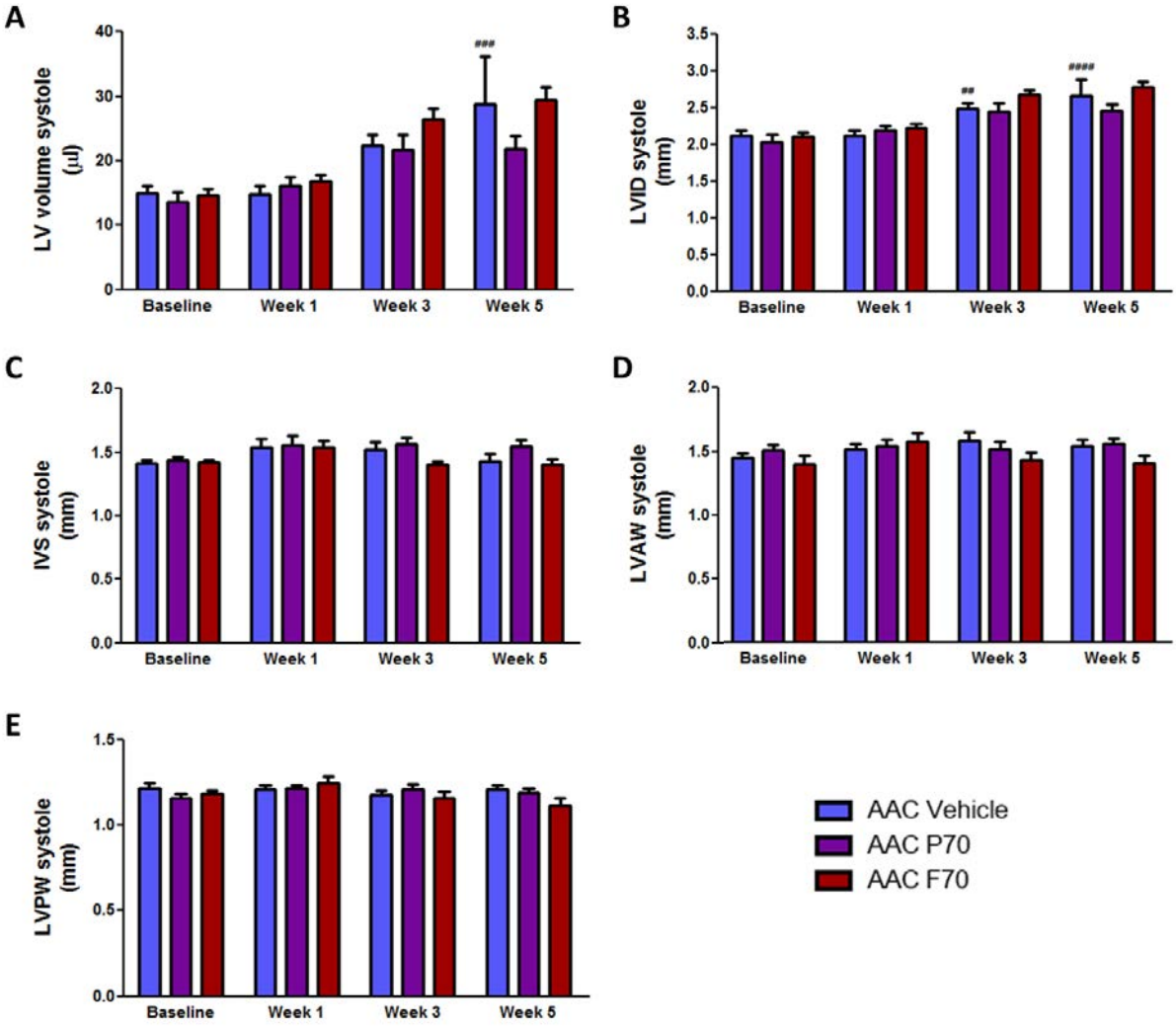

Figure 6.12. Effects of perhexiline and FPER-1 on cardiac volumes and dimensions at end-systole in AAC mice

Values measured in AAC mice treated with either vehicle, 70 mg/kg perhexiline (P70), or 70 mg/kg FPER-1 (F70), pre-surgery (baseline) and post-surgery (at week 1, 3 and 5). **A:** Left ventricular (LV) volume. **B:** Left ventricular internal diameter (LVID). **C:** Interventricular septal wall (IVS) thickness. **D:** Left ventricular anterior wall (LVAW) thickness. **E:** Left ventricular posterior wall (LVPW) thickness. Data are presented as mean ±SEM; n = 9 mice. *##p<0.01* vs Baseline; *###p<0.001* vs Baseline; *####p<0.0001* vs Baseline (Two-way ANOVA followed by Bonferroni post-hoc test).

6.3.3.3. Effects of perhexiline and FPER-1 on aortic and mitral valve variables in AAC mice

Aortic and mitral valve Doppler measurements did not differ significantly between perhexiline- or FPER-1-treated AAC mice relative to vehicle-treated AAC mice **[Figure 6.13]**. Interestingly mitral VTI was significantly reduced at week 5 in vehicle-treated AAC mice relative to baseline (1.2-fold; *p<0.01*) **[Figure 6.13D]**, despite this decrease not having been

observed in untreated AAC mice in section 6.3.1.3. The limitations of this are discussed in section 6.4.3 and 6.4.5.

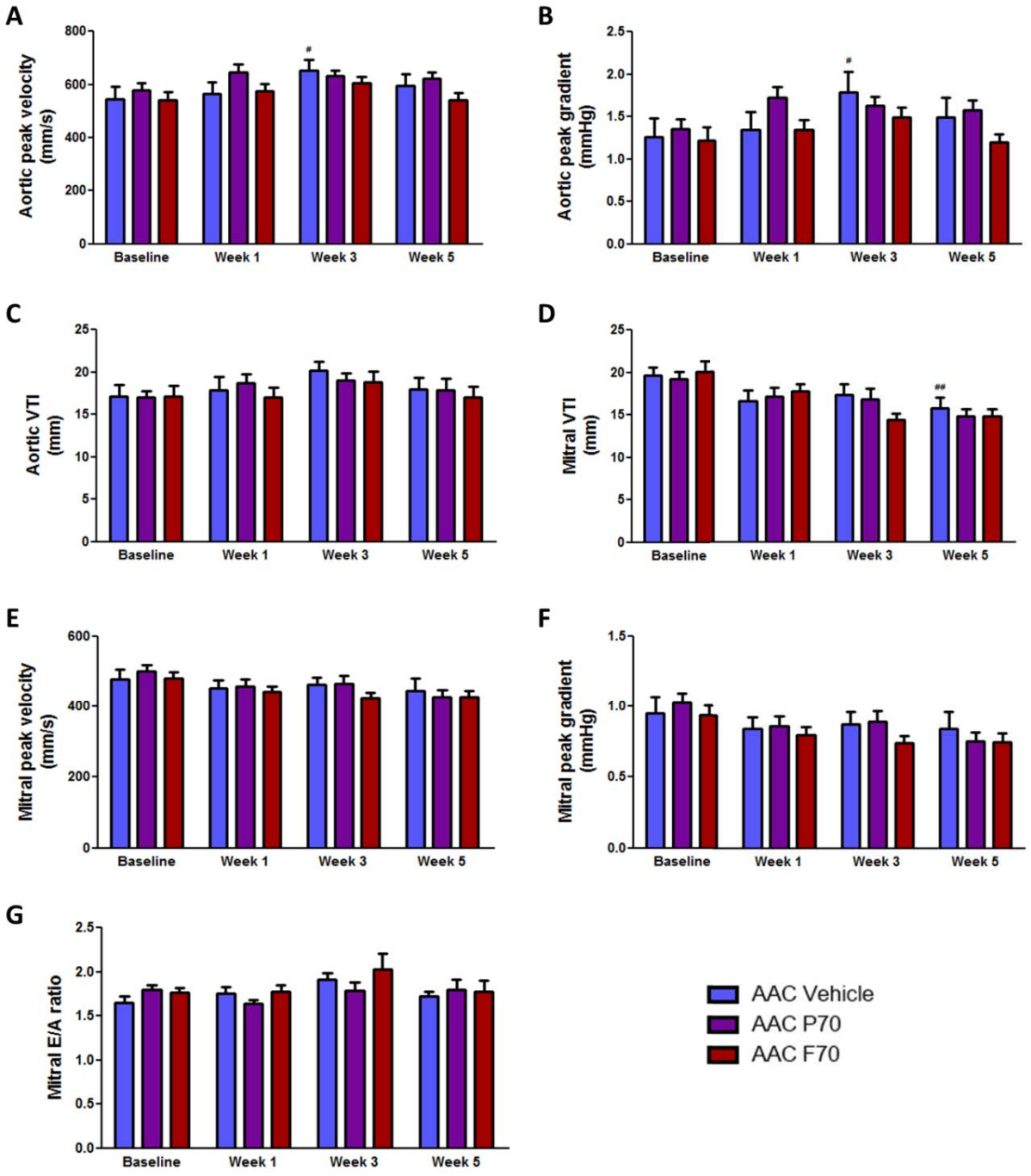

Figure 6.13. Effects of perhexiline and FPER-1 on aortic and mitral valve variables in AAC mice

Values measured in AAC mice treated with either vehicle, 70 mg/kg perhexiline (P70), or 70 mg/kg FPER-1 (F70), pre-surgery (baseline) and post-surgery (at week 1, 3 and 5). **A:** Aortic peak velocity. **B:** Aortic peak gradient. **C:** Aortic velocity time integral (VTI). **D:** Mitral velocity time integral (VTI). **E:** Mitral peak velocity **F:** Mitral peak gradient. **G:** Mitral E/A ratio. Data are presented as mean ±SEM; n = 9 mice. #*p<0.05* vs Baseline; ##*p<0.01* vs Baseline (Two-way ANOVA followed by Bonferroni post-hoc test).

6.3.4. Investigating potential cardioprotective mechanism(s) of perhexiline and FPER-1 treatment in AAC mice

The expression and/or phosphorylation of proteins investigated in Chapter 4 were measured in AAC-treated mice.

6.3.4.1. Effects of perhexiline and FPER-1 on PLB expression and phosphorylation in AAC mice

There was no significant difference in phospholamban (PLB) expression (*p=0.63*) between sham-operated controls and vehicle-treated AAC controls whilst any difference in phosphorylation at PLB^{Ser16} (1.4-fold decrease; *p=0.22*) or PLB^{Thr17} (1.6-fold decrease; *p=0.09*) was not significant **[Figure 6.14]**. In AAC mice, perhexiline or FPER-1 treatment did not alter PLB expression compared to vehicle-treated mice (*p=0.97*) **[Figure 6.14A+D]**. In contrast, perhexiline induced a significant increase in PLB phosphorylation at Thr17 (1.3-fold; *p<0.05*) but any effect on phosphorylated PLB^{Ser16} was not significant (1.5-fold increase; *p=0.16*) relative to the vehicle-treated AAC group **[Figure 6.14A-C]**. However, FPER-1 did not alter PLB phosphorylation at either site (Ser16 or Thr17) (*p>0.99* and *=0.16* respectively).

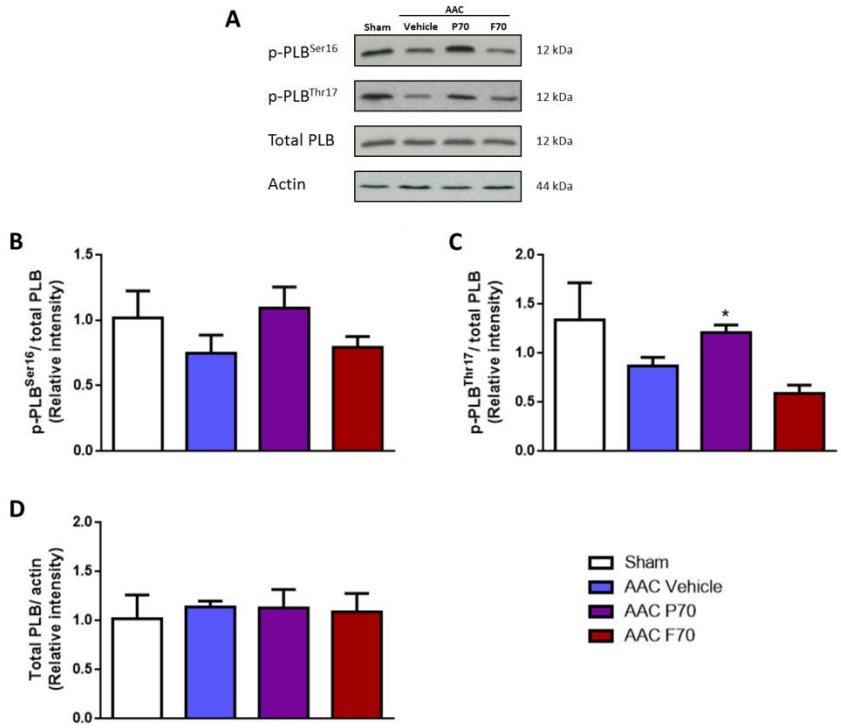

Figure 6.14. Effects of perhexiline and FPER-1 on PLB expression and phosphorylation in AAC mice

Sham mice were treated with vehicle, and AAC mice treated with either 1) vehicle, 2) 70 mg/kg perhexiline (P70) or 3) 70 mg/kg FPER-1 (F70). **A:** Representative Western blots for phosphorylated PLB Ser16, Thr17, total PLB and loading control actin. **B:** Mean phosphorylated PLB^{Ser16} over total PLB. **C:** Mean phosphorylated PLB^{Thr17} over total PLB. **D:** Mean total PLB over actin. Data are presented as mean ±SEM; n = 6-9 mice. *$p<0.05$ vs AAC Vehicle (One-way ANOVA followed by Bonferroni post-hoc test).

6.3.4.2. Effects of perhexiline and FPER-1 on CPT1B expression in AAC mice

Compared to sham-operated controls, any difference in CPT1B expression observed in vehicle-treated AAC mice was not significant (1.6-fold increase; *p=0.14*) **[Figure 6.15]**. Treatment with perhexiline or FPER-1 did not alter CPT1B expression compared to vehicle-treated AAC mice (*p=0.88*).

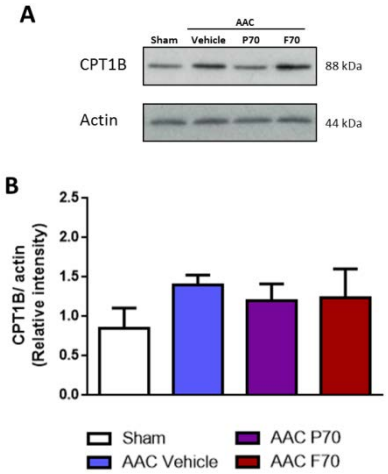

Figure 6.15. Effects of perhexiline and FPER-1 on CPT1B expression in AAC mice

Sham mice were treated with vehicle, and AAC mice treated with either 1) vehicle, 2) 70 mg/kg perhexiline (P70) or 3) 70 mg/kg FPER-1 (F70). **A:** Representative Western blots for total CPT1B and loading control actin. **B:** Mean total CPT1B over actin. Data are presented as mean ±SEM; n = 6-8 mice

6.3.4.3. Effects of perhexiline and FPER-1 on PDH, GSK3αβ, Akt and ERK1/2 expression and/or phosphorylation in AAC mice

No difference in expression or phosphorylation (at Ser232, 293 or 300) of PDH was observed between sham-operated mice and vehicle-treated AAC mice (*p=0.78*, *0.62*, *0.51* and *0.7* respectively) **[Figure 6.16]**. Therefore, as expected, perhexiline or FPER-1 treatment had no effect on PDH expression or phosphorylation (at Ser232, 293 or 300) relative to vehicle-treated AAC mice (*p=0.98*, *0.77*, *0.94* and *0.56* respectively).

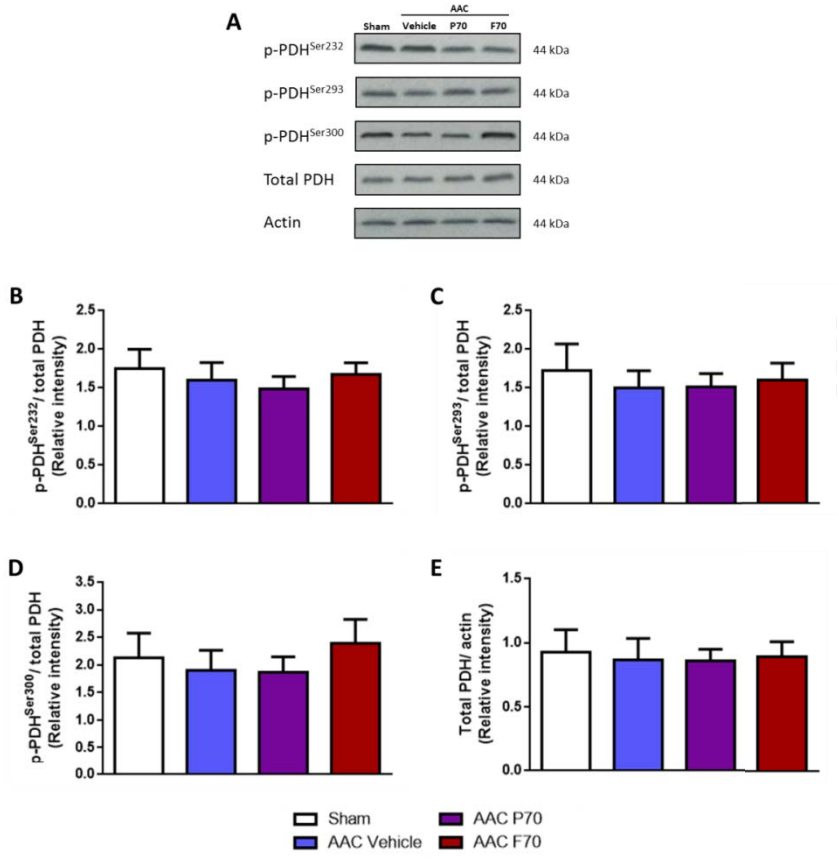

Figure 6.16. Effects of perhexiline and FPER-1 on PDH expression and phosphorylation in AAC mice

Sham mice were treated with vehicle, and AAC mice treated with either 1) vehicle, 2) 70 mg/kg perhexiline (P70) or 3) 70 mg/kg FPER-1 (F70). **A:** Representative Western blots for phosphorylated PDH Ser232, 293, 300, total PDH and loading control actin. **B:** Mean phosphorylated PDH^{Ser232} over total PDH. **C:** Mean phosphorylated PDH^{Ser293} over total PDH. **D:** Mean phosphorylated PDH^{Ser300} over total PDH. **E:** Mean total PDH over actin. Data are presented as mean ±SEM; n = 6-9 mice.

Similarly, phosphorylation of glycogen synthase kinase 3αβ (GSK3αβ), protein kinase B (Akt) and extracellular signal-regulated kinase 1/2 (ERK1/2) were not altered in AAC mice relative to sham controls (*p=0.98*, *0.67* and *0.95* respectively) and drug treatment had no effect on Akt or ERK1/2 phosphorylation relative to the vehicle-treated AAC group (*0.52* and *0.49* respectively) **[Figure 6.17]**. Regarding GSK3αβ phosphorylation at Ser21/9, any effect observed in perhexiline-treated (1.3-fold increase; *p=0.87*) or FPER-1-treated (1.4-fold

increase; *p=0.58*) AAC mice was not significant compared to the vehicle-treated AAC mice **[Figure 6.17A+B]**.

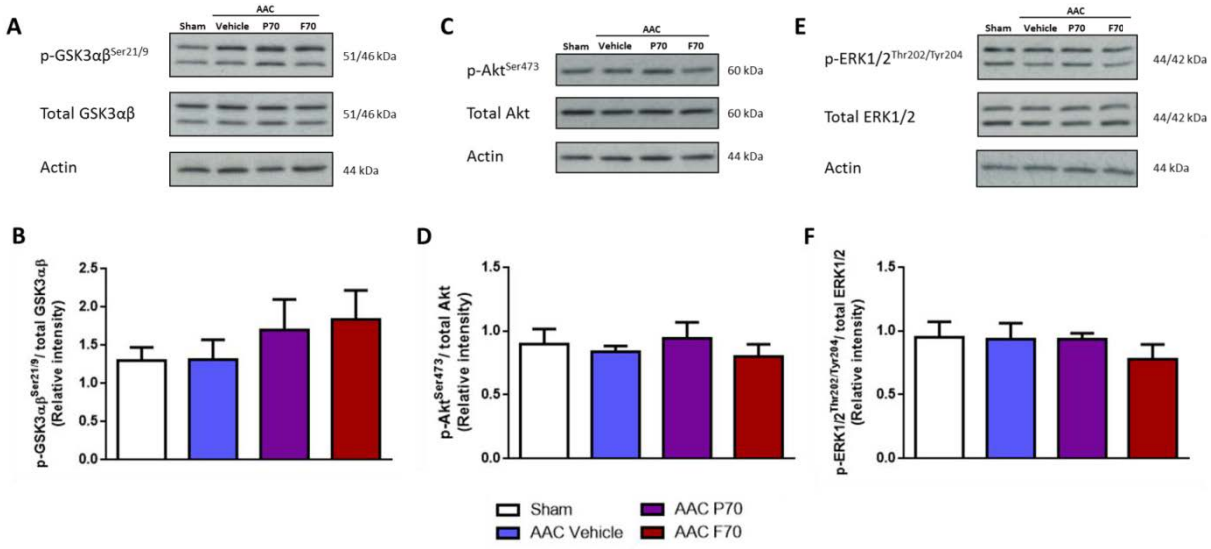

Figure 6.17. Effects of perhexiline and FPER-1 on GSK3αβ, Akt and ERK1/2 phosphorylation in AAC mice

Sham mice were treated with vehicle, and AAC mice treated with either 1) vehicle, 2) 70 mg/kg perhexiline (P70) or 3) 70 mg/kg FPER-1 (F70). **A:** Representative Western blots for phosphorylated GSK3αβ Ser21/9, total GSK3αβ and loading control actin. **B:** Mean phosphorylated GSK3αβ$^{Ser21/9}$ over total GSK3αβ. **C:** Representative Western blots for phosphorylated Akt Ser473, total Akt and loading control actin. **D:** Mean phosphorylated Akt^{Ser473} over total Akt. **E:** Representative Western blots for phosphorylated ERK1/2 Thr202/Tyr204, total ERK1/2 and loading control actin. **F:** Mean phosphorylated ERK1/2$^{Thr202/Tyr204}$ over total ERK1/2. Data are presented as mean ±SEM; n = 6-9 mice.

6.3.4.4. Effects of perhexiline and FPER-1 on TXNIP, UCP3 and ANT expression in AAC mice

No differences were observed in TXNIP or ANT expression in sham-operated controls relative to vehicle-treated AAC mice, and any effect on UCP3 expression was not significant (1.2-fold increase; *p=0.11*) **[Figure 6.18]**. Not surprisingly, neither perhexiline nor FPER-1 treatment altered either TXNIP or ANT levels in AAC mice relative to the vehicle-treated AAC group (*p=0.78* and *0.59* respectively) **[Figure 6.18A+B and 6.18E+F]**. In contrast, both perhexiline and FPER-1 treatment significantly decreased UCP3 expression in AAC mice relative to

vehicle-treated AAC mice (1.3-fold and 1.4-fold respectively; *p<0.05* for both) **[Figure 6.18C+D]**.

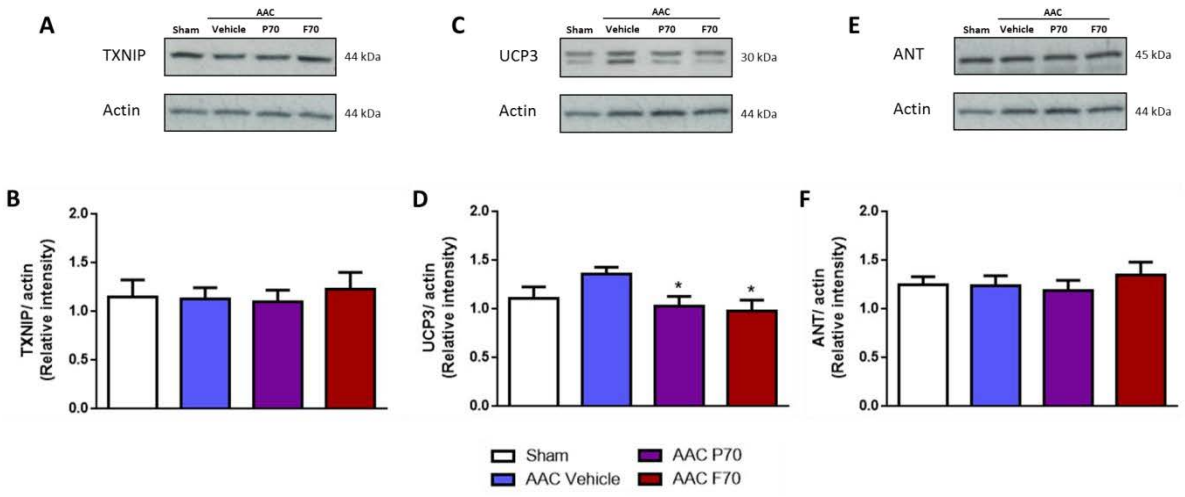

Figure 6.18. Effects of perhexiline and FPER-1 on TXNIP, UCP3 and ANT expression in AAC mice

Sham mice were treated with vehicle, and AAC mice treated with either 1) vehicle, 2) 70 mg/kg perhexiline (P70) or 3) 70 mg/kg FPER-1 (F70). **A:** Representative Western blots for total TXNIP and loading control actin. **B:** Mean total TXNIP over actin. **C:** Representative Western blots for total UCP3 and loading control actin. **D:** Mean total UCP3 over actin. **E:** Representative Western blots for total ANT and loading control actin. **F:** Mean total ANT over actin. Data are presented as mean ±SEM; n = 6-9 mice. **p<0.05* vs AAC Vehicle (One-way ANOVA followed by Bonferroni post-hoc test).

6.4. Discussion

To date, perhexiline has had promising therapeutic effects in patients with HF (Lee et al., 2005; Phan et al., 2009b; Beadle et al., 2015) but its full therapeutic capability and mechanism of action are not well understood. In addition, the novel derivative FPER-1 has yet to be tested in a model of HF. Therefore, the work in this chapter aimed to assess both metabolic drugs in a murine model of hypertrophy and progression to HF, and to determine whether these drugs could delay disease progression. To do this, it was important to first establish the *in vivo* model and ensure that the results would be reproducible.

6.4.1. Establishing a model of cardiac hypertrophy and progression to failure

Various HF animal models exist which involve subjecting the myocardium to a cardiac stress, to trigger hypertrophic remodelling that eventually progresses into failure (Berry et al., 2007; Gomes et al., 2013). This includes infusing a neurohormonal stressor such as angiotensin (Guan et al., 2017; Shimizu et al., 2017), causing ischaemic stress by coronary artery ligation (Antoniak et al., 2013; Muthuramu et al., 2014), volume overload by an aortocaval shunt (Wu et al., 2015; Mohamed et al., 2016) or inducing pressure overload, achieved through either a high-salt diet in Dahl salt-sensitive rats (Huang et al., 2017; Amara et al., 2017), renal wrapping (Morioka and Simon, 1982) or aortic constriction (Zhou et al., 2017; C. Li et al., 2017). Of these techniques pressure overload by aortic constriction is one of the most common (Gomes et al., 2013) and holds greater clinical relevance due to the gradual transition from a stable compensated hypertrophy to enlargement of the heart chambers and deterioration in LV function (decompensated state), terminating in HF with augmented hypertrophy, all of which correlate with the disease progression in humans (Boluyt et al., 2005). Clinically, HF induced by pressure overload (i.e. hypertension) is well-characterised by detrimental changes in cardiac metabolism (Sankaralingam and Lopaschuk, 2015). Experimentally, the surgical technique of inducing pressure overload holds the advantage of allowing manipulation of the level of pressure overload, by changing the severity of constriction (Duan et al., 2007; Moens et al., 2009).

Aortic constriction can be achieved by ligating the ascending aorta (close to the aortic root), transverse aorta (at the aortic arch) or descending aorta (abdominally, above or below the renal arteries) (Gomes et al., 2013). In recent years, abdominal aortic constriction (AAC) has

become more widely used than thoracic aortic constriction (TAC; ascending aorta and transverse aorta) because the operative procedure is less complex and does not require open-chest surgery or mechanical ventilation. Furthermore, for the same given stenosis size, the effects are more pronounced following TAC due to the closer proximity to the heart (Rockman et al., 1991), leading to rapid disease progression, whilst AAC causes a more gradual rise in pressure (Ku et al., 2016). As such, AAC is considered a less traumatic and less severe model, as demonstrated by its associated lower mortality rate (as low as 10%) (Gomes et al., 2013). Thus, the AAC model of cardiac hypertrophy and HF was chosen for the present study, using the well-established protocol from Queen Mary University of London to constrict the abdominal aorta against a 27-gauge needle (Moyes et al., 2015).

To assess LV function, ejection fraction (EF) and fractional shortening (FS) were measured, both of which are important clinical markers and indicators of myocardial contractile efficiency (The Japan Society of Ultrasonics in Medicine, 2006). EF describes the percentage of blood ejected from the heart upon each contraction whilst FS refers to the reduction of length (degree of shortening) of the LV diameter between end-diastole and end-systole (The Japan Society of Ultrasonics in Medicine, 2006). In the present study, both parameters were significantly reduced 3 weeks post-AAC, and the reduction became more pronounced with time, resulting in a 20% decrease in EF and a 14.1% decrease in FS by week 5; indicative of mild LV systolic dysfunction. These results corroborate those of Heinecke and co-workers (2017) who, using a 27-gauge needle and AAC, observed a ~20% decrease in EF and a fall in FS at week 4 in AAC mice. Other murine AAC studies have also observed significant reductions in EF and FS by week 6 when using a 27-gauge needle (Ruetten et al., 2005; C. Li

et al., 2017). Furthermore, the present results are consistent with murine AAC studies that used a 26-gauge needle for constriction and demonstrated a 20% fall in EF (C.Z. Zhao et al., 2016; Aubdool et al., 2017) and a 15.5% fall in FS (Gravning et al., 2013).

In addition, the present markers of hypertrophic growth (LV mass and HW) indicated that compensated hypertrophy was not instantaneous following AAC, but gradual after the first week in the presence of preserved LV function (EF and FS unchanged). By week 3, decompensated hypertrophy had taken place as the LV mass had continued to rise in parallel with a loss of function (decrease in EF and FS). Moreover, by week 5, the LV mass/BW had significantly increased by 40% whilst the HW/BW ratio was 44% greater than that of the sham controls. Ruetten and colleagues (2005) observed similar hypertrophic results, with an increase of 46% in LV mass/BW ratio in mice 6 weeks post-aortic constriction, compared to the sham group when they used a 27-gauge needle. Other AAC mice studies also demonstrated compensatory increases in LV mass followed by decompensated hypertrophy by the end of a 4-6 week study (Hara et al., 2002; Duan et al., 2007; Hua et al., 2012; Xu et al., 2014; Aubdool et al., 2017; Heinecke et al., 2017; C. Li et al., 2017).

In the present study, cardiac remodelling (hypertrophy and/or dilatation) was further assessed by measuring ventricular dimensions (volumes and wall thickness). Increases in interventricular septal wall (IVS), posterior wall (LVPW) and anterior wall (LVAW) thickness were observed at end-diastole by week 5 in AAC mice. These results corroborate those of Weng et al. (2012), Zhang et al. (2013), Boguslavskyi et al. (2014) and C.Z. Zhao et al. (2016) who all observed increases in end-diastolic IVS and LVPW thickness in AAC mice. Other

studies also demonstrated increases in these cardiac dimensions in AAC mice (Zou et al., 2001; Zahabi et al., 2003; Xu et al., 2014; Gravning et al., 2013; Aubdool et al., 2017; Heinecke et al., 2017).

In the present study, increases in LV end-systolic volume and end-systolic LV internal diameter (LVID) also occurred, further indicating contractile dysfunction. This is consistent with previous studies which demonstrated an increase in end-systolic LVID (C.Z. Zhao et al., 2016; Heinecke et al., 2017) and LV end-systolic volume (Boguslavskyi et al., 2014; C. Li et al., 2017) in AAC mice. Of note, end-diastolic LVID, an indicator of cardiac dilatation, was not altered in the present study.

Finally, aortic and mitral valve velocity time integral (VTI), indicators of the corresponding valve area which can also reflect the stroke volume (SV), and peak velocity and peak gradient were measured; when the latter two are increased this indicates a decrease in valve area (Otto., 2006). By week 5, AAC mice displayed a significant increase in both aortic peak velocity and gradient, but a contradictory *increase* in aortic VTI. Boguslavskyi and colleagues (2014) also observed significant increases in aortic peak velocity and gradient at week 6 in AAC mice, but a marginal decrease in VTI. On the other hand, in the present study, AAC did not alter mitral valve VTI, peak velocity or gradient, useful variables for evaluating diastolic filling clinically (Daneshvar et al., 2010). Moreover, the mitral E/A ratio (a ratio of the early and late ventricular filling velocity), a measure of diastolic dysfunction (Daneshvar et al., 2010), remained unchanged in the present AAC mice, as in the AAC study performed by Ruetten and colleagues (2005).

Healthy LV diastolic function is confirmed by a mitral E wave which is higher than the A wave and this relationship becomes reversed at the onset of impaired relaxation. However, in moderate diastolic dysfunction, pseudonormalisation of the E/A ratio occurs in which the transmitral Doppler waveform appears normal because the impaired early LV filling is compensated by an increase in left atrial pressure (Little et al., 1998). It is therefore possible that the present AAC model induced moderate diastolic dysfunction resulting in pseudonormalised LV filling, and thus the model would be one of mild HF rather than of hypertrophy and mild LV systolic dysfunction. Further analysis, such as measuring the E wave deceleration time, would be required to confirm this.

Circulating BNP plasma levels, an important incipient and prognostic marker of HF (Khanam et al., 2017), were also assessed from sham-operated mice and vehicle-treated AAC mice. Due to time constraints, BNP plasma levels were not assessed in untreated mice. In the present AAC mice there was no increase in BNP relative to the sham controls. This is consistent with the echocardiographic data in demonstrating that the present AAC model induced mild LV systolic dysfunction but not frank HF. This conclusion agrees with the functional data given that LV end-diastolic volume remained unchanged (i.e. no LV dilatation) whilst EF fell only to ~50% in AAC mice, still within the normal LVEF range: HFrEF is clinically defined as an EF of <40% (Ponikowski et al., 2016). In this respect the present AAC model resembled HFpEF rather than HFrEF. Measurements of the mitral E wave deceleration time would help to clarify this by providing information of whether diastolic function was indeed impaired, as occurs in HFpEF.

It could be argued that measuring BNP protein levels in plasma using an immunoassay may not have be the most sensitive technique given that most aortic constriction mouse studies have instead measured myocardial BNP messenger ribonucleic acid (mRNA) expression via quantitative polymerase chain reaction (qPCR) (Zou et al., 2001; Gravning et al., 2013; Xu et al., 2014; C.Z. Zhao et al., 2016; Aubdool et al., 2017; J. Li et al., 2017). However, the immunoassay kit used in the present study was used in a TAC-induced HF mouse model (Bhushan et al., 2014). The authors reported similar BNP levels in their sham-operated mice as in the present study (~1 µg/µl), but BNP levels were almost double this (~2 µg/µl) in TAC mice at 9 weeks, and this was accompanied by a 40% decrease in EF (compared to the 20% decrease in the present AAC mice). This finding suggests that a more severe AAC (as achieved by TAC) would be required to observe an increase in plasma BNP when using immunoassay.

Nevertheless, in combination, the results of the present study replicated that of other studies on AAC mice, confirming that the methodology produced a model of cardiac hypertrophy and progression to HF, which showed significant and reproducible hypertrophy by week 3 post-surgery.

6.4.2. Survival, drug toxicity and drug pharmacokinetics in AAC mice

Having established the AAC model, drug treatment was commenced. Alongside the functional and morphometric measurements discussed below (section 6.4.3), animal survival following AAC was assessed, as well as drug pharmacokinetics and *in vivo* toxicity following 4-week treatment. Survival rates post-AAC were high (90.2%), with the majority of deaths

being perioperative due to surgical complications. In fact, the first week post-surgery was identified as the critical period, most deaths taking place at this point. Importantly, the gavage procedure and daily treatment with perhexiline or FPER-1 did not affect survival. Furthermore, the AAC procedure did not affect the normal gain in weight over the 5-week study period and AAC mice were not phenotypically different from the sham-operated mice despite the gradual development of pathological hypertrophy. It may be noted that perhexiline caused marked body weight loss in angina patients (Myers and Ronthal, 1978) and short-term treatment for 3-4 months caused transient weight loss (2-4 kg) in chronic HF patients (Phan et al., 2009b), but these data were collected following a longer treatment period than in the present study.

As expected from the results of Chapter 5, daily gavage with 70 mg/kg perhexiline was sufficient to achieve detectable drug plasma levels; plasma levels were in fact 1.4-fold higher than the established therapeutic range (0.15 – 0.6 mg/L) and higher than those measured in Chapter 5 (section 5.3.2). As was also expected, the perhexiline metabolite (OH-perhexiline) was present at a lower level than its parent drug, whereas FPER-1 plasma levels were several times higher than perhexiline, confirming the differences between FPER-1 and perhexiline metabolism and stability. Nonetheless, 4-week gavage treatment in AAC mice with perhexiline or FPER-1 was safe in that no drug-induced deaths took place during the study despite the slightly higher than expected perhexiline plasma levels. Importantly, the dose of 70 mg/kg for both drugs was not hepatotoxic as assessed by histopathology and plasma ALT levels, confirming the results from Chapter 5 (section 5.3.3). Clinical studies have reported similar findings, demonstrating that when maintained within the established therapeutic

plasma range, prolonged perhexiline therapy does not induce hepatotoxicity or significant side effects (Unger et al., 1997; Lee et al., 2005; Abozguia et al., 2010; Beadle et al., 2015; Drury et al., 2015).

6.4.3. Effects of perhexiline and FPER-1 treatment on cardiac function and remodelling in AAC mice

Following the induction of pressure overload by AAC, vehicle or drug treatment were commenced by daily oral gavage 1 week post-surgery. Vehicle-treated AAC mice displayed the same development of compensated hypertrophy at week 1, followed by decompensated hypertrophy (increase in LV mass/BW and HW/BW ratio) and cardiac dysfunction (20% decrease in EF and decrease in FS) by week 5, as the untreated AAC mice discussed in section 6.4.1. Furthermore, vehicle-treated AAC mice showed the same form of cardiac remodelling as the untreated AAC mice (increase in end-diastolic IVS, LVAW and LVPW thickness and increase in end-systolic LV volume and LVID), confirming the reproducibility of the model. The mitral E/A ratio was also similarly unchanged in vehicle-treated AAC mice, although as discussed above (section 6.4.1), it is possible this reflected pseudonormalisation. However, whilst an increase in aortic peak velocity and gradient were observed in vehicle-treated AAC mice, aortic VTI was unchanged and mitral VTI was reduced, the latter suggestive of reduced SV, in contrast to what was observed in the untreated AAC mice. This disparity indicates that the Doppler flow echocardiographic measurements were not as reproducible as the functional and morphological measures (for further discussion see study limitations; section 6.4.5).

Considering the effects of drug treatment, the present results revealed that 70 mg/kg perhexiline alleviated cardiac dysfunction by attenuating the fall in both EF and FS at week 5. This corresponds to results in mice with experimentally-induced irreversible HF, in which perhexiline therapy attenuated cardiac dysfunction (Stapel et al., 2017). The present results are also consistent with findings from the clinical trial by Lee and colleagues (2005) who observed an improvement in LVEF (10% increase vs placebo treated) in chronic HF patients, following 8 weeks drug therapy. In contrast Beadle and colleagues (2015) observed no improvement in LVEF in HFrEF patients, following short-term (4 weeks) perhexiline treatment despite plasma levels falling within the therapeutic range. Moreover, EF was also unaltered in perhexiline-treated patients with non-obstructive HCM (Abozguia et al., 2010) and FS unaltered following perhexiline therapy in a genetic mouse model of HCM (Gehmlich et al., 2015). In addition, although perhexiline did not significantly improve LV end-systolic volume in the present study, this effect has been reported clinically in chronic HF patients as perhexiline therapy reduced LV end-systolic volume by 20% and improved long-axis systolic function by 24% (Lee et al., 2005).

In contrast, 70 mg/kg FPER-1 did not replicate perhexiline's therapeutic effects on function as EF and FS continued to decrease over the 5-week study and thus cardiac dysfunction was not prevented. However, surprisingly only FPER-1 attenuated the increase in end-diastolic LVAW thickness; this parameter remained unchanged with perhexiline, despite perhexiline attenuating the increase in end-diastolic LVAW thickness in mice with hypertrophic hearts (Gehmlich et al., 2015).

Despite these differences, both perhexiline and FPER-1 treatment in AAC mice had similar therapeutic effects on cardiac hypertrophy as they both attenuated the increase in HW/BW, although their effects on LV mass/BW were not statistically significant. Improvements in LV mass, but not HW/BW, were previously demonstrated in a genetic mouse model of HCM following 6 weeks twice-daily dosing with perhexiline (Gehmlich et al., 2015). Moreover, in the present study, both perhexiline and FPER-1 reduced LVPW thickness at end-diastole, also indicative of reduced hypertrophy and remodelling. However, interestingly, neither perhexiline nor FPER-1 improved LVID at end-systole, a marker of systolic function, nor affected aortic or mitral valve measurements, or mitral E/A ratio (indicative of end-diastolic pressure). The lack of change in mitral E/A ratio in the present study may be due to the present AAC mice having mild LV dysfunction and not frank HF, for perhexiline reduced the mitral E/A ratio by 24% in patients with chronic HF (Lee et al., 2005), and in HCM patients it normalised diastolic LV filling on exercise (Abozguia et al., 2010).

Nevertheless, in combination, the results of the present study complement the current literature (Lee et al., 2005; Phan et al., 2009b; Abozguia et al., 2010; Beadle et al., 2015; Gehmlich et al., 2015; Stapel et al., 2017). By assessing a broad range of end-diastolic and end-systolic parameters for the first time, the present results demonstrate that perhexiline has the potential to prevent cardiac dysfunction and remodelling (prominent features of HF). Furthermore, the present study also provides novel evidence that the new derivative FPER-1, given at the same dose as perhexiline, can replicate the beneficial effects on hypertrophy and remodelling. The lack of effect of FPER-1 on systolic function suggests that despite plasma levels being ~4-fold higher than the parent drug, the dose used may be at the lower

end of FPER-1's therapeutic range. Therefore, further work is required to establish the FPER-1 dose required to achieve full effects on function and morphology. Moreover, it suggests that different mechanisms may be involved in preventing hypertrophy versus dysfunction.

6.4.4. Potential cardioprotective mechanisms of perhexiline and FPER-1 in AAC mice

6.4.4.1. Effects of perhexiline and FPER-1 on the cardiac contractility-relaxation pathway in AAC mice

As discussed in Chapter 1 (section 1.4.1), dysregulation of cardiac contractility occurs in HF (Dorn and Molkentin, 2004). Such dysfunction is thought to involve increased PLB activity (PLB dephosphorylation), resulting in increased sarco-endoplasmic reticulum Ca^{2+}-ATPase (SERCA) inhibition and thus reduced Ca^{2+} cycling in the myocardium which impairs cardiac contractility and relaxation (Haghighi et al., 2014). In the present AAC model, PLB expression was not altered; similar findings were made in a rat model of ascending aortic constriction (Miyamoto et al., 2000) and in TAC mouse models (Buys et al., 2007; Toischer et al., 2010; Kho et al., 2011). However, PLB dephosphorylation at both Ser16 and Thr17 did appear to increase in the present AAC mice, which is consistent with the decreased cardiac function observed in these mice compared to the sham controls, but this effect was not significant. Significant increases in PLB dephosphorylation, which suggest increased PLB activity, have been reported in several TAC mice studies (Buys et al., 2007; Loyer et al., 2008; Gelpi et al., 2009; Pereira et al., 2013; Chen et al., 2016; Aoyama et al., 2016).

The present data also provided novel evidence that 70 mg/kg perhexiline decreased PLB activity in AAC mice, judged by increased phosphorylation at Thr17. This result was not

replicated by FPER-1 and therefore accords with the lack of improvement in cardiac function following 70 mg/kg FPER-1 treatment.

These data therefore complement the literature which has shown that increased PLB phosphorylation improves contractile function (attenuates the fall in EF and/or FS) in AAC rats (Pritchard et al., 2013) and in rats with isoproterenol-induced HF (P.X. Wang et al., 2017). Increased PLB phosphorylation at Ser16 and Thr17 (PLB inhibition) also attenuated hypertrophic growth and delayed the onset of HF in TAC mice (Pathak et al., 2005), halted cardiac remodelling in AAC rats (Pritchard et al., 2013) and decreased LVID in rats with isoproterenol-induced HF (P.X. Wang et al., 2017). However, in the present study, both perhexiline and FPER-1 attenuated hypertrophy and remodelling even though only perhexiline inhibited PLB, thereby suggesting that PLB was not involved in this protection.

6.4.4.2. Effects of perhexiline and FPER-1 on fatty acid metabolism in AAC mice

The downregulation of both the FA and glucose oxidation pathway have been described in various HF studies (Tuunanen et al., 2006; Doenst et al., 2010; Kaimoto et al., 2017), however, upregulating glucose oxidation in parallel to decreasing FA oxidation produces a more favourable oxygen sparing effect; this evidence is discussed in greater detail in Chapter 1 (section 1.7).

In the present AAC mice, the expression of the rate-limiting enzyme for FA oxidation, CPT1B, was not significantly altered. This was interesting as previous pressure overload studies have described a *decrease* in FA oxidation and CPT1B expression in TAC mice (Lai et al., 2014;

Dong et al., 2017) and AAC rats (Akki et al., 2008). A decrease in FA oxidation was also reported in other TAC mice studies (Kolwicz et al., 2012; Kaimoto et al., 2017). However, Zhabyeyev and colleagues (2013) observed no change in FA oxidation in TAC mice and Nguyen and co-workers (2015) reported no change in FA oxidation in AAC rats. In addition, CPT1B expression remained unaltered in AAC rats (Dobrzyn et al., 2013), in ascending aortic-constricted mice (Nakajima et al., 2013) and in TAC mice (Pereira et al., 2013), demonstrating the variability in results amongst these pressure overload studies. On the other hand, an increase in FA oxidation, of up to 40%, was described clinically in patients with congestive HF (Paolisso et al., 1994). Additionally, increases in FA accumulation are known to occur during pathological hypertrophy and LV dysfunction (Chiu et al., 2001).

In the present study, neither perhexiline nor FPER-1 treatment altered CPT1B expression in AAC mice supporting the concept that CPT1B may not be involved in perhexiline-mediated protection. This finding is consistent with the results obtained in patients with HFrEF, in which perhexiline therapy did not alter FA uptake from the blood despite improvements in the New York Heart Association (NYHA) functional class (Beadle et al., 2015). However, Gehmlich and colleagues (2015) reported that daily injection with perhexiline decreased long chain FAs in hypertrophic mouse hearts, indicative of decreased CPT1B activity. Similar results, i.e. a decrease in serum FA levels, were also observed clinically in HCM patients treated with perhexiline (Abozguia et al., 2010). Furthermore, decreased intracellular FA levels were suggested to ameliorate cardiac hypertrophy in AAC rats (Gao et al., 2015) whilst direct CPT1B inhibition with oxfenicine abrogated LV remodelling and delayed progression to failure in dogs with pacing-induced HF (Lionetti et al., 2005). Moreover, in TAC rats, etomoxir

treatment did not alter CPT1B activity and thus failed to reverse progression to failure (Schwarzer et al., 2009). Together these studies suggest that a decrease in FA metabolism, whether through CPT1B downregulation or not, *is* protective in HF.

6.4.4.3. Effects of perhexiline and FPER-1 on glucose metabolism in AAC mice

In the present study, the expression and activity of PDH, the rate limiting enzyme for glucose metabolism, were not altered in AAC mice. Similarly, PDH expression was unaltered in AAC rats (Seymour and Chatham, 1997), PDH activity unchanged in ascending aortic constricted rats (Schwarzer et al., 2009) and PDH expression and activity unchanged in TAC mice (Carley et al., 2015). However, in some contrast to these findings, a reduction in glucose oxidation was described in other TAC mice studies (Dai et al., 2012; Zhabyeyev et al., 2013; Kaimoto et al., 2017), in TAC rats (Sorokina et al., 2007; Doenst et al., 2010) and in AAC mice (Zhang et al., 2013) implicating other proteins involved in glucose metabolism.

In the present study, 4-week perhexiline or FPER-1 treatment did not affect PDH expression or increase its activity in AAC mice as judged by absence of PDH dephosphorylation. This may be related to the lack of pathological downregulation of PDH in the present AAC model, despite reports that PDH activity is reduced in hypertrophic rat hearts (Seymour and Chatham, 1997). However, Yin and colleagues (2013) observed an increase in myocardial PDH activity (decrease in total phosphorylation) in healthy mice, fed perhexiline for 4 weeks. Perhexiline also increased intermediates of the glycolytic, glycerol and pentose phosphate pathway in mice with hypertrophic hearts, suggesting increased glucose metabolism (Gehmlich et al., 2015). However, in both of these studies, perhexiline treatment was

maintained over a 24 h period to ensure plasma levels were sustained within the therapeutic range throughout the course of the study. Thus, the lack of effect of perhexiline in the present study may be explained by the fact that the once-daily gavage did not achieve constant perhexiline or FPER-1 levels throughout each day. It would be necessary to collect plasma samples at additional time points from drug-treated AAC mice to test this proposal. The evidence from clinical studies is equivocal on whether perhexiline affects glucose metabolism. To expand, Abozguia and colleagues (2010) observed a decrease in serum glucose levels following perhexiline treatment in HCM patients, but Beadle and colleagues (2015) reported that perhexiline therapy did not alter myocardial or serum glucose levels in HFrEF patients. Concerning FPER-1, the levels achieved in plasma were likely to have been better maintained between doses than was the case for perhexiline (see Chapter 5, section 5.3.2). However, the lack of effect FPER-1 had on PDH may reflect the absolute plasma level rather than the constancy of it. In summary, the present results suggest that PDH activation was not a cardioprotective mechanism of perhexiline or FPER-1 in AAC mice.

Phosphorylation and thus activity of GSK3αβ, which was demonstrated to inhibit PDH activity (Hoshi et al., 1996), was also unchanged in the present AAC mice. Perhexiline and FPER-1 treatment also had no significant effect on GSK3αβ phosphorylation in AAC mice, thus indicating that GSK3αβ inhibition did not underlie the improvements in hypertrophy and remodelling achieved with both drugs, even though GSK3αβ inhibition is regarded as cardioprotective. To clarify, genetic inhibition of GSK3αβ improved LV contractile function in TAC mice (Hirotani et al., 2007) whilst pharmacological GSK3αβ inhibition protected against ischaemia in hypertrophic rabbit hearts (Barillas et al., 2007). It should be noted that

interpreting the effects of GSK3αβ expression/phosphorylation are not straightforward for Matsuda and colleagues (2008) reported that inhibition of GSK3β *contributed* to pathological hypertrophy, whereas inhibition of GSK3α was protective in TAC mice. Therefore it is possible that perhexiline or FPER-1 treatment had differential effects on the GSK3α and GSK3β isoforms in the present study and this could not be discerned by considering the two isoforms together.

6.4.4.4. Effects of perhexiline and FPER-1 upstream of GSK3αβ in AAC mice

The activity of Akt and ERK1/2, proteins upstream of GSK3αβ, were assessed. Due to their role in potentiating physiological cell survival (Hausenloy and Yellon, 2007), hypertrophy and cardiac growth, Akt and ERK1/2 activity in pathological cardiac remodelling and HF becomes maladaptive (Shiojima and Walsh, 2006; Rose et al., 2010). As such, increases in ERK1/2 phosphorylation are often used as a marker of pathological cardiac hypertrophy and failure in TAC (J. Zhang et al., 2016) and AAC (Hua et al., 2013) mouse models. In the present AAC mice, phosphorylation of Akt and ERK1/2 (indicating activation) was not altered relative to sham-operated mice. This is in contrast to the increases in Akt and ERK1/2 phosphorylation described in TAC mouse models of HF (Xu et al., 2008; Sbroggiò et al., 2011; L. Zhao et al., 2016) and clinically in failing human hearts (Haq et al., 2001; Baba et al., 2003). However, Sopontammarak and colleagues (2005) reported that ERK1/2 activation may be dependent on the severity of pressure overload used whilst Rothermel and co-workers (2005) reported no change in Akt activity in another TAC mouse study. Thus, it may be that the pressure overload produced in the present AAC model was not great enough to affect Akt or ERK1/2 activity.

In the present study, 4-week treatment with perhexiline or FPER-1 in AAC mice had no effect on Akt or ERK1/2 phosphorylation, suggestive of unaltered activity. Therefore, it appears that modulation of these pro-survival proteins was not involved in the functional improvements observed with perhexiline, or the reduction in cardiac hypertrophy and remodelling observed with both perhexiline and FPER-1, even though modulation of these proteins in TAC mice attenuated hypertrophy (Wei et al., 2016; X. Wang et al., 2017; Gao et al., 2017), prevented cardiac remodelling (Wei et al., 2012; Ye et al., 2015; Li et al., 2016), improved LV function (Wei et al., 2012; Ye et al., 2015; J. Li et al., 2017) and prevented HF disease progression (Qi et al., 2017).

6.4.4.5. Effects of perhexiline and FPER-1 on redox-sensitive proteins in AAC mice

Redox-sensitive proteins TXNIP and ANT remained unchanged in AAC mice, and any difference in UCP3 expression was not significant, despite evidence that these proteins all play a role in the pathogenesis of HF; oxidative stress induces contractile dysfunction, cardiac remodelling, hypertrophy and fibrosis (discussed in Chapter 1, section 1.7.8) (Tsutsui et al., 2011). It is possible that these results occurred because the present AAC mice had mild LV dysfunction rather than severe HF. In support of this, the more severe mouse model of TAC-induced HF induced a 40% reduction in TXNIP expression (Yoshioka et al., 2004) whilst TXNIP-null mice developed maladaptive cardiac remodelling 8 weeks post-surgery, despite initially having a reduction in hypertrophy and preserved LV function 4 weeks post-surgery (Yoshioka et al., 2007). Furthermore, although reduced TXNIP expression is implicated as a cardioprotective mechanism of perhexiline in ischaemia/reperfusion injury (Ngo et al., 2011), neither perhexiline nor FPER-1 affected TXNIP expression in the present AAC mice.

Regarding UCP3, significant increases in UCP3 expression were reported in failing human hearts and isoproterenol infusion-induced HF in mice in parallel with cardiac hypertrophy (Planavila et al., 2015). UCP3 levels were also increased in obese diabetic mice with HF (Chen et al., 2010) and increased by 53% in infarcted failing rat hearts (Murray et al., 2008); these effects were accompanied by reduced cardiac efficiency. Moreover, in mitochondria from hypertrophied rat hearts, UCP3 levels were increased by 32%, and this was associated with reduced myocardial efficiency (Boehm et al., 2001). In contrast, UCP3 expression was *reduced* in rats with doxorubicin-induced HF (Bugger et al., 2011), in TAC mice (Riehle et al., 2011; Westenbrink et al., 2015), in AAC rats (Akki et al., 2008) and reduced by 80% in failing human heart biopsies (Razeghi et al., 2002). These differences in the literature indicate that the model severity may influence the change in UCP3 expression observed. The extent of model severity may also explain why UCP3 expression was not significanly altered in the present study as the AAC mice did not have severe HF.

The present study provided novel evidence that both perhexiline and FPER-1 significantly decrease UCP3 expression in AAC mice. Decreasing UCP expression is suggested to be cardioprotective as when UCP1 expression was reduced by ranolazine therapy in AAC mice cardiac function was improved (AbdAlla et al., 2011) and moreover, increases in UCP2 expression observed in rats with HF induced by aortic regurgitation were accompanied by hypertrophy and LV remodelling (Noma et al., 2001; Murakami et al., 2002). Furthermore, increased UCP2 expression was correlated with increased pathological cardiac remodelling i.e. LV dilatation in coronary artery ligated rats (Guo et al., 2005). It can therefore be suggested that UCP3 downregulation in pressure-overloaded mice may be a key metabolic

mechanism in the attenuation of hypertrophic growth and remodelling that were observed following treatment with both perhexiline and FPER-1 in the present study.

Turning to ANT, in contrast to the present finding that ANT expression was unchanged in AAC mice, an increase in ANT1 with a concomitant decrease in ANT2 was described in dogs with pacing induced-HF (Rosca et al., 2009) and in patients with dilated cardiomyopathy (Dörner et al., 2006). This shift in ANT isoform expression is thought to be adaptive as ANT1 overexpression attenuated cardiac dysfunction caused by diabetic cardiomyopathy in mice (Wang et al., 2009) whilst ANT1 knock-out mice developed LV hypertrophy and dilatation (Narula et al., 2011). In addition, ANT1 is thought to be involved in the adaptive apoptosis that takes place to reduce hypertrophy in TAC mice (Hang et al., 2006). However, ANT1 overexpression can be cytotoxic by upregulating ROS (Baines and Molkentin, 2009). Thus, differential changes in expressions of the ANT isoforms during hypertrophy may explain an apparent lack of change in ANT expression in the present study between sham-operated and AAC mice as well as between vehicle- and drug-treated AAC mice because the expressions of all four ANT isoforms (ANT1/2/3/4) were assessed in combination. It is therefore impossible to conclude whether or not modulation of the individual ANT isoforms was involved in the observed perhexiline- or FPER-1-induced protection.

6.4.5. Study limitations

To assess both perhexiline and FPER-1, in a model of cardiac hypertrophy and progression to HF, it was necessary to first establish the AAC murine model at Birmingham. As with all newly established techniques variability of the procedure was a concern. For this reason,

drug treatment was only commenced once the AAC results were reproducible i.e. a consistent fall in EF during the 5-week study. Despite this, there were slightly different changes in the pattern of flow within the heart i.e. a decrease in mitral VTI in the vehicle-treated AAC mice which was not observed in the untreated AAC mice. The AAC procedure involves inducing a diameter of stenosis, with a suture, which is consistent throughout the study and between animals. However, there will always be a possibility for the suture knot to either become undone post-surgery, loosen overtime, or even become internalised resulting in de-banding. Therefore, it is inevitable that consistency cannot be guaranteed (Lygate et al., 2006).

To reduce such problems in the present study, the same 27-gauge needle was used for each AAC surgery and the suture was pulled as tightly as possible during the procedure to create a constriction of uniform cross-sectional area. Furthermore, at the end of the 5-week study, following organ harvest, the suture was located and isolated from each AAC mouse to ensure it had remained intact. However, in hind sight it would have been more robust to carry out a post-mortem measurement of the residual luminal diameter of the constriction knot to determine whether it remained consistent between all mice as previously described (Boguslavskyi et al., 2014). When using the AAC model inter-individual variability may also exist in response to pressure overload (Mohammed et al., 2012b). To combat this, animals were randomly assigned to treatment groups and where possible blinding was used such that echocardiography was carried out without knowledge of animal identity, weight, treatment or surgical group to avoid bias. Nonetheless, complete blinding was not possible given the present author was the *in vivo* surgeon, and also conducted the echocardiography,

daily gavage treatment and study analysis. It would have been ideal to have one of these steps, e.g. the treatment or echocardiographies, carried out by another researcher.

Difficulties were also faced with the echocardiography component of the study, which in itself can be challenging. However, anatomical markers such as the papillary muscle were used to ensure echocardiographic images were taken at the same position of the heart at each time point (baseline to week 5) and for each mouse (vehicle and drug-treated). In addition, any inaccuracies in the procedure were probably consistent as all measurements were carried out by one person, so as to reduce variability. Nevertheless, variability between groups of animals was particularly likely for the Doppler echocardiography aortic and mitral valve measurements, which required more precise probe placement (Hartley et al., 2011; Fayssoil and Tournoux, 2013). However, as noted above, the AAC procedure itself can produce variable effects between groups of animals which may explain the differences in aortic and mitral VTI between the untreated and vehicle-treated AAC mice of the present study. It should also be noted that the present aortic valve measurement values were lower than those of Boguslavskyi and colleagues (2014). This may reflect differences in the precise positioning of the Doppler probe, but may also reflect differences in the depth of anaesthesia used. In future, care should be taken to standardise these issues between groups of animals. Additionally measurements of aortic and mitral valve area would allow for more complete interpretation of the data and calculation of SV.

Whilst the AAC pressure overload technique is less surgically complex, minimally invasive and provides muscle-sparing access to the abdominal aorta, the onset of pathological hypertrophy and development of HF in mice takes longer than with other procedures such as

TAC or isoproterenol infusion. In AAC mice, it was reported that cardiac remodelling and injury is observed 10 weeks post-surgery (Ku et al., 2016) whereas HF appears to only develop 15-21 weeks post-surgery (Wettschureck et al., 2001; Hara et al., 2002). Therefore, whether a decrease in EF of 20% during the present 5-week study was sufficient for testing the therapeutic efficacy of perhexiline and FPER-1, or whether a more severe cardiac insult is required could be questioned. Moreover, the suprarenal aortic constriction used in the AAC model causes renal hypoperfusion (Cantor et al., 2005); a cause for concern given that a clinical trial revealed that pre-operative perhexiline treatment in CABG patients led to renal impairment (Senanayake et al., 2015).

Mice that underwent AAC were administered the drug treatments once daily by oral gavage based on the results from Chapter 5. Once-daily dosing meant that it was likely the perhexiline and FPER-1 plasma levels were not maintained at a constant level throughout the day, although measurements of plasma levels at additional time points would be required to confirm this. Fluctuations in the drug plasma levels may account for the lack of effect on the investigated molecular mechanisms despite the prolonged 4-week treatment. The present study can also be criticised because the concentration of drug reaching the myocardium was not measured due to time constraints which may be implicated in the lack of effect of FPER-1 on cardiac function, or lack of effect of both drugs on end-systolic remodelling or Doppler measurements. Nonetheless, improvements in function and/or end-diastolic remodelling were observed with both drugs in the present study; consistent with a clinical study by Drury and colleagues (2014) which showed that the perhexiline plasma concentration was predicative of the myocardial concentration in patients undergoing CABG, following

perhexiline treatment for 8.5 days. Furthermore, it has been recognised that due to perhexiline's amphiphilic nature, it can accumulate up to 30-fold higher in the heart than in the plasma, the concentration around the cardiac mitochondria being expected to exceed this (Ashrafian et al., 2007b). Drury and co-workers (2014) confirmed this finding as they observed cellular perhexiline concentrations much higher than the plasma concentrations, although a substantial lag existed between the therapeutic plasma levels and steady state cellular levels. Concerning FPER-1 plasma levels, although at higher levels than perhexiline, the optimal therapeutic/working dose *in vivo* is still unknown as only one dose was tested.

Finally, the cardiac samples used for molecular analysis in the present study were not snap-frozen immediately in liquid nitrogen following extraction (see section 6.2 or Chapter 2, section 2.12.3). Time delay from organ harvest to snap-freezing can have a significant impact on protein phosphorylation status (Kofanova et al., 2013). Moreover, the left ventricle was not isolated from the right ventricle and therefore Western blot analysis included a mixture of proteins from both chambers. It was reported that key differences exist in the expression and/or phosphorylation of contractile, metabolic and pro-survival proteins from the left and right ventricle when assessed in explanted failing human hearts (Su et al., 2015), which may have had an impact on the results collated in the present study.

6.4.6. Future considerations

As discussed above (section 6.4.5) the AAC model comes with limitations that should be considered in future. Firstly, larger experimental groups will certainly be required due to the variability that exists with using this model and power calculations signifying a required

group size of 20-25 for functional and molecular experiments. It would also be useful to extend the study duration to increase the severity of symptoms (further reduction in function and greater degree of hypertrophy and remodelling). This would be helpful for determining the therapeutic efficacy of perhexiline and FPER-1, as well as possible side effects. Alternatively, the severity of symptoms could be increased by using a smaller needle size for constriction, such as 29-gauge which has been used in other AAC studies (Niu et al., 2004; Xu et al., 2013).

Additional markers for cardiac dysfunction/failure should also be considered in conjunction with the echocardiographic measurements. This would include measurements of arterial blood pressure which is deemed a useful diagnostic and prognostic marker of HF (Braz Nogueira, 2017). This has been achieved in previous pressure overload studies (Luther et al., 2012; Gu et al., 2015) and can easily be done non-invasively using a tail cuff. Cardiac mRNA expression or plasma levels of biochemical markers such as atrial natriuretic peptide (Sato et al., 2012) could also be assessed in addition to BNP which was measured in the plasma alone in the present study. Moreover, cardiac histopathology would be a valuable marker of hypertrophy and fibrosis to assess disease progression and drug-induced protection. With regards to drug treatment, additional doses of FPER-1 require testing to determine its therapeutic range and the dose required to retain all of perhexiline's observed effects.

Lastly, based on the molecular results in this chapter, additional proteins such as SERCA and ryanodine receptor involved in contractility (Armoundas et al., 2007; Lu et al., 2011) and UCP2 (Akki et al., 2008) could be assessed to expand the cardioprotective mechanisms of

perhexiline and FPER-1 in AAC mice. Directly measuring FA and glucose oxidation/utilisation as well as ATP production would also be important.

6.4.7. Conclusion

In the present chapter the *in vivo* murine model of AAC-induced cardiac hypertrophy and progression to HF was used to determine whether daily oral treatment with perhexiline or FPER-1 would delay disease progression. The results revealed that both drugs attenuated hypertrophic growth and cardiac remodelling in AAC mice. Cardiac systolic function was also improved following 70 mg/kg perhexiline treatment in AAC mice. In contrast, the novel derivative FPER-1 did not improve function in AAC mice thereby not fully replicating the effects of its parent drug, despite being present at a higher plasma concentration than perhexiline. The molecular mechanisms by which perhexiline acted *in vivo* appeared to involve a decrease in PLB activity, which may be involved with the improvement in cardiac function that it induced. Moreover, treatment with both perhexiline and FPER-1 was associated with a decrease in UCP3 expression, which may have contributed to or have been caused by the attenuation of hypertrophy and remodelling induced by both drugs.

Chapter 7:
General discussion

Chapter 7: General Discussion

7.1. Heart failure and metabolic modulation

Heart failure (HF) is a severe clinical syndrome, affecting around 26 million people worldwide (Ambrosy et al., 2014). Although evidence-based pharmacological interventions exist for heart failure with reduced ejection fraction (HFrEF), morbidity and mortality remain high. Furthermore, there are no established agents for heart failure with preserved ejection fraction (HFpEF); accountable for over half the HF population (Borlaug and Kass, 2011). As such, novel pharmacological agents are urgently required. It is becoming increasingly recognised that metabolic impairment occurs in both types of HF, including mitochondrial dysfunction, oxidative stress and disrupted cardiac substrate utilisation (Siddiqi et al., 2013; Tuomainen and Tavi, 2017). Substrate utilisation offers the most potential for pharmacological targeting, therefore, metabolic drugs such as perhexiline, which modulate this, are considered for clinical use (Noordali et al., 2018). Perhexiline has proved successful clinically, but its highly polymorphic metabolism by cytochrome P450 2D6 (CYP2D6) and toxicity when at high concentrations remain problematic, despite the establishment of an effective therapeutic dose (Horowitz et al., 1986) and an appropriate drug-loading regimen (Philpott et al., 2004). Therefore, a novel analogue of perhexiline, fluoroperhexiline-1 (FPER-1), which has a similar chemical structure, *in vitro* drug potency and *in vivo* myocardial selective accumulation, in the absence of CYP2D6 metabolic liability has been developed and synthesised by Signal Pharma.

7.2. Summary of thesis aims

Against this background, the aim of the work in this thesis was to first determine whether perhexiline and FPER-1 could improve cardiac haemodynamics *ex vivo* in an isolated mouse heart Langendorff model, pre- and post-global ischaemia (Chapter 3) and to explore potential cardioprotective molecular mechanisms (Chapter 4).

The secondary aim was to determine whether perhexiline and FPER-1 could delay progression from left ventricular (LV) hypertrophy to failure *in vivo* and elucidate the molecular mechanism(s) by which perhexiline and FPER-1 act in this model (Chapter 6). To achieve this it was first necessary to identify an optimal and safe drug dose and route of administration (Chapter 5), followed by establishing, in Birmingham, the *in vivo* model using abdominal aortic constriction (AAC) (Chapter 6).

7.3. Effects of perhexiline and FPER-1 in the *ex vivo* Langendorff model

Myocardial ischaemia is a common feature of HF, resulting from diminished cardiac output to the heart itself and reduced myocardial blood flow reserve (van Veldhuisen et al., 1998). This culminates in impaired oxygen supply, a major cause of LV dysfunction and metabolic impairment (e.g. reduced substrate oxidation, adenosine triphosphate (ATP) depletion) observed in HF (de Boer et al., 2003). Ischaemia also induces aberrant cardiac remodelling (Remme, 2000) and diastolic dysfunction (particularly during exercise) (van Veldhuisen and de Boer, 2016). Moreover, ischaemic heart disease is causally implicated in HFrEF and recently identified as an important prognostic factor for HFpEF (Vedin et al., 2017). Thus, it was of particular interest to test the effects of perhexiline and FPER-1 in ischaemia and on

subsequent reperfusion. Perhexiline has proven therapeutic value in cardiovascular diseases characterised by ischaemia such as angina (Phan et al., 2009b) and aortic stenosis (Unger et al., 1997) although recent clinical trials suggested it was ineffective in ischaemia/reperfusion (Drury et al., 2015; Senanayake et al., 2015).

To accomplish this, in Chapter 3, hearts were perfused with a high-fat buffer on the Langendorff system, given that fatty acid overload occurs in HF (Lopaschuk et al., 2010) and following ischaemia i.e. post-myocardial infarction (Mueller and Ayres, 1978). Under these conditions, 2 µM perhexiline not only enhanced cardiac inotropy and lusitropy during normoxia, but also protected the heart following global ischaemia, by attenuating the increase in LV end-diastolic pressure (LVEDP), improving coronary flow rate (CFR) and attenuating hypercontracture magnitude. Additionally, the novel derivative FPER-1 at 10 µM, but not 2 µM, replicated the positive inotropic and lusitropic effects of perhexiline in normoxia, and FPER-1 also replicated the post-ischaemic improvements in LVEDP, CFR and hypercontracture. Interestingly, in contrast to 2 µM perhexiline, 10 µM FPER-1 unfavourably increased LVEDP in normoxia whilst FPER-1 at both doses favourably augmented LV developed pressure (LVDP) post-ischaemia, indicating a positive inotropic effect.

These *ex vivo* findings indicate that perhexiline and especially FPER-1, would have therapeutic potential in clinical situations of ischaemia/reperfusion, such as coronary artery bypass graft (CABG) surgery, whilst also suggesting FPER-1 would be required at plasma levels ~5-fold higher than perhexiline to have its full effects. However, it must be acknowledged that the effect of either drug on infarct size post-ischaemia was not tested

which should certainly be done in future studies. Moreover, the disparity between the present results and the disappointing effects of perhexiline in CABG patients (e.g. Drury et al., 2015) may be associated with the fact that the present study was performed on otherwise healthy young hearts, whereas CABG was necessarily performed on diseased older hearts. It seems therefore reasonable to argue that further studies on diseased mouse hearts are required to better understand the conditions under which these drugs are effective. The present results also indicate that these agents may be therapeutic in HF given that increases in LVEDP occur in HFrEF and HFpEF and are correlated with HF-related mortality (Mielniczuk et al., 2007), whilst changes in Langendorff cardiac haemodynamics were predicative of changes in ejection fraction (EF) in failing rabbit hearts (Pye et al., 1996).

Regarding potential mechanisms, the results of Chapter 4 demonstrated for the first time, that in Langendorff hearts, both perhexiline and FPER-1 increased phospholamban (PLB) phosphorylation at Ser16 and Thr17 in normoxia, consistent with PLB inhibition, but had no effect on CPT1B, or other metabolic pathways. This novel finding revealed that these 'metabolic' agents *can* target non-metabolic pathways, but also provided an explanation for their positive inotropic and lusitropic effects during normoxia. The fact that neither drug affected PLB phosphorylation in ischaemia indicates that the positive inotropic effects of FPER-1 post-ischaemia must involve other mechanisms and raises the question of whether the influences of both drugs on PLB are O_2-dependent.

Although perhexiline is a potent CPT1 inhibitor, it is argued that this is not its cardioprotective mechanism (George et al., 2016). In agreement with this, the present study

revealed that 2 μM perhexiline had no significant effect on CPT1B expression in normoxia or ischaemia, despite improved function under both conditions. This accords with previous reports that perhexiline had no effect on CPT1B activity in ischaemic mouse hearts (Kennedy et al., 2000) or during ischaemia/reperfusion, in CABG patients (Drury et al., 2015). Interestingly, in the present study, FPER-1 at 10 μM only, *decreased* CPT1B expression in ischaemia, but had no obvious additional effects post-ischaemia relative to 2 μM FPER-1 or perhexiline. Therefore, the role of CPT1B remains unclear.

Recently, it was proposed from an *in vivo* study on healthy mice that perhexiline increases pyruvate dehydrogenase (PDH) activity and therefore, upregulates glucose metabolism (Yin et al., 2013). The present study substantiated this idea, providing new evidence that during ischaemia, perhexiline dephosphorylates PDH, consistent with PDH activation, and that Ser293 and Ser300 are the target sites of action. Importantly, FPER-1 had comparable effects to perhexiline demonstrating that this action is preserved in this derivative. Furthermore, the present findings showed for the first time that both drugs increased GSK3αβ phosphorylation at Ser21/9 in ischaemia, suggesting GSK3αβ inactivation. Since GSK3 is an upstream inhibitor of PDH (Hoshi et al., 1996), GSK3αβ inhibition would be expected to promote PDH activity. In contrast, Akt and ERK1/2 activity, cardioprotective proteins upstream of GSK3αβ, were unaffected by either drug, as judged by the absence of increased phosphorylation.

The expression of redox-sensitive proteins TXNIP, ANT and UCP3 were also investigated given their role in oxidative stress and myocardial ischaemia (Tsutsui et al., 2011). The study

design did not allow assessment of the effects of ischaemia alone on their expression, but this could be resolved in future studies. Nevertheless, the results of Chapter 4 indicated that neither perhexiline nor FPER-1 affected TXNIP, UCP3 or ANT expression in normoxia or ischaemia. It would be interesting in future studies to follow their expression in reperfusion.

In summary, the results of Chapter 4 provided new evidence that perhexiline and FPER-1 are capable of improving cardiac metabolism under ischaemic conditions. Together with the results of Chapter 3, they indicated that the improvements in post-ischaemic function were in part due to perhexiline's and FPER-1's ability to upregulate glucose metabolism.

7.4. Effects of perhexiline and FPER-1 *in vivo*

The dosing studies in Chapter 5 demonstrated in healthy mice, that 1-week daily oral gavage of 70 mg/kg perhexiline achieved plasma levels within the established therapeutic range at 1 and 8 h, and was non-toxic as judged by liver histology and plasma ALT levels. At the same dose, FPER-1 plasma levels were much higher, consistent with its altered metabolism, but also non-toxic. Admittedly, it was predictable that plasma levels following daily dosing with 70 mg/kg perhexiline would fall below the therapeutic level within the 24 h between doses and limit its therapeutic capability. Furthermore, although plasma levels of FPER-1 were better maintained than perhexiline, whether 70 mg/kg would be effective could only be discerned in the functional studies of Chapter 6.

In Chapter 6, the *in vivo* model of cardiac hypertrophy progressing to HF was established for the first time at Birmingham. The model was successful as survival rates post-surgery were

high and importantly, significant reproducible cardiac hypertrophy, remodelling and cardiac dysfunction (i.e. 20% fall in EF) were achieved by week 5. However, the progressive fall in EF to 50% at 5 weeks post-AAC may be more representative of mild LV dysfunction or HFpEF than HFrEF (LVEF <40%) and thus, in retrospect, extending the study length to achieve HFrEF may have allowed for more complete assessment of the efficacies of both drugs.

Nevertheless, the present findings showed that gavage treatment with each drug produced significant improvements. To elaborate, 70 mg/kg perhexiline improved cardiac function and contractility (improved EF and fractional shortening), whereas both 70 mg/kg perhexiline and FPER-1 attenuated LV hypertrophy and abrogated end-diastolic cardiac remodelling, but aortic and mitral valve variables were unchanged. The preferential effect of both drugs on diastolic parameters, as observed in the Langendorff model, is particularly promising given that diastolic dysfunction is a key trait of HFpEF and that the majority of pharmacological interventions for HF focus on improving systolic function alone (Loudon et al., 2016).

Regarding molecular mechanisms in this AAC model, the work in Chapter 6 demonstrated that perhexiline, though not FPER-1, inhibited PLB activity (judged by increased PLB phosphorylation at Thr17). This effect suggests improved Ca^{2+} cycling contributed to the marked improvement in cardiac function induced by perhexiline. This is also consistent with the lack of FPER-1 effect on PLB activity and cardiac function in AAC mice. Given that FPER-1 at a dose 5-fold greater than perhexiline was equally effective in attenuating PLB activity in the Langendorff preparation, it would be interesting to test a higher FPER-1 dose on PLB and cardiac function in AAC mice.

Neither perhexiline nor FPER-1 altered CPT1B expression, nor PDH, GSK3αβ, Akt or ERK1/2 phosphorylation in AAC mice, but it should be noted that their phosphorylation were not changed in vehicle-treated AAC mice. Given the *ex vivo* findings of Chapters 3 and 4 which showed that during ischaemia, both perhexiline and FPER-1 *did* modulate PDH and GSK3αβ activity, and that FPER-1 also inhibited CPT1B, it is reasonable to conclude that the HF severity achieved in the present study was not accompanied by sufficient myocardial ischaemia for either drug to show these effects. Therefore, it would be interesting to test both drugs in an AAC model that progressed to frank HF, especially because metabolic dysregulation becomes more pronounced as disease severity increases (Chaanine et al., 2017).

Lastly, regarding the redox-sensitive proteins, TXNIP and ANT expression were unaltered in the vehicle-treated or drug-treated AAC mice. Any difference in UCP3 levels in vehicle-treated AAC mice was not significant; however, both perhexiline and FPER-1 significantly *decreased* UCP3 expression. This provides novel evidence that UCP3 may be one the earliest of these redox-sensitive proteins to begin to change expression during HF development and that it is also a metabolic target for perhexiline and FPER-1. Increased UCP3 expression is correlated with oxidative stress, which causes contractile dysfunction, and leads to fibrosis that contributes to cardiac hypertrophy and remodelling (Tsutsui et al., 2011). Thus, it is possible that both perhexiline and FPER-1 achieved their beneficial effects on cardiac hypertrophy and remodelling in part by modulating UCP3, but it also probable that UCP3 expression was reduced as a consequence of the drug-induced changes in hypertrophy and remodelling. Moreover it is likely that additional mechanisms remain to be identified.

Together, the results of the present AAC study indicated that perhexiline and FPER-1 have the ability to delay HF progression. Similar to the Langendorff study, these therapeutic effects involved both metabolic and non-metabolic mechanisms. On this basis the main findings of this thesis, with proposed mechanisms, are presented in **Figure 7.1**.

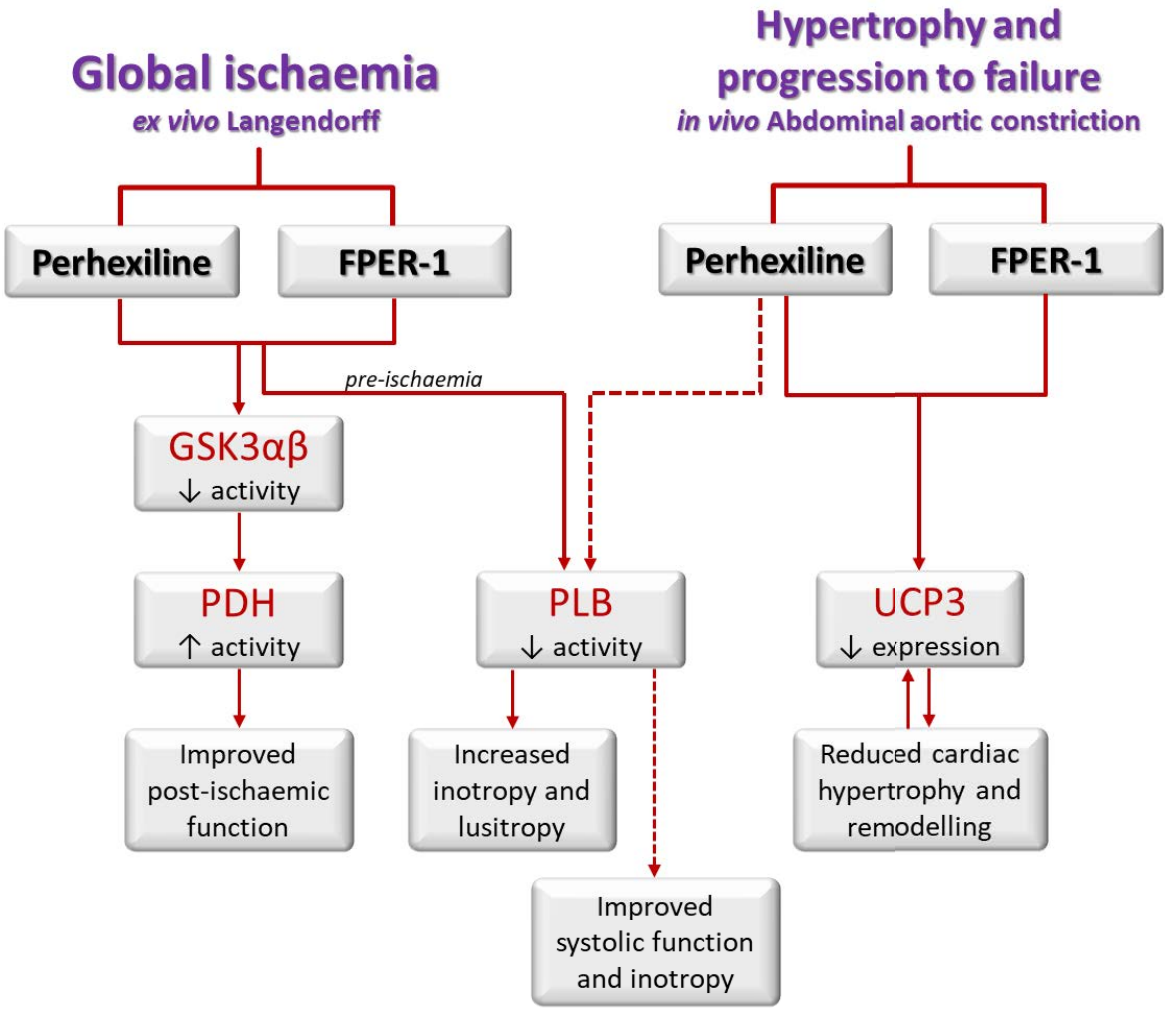

Figure 7.1. Proposed *ex vivo* and *in vivo* mechanisms of action of perhexiline and FPER-1

In both the Langendorff and abdominal aortic constriction (AAC) model, perhexiline was demonstrated to be cardioprotective, involving metabolic (GSK3αβ, PDH or UCP3) and non-metabolic (PLB) protein pathways. It is also probable that the changes in UCP3 expression observed in the AAC model were a consequence of the drug-induced reduction in hypertrophy and remodelling. FPER-1 replicated all beneficial effects in the Langendorff model and retained the ability to attenuate hypertrophy and remodelling in the *in vivo* model by targeting the same molecular pathways as perhexiline. FPER-1, and not perhexiline, also decreased carnitine palmitoyltransferase 1B (CPT1B) expression *ex vivo*, but this did not appear to induce any additional protective effects. Therefore, as discussed in section 7.4, the role of CPT1B inhibition remains unclear.

FPER-1, fluoroperhexiline-1; GSK3αβ, glycogen synthase kinase 3αβ; PDH, pyruvate dehydrogenase; PLB, phospholamban; UCP3, uncoupling protein 3.

7.5. Future considerations

Both the Langendorff global ischaemia model and the AAC pressure overload model used for the work in this thesis are well-established techniques for assessing cardiovascular integrity and pharmacological efficacy (Liao et al., 2012; Gomes et al., 2013). Future work on perhexiline and FPER-1 in both models would be beneficial to further explore their therapeutic potential. Importantly, the studies in this thesis are the first to investigate FPER-1, thus it would be imperative to assess a range of FPER-1 doses in both models as only two *ex vivo* concentrations and one *in vivo* dose were tested. In this manner a therapeutic range for FPER-1, which would be useful and safe to test clinically, could be established.

As previously discussed, increasing the severity of the AAC model by creating a smaller stenosis and/or prolonging the study duration would be essential to fully assess the ability of these agents to reduce HF progression and metabolic dysregulation. It would also be interesting to assess cardiac haemodynamics in hearts from AAC mice (vehicle and drug-treated) on the Langendorff system, in addition to echocardiography. Moreover, the present AAC study assessed the effects of perhexiline and FPER-1 in a model of *progression* to failure rather than established HF. This may explain some of the disparities between the present findings and those of clinical studies, in which perhexiline was administered when hypertrophy/HF had already developed. Thus, investigating these drugs in the AAC model after HF has developed to see if they can correct dysfunction would also be useful.

Regarding cardioprotective mechanisms of perhexiline and FPER-1, additional metabolic proteins such as UCP2 should be considered as well as those involved in cardiac contractility-

relaxation. Furthermore, directly assessing ATP production, oxidative phosphorylation and substrate oxidation/utilisation would be valuable in determining whether the observed protein changes lead to improvements in cardiac energetics and metabolic efficiency.

7.6. Concluding remarks

The primary aims of the work in this thesis were to determine the therapeutic potential of perhexiline, whether the novel derivative FPER-1 is capable of replicating these effects, and to gain insights into possible molecular mechanisms. These aims were accomplished in that the work in this thesis provides both complementary and novel findings on the cardioprotective potential and mechanisms of perhexiline and most importantly demonstrates that FPER-1 can reproduce these effects *ex vivo* and *in vivo*. Both agents had positive inotropic and lusitropic effects during normoxia and improved post-ischaemic recovery in the Langendorff-perfused isolated mouse hearts. Furthermore, both drugs attenuated cardiac hypertrophy and remodelling *in vivo* in the murine AAC model, demonstrating their potential to delay HF progression. Perhexiline at a therapeutic dose also alleviated cardiac dysfunction, but this was not replicated by FPER-1 indicating that the optimal efficacious dose of FPER-1 still requires investigation. Their mechanisms of action were shown to involve metabolic (GSK3αβ, PDH or UCP3) and non-metabolic (PLB) proteins highlighting that perhexiline-mediated protection is not restricted to CPT1 modulation. Overall, the work in this thesis provides promising evidence for the clinical use of perhexiline and FPER-1 for the treatment and management of HF.

Chapter 8: References

Chapter 8: References

Aasum, E., Hafstad, A.D. and Larsen, T.S. (2003) Changes in substrate metabolism in isolated mouse hearts following ischemia-reperfusion. *Mol Cell Biochem*, 249 (1-2), pp. 97-103.

AbdAlla, S., Fu, X., S Elzahwy, S., Klaetschke, K., Streichert, T. and Quitterer, U. (2011) Up-regulation of the cardiac lipid metabolism at the onset of heart failure. *Cardiovasc Hematol Agents Med Chem*, 9 (3), pp. 190-206.

Abebe, T.B., Gebreyohannes, E.A., Tefera, Y.G. and Abegaz, T.M. (2016) Patients with HFpEF and HFrEF have different clinical characteristics but similar prognosis: a retrospective cohort study. *BMC Cardiovasc Disord*, 16 (1), p. 232.

Abozguia, K., Elliott, P., McKenna, W., Phan, T.T., Nallur-Shivu, G. and Ahmed, I. et al. (2010) Metabolic modulator perhexiline corrects energy deficiency and improves exercise capacity in symptomatic hypertrophic cardiomyopathy. *Circulation*, 122 (16), pp. 1562-1569.

Ahmed, A., Rich, M.W., Fleg, J.L., Zile, M.R., Young, J.B. and Kitzman, D.W. et al. (2006) Effects of digoxin on morbidity and mortality in diastolic heart failure. *Circulation*, 114 (5), pp. 397-403.

AIRE Study Investigators (1993) Effect of ramipril on mortality and morbidity of survivors of acute myocardial infarction with clinical evidence of heart failure. *Lancet*, 342 (8875), pp. 821-828.

Akhmedov, A.T., Rybin, V. and Marín-García, J. (2015) Mitochondrial oxidative metabolism and uncoupling proteins in the failing heart. *Heart Fail Rev*, 20 (2), pp. 227-249.

Akki, A., Smith, K. and Seymour, A.M.L. (2008) Compensated cardiac hypertrophy is characterised by a decline in palmitate oxidation. *Mol Cell Biochem*, 311 (1-2), pp. 215-224.

Alcocer, L., Aspe, J. and Arce-Gomez, E. (1973) Effects of perhexiline maleate in patients with angina pectoris unrelieved by other antianginal agent. *Curr Ther Res Clin Exp*, 15 (7), pp. 349-357.

Allison, S.P., Chamberlain, M.J. and Hinton, P. (1969) Intravenous glucose tolerance, insulin, glucose, and free fatty acid levels after myocardial infarction. *Br Med J*, 4 (5686), pp. 776-778.

Amara, V.R., Surapaneni, S.K. and Tikoo, K. (2017) Dysregulation of microRNAs and renin-angiotensin system in high salt diet-induced cardiac dysfunction in uninephrectomized rats. *PLoS One*, 12 (7), p. e0180490.

Ambrosy, A.P., Fonarow, G.C., Butler, J., Chioncel, O., Greene, S.J. and Vaduganathan, M. et al. (2014) The global health and economic burden of hospitalizations for heart failure: lessons learned from hospitalized heart failure registries. *J Am Coll Cardiol*, 63 (12), pp. 1123-1133.

Andreadou, I., Bibli, S.I., Efentakis, P., Vasileiou, S., Pouli, N. and Zoga, A. et al. (2013) Ranolazine triggers pharmacological preconditioning and postconditioning in anesthetized rabbits through activation of RISK pathway. *Eur J Pharmacol*, 789, pp. 431-438.

Antoniak, S., Sparkenbaugh, E.M., Tencati, M., Rojas, M., Mackman, N. and Pawlinski, R. (2013) Protease activated receptor-2 contributes to heart failure. *PLoS One*, 8 (11), p. e81733.

Aoyama, M., Kawase, H., Bando, Y.K., Monji, A. and Murohara, T. (2016) Dipeptidyl peptidase 4 inhibition alleviates shortage of circulating glucagon-like peptide-1 in heart failure and mitigates myocardial remodeling and apoptosis via the exchange protein directly activated by cyclic AMP 1/Ras-Related protein 1 axis. *Circ Heart Fail*, 9 (1), p. e002081.

Apstein, C.S., Deckelbaum, L., Mueller, M., Hagopian, L. and Hood, W.B. (1977) Graded global ischemia and reperfusion. Cardiac function and lactate metabolism. *Circulation*, 55 (6), pp. 864-872.

Arany, Z., Novikov, M., Chin, S., Ma, Y., Rosenzweig, A. and Spiegelman, B.M. (2006) Transverse aortic constriction leads to accelerated heart failure in mice lacking PPAR-γ coactivator 1α. *Proc Natl Acad Sci U S A*, 103 (26), pp. 10086-10091.

Armoundas, A.A., Rose, J., Aggarwal, R., Stuyvers, B.D., O'Rourke, B. and Kass, D.A. et al. (2007) Cellular and molecular determinants of altered Ca 2+ handling in the failing rabbit heart: primary defects in SR Ca 2+ uptake and release mechanisms. *Am J Physiol Heart Circ Physiol*, 292 (3), pp. H1607-H1618.

Armstrong, M.L. (1973) Proceedings: A comparative study of perhexiline, beta-adrenergic blocking agents and placebos in the management of angina pectoris. *Postgrad Med J*, 49 (S3), pp. 108-112.

Arumugam, S., Sreedhar, R., Thandavarayan, R.A., Karuppagounder, V. and Watanabe, K. (2016) Targeting fatty acid metabolism in heart failure: is it a suitable therapeutic approach? *Drug Discov Today*, 21 (6), pp. 1003-1008.

Ashrafian, H., Frenneaux, M.P. and Opie, L.H. (2007a) Metabolic mechanisms in heart failure. *Circulation*, 116 (4), pp. 434-448.

Ashrafian, H., Horowitz, J.D. and Frenneaux, M.P. (2007b). Perhexiline. *Cardiovasc Drug Rev*, 25 (1), pp. 76-97.

Asimakis, G.K. and Conti, V.R. (1984) Myocardial ischemia: correlation of mitochondrial adenine nucleotide and respiratory function. *J Mol Cell Cardiol*, 16 (5), pp. 439-447.

Atherton, J.J., Moore, T.D., Lele, S.S., Thomson, H.L., Galbraith, A.J. and Belenkie, I. et al. (1997) Diastolic ventricular interaction in chronic heart failure. *Lancet*, 349 (9067), pp. 1720-1724.

Atkinson, A.B., McAreavey, D. and Trope, G. (1980) Papilloedema and hepatic dysfunction apparently induced by perhexiline maleate (Pexid). *Heart*, 43 (4), pp. 490-491.

Aubdool, A.A., Thakore, P., Argunhan, F., Smillie, S.J., Schnelle, M. and Srivastava, S. et al. (2017) A Novel α-Calcitonin Gene-Related Peptide Analogue Protects Against End-Organ Damage in Experimental Hypertension, Cardiac Hypertrophy and Heart Failure. *Circulation*, 136 (4), pp. 367-383.

Azzu, V. and Brand, M.D. (2010) The on-off switches of the mitochondrial uncoupling proteins. *Trends Biochem Sci*, 35 (5), pp. 298-307.

Baba, H.A., Stypmann, J., Grabellus, F., Kirchhof, P., Sokoll, A. and Schäfers, M. et al. (2003) Dynamic regulation of MEK/Erks and Akt/GSK-3β in human end-stage heart failure after left ventricular mechanical support: myocardial mechanotransduction-sensitivity as a possible molecular mechanism. *Cardiovasc Res*, 59 (2), pp. 390-399.

Bady, B., Bourrat, C., Trillet, M., Girard, P.F. and Carrier, H. (1978) Toxic neurologic manifestations during angina pectoris treatment (perhexiline maleate and amiotadone hydrochloride). *Int J Neurol*, 11 (4), pp. 371-82.

Baicu, C.F., Zile, M.R., Aurigemma, G.P. and Gaasch, W.H. (2005) Left ventricular systolic performance, function, and contractility in patients with diastolic heart failure. *Circulation*, 111 (18), pp. 2306-2312.

Baines, C.P. and Molkentin, J.D. (2009) Adenine nucleotide translocase-1 induces cardiomyocyte death through upregulation of the pro-apoptotic protein Bax. *J Mol Cell Cardiol*. 46 (6), pp. 969-977.

Balgi, A.D., Fonseca, B.D., Donohue, E., Tsang, T.C., Lajoie, P. and Proud, C.G. et al. (2009) Screen for chemical modulators of autophagy reveals novel therapeutic inhibitors of mTORC1 signaling. *PLoS One*, 4 (9), p. e7124.

Bansal, M., Chan, J., Leano, R., Pillans, P., Horowitz, J. and Marwick, T.H. (2010) Effects of perhexiline on myocardial deformation in patients with ischaemic left ventricular dysfunction. *Int J Cardiol*, 139 (2), pp. 107-112.

Barclay, M.L., Sawyers, S.M., Begg, E.J., Zhang, M., Roberts, R.L. and Kennedy, M.A. et al. (2003) Correlation of CYP2D6 genotype with perhexiline phenotypic metabolizer status. *Pharmacogenetics*, 13 (10), pp. 627-632.

Barger, P.M., Brandt, J.M., Leone, T.C., Weinheimer, C.J. and Kelly, D.P. (2000) Deactivation of peroxisome proliferator–activated receptor-α during cardiac hypertrophic growth. *J Clin Invest*, 105 (12), p. 1723-1730.

Barillas, R., Friehs, I., Cao-Danh, H., Martinez, J.F. and Pedro, J. (2007) Inhibition of glycogen synthase kinase-3β improves tolerance to ischemia in hypertrophied hearts. *Ann Thorac Surg*, 84 (1), pp. 126-133.

Barry, W.H., Horowitz, J.D. and Smith, T.W. (1985) Comparison of negative inotropic potency, reversibility, and effects on calcium influx of six calcium channel antagonists in cultured myocardial cells. *Br J Pharmacol*, 85 (1), pp. 51-59.

Baumgardt, S.L., Paterson, M., Leucker, T.M., Fang, J., Zhang, D.X. and Bosnjak, Z.J. et al. (2016) Chronic co-administration of sepiapterin and l-citrulline ameliorates diabetic cardiomyopathy and myocardial ischemia/reperfusion injury in obese type 2 diabetic mice. *Circ Heart Fail*, 9 (1), p. e002424.

Beadle, R.M., Williams, L.K., Kuehl, M., Bowater, S., Abozguia, K. and Leyva, F. et al. (2015) Improvement in cardiac energetics by perhexiline in heart failure due to dilated cardiomyopathy. *JACC Heart Fail*, 3 (3), pp. 202-211.

Beaugrand, M., Chousterman, M., Callard, P., Camilleri, J.P., Petite, J. and Ferrier, J.P. (1977) Hepatitis due to perhexiline maleate. Development of cirrhosis after interruption of the drug. Report of two cases (author's transl). *Gastroenterol Clin Biol*, 1 (10), pp. 745-750.

Beaugrand, M., Poupon, R., Levy, V.G., Callard, P., Lageron, A. and Lecomte, D. et al. (1978) Hepatic lesions due to perhexiline maleate (author's transl). *Gastroenterol Clin Biol*, 2 (6-7), pp. 579-588.

Beer**,** M., Seyfarth, T., Sandstede, J., Landschütz, W., Lipke, C. and Köstler, H. et al. (2002) Absolute concentrations of high-energy phosphate metabolites in normal, hypertrophied, and failing human myocardium measured noninvasively with 31 P-SLOOP magnetic resonance spectroscopy. *J Am Coll Cardiol*, 40 (7), pp. 1267-1274.

Belke, D.D., Larsen, T.S., Lopaschuk, G.D. and Severson, D.L (1999) Glucose and fatty acid metabolism in the isolated working mouse heart. *Am J Physiol*, 277 (4 Pt 2), pp. 1210-1217.

Bell, R.M., Mocanu, M.M. and Yellon, D.M. (2011) Retrograde heart perfusion: the Langendorff technique of isolated heart perfusion. *J Mol Cell Cardiol*, 50 (6), pp. 940-950.

Benedek, A., Móricz, K., Jurányi, Z., Gigler, G., Lévay, G. and Hársing, L.G. et al. (2006) Use of TTC staining for the evaluation of tissue injury in the early phases of reperfusion after focal cerebral ischemia in rats. *Brain Res*, 1116 (1), pp. 159-165.

Bennett, M.K., Sweet, W.E., Baicker-McKee, S., Looney, E., Karohl, K. and Mountis, M. et al. (2014) S100A1 in Human Heart Failure. *Circ Heart Fail*, 7 (4), pp. 612-618.

Berenji, K., Drazner, M.H., Rothermel, B.A. and Hill, J.A. (2005) Does load-induced ventricular hypertrophy progress to systolic heart failure? *Am J Physiol Heart Circ Physiol*, 289 (1), pp. H8-H16.

Berry, J.M., Naseem, R.H., Rothermel, B.A. and Hill, J.A. (2007) Models of cardiac hypertrophy and transition to heart failure. *Drug Discov Today Dis Models*, 4 (4), pp. 197-206.

Bersin, R.M., Wolfe, C., Kwasman, M., Lau, D., Klinski, C. and Tanaka, K. et al. (1994) Improved hemodynamic function and mechanical efficiency in congestive heart failure with sodium dichloroacetate. *J Am Coll Cardiol*, 23 (7), pp. 1617-1624.

Bhatia, R.S., Tu, J.V., Lee, D.S., Austin, P.C., Fang, J. and Haouzi, A. et al. (2006) Outcome of heart failure with preserved ejection fraction in a population-based study. *N Engl J Med*, 355 (3), pp. 260-269.

Bhushan, S., Kondo, K., Polhemus, D.J., Otsuka, H., Nicholson, C. and Tao, Y.X. et al. (2014) Nitrite Therapy Improves Left Ventricular Function During Heart Failure via Restoration of Nitric Oxide (NO) Mediated Cytoprotective Signaling. *Circ Res*, 114 (8), pp. 1281-1291.

Bing, R.J., Siegel, A., Ungar, I. and Gilbert, M. (1954) Metabolism of the human heart: II. Studies on fat, ketone and amino acid metabolism. *Am J Med*, 16 (4), pp. 504-515.

Bishu, K., Deswal, A., Chen, H.H., LeWinter, M.M., Lewis, G.D. and Semigran, M.J. et al. (2012) Biomarkers in acutely decompensated heart failure with preserved or reduced ejection fraction. *Am Heart J*, 164 (5), pp. 763-770.

Bleifer, D.J., Bleifer, S.B. and Okun, R. (1972) Perhexiline maleate in angina pectoris. A controlled, double-blind clinical trial. *Geriatrics*, 27 (9), p. 109-115.

Boehm, E.A., Jones, B.E., Radda, G.K., Veech, R.L. and Clarke, K. (2001) Increased uncoupling proteins and decreased efficiency in palmitate-perfused hyperthyroid rat heart. *Am J Physiol Heart Circ Physiol*, 280 (3), pp. H977-H983.

Boguslavskyi, A., Pavlovic, D., Aughton, K., Clark, J.E., Howie, J. and Fuller, W. et al. (2014) Cardiac hypertrophy in mice expressing unphosphorylatable phospholemman. *Cardiovasc Res*, 104 (1), pp. 72-82.

Boluyt, M.O., Robinson, K.G., Meredith, A.L., Sen, S., Lakatta, E.G. and Crow, M.T. et al. (2005) Heart failure after long-term supravalvular aortic constriction in rats. *Am J Hypertens*, 18 (2), pp. 202-212.

Bonnefont, J.P., Djouadi, F., Prip-Buus, C., Gobin, S., Munnich, A. and Bastin, J. (2004) Carnitine palmitoyltransferases 1 and 2: biochemical, molecular and medical aspects. *Mol Aspects Med*, 25 (5), pp. 495-520.

Bonnet, P., Jourdan, J., Janbon, F., Michel, H. and Bertrand, A. (1978) Liver cirrhosis after 2 years of perhexiline maleate treatment. *Nouv Presse Med*, 7 (3), p. 208.

Borbély, A., Falcao-Pires, I., Van Heerebeek, L., Hamdani, N., Edes, I. and Gavina, C. et al. (2009) Hypophosphorylation of the Stiff N2B titin isoform raises cardiomyocyte resting tension in failing human myocardium. *Circ Res*, 104 (6), pp. 780-786.

Borlaug, B.A. and Kass, D.A. (2009) Invasive hemodynamic assessment in heart failure. *Heart Fail Clin*, 5 (2), pp. 217-228.

Borlaug, B.A. and Kass, D.A. (2011) Ventricular–vascular interaction in heart failure. *Cardiol Clin*, 29 (3), pp. 447-459.

Borlaug, B.A., Melenovsky, V., Russell, S.D., Kessler, K., Pacak, K. and Becker, L.C. et al. (2006) Impaired chronotropic and vasodilator reserves limit exercise capacity in patients with heart failure and a preserved ejection fraction. *Circulation*, 114 (20), pp. 2138-2147.

Borlaug, B.A., Nishimura, R.A., Sorajja, P., Lam, C.S. and Redfield, M.M. (2010) Exercise hemodynamics enhance diagnosis of early heart failure with preserved ejection fraction. *Circ Heart Fail*, 3 (5), pp. 588-595.

Borlaug, B.A. and Redfield, M.M. (2011) Diastolic and systolic heart failure are distinct phenotypes within the heart failure spectrum. *Circulation*, 123 (18), pp. 2006-2013.

Bouche, P., Bousser, M.G., Peytour, M.A. and Cathala, H.P. (1979) Perhexiline maleate and peripheral neuropathy. *Neurology*, 29 (5), pp. 739-739.

Bourrat, C., Viala, J.J. and Guastala, J.P. (1975) Peripheral neuropathy after prolonged adsorption of perhexiline maleate. 2 cases. *Nouv Presse Med*, 4 (35), p. 2528.

Bousser, M.G., Bouche, P., Brochard, C. and Herreman, G. (1976) Letter: 7 peripheral neuropathies after treatment by perhexiline maleate. *Nouv Presse Med*, 5 (10), pp. 652-653.

Braissant, O., Foufelle, F., Scotto, C., Dauça, M. and Wahli, W. (1996) Differential expression of peroxisome proliferator-activated receptors (PPARs): tissue distribution of PPAR-alpha,-beta, and-gamma in the adult rat. *Endocrinology*, 137 (1), pp. 354-366.

Brancaccio, P., Lippi, G. and Maffulli, N. (2010) Biochemical markers of muscular damage. *Clin Chem Lab Med*, 48 (6), pp. 757-767.

Braz Nogueira, J. (2017) Serum sodium levels and blood pressure monitoring in heart failure: Added diagnostic and prognostic value. *Rev Port Cardiol*, 36 (7-8), pp. 521-523.

Bristow, M.R., Ginsburg, R., Minobe, W., Cubicciotti, R.S., Sageman, W.S. and Lurie, K. et al. (1982) Decreased catecholamine sensitivity and β-adrenergic-receptor density in failing human hearts. *N Engl J Med*, 307 (4), pp. 205-211.

British Heart Foundation (BHF) (no date) *How a healthy heart works*. Available at: https://www.bhf.org.uk/heart-health/how-your-heart-works/how-a-healthy-heart-works (Accessed: 15 November 2017).

Brown, M.J., Horowitz, J.D. and Mashford, M.L. (1976) A double-blind trial of perhexiline maleate in the prophylaxis of angina pectoris. *Med J Aust*, 1 (9), pp. 260-263.

Bugger, H., Guzman, C., Zechner, C., Palmeri, M., Russell, K.S. and Russell, R.R. (2011) Uncoupling protein downregulation in doxorubicin-induced heart failure improves mitochondrial coupling but increases reactive oxygen species generation. *Cancer Chemother Pharmacol*, 67 (6), pp. 1381-1388.

Bugger, H., Schwarzer, M., Chen, D., Schrepper, A., Amorim, P.A. and Schoepe, M. et al. (2010) Proteomic remodelling of mitochondrial oxidative pathways in pressure overload-induced heart failure. *Cardiovasc Res*, 85 (2), pp. 376-384.

Burkhoff, D. (2011) Mortality in heart failure with preserved ejection fraction: an unacceptably high rate. *Eur Heart J*, 33 (14), pp. 1718-1720.

Burns-Cox, C.J., Chandrasekhar, K.P., Ikram, H., Peirce, T.H., Pilcher, J. and Quinlan, C.D.M. et al. (1971) Clinical evaluation of perhexiline maleate in patients with angina pectoris. *Br Med J*, 4 (5787), pp. 586-588.

Buys, E.S., Raher, M.J., Blake, S.L., Neilan, T.G., Graveline, A.R. and Passeri, J.J. et al. (2007) Cardiomyocyte-restricted restoration of nitric oxide synthase 3 attenuates left ventricular remodeling after chronic pressure overload. *Am J Physiol Heart Circ Physiol*, 293 (1), pp. H620-H627.

Cairns, R.A., Harris, I.S. and Mak, T.W. (2011) Regulation of cancer cell metabolism. *Nat Rev Cancer*, 11 (2), pp. 85-95.

Calcutt, N.A., Lopez, V.L., Bautista, A.D., Mizisin, L.M., Torres, B.R. and Shroads, A.L. et al. (2009) Peripheral neuropathy in rats exposed to dichloroacetate. *J Neuropathol Exp Neurol*, 68 (9), pp. 985-993.

Cantor, E.J., Babick, A.P., Vasanji, Z., Dhalla, N.S. and Netticadan, T. (2005) A comparative serial echocardiographic analysis of cardiac structure and function in rats subjected to pressure or volume overload. *J Mol Cell Cardiol*, 38 (5), pp. 777-786.

Cappola, T.P. (2015) Perhexiline: Lessons for Heart Failure Therapeutics. *JACC Heart Fail*, 3 (3), pp. 212-213.

Carley, A.N., Taglieri, D.M., Bi, J., Solaro, R.J. and Lewandowski, E.D. (2015) Metabolic efficiency promotes protection from pressure overload in hearts expressing slow skeletal troponin I. *Circ Heart Fail*, 8 (1), pp. 119-127.

Cave, A.C., Ingwall, J.S., Friedrich, J., Liao, R., Saupe, K.W. and Apstein, C.S. et al. (2000) ATP synthesis during low-flow ischemia. *Circulation*, 101 (17), pp. 2090-2096.

Chaanine, A.H., Nair, K.S., Bergen, R.H., Klaus, K., Guenzel, A.J. and Hajjar, R.J. et al. (2017) Mitochondrial Integrity and Function in the Progression of Early Pressure Overload–Induced Left Ventricular Remodeling. *J Am Heart Assoc*, 6 (6), p. e005869.

Chandran, K., Aggarwal, D., Migrino, R.Q., Joseph, J., McAllister, D. and Konorev, E.A. et al. (2009) Doxorubicin inactivates myocardial cytochrome c oxidase in rats: cardioprotection by Mito-Q. *Biophys J*, 96 (4), pp. 1388-1398.

Charles River (2011) *C57BL/6 mice nomenclature: C57BL/6NCrl (information sheet)*. Available at: https://www.criver.com/sites/default/files/resources/C57BL6MouseModelInformationSheet.pdf (Accessed: 18 June 2017).

Chen, M., Xin, J., Liu, B., Luo, L., Li, J. and Yin, W. et al. (2016) Mitogen-Activated Protein Kinase and Intracellular Polyamine Signaling Is Involved in TRPV1 Activation–Induced Cardiac Hypertrophy. *J Am Heart Assoc*, 5 (8), p. e003718.

Chen, R., Liang, F., Morimoto, S., Li, Q., Moriya, J. and Yamakawa, J.I. et al. (2010) The Effects of a PPARα Agonist on Myocardial Damage in Obese Diabetic Mice With Heart Failure. *Int Heart J*, 51 (3), pp. 199-206.

Chiu, H.C., Kovacs, A., Ford, D.A., Hsu, F.F., Garcia, R. and Herrero, P. et al. (2001) A novel mouse model of lipotoxic cardiomyopathy. *J Clin Invest*, 107 (7), p. 813-822.

Cho, Y.W., Belej, M. and Aviado, D.M. (1970) Pharmacology of a New Antianginal Drug: Perhexiline: I. Coronary Circulation and Myocardial Metabolism. *Chest*, 58 (6), pp. 577-581.

Chokshi, A., Drosatos, K., Cheema, F.H., Ji, R., Khawaja, T. and Yu, S. et al. (2012) Ventricular Assist Device Implantation Corrects Myocardial Lipotoxicity, Reverses Insulin Resistance and Normalizes Cardiac Metabolism in Patients with Advanced Heart Failure. *Circulation*, 125 (23), pp. 2844-2853.

Chong, C.R., Chan, W.P.A., Nguyen, T.H., Liu, S., Procter, N.E. and Ngo, D.T. et al. (2014) Thioredoxin-interacting protein: pathophysiology and emerging pharmacotherapeutics in cardiovascular disease and diabetes. *Cardiovasc Drugs Ther*, 28 (4), pp. 347-360.

Chong, C.R., Sallustio, B. and Horowitz, J.D. (2016) Drugs that Affect Cardiac Metabolism: Focus on Perhexiline. *Cardiovasc Drugs Ther*, 30 (4), pp. 399-405.

CIBIS-II Investigators and Committees. (1999) The Cardiac Bisoprolol Study II (CIBI-II): A randomized trial. *Lancet*, 353 (1999), pp. 9-13

Circu, M.L. and Aw, T.Y. (2010) Reactive oxygen species, cellular redox systems, and apoptosis. *Free Radic Biol Med*, 48 (6), pp. 749-762.

Clarke, B., Spedding, M., Patmore, L. and McCormack, J.G. (1993) Protective effects of ranolazine in guinea-pig hearts during low-flow ischaemia and their association with increases in active pyruvate dehydrogenase. *Br J Pharmacol*, 109 (3), pp. 748-750.

Clarke, B., Wyatt, K.M. and McCormack, J.G. (1996) Ranolazine increases active pyruvate dehydrogenase in perfused normoxic rat hearts: evidence for an indirect mechanism. *J Mol Cell Cardiol*, 28 (2), pp. 341-350.

Cleland, J.G., Tendera, M., Adamus, J., Freemantle, N., Polonski, L. and Taylor, J. (2006) The perindopril in elderly people with chronic heart failure (PEP-CHF) study. *Eur Heart J*, 27 (19), pp. 2338-2345.

Cohn, J.N., Archibald, D., Ziesche, S., Franciosa, J., Harston, W. and Tristani, F. et al. (1986) Effect of Vasodilator Therapy on Mortality in Chronic Congestive Heart Failure. Results of a Veterans Administration Cooperative Study. *N Engl J Med*, 314 (24), pp. 1547-1552.

Cohn, J.N., Johnson, G., Ziesche, S., Cobb, F., Francis, G. and Tristani, F. et al. (1991) A comparison of enalapril with hydralazine–isosorbide dinitrate in the treatment of chronic congestive heart failure. *N Engl J Med*, 325 (5), pp. 303-310.

Cohn, J.N. and Tognoni, G. (2001) A randomized trial of the angiotensin-receptor blocker valsartan in chronic heart failure. *N Engl J Med*, 345 (23), pp. 1667-1675.

Cole, P.L., Beamer, A.D., McGowan, N., Cantillon, C.O., Benfell, K. and Kelly, R.A. et al. (1990) Efficacy and safety of perhexiline maleate in refractory angina. A double-blind placebo-controlled clinical trial of a novel antianginal agent. *Circulation*, 81 (4), pp. 1260-1270.

Colyer, J. (1998) Phosphorylation States of Phospholambana. *Ann N Y Acad Sci*, 853 (1), pp.79-91.

Conraads, V.M., Metra, M., Kamp, O., De Keulenaer, G.W., Pieske, B. and Zamorano, J. et al. (2012) Effects of the long-term administration of nebivolol on the clinical symptoms, exercise capacity, and left ventricular function of patients with diastolic dysfunction: results of the ELANDD study. *Eur J Heart Fail*, 14 (2), pp. 219-225.

CONSENSUS Trial Study Group (1987) Effects of enalapril on mortality in severe congestive heart failure. Results of the Cooperative North Scandinavian Enalapril Survival Study (CONSENSUS). *New Engl J Med*, 316 (23), pp. 1429-1435.

Cooper, R.G., Evans, D.A. and Whibley, E.J. (1984) Polymorphic hydroxylation of perhexiline maleate in man. *J Med Genet*, 21 (1), pp. 27-33.

Crinquette, J.F., Pirot, J., Lugand, J.J., Dessaint, J.P., Houcke, M. and Mazzuga, M. et al. (1981) Perhexiline maleate induced cirrhosis (author's transl). *Acta Gastroenterol Belg*, 44 (9-10), pp. 391-395.

Dai, D.F., Chen, T., Szeto, H., Nieves-Cintrón, M., Kutyavin, V. and Santana, L.F. et al. (2011) Mitochondrial targeted antioxidant peptide ameliorates hypertensive cardiomyopathy. *J Am Coll Cardiol*, 58 (1), pp. 73-82.

Dai, D.F., Hsieh, E.J., Chen, T., Menendez, L.G., Basisty, N.B. and Tsai, L. et al. (2013) Global Proteomics and Pathway Analysis of Pressure-overload Induced Heart Failure and Its Attenuation by Mitochondrial Targeted Peptides. *Circ Heart Fail*, 6 (5), pp. 1067-1076.

Dai, D.F., Hsieh, E.J., Liu, Y., Chen, T., Beyer, R.P. and Chin, M.T. et al. (2012) Mitochondrial proteome remodelling in pressure overload-induced heart failure: the role of mitochondrial oxidative stress. *Cardiovasc Res*, 93 (1), pp. 79-88.

Dally, S., Lagier, G., Assan, R. and Gaultier, M. (1977) Hypoglycemia in 2 patients treated with perhexiline maleate. *Nouv Presse Med*, 6 (19), pp. 1643-4.

Daneshvar, D., Wei, J., Tolstrup, K., Thomson, L.E., Shufelt, C. and Merz, C.N.B. (2010) Diastolic dysfunction: improved understanding using emerging imaging techniques. *Am Heart J*, 160 (3), pp. 394-404.

Daniell, H.B., Privitera, P.J., Conradi, S.E. and Gaffney, T.E. (1977) Effects of perhexiline on survival time and infarct size in experimental myocardial infarction. *J Pharmacol Exp Ther*, 200 (1), pp. 155-165.

Davies, B.J., Coller, J.K., James, H.M., Gillis, D., Somogyi, A.A. and Horowitz, J.D. et al. (2004) Clinical inhibition of CYP2D6-catalysed metabolism by the antianginal agent perhexiline. *Br J Clin Pharmacol*, 57 (4), pp. 456-463.

Davies, B.J., Coller, J.K., James, H.M., Somogyi, A.A., Horowitz, J.D. and Sallustio, B.C. (2006) The influence of CYP2D6 genotype on trough plasma perhexiline and cis-OH-perhexiline concentrations following a standard loading regimen in patients with myocardial ischaemia. *Br J Clin Pharmacol*, 61 (3), pp. 321-325.

Dawes, P. and Moulder, C. (1982) Perhexiline hepatitis and HLA B8. *Lancet*, 2 (8289), p. 109.

de Boer, R.A., Pinto, Y.M. and Van Veldhuisen, D.J. (2003) The imbalance between oxygen demand and supply as a potential mechanism in the pathophysiology of heart failure: the role of microvascular growth and abnormalities. *Microcirculation*, 10 (2), pp. 113-126.

de Brouwer, K.F., Degens, H., Aartsen, W.M., Lindhout, M., Bitsch, N.J. and Gilde, A.J. et al. (2006) Specific and sustained down-regulation of genes involved in fatty acid metabolism is not a hallmark of progression to cardiac failure in mice. *J Mol Cell Cardiol*, 40 (6), pp. 838-845.

de Oliveira, J.M. and Amado, J.N. (1970) Perhexilene maleate in the treatment of angina pectoris. *Hospital (Rio J)*, 77 (5), pp. 1511-1518.

de Roos, A., Doornbos, J., Luyten, P.R., Oosterwaal, L.J., den Hollander, J.A. and van der Wall, E.E. (1992) Cardiac metabolism in patients with dilated and hypertrophic cardio-myopathy: Assessment with proton-decoupled P-31 MR spectroscopy. *J Magn Reson Imaging*, 2 (6), pp. 711-719.

Dedkova, E.N., Seidlmayer, L.K. and Blatter, L.A. (2013) Mitochondria-mediated cardioprotection by trimetazidine in rabbit heart failure. *J Mol Cell Cardiol*, 59, pp. 41-54.

Deng, S., Yang, Y., Han, Y., Li, X., Wang, X. and Li, X. et al. (2012) UCP2 inhibits ROS-mediated apoptosis in A549 under hypoxic conditions. *PLoS One*, 7 (1), p. e30714.

Deschamps, D., DeBeco, V., Fisch, C., Fromenty, B., Guillouzo, A. and Pessayre, D. (1994) Inhibition by perhexiline of oxidative phosphorylation and the β-oxidation of fatty acids: Possible role in pseudoalcoholic liver lesions. *Hepatology*, 19 (4), pp. 948-961.

Deswal, A., Richardson, P., Bozkurt, B. and Mann, D.L. (2011) Results of the randomized aldosterone antagonism in heart failure with preserved ejection fraction trial (RAAM-PEF). *J Card Fail*, 17 (8), pp. 634-642.

Digitalis Investigation Group (1997) The effect of digoxin on mortality and morbidity in patients with heart failure. *N Engl J Med*, 336 (8), pp. 525-533.

Dmitriev, Y.V., Minasian, S.M., Demchenko, E.A. and Galagudza, M.M. (2012) Cardioprotective Properties of Dimethyl Sulfoxide during Global Ischemia–Reperfusion of Isolated Rat Heart. *Bull Exp Biol Med*, 154 (1), pp. 47-50.

Dobrzyn, P., Pyrkowska, A., Duda, M.K., Bednarski, T., Maczewski, M. and Langfort, J. et al. (2013) Expression of lipogenic genes is upregulated in the heart with exercise training-induced but not pressure overload-induced left ventricular hypertrophy. *Am J Physiol Endocrinol Metab*, 304 (12), pp. E1348-E1358.

Doehner, W., Frenneaux, M. and Anker, S.D. (2014) Metabolic impairment in heart failure. *J Am Coll Cardiol*, 64 (13), pp. 1388-1400.

Doenst, T., Nguyen, T.D. and Abel, E.D. (2013) Cardiac metabolism in heart failure: implications beyond ATP production. *Circ Res*, 113 (6), pp. 709-724.

Doenst, T., Pytel, G., Schrepper, A., Amorim, P., Färber, G. and Shingu, Y. et al. (2010) Decreased rates of substrate oxidation ex vivo predict the onset of heart failure and contractile dysfunction in rats with pressure overload. *Cardiovasc Res*, 86 (3), pp. 461-470.

Dong, Z., Zhao, P., Xu, M., Zhang, C., Guo, W. and Chen, H. et al. (2017) Astragaloside IV alleviates heart failure via activating PPARα to switch glycolysis to fatty acid β-oxidation. *Sci Rep*, 7 (1), p. 2691.

Dorn, G.W. and Molkentin, J.D. (2004) Manipulating cardiac contractility in heart failure. *Circulation*, 109 (2), pp. 150-158.

Dörner, A., Giessen, S., Gaub, R., Siestrup, H.G., Schwimmbeck, P.L. and Hetzer, R. et al. (2006) An isoform shift in the cardiac adenine nucleotide translocase expression alters the kinetic properties of the carrier in dilated cardiomyopathy. *Eur J Heart Fail*, 8 (1), pp. 81-89.

Doucette, T.A., Ryan, C.L. and Tasker, R.A. (2000) Use of osmotic minipumps for sustained drug delivery in rat pups: effects on physical and neurobehavioural development. *Physiol Behav*, 71 (1), pp. 207-212.

Drew, B. and Leeuwenburgh, C. (2003) Method for measuring ATP production in isolated mitochondria: ATP production in brain and liver mitochondria of Fischer-344 rats with age and caloric restriction. *Am J Physiol Regul Integr Comp Physiol*, 285 (5), pp. R1259-R1267.

Drury, N.E., Howell, N.J., Calvert, M.J., Weber, R.J., Senanayake, E.L. and Lewis, M.E. et al. (2015) The effect of perhexiline on myocardial protection during coronary artery surgery: a two-centre, randomized, double-blind, placebo-controlled trial. *Eur J Cardiothorac Surg*, 47 (3), pp. 464-472.

Drury, N.E., Licari, G., Chong, C.R., Howell, N.J., Frenneaux, M.P. and Horowitz, J.D. et al. (2014) Relationship between plasma, atrial and ventricular perhexiline concentrations in humans: insights into factors affecting myocardial uptake. *Br J Clin Pharmacol*, 77 (5), pp. 789-795.

Duan, J. and Karmazyn, M. (1989) Relationship between oxidative phosphorylation and adenine nucleotide translocase activity of two populations of cardiac mitochondria and mechanical recovery of ischemic hearts following reperfusion. *Can J Physiol Pharmacol*, 67 (7), pp. 704-709.

Duan, S.Z., Ivashchenko, C.Y., Whitesall, S.E., D'Alecy, L.G. and Mortensen, R.M. (2007) Direct monitoring pressure overload predicts cardiac hypertrophy in mice. *Physiol Meas*, 28 (11), pp. 1329-1339.

Durkot, M.J., De Garavilla, L., Caretti, D. and Francesconi, R. (1995) The effects of dichloroacetate on lactate accumulation and endurance in an exercising rat model. *Int J Sports Med*, 16 (3), pp. 167-171.

Eaton, C.B., Pettinger, M., Rossouw, J., Martin, L.W., Foraker, R. and Quddus, A. et al. (2016) Risk factors for incident hospitalized heart failure with preserved versus reduced ejection fraction in a multiracial cohort of postmenopausal women. *Circ Heart Fail*, 9 (10), p. e002883.

Edelmann, F., Wachter, R., Schmidt, A.G., Kraigher-Krainer, E., Colantonio, C. and Kamke, W. et al. (2013) Effect of spironolactone on diastolic function and exercise capacity in patients with heart failure with preserved ejection fraction: the Aldo-DHF randomized controlled trial. *Jama*, 309 (8), pp. 781-791.

Efentakis, P., Andreadou, I., Bibli, S.I., Vasileiou, S., Dagres, N. and Zoga, A. et al. (2016) Ranolazine triggers pharmacological preconditioning and postconditioning in anesthetized rabbits through activation of RISK pathway. *Eur J Pharmacol*, 789, pp. 431-438.

Eisner, D.A., Caldwell, J.L., Kistamás, K. and Trafford, A.W. (2017) Calcium and excitation-contraction coupling in the heart. *Circ Res*, 121 (2), pp. 181-195.

Embi, N., Rylatt, D.B. and Cohen, P. (1980) Glycogen synthase kinase-3 from rabbit skeletal muscle. *Eur J Biochem*, 107 (2), pp. 519-527.

Endo, M., Tanaka, M. and Ogawa, Y. (1970) Calcium induced release of calcium from the sarcoplasmic reticulum of skinned skeletal muscle fibres. *Nature*, 228 (5266), pp. 34-36.

Esposito, S., Bracacel, E., Nibbio, M., Speziale, R., Orsatti, L. and Veneziano, M. et al. (2016) Use of 'dilute-and-shoot'liquid chromatography-high resolution mass spectrometry in preclinical research: application to a DMPK study of perhexiline in mouse plasma. *Journal Pharm Biomed Anal*, 118, pp. 70-80.

Evans, W.E., Relling, M.V., Rahman, A., McLeod, H.L., Scott, E.P. and Lin, J.S. (1993) Genetic basis for a lower prevalence of deficient CYP2D6 oxidative drug metabolism phenotypes in black Americans. *J Clin Invest*, 91 (5), pp. 2150-2154.

Faadiel Essop, M. and Opie, L.H. (2004) Metabolic therapy for heart failure. *Eur Heart J*, 25 (20), pp. 1765-1768.

Fang, Y.H., Piao, L., Hong, Z., Toth, P.T., Marsboom, G. and Bache-Wiig, P. et al. (2012) Therapeutic inhibition of fatty acid oxidation in right ventricular hypertrophy: exploiting Randle's cycle. *J Mol Med*, 90 (1), pp. 31-43.

Fardeau, M., Tomé, F.M.S. and Simon, P. (1979) Muscle and nerve changes induced by perhexiline maleate in man and mice. *Muscle Nerve*, 2 (1), pp. 24-36.

Fath-Ordoubadi, F. and Beatt, K.J. (1997) Glucose-insulin-potassium therapy for treatment of acute myocardial infarction. *Circulation*, 96 (4), pp. 1152-1156.

Fayssoil, A. and Tournoux, F. (2013) Analyzing left ventricular function in mice with Doppler echocardiography. *Heart Fail Rev*, 18 (4), pp. 511-516.

Felker, G.M., Lee, K.L., Bull, D.A., Redfield, M.M., Stevenson, L.W. and Goldsmith, S.R. et al. (2011) Diuretic strategies in patients with acute decompensated heart failure. *N Engl J Med*, 364 (9), pp. 797-805.

Feng, G., Yang, Y., Chen, J., Wu, Z., Zheng, Y. and Li, W. et al. (2016) Ranolazine attenuated heightened plasma norepinephrine and B-Type natriuretic peptide-45 in improving cardiac function in rats with chronic ischemic heart failure. *Am J Transl Res*, 8 (2), pp. 1295-1301.

Fillmore, N. and Lopaschuk, G.D. (2013) Targeting mitochondrial oxidative metabolism as an approach to treat heart failure. *Biochim Biophys Acta*, 1833 (4), pp. 857-865.

Fillmore, N., Mori, J. and Lopaschuk, G.D. (2014) Mitochondrial fatty acid oxidation alterations in heart failure, ischaemic heart disease and diabetic cardiomyopathy. *Br J Pharmacol*, 171 (8), pp. 2080-2090.

Flather, M.D., Shibata, M.C., Coats, A.J., Van Veldhuisen, D.J., Parkhomenko, A. and Borbola, J. et al. (2005) Randomized trial to determine the effect of nebivolol on mortality and cardiovascular hospital admission in elderly patients with heart failure (SENIORS). *Eur Heart J*, 26 (3), pp. 215-225.

Forbes, G.B., Rake, M.O. and Taylor, D.J. (1979) Liver damage due to perhexiline maleate. *J Clin Pathol*, 32 (12), pp. 1282-1285.

Foster, D.W. (2012) Malonyl-CoA: the regulator of fatty acid synthesis and oxidation. *J Clin Invest*, 122 (6), p.1958-1958.

Fotino, A.D., Thompson-Paul, A.M. and Bazzano, L.A. (2013) Effect of coenzyme Q10 supplementation on heart failure: a meta-analysis. *Am J Clin Nutr*, 97 (2), pp. 268-275.

Fragasso, G., Palloshi, A., Puccetti, P., Silipigni, C., Rossodivita, A. and Pala, M. et al. (2006) A randomized clinical trial of trimetazidine, a partial free fatty acid oxidation inhibitor, in patients with heart failure. *J Am Coll Cardiol*, 48 (5), pp. 992-998.

Franssen, C. and González Miqueo, A. (2016) The role of titin and extracellular matrix remodelling in heart failure with preserved ejection fraction. *Neth Heart J*, 24 (4), pp. 259-267.

Fraser, D.M., Campbell, I.W. and Miller, H.C. (1977) Peripheral and autonomic neuropathy after treatment with perhexiline maleate. *Br Med J*, 2 (6088), p. 675-676.

Fraser, D.M. and Miller, H.C. (1978) Perhexilline-induced neuropathy. *Br Med J*, 1 (6116), pp. 858-859.

Frenneaux, M. and Williams, L. (2007) Ventricular-arterial and ventricular-ventricular interactions and their relevance to diastolic filling. *Prog Cardiovasc Dis*, 49 (4), pp. 252-262.

Fromenty, B. and Pessayre, D. (1995) Inhibition of mitochondrial beta-oxidation as a mechanism of hepatotoxicity. *Pharmacol Ther*, 67 (1), pp. 101-154.

Fu, Z., Zhao, L., Chai, W., Dong, Z., Cao, W. and Liu, Z. (2013) Ranolazine recruits muscle microvasculature and enhances insulin action in rats. *J Physiol*, 591 (20), pp. 5235-5249.

Fukushima, A. and Lopaschuk, G.D. (2016) Acetylation control of cardiac fatty acid β-oxidation and energy metabolism in obesity, diabetes, and heart failure. *Biochim Biophys Acta*, 1862 (12), pp. 2211-2220.

Furberg, C.D. and Yusuf, S. (1985) Effect of vasodilators on survival in chronic congestive heart failure. *Am J Cardiol*, 55 (8), pp. 1110-1113.

Gao, H., Feng, X.J., Li, Z.M., Li, M., Gao, S. and He, Y.H. et al. (2015) Downregulation of adipose triglyceride lipase promotes cardiomyocyte hypertrophy by triggering the accumulation of ceramides. *Arch Biochem Biophys*, 565, pp. 76-88.

Gao, L., Yao, R., Liu, Y., Wang, Z., Huang, Z. and Du, B. et al. (2017) Isorhamnetin protects against cardiac hypertrophy through blocking PI3K–AKT pathway. *Mol Cell Biochem*, 429 (1-2), pp. 167-177.

Gao, D., Zhang, L., Dhillon, R., Hong, T.T., Shaw, R.M. and Zhu, J. (2013) Dynasore protects mitochondria and improves cardiac lusitropy in Langendorff perfused mouse heart. *PLoS One*, 8 (4), p. e60967.

García, E.H., Perna, E.R., Farías, E.F., Obregón, R.O., Macin, S.M. and Parras, J.I. et al. (2006) Reduced systolic performance by tissue Doppler in patients with preserved and abnormal ejection fraction: new insights in chronic heart failure. *Int J Cardiol*, 108 (2), pp. 181-188.

Gatto, G.J. Jr., Ao, Z., Kearse, M.G., Zhou, M., Morales, C.R. and Daniels, E. et al. (2013) NADPH oxidase-dependent and-independent mechanisms of reported inhibitors of reactive oxygen generation. *J Enzyme Inhib Med Chem*, 28 (1), pp. 95-104.

Gattoni, S., Treu Røe, Å., Aronsen, J.M., Sjaastad, I., Louch, W.E. and Smith, N.P. et al. (2017) Compensatory and decompensatory alterations in cardiomyocyte Ca2+ dynamics in hearts with diastolic dysfunction following aortic banding. *J Physiol*, 595 (12), pp. 3867-3889.

Gehmlich, K., Dodd, M.S., Allwood, J.W., Kelly, M., Bellahcene, M. and Lad, H.V. et al. (2015) Changes in the cardiac metabolome caused by perhexiline treatment in a mouse model of hypertrophic cardiomyopathy. *Mol BioSyst*, 11 (2), pp. 564-573.

Gelpi, R.J., Gao, S., Zhai, P., Yan, L., Hong, C. and Danridge, L.M. et al. (2009) Genetic inhibition of calcineurin induces diastolic dysfunction in mice with chronic pressure overload. *Am J Physiol Heart Circ Physiol*, 297 (5), pp. H1814-H1819.

George, C.H., Mitchell, A.N., Preece, R., Bannister, M.L. and Yousef, Z. (2016) Pleiotropic mechanisms of action of perhexiline in heart failure. *Expert Opin Ther Pat*, 26 (9), pp. 1049-1059.

Gertz, E.W., Wisneski, J.A., Stanley, W.C. and Neese, R.A. (1988) Myocardial substrate utilization during exercise in humans. Dual carbon-labeled carbohydrate isotope experiments. *J Clin Invest*, 82 (6), pp. 2017-2025.

Gmeiner, R., Apstein, C.S. and Brachfeld, N. (1975) Effect of palmitate on hypoxic cardiac performance. *J Mol Cell Cardiol*, 7(4), pp. 227-235.

Goble, A.J. and Horowitz, J.D. (1984) Perhexilene neuropathy: A report of two cases. *Int Med J*, 14 (3), pp. 279-279.

Gomes, A.C., Falcao-Pires, I., Pires, A.L., Brás-Silva, C. and Leite-Moreira, A.F. (2013) Rodent models of heart failure: an updated review. *Heart Fail Rev*, 18 (2), pp. 219-249.

Gordon, M. and Gordon, A.S. (1981) Perhexiline maleate as a cause of reversible parkinsonism and peripheral neuropathy. *J Am Geriatr Soc*, 29 (6), pp. 259-262.

Gottlieb, R. and Magnus, R. (1904) Digitalis und Herzabeit. Nach Versuchen an uberlebenden Warmbluterherzen. *Arch Für Exp Pathol Pharmakol*, 51 (1), pp. 30-63.

Gowda, S., Desai, P.B., Hull, V.V., Math, A.A.K., Vernekar, S.N. and Kulkarni, S.S. (2009) A review on laboratory liver function tests. *Pan Afr Med J*, 3, p. 17.

Graham, D., Huynh, N.N., Hamilton, C.A., Beattie, E., Smith, R.A. and Cochemé, H.M. et al. (2009) Mitochondria-targeted antioxidant MitoQ10 improves endothelial function and attenuates cardiac hypertrophy. *Hypertension*, 54 (2), pp. 322-328.

Granger, C.B., McMurray, J.J., Yusuf, S., Held, P., Michelson, E.L. and Olofsson, B. et al. (2003) Effects of candesartan in patients with chronic heart failure and reduced left-ventricular systolic function intolerant to angiotensin-converting-enzyme inhibitors: the CHARM-Alternative trial. *Lancet*, 362 (9386), pp. 772-776.

Grassian, A.R., Metallo, C.M., Coloff, J.L., Stephanopoulos, G. and Brugge, J.S. (2011) Erk regulation of pyruvate dehydrogenase flux through PDK4 modulates cell proliferation. *Genes Dev*, 25 (16), pp. 1716-1733.

Gravning, J., Ahmed, M.S., von Lueder, T.G., Edvardsen, T. and Attramadal, H. (2013) CCN2/CTGF attenuates myocardial hypertrophy and cardiac dysfunction upon chronic pressure-overload. *Int J Cardiol*, 168 (3), pp. 2049-2056.

Grima, M., Velly, J., Decker, N., Marciniak, G. and Schwarte, J. (1988) Inhibitory effects of some cyclohexylaralkylamines related to perhexiline on sodium influx, binding of [3H] batrachotoxinin A 20-α-benzoate and [3H] nitrendipine and on guinea pig left atria contractions. *Eur J Pharmacol*, 147 (2), pp. 173-185.

Grupp, I.L., Bunde, C.A. and Grupp, G. (1970) Effects of Perhexiline Maleate on Exercise-Induced Tachycardia. *J Clin Pharmacol*, 10 (5), pp. 312-315.

Gu, W.L., Chen, C.X., Huang, X.Y. and Gao, J.P. (2015) The effect of angoroside C on pressure overload-induced ventricular remodeling in rats. *Phytomedicine*, 22 (7), pp. 705-712.

Guan, X.H., Hong, X., Zhao, N., Liu, X.H., Xiao, Y.F. and Chen, T.T. et al. (2017). CD38 promotes angiotensin II-induced cardiac hypertrophy. *J Cell Mol Med*, 21 (8), pp. 1492-1502.

Guazzi, M. and Borlaug, B.A. (2012) Pulmonary hypertension due to left heart disease. *Circulation*, 126 (8), pp. 975-990.

Guo, P., Mizushige, K., Noma, T., Murakami, K., Namba, T. and Ishizawa, M. et al. (2005) Association of uncoupling protein-2 expression with increased reactive oxygen species in residual myocardium of the enlarged left ventricle after myocardial infarction. *Heart Vessels*, 20 (2), pp. 61-65.

Guo, Y., Fan, Y., Zhang, J., Lomberk, G.A., Zhou, Z. and Sun, L. et al. (2015) Perhexiline activates KLF14 and reduces atherosclerosis by modulating ApoA-I production. *J Clin Invest*, 125 (10), pp. 3819-3830.

Gupta, V. (2013) Glucagon-like peptide-1 analogues: an overview. *Indian J Endocrinol Metab*, 17 (3), pp. 413-421.

Haemmerle, G., Moustafa, T., Woelkart, G., Büttner, S., Schmidt, A. and Van De Weijer, T. et al. (2011) ATGL-mediated fat catabolism regulates cardiac mitochondrial function via PPAR-[alpha] and PGC-1. *Nat Med*, 17 (9), pp. 1076-1085.

Haghighi, K., Bidwell, P. and Kranias, E.G. (2014) Phospholamban interactome in cardiac contractility and survival: A new vision of an old friend. *J Mol Cell Cardiol*, 77, pp. 160-167.

Haim, T.E., Wang, W., Flagg, T.P., Tones, M.A., Bahinski, A. and Numann, R.E. et al. (2009) Palmitate attenuates myocardial contractility through augmentation of repolarizing Kv currents. *J Mol Cell Cardiol*, 48 (2), pp. 395-405.

Halbirk, M., Nørrelund, H., Møller, N., Holst, J.J., Schmitz, O. and Nielsen, R. et al. (2010) Cardiovascular and metabolic effects of 48-h glucagon-like peptide-1 infusion in compensated chronic patients with heart failure. *Am J Physiol Heart Circ Physiol*, 298 (3), pp. H1096-H1102.

Hamdani, N., Franssen, C., Lourenço, A., Falcão-Pires, I., Fontoura, D. and Leite, S. et al. (2013) Myocardial titin hypophosphorylation importantly contributes to heart failure with preserved ejection fraction in a rat metabolic risk model. *Circ Heart Fail*, 6 (6, pp. 1239-1249.

Hamer, A.W., Arkles, L.B. and Johns, J.A. (1989) Beneficial effects of low dose amiodarone in patients with congestive cardiac failure: a placebo-controlled trial. *J Am Coll Cardiol*, 14 (7), pp. 1768-1774.

Hamichi, L., Pirotte, J., Borlee, G. and Jardon, J. (1982) Perhexiline maleate-induced cirrhosis. *Acta Gastroenterol Belg*, 45 (5-6), pp. 210-214.

Hang, T., Huang, Z., Jiang, S., Gong, J., Wang, C. and Xie, D. et al. (2006) Apoptosis in pressure overload-induced cardiac hypertrophy is mediated, in part, by adenine nucleotide translocator-1. *Ann Clin Lab Sci*, 36 (1), pp. 88-95.

Hanrath, P., Mathey, D.G., Siegert, R. and Bleifeld, W. (1980) Left ventricular relaxation and filling pattern in different forms of left ventricular hypertrophy: an echocardiographic study. *Am J Cardiol*, 45 (1), pp. 15-23.

Haq, S., Choukroun, G., Lim, H., Tymitz, K.M., del Monte, F. and Gwathmey, J. et al. (2001) Differential activation of signal transduction pathways in human hearts with hypertrophy versus advanced heart failure. *Circulation*, 103 (5), pp. 670-677.

Hara, M., Ono, K., Hwang, M.W., Iwasaki, A., Okada, M. and Nakatani, K. et al. (2002) Evidence for a role of mast cells in the evolution to congestive heart failure. *J Exp Med*, 195 (3), pp. 375-381.

Hardie, D.G., Ross, F.A. and Hawley, S.A. (2012) AMPK: a nutrient and energy sensor that maintains energy homeostasis. *Nat Rev Mol Cell Biol*, 13 (4), pp. 251-262.

Hart, C.Y., Meyer, D.M., Tazelaar, H.D., Grande, J.P., Burnett Jr, J.C. and Housmans, P.R. et al. (2001) Load versus humoral activation in the genesis of early hypertensive heart disease. *Circulation*, 104 (2), pp. 215-220.

Hartley, C.J., Reddy, A.K., Madala, S., Entman, M.L., Michael, L.H. and Taffet, G.E. (2011). Doppler velocity measurements from large and small arteries of mice. *Am J Physiol Heart Circ Physiol*, 301 (2), pp. H269-H278.

Hausenloy, D.J. and Yellon, D.M. (2007) Reperfusion injury salvage kinase signalling: taking a RISK for cardioprotection. *Heart Fail Rev*, 12 (3-4), pp. 217-234.

Hay, D.R. and Gwynne, J.F. (1983) Cirrhosis of the liver following therapy with perhexiline maleate. *N Z Med J*, 96 (728), pp. 202-204.

Heinecke, K., Heuser, A., Blaschke, F., Jux, C., Thierfelder, L. and Drenckhahn, J.D. (2017) Preserved heart function after left ventricular pressure overload in adult mice subjected to neonatal cardiac hypoplasia. *J Dev Orig Health Dis*, 24 pp. 1-13.

Heinzel, F.R., Hohendanner, F., Jin, G., Sedej, S. and Edelmann, F. (2015) Myocardial hypertrophy and its role in heart failure with preserved ejection fraction. *J Appl Physiol*, 119 (10), pp. 1233-1242.

Herr, D.J., Aune, S.E. and Menick, D.R. (2015) Induction and Assessment of Ischemia-reperfusion Injury in Langendorff-perfused Rat Hearts. *J Vis Exp*, (101), e52908.

Hess, O.M., Grimm, J. and Krayenbuehl, H.P. (1979) Diastolic simple elastic and viscoelastic properties of the left ventricle in man. *Circulation*, 59 (6), pp. 1178-1187.

Higgins, A.J., Morville, M., Burges, R.A., Gardiner, D.G., Page, M.G. and Blackburn, K.J. (1980) Oxfenicine diverts rat muscle metabolism from fatty acid to carbohydrate oxidation and protects the ischaemic rat heart. *Life Sci*, 27 (11), pp. 963-970.

Hirasaka, K., Lago, C.U., Kenaston, M.A., Fathe, K., Nowinski, S.M. and Nikawa, T. et al. (2011) Identification of a redox-modulatory interaction between uncoupling protein 3 and thioredoxin 2 in the mitochondrial intermembrane space. *Antioxid Redox Signal*, 15 (10), pp. 2645-2661.

Hirotani, S., Zhai, P., Tomita, H., Galeotti, J., Marquez, J.P. and Gao, S. et al. (2007) Inhibition of glycogen synthase kinase 3β during heart failure is protective. *Circ Res*, 101 (11), pp. 1164-1174.

Hirshleifer, I. (1969) Perhexiline maleate in the treatment of angina pectoris. *Curr Ther Res Clin Exp*, 11 (3), pp. 99-105.

Hogan, Q., Sapunar, D., Modric-Jednacak, K. and McCallum, J.B. (2004) Detection of neuropathic pain in a rat model of peripheral nerve injury. *Anesthesiology*, 101 (2), pp. 476-487.

Holmström, K.M. and Finkel, T. (2014) Cellular mechanisms and physiological consequences of redox-dependent signalling. *Nat Rev Mol Cell Biol*, 15 (6), pp. 411-421.

Hölscher, M., Schäfer, K., Krull, S., Farhat, K., Hesse, A. and Silter, M. et al. (2012) Unfavourable consequences of chronic cardiac HIF-1α stabilization. *Cardiovasc Res*, 94 (1), pp. 77-86.

Holubarsch, C.J., Rohrbach, M., Karrasch, M., Boehm, E., Polonski, L. and Ponikowski, P. et al. (2007) A double-blind randomized multicentre clinical trial to evaluate the efficacy and safety of two doses of etomoxir in comparison with placebo in patients with moderate congestive heart failure: the ERGO (etomoxir for the recovery of glucose oxidation) study. *Clin Sci (Lond)*, 113 (4), pp. 205-212.

Horowitz, J.D., Button, I.K. and Wing, L. (1995) Is perhexiline essential for the optimal management of angina pectoris? *Aust N Z J Med*, 25 (2), pp. 111-113.

Horowitz, J.D., Chirkov, Y.Y., Kennedy, J.A. and Sverdlov, A.L. (2010) Modulation of myocardial metabolism: an emerging therapeutic principle. *Curr Opin Cardiol*, 25 (4), pp. 329-334.

Horowitz, J.D., Goble, A.J., Morris, P.M., Drummer, O.H. and Louis, W.J. (1981) High-performance liquid chromatographic assay of perhexiline maleate in plasma. *J Pharm Sci*, 70 (3), pp. 320-322.

Horowitz, J.D. and Mashford, M.L. (1979) Perhexiline maleate in the treatment of severe angina pectoris. *Med J Aust*, 1 (11), pp. 485-488.

Horowitz, J.D., Sia, S.T.B., Macdonald, P.S., Goble, A.J. and Louis, W.J. (1986) Perhexiline maleate treatment for severe angina pectoris—correlations with pharmacokinetics. *Int J Cardiol*, 13 (2), pp. 219-229.

Horowitz, J.D., White, H.D. and Goble, A.J. (1982) Liver disease induced by perhexiline maleate. *Med J Aust*, 2 (1), pp. 9-10.

Hoshi, M., Takashima, A., Noguchi, K., Murayama, M., Sato, M. and Kondo, S. et al. (1996) Regulation of mitochondrial pyruvate dehydrogenase activity by tau protein kinase I/glycogen synthase kinase 3beta in brain. *Proc Natl Acad Sci U S A*, 93 (7), pp. 2719-2723.

Hua, Y., Xu, X., Shi, G.P., Chicco, A.J., Ren, J. and Nair, S. (2013) Cathepsin K Knockout Alleviates Pressure Overload–Induced Cardiac HypertrophyNovelty and Significance. *Hypertension*, 61 (6), pp. 1184-1192.

Hua, Y., Zhang, Y. and Ren, J. (2012) IGF-1 deficiency resists cardiac hypertrophy and myocardial contractile dysfunction: role of microRNA-1 and microRNA-133a. *J Cell Mol Med*, 16 (1), pp. 83-95.

Huang, P., Shen, Z., Yu, W., Huang, Y., Tang, C. and Du, J. et al. (2017) Hydrogen sulfide inhibits high-salt diet-induced myocardial oxidative stress and myocardial hypertrophy in Dahl rats. *Front Pharmacol*, 8, p. 128.

Huang, Q., Zhou, H.J., Zhang, H., Huang, Y., Hinojosa-Kirschenbaum, F. and Fan, P. et al. (2015) Thioredoxin-2 inhibits mitochondrial ROS generation and ASK1 activity to maintain cardiac function. *Circulation*, 131 (12), 1082-1097.

Hudak, W.J., Lewis, R.E. and Kuhn, W.L. (1970) Cardiovascular pharmacology of perhexiline. *J Pharmacol Exp Ther*, 173 (2), pp. 371-382.

Hudak, W.J., Lewis, R.E., Lucas, R.W. and Kuhn, W.L. (1973) Proceedings: Review of the cardiovascular pharmacology of perhexiline. *Postgrad Med J*, 49, p. S3.

Hundley, W.G., Bayram, E., Hamilton, C.A., Hamilton, E.A., Morgan, T.M. and Darty, S.N. et al. (2007) Leg flow-mediated arterial dilation in elderly patients with heart failure and normal left ventricular ejection fraction. *Am J Physiol Heart Circ Physiol*, 292 (3), pp. H1427-H1434.

Hundley, W.G., Kitzman, D.W., Morgan, T.M., Hamilton, C.A., Darty, S.N. and Stewart, K.P. et al. (2001) Cardiac cycle-dependent changes in aortic area and distensibility are reduced in older patients with isolated diastolic heart failure and correlate with exercise intolerance. *J Am Coll Cardiol*, 38 (3), pp. 796-802.

Hunter, W.G., Kelly, J.P., McGarrah III, R.W., Kraus, W.E. and Shah, S.H. (2016) Metabolic dysfunction in heart failure: diagnostic, prognostic, and pathophysiologic insights from metabolomic profiling. *Curr Heart Fail Rep*, 13 (3), pp. 119-131.

Iaizzo, P.A. (2015) *Handbook of Cardiac Anatomy, Physiology, and Devices*. 3rd ed. Springer International Publishing.

Ide, T., Tsutsui, H., Kinugawa, S., Utsumi, H., Kang, D. and Hattori, N. et al. (1999) Mitochondrial electron transport complex I is a potential source of oxygen free radicals in the failing myocardium. *Circ Res*, 85 (4), pp. 357-363.

Igishu, J. (1976) Long-term perhexiline maleate and liver function. *Br Med J*, 1 (6002), p. 133.

Ikizler, M., Dernek, S., Sevin, B. and Kural, T. (2003) Trimetazidine improves recovery during reperfusion in isolated rat hearts after prolonged ischemia. *Anadolu Kardiyol Derg*, 3 (4), pp. 303-308.

Ileana, T., Anna, M., Pamela, S., Fernanda, V., Stefano, B. and Livio, L. (2017) Ranolazine promotes muscle differentiation and reduces oxidative stress in C2C12 skeletal muscle cells. *Endocrine*, 58 (1), pp. 33-45.

Inglis, S. and Stewart, S. (2006) Metabolic therapeutics in angina pectoris: history revisited with perhexiline. *Eur J Cardiovasc Nurs*, 5 (2), pp. 175-184.

Ingwall, J.S. (1984) The hypertrophied myocardium accumulates the MB-creatine kinase isozyme. *Eur Heart J*, 5(SF), pp. 129-139.

Inserte, J., Barba, I., Hernando, V., Abellán, A., Ruiz-Meana, M. and Rodríguez-Sinovas, A. et al. (2008) Effect of acidic reperfusion on prolongation of intracellular acidosis and myocardial salvage. *Cardiovasc Res*, 77 (4), pp. 782-790.

Jackson, G., Gibbs, C.R., Davies, M.K. and Lip, G.Y.H. (2000) ABC of heart failure: Pathophysiology. *BMJ*, 320 (7228), pp. 167-170.

Jameel, M.N., Xiong, Q., Mansoor, A., Bache, R.J. and Zhang, J. (2016) ATP sensitive K+ channels are critical for maintaining myocardial perfusion and high energy phosphates in the failing heart. *J Mol Cell Cardiol*, 92, pp. 116-121.

Jaswal, J.S., Keung, W., Wang, W., Ussher, J.R. and Lopaschuk, G.D. (2011) Targeting fatty acid and carbohydrate oxidation—a novel therapeutic intervention in the ischemic and failing heart. *Biochim Biophys Acta*, 1813 (7), pp. 1333-1350.

Jeffrey, F.M.H., Alvarez, L., Diczku, V., Sherry, D. and Malloy, C.R. (1995) Direct evidence that perhexiline modifies myocardial substrate utilization from fatty acids to lactate. *J Cardiovasc Pharmacol*, 25 (3), pp. 469-472.

Juhaszova, M., Zorov, D.B., Kim, S.H., Pepe, S., Fu, Q. and Fishbein, K.W. et al. (2004) Glycogen synthase kinase-3β mediates convergence of protection signaling to inhibit the mitochondrial permeability transition pore. *J Clin Invest*, 113 (11), p.1535-1549.

Kabir, M.E., Singh, H., Lu, R., Olde, B., Leeb-Lundberg, L.F. and Bopassa, J.C. (2015) G Protein-coupled estrogen receptor 1 mediates acute estrogen-induced cardioprotection via MEK/ERK/GSK-3β pathway after ischemia/reperfusion. *PLoS One*, 10 (9), p. e0135988.

Kaimoto, S., Hoshino, A., Ariyoshi, M., Okawa, Y., Tateishi, S. and Ono, K. et al. (2017) Activation of PPAR-α in the early stage of heart failure maintained myocardial function and energetics in pressure-overload heart failure. *Am J Physiol Heart Circ Physiol*, 312 (2), pp. H305-H313.

Kalay, N., Ozdogru, I., Gul, A., Yucel, Y., Cetinkaya, Y. and Inanc, M.T. et al. (2008) Effects of intermittent and long-term glucose-insulin-potassium infusion in patients with systolic heart failure. *Exp Clin Cardiol*, 13 (2), pp. 85-88.

Kalogeris, T., Baines, C.P., Krenz, M. and Korthuis, R.J. (2012) Cell biology of ischemia/reperfusion injury. *Int Rev Cell Mol Biol*, 298, p. 229-317.

Kantor, P.F., Lucien, A., Kozak, R. and Lopaschuk, G.D. (2000) The antianginal drug trimetazidine shifts cardiac energy metabolism from fatty acid oxidation to glucose oxidation by inhibiting mitochondrial long-chain 3-ketoacyl coenzyme A thiolase. *Circ Res*, 86 (5), pp. 580-588.

Kara, A.F., Demiryürek, Ş., Çelik, A., Tarakçıoğlu, M. and Demiryürek, A.T. (2006) Effects of chronic trimetazidine treatment on myocardial preconditioning in anesthetized rats. *Fundam Clin Pharmacol*, 20 (5), pp. 449-459.

Karbowska, J., Kochan, Z. and Smolenski, R.T. (2003) Peroxisome proliferator-activated receptor alpha is downregulated in the failing human heart. *Cell Mol Biol Lett*, 8 (1), pp. 49-54.

Kasner, M., Westermann, D., Lopez, B., Gaub, R., Escher, F. and Kühl, U. et al. (2011) Diastolic tissue Doppler indexes correlate with the degree of collagen expression and cross-linking in heart failure and normal ejection fraction. *J Am Coll Cardiol*, 57 (8), pp. 977-985.

Kass, D.A., Maughan, W.L., Guo, Z.M., Kono, A., Sunagawa, K. and Sagawa, K. (1987) Comparative influence of load versus inotropic states on indexes of ventricular contractility: experimental and theoretical analysis based on pressure-volume relationships. *Circulation*, 76 (6), pp. 1422-1436.

Kato, S., Spinale, F.G., Tanaka, R., Johnson, W., Cooper, G.T. and Zile, M.R. (1995) Inhibition of collagen cross-linking: effects on fibrillar collagen and ventricular diastolic function. *Am J Physiol Heart Circ Physiol*, 269 (3), pp. H863-H868.

Kato, T., Niizuma, S., Inuzuka, Y., Kawashima, T., Okuda, J. and Tamaki, Y. et al. (2010) Analysis of metabolic remodeling in compensated left ventricular hypertrophy and heart failure. *Circ Heart Fail*, 3 (3), pp. 420-430.

Katz, A.M. (2010) *Physiology of the Heart*. 5th revised edn. Lippincott Williams and Wilkins.

Kawaguchi, M., Hay, I., Fetics, B. and Kass, D.A. (2003) Combined ventricular systolic and arterial stiffening in patients with heart failure and preserved ejection fraction. *Circulation*, 107 (5), pp. 714-720.

Kemp, C.D. and Conte, J.V. (2012) The pathophysiology of heart failure. *Cardiovasc Pathol*, 21 (5), pp. 365-371.

Kennedy, J.A., Beck-Oldach, K., McFadden-Lewis, K., Murphy, G.A., Wong, Y.W. and Zhang, Y. et al. (2006) Effect of the anti-anginal agent, perhexiline, on neutrophil, valvular and vascular superoxide formation. *Eur J Pharmacol*, 531 (1), pp. 13-19.

Kennedy, J.A., Kiosoglous, A.J., Murphy, G.A., Pelle, M.A. and Horowitz, J.D. (2000) Effects of perhexiline and oxfenicine on myocardial function and metabolism during low-flow ischaemia/ reperfusion in the isolated rat heart. *J Cardiovasc Pharmacol*, 36 (6), pp. 794-801.

Kennedy, J.A., Mohan, P., Pelle, M.A., Wade, S.R. and Horowitz, J.D. (1999) The effects of perhexiline on the rat coronary vasculature. *Eur J Pharmacol*, 370 (3), pp. 263-270.

Kennedy, J.A., Unger, S.A. and Horowitz, J.D. (1996) Inhibition of carnitine palmitoyltransferase-1 in rat heart and liver by perhexiline and amiodarone. *Biochem Pharmacol*, 52 (2), pp. 273-280.

Keung, W., Ussher, J.R., Jaswal, J.S., Raubenheimer, M., Lam, V.H. and Wagg, C.S. et al. (2013) Inhibition of carnitine palmitoyltransferase-1 activity alleviates insulin resistance in diet-induced obese mice. *Diabetes*, 62 (3), pp. 711-720.

Khanam, S.S., Son, J.W., Lee, J.W., Youn, Y.J., Yoon, J. and Lee, S.H. et al. (2017) Prognostic value of short-term follow-up BNP in hospitalized patients with heart failure. *BMC Cardiovasc Disord*, 17 (1), p. 215

Kho, C., Lee, A., Jeong, D., Oh, J.G., Chaanine, A.H. and Kizana, E. et al. (2011) SUMO1-dependent modulation of SERCA2a in heart failure. *Nature*, 477 (7366), pp. 601-605.

Killalea, S.M. and Krum, H. (2001) Systematic review of the efficacy and safety of perhexiline in the treatment of ischemic heart disease. *Am J Cardiovasc Drugs*, 1 (3), pp. 193-204.

Kim, W., Flamm, S.L., Di Bisceglie, A.M. and Bodenheimer, H.C. (2008) Serum activity of alanine aminotransferase (ALT) as an indicator of health and disease. *Hepatology*, 47 (4), pp. 1363-1370.

Kirchberger, M.A. and Antonetz, T. (1982) Phospholamban: dissociation of the 22,000 molecular weight protein of cardiac sarcoplasmic reticulum into 11,000 and 5,500 molecular weight forms. *Biochem Biophys Res Commun*, 105 (1), pp. 152-156.

Kitzman, D.W., Hundley, W.G., Brubaker, P.H., Morgan, T., Moore, J.B. and Stewart, K.P. et al. (2010) A randomized, double-blinded trial of enalapril in older patients with heart failure and preserved ejection fraction: effects on exercise tolerance and arterial distensibility. *Circ Heart Fail*, 3 (4), pp. 477-485.

Klassen, G.A., Sestier, F., L'abbate, A., Mildenberger, R.R. and Zborowska-Sluis, D.T. (1976) Effects of perhexiline maleate on coronary flow distribution in the ischemic canine myocardium. *Circulation*, 54 (1), pp. 14-20.

Køber, L., Torp-Pedersen, C., McMurray, J.J., Gøtzsche, O., Lévy, S. and Crijns, H. et al. (2008) Increased mortality after dronedarone therapy for severe heart failure. *N Engl J Med*, 358 (25), pp. 2678-2687.

Kofanova, O.A., Fack, F., Niclou, S.P. and Betsou, F. (2013) Combined effect of tissue stabilization and protein extraction methods on phosphoprotein analysis. *Biopreserv Biobanking*, 11 (3), pp. 161-165.

Kolobova, E., Tuganova, A., Boulatnikov, I. and Popov, K.M. (2001) Regulation of pyruvate dehydrogenase activity through phosphorylation at multiple sites. *Biochem J*, 358 (1), pp. 69-77.

Kolwicz, S.C., Olson, D.P., Marney, L.C., Garcia-Menendez, L., Synovec, R.E. and Tian, R. (2012) Cardiac-Specific Deletion of Acetyl CoA Carboxylase 2 Prevents Metabolic Remodeling During Pressure-Overload Hypertrophy. *Circ Res*, 111 (6), pp. 728-738.

Kopelman, P. and Morgan, P.G.M. (1977) Liver damage after perhexiline maleate. *Lancet*, 309 (8013), p. 705.

Korvald, C., Elvenes, O.P. and Myrmel, T. (2000) Myocardial substrate metabolism influences left ventricular energetics in vivo. *Am J Physiol Heart Circ Physiol*, 278 (4), pp. H1345-H1351.

Kosmala, W., Holland, D.J., Rojek, A., Wright, L., Przewlocka-Kosmala, M. and Marwick, T.H. (2013) Effect of I f-channel inhibition on hemodynamic status and exercise tolerance in heart failure with preserved ejection fraction: a randomized trial. *J Am Coll Cardiol*, 62 (15), pp. 1330-1338.

Kovacs, K., Hanto, K., Bognar, Z., Tapodi, A., Bognar, E. and Kiss, G.N. et al. (2009) Prevalent role of Akt and ERK activation in cardioprotective effect of Ca2+ channel-and beta-adrenergic receptor blockers. *Mol Cell Biochem*, 321 (1-2), pp. 155-164.

Kranias, E.G. and Hajjar, R.J. (2012) Modulation of cardiac contractility by the phopholamban/SERCA2a regulatome. *Circ Res*, 110 (12), pp. 1646-1660.

Ku, H.C., Lee, S.Y., Wu, Y.K.A., Yang, K.C. and Su, M.J. (2016) A Model of Cardiac Remodeling Through Constriction of the Abdominal Aorta in Rats. *J Vis Exp*, (118), p. e54818.

Kuzmicic, J., Parra, V., Verdejo, H.E., López-Crisosto, C., Chiong, M. and García, L. et al. (2014) Trimetazidine prevents palmitate-induced mitochondrial fission and dysfunction in cultured cardiomyocytes. *Biochem Pharmacol*, 91 (3), pp. 323-336.

Ky, B., French, B., Khan, A.M., Plappert, T., Wang, A. and Chirinos, J.A. et al. (2013) Ventricular-arterial coupling, remodeling, and prognosis in chronic heart failure. *J Am Coll Cardiol*, 62 (13), pp. 1165-1172.

Lageron, A. (1979) Histoenzymologic modifications induced by perhexiline maleate in human liver. *Méd Chir Dig*, 8 (5), p. 415-417.

Lageron, A., Scotto, J. and Gautier, M. (1981) Effects of pexid on liver cell cultures ultrastructural and histoenzymological studies. *Eur J Clin Pharmacol*, 19 (6), pp. 417-421.

Lahey, R., Wang, X., Carley, A.N. and Lewandowski, E.D. (2014) Dietary fat supply to failing hearts determines dynamic lipid signaling for nuclear receptor activation and oxidation of stored triglyceride. *Circulation*, 130 (20), pp. 1790-9.

Lai, L., Leone, T.C., Keller, M.P., Martin, O.J., Broman, A.T. and Nigro, J. et al. (2014) Energy metabolic re-programming in the hypertrophied and early stage failing heart: a multi-systems approach. *Circ Heart Fail*, 7 (6), pp. 1022-1031.

Lainscak, M., Pelliccia, F., Rosano, G., Vitale, C., Schiariti, M. and Greco, C. et al. (2015) Safety profile of mineralocorticoid receptor antagonists: Spironolactone and eplerenone. *Int J Cardiol*, 200, pp. 25-29.

Lam, C.S., Roger, V.L., Rodeheffer, R.J., Bursi, F., Borlaug, B.A. and Ommen, S.R. et al. (2007) Cardiac structure and ventricular–vascular function in persons with heart failure and preserved ejection fraction from Olmsted County, Minnesota. *Circulation*, 115 (15), pp. 1982-1990.

Langendorff, O. (1897) Untersuchungen am überlebenden Säugethierherzen. *Pflügers Archiv Eur J Physiol*, 66 (7), pp. 355-400.

Laplane, D. and Bousser, M.G. (1981) Polyneuropathy during perhexiline maleate therapy. *Int J Neurol*, 15 (3-4), pp. 293-300.

Le Gall, J.Y., Guillouzo, A., Glaise, D., Deugnier, Y., Messner, M. and Bourel, M. (1980) Perhexiline maleate toxicity on human liver cell lines. *Gut*, 21 (11), pp. 977-984.

Leclerc, G., Decker, N. and Schwartz, J. (1982) Synthesis and cardiovascular activity of a new series of cyclohexylaralkylamine derivatives related to perhexiline. *J Med Chem*, 25 (6), pp. 709-714.

Lee, C.F. and Tian, R. (2015) Mitochondrion as a Target for Heart Failure Therapy - Role of Protein Lysine Acetylation. *Circ J*, 79 (9), pp. 1863-1870.

Lee, J.F., Barrett-O'Keefe, Z., Garten, R.S., Nelson, A.D., Ryan, J.J. and Nativi, J.N. et al. (2016) Evidence of microvascular dysfunction in heart failure with preserved ejection fraction. *Heart*, 102 (4), pp. 278-284.

Lee, L., Campbell, R., Scheuermann-Freestone, M., Taylor, R., Gunaruwan, P. and Williams, L. et al. (2005) Metabolic modulation with perhexiline in chronic heart failure. *Circulation*, 112 (21), pp. 3280-3288.

Lei, B., Lionetti, V., Young, M.E., Chandler, M.P., d'Agostino, C. and Kang, E. et al. (2004) Paradoxical downregulation of the glucose oxidation pathway despite enhanced flux in severe heart failure. *J Mol Cell Cardiol*, 36 (4), pp. 567-576.

Lei, L., Mason, S., Liu, D., Huang, Y., Marks, C. and Hickey, R. et al. (2008) Hypoxia-inducible factor-dependent degeneration, failure, and malignant transformation of the heart in the absence of the von Hippel-Lindau protein. *Mol Cell Biol*, 28 (11), pp. 3790-3803.

Lele, S.S., Macfarlane, D., Morrison, S., Thomson, H., Khafagi, F. and Frenneaux, M. (1996) Determinants of exercise capacity in patients with coronary artery disease and mild to moderate systolic dysfunction: Role of heart rate and diastolic filling abnormalities. *Eur Heart J*, 17 (2), pp. 204-212.

Lenoir, C. and Blanchon, P. (1978) Hepatitis caused by perhexiline maleate. *Coeur Med Interne*, 17 (1), pp. 69-75.

Levelt, E., Rodgers, C., Clarke, W.T., Mahmod, M., Ariga, R. and Francis, J.M. et al. (2015) Effect of exercise on myocardial energy metabolism and relationship between coronary microvascular dysfunction and abnormal myocardial energetics in diabetic cardiomyopathy. *J Cardiovasc Magn Reson*, 17 (S1), p. O98.

Levick, R.L. (2009) *An Introduction to Cardiovascular Physiology*. 5th edn. CRC press.

Lewis, D., Wainwright, H.C., Kew, M.C., Zwi, S. and Isaacson, C. (1979) Liver damage associated with perhexiline maleate. *Gut*, 20 (3), pp. 186-189.

Lhermitte, F., Fardeau, M., Chedru, F. and Mallecourt, J. (1976) Polyneuropathy after perhexiline maleate therapy. *Br Med J*, 1 (6020), p. 1256.

Li, C., Sun, X.N., Zeng, M.R., Zheng, X.J., Zhang, Y.Y. and Wan, Q. et al. (2017) Mineralocorticoid Receptor Deficiency in T Cells Attenuates Pressure Overload–Induced Cardiac Hypertrophy and Dysfunction Through Modulating T-Cell Activation. *Hypertension*, 70 (1), pp.137-147.

Li, J., Yousefi, K., Ding, W., Singh, J. and Shehadeh, L.A. (2017) Osteopontin RNA aptamer can prevent and reverse pressure overload-induced heart failure. *Cardiovasc Res*, 113 (6), pp. 633-643.

Li, M., Wang, X.F., Shi, J.J., Li, Y.P., Yang, N. and Zhai, S. et al. (2015) Caffeic acid phenethyl ester inhibits liver fibrosis in rats. *World J Gastroenterol*, 21 (13), pp. 3893-38903.

Li, Y., Tang, X.H., Li, X.H., Dai, H.J., Miao, R.J. and Cai, J.J. et al. (2016) Regulator of G protein signalling 14 attenuates cardiac remodelling through the MEK–ERK1/2 signalling pathway. *Basic Res Cardiol*, 111 (4), p. 1-19.

Liao, R., Podesser, B.K. and Lim, C.C. (2012) The continuing evolution of the Langendorff and ejecting murine heart: new advances in cardiac phenotyping. *Am J Physiol Heart Circ Physiol*, 303 (2), pp. H156-H167.

Liberman, Z. and Eldar-Finkelman, H. (2005) Serine 332 phosphorylation of insulin receptor substrate-1 by glycogen synthase kinase-3 attenuates insulin signaling. *J Biol Chem*, 280 (6), pp. 4422-4428.

Liberts, E.A., Willoughby, S.R., Kennedy, J.A. and Horowitz, J.D. (2007) Effects of perhexiline and nitroglycerin on vascular, neutrophil and platelet function in patients with stable angina pectoris. *Eur J Pharmacol*, 560 (1), pp. 49-55.

Licari, G., Somogyi, A.A., Milne, R.W. and Sallustio, B.C. (2015) Comparison of CYP2D metabolism and hepatotoxicity of the myocardial metabolic agent perhexiline in Sprague–Dawley and Dark Agouti rats. *Xenobiotica*, 45 (1), pp. 3-9.

Lin, C.L., Tseng, H.C., Chen, W.P., Su, M.J., Fang, K.M. and Chen, R.F. et al. (2011) Intracellular zinc release-activated ERK-dependent GSK-3β–p53 and Noxa–Mcl-1 signaling are both involved in cardiac ischemic-reperfusion injury. *Cell Death Differ*, 18 (10), pp. 1651-1663.

Ling, L.H., Khammy, O., Byrne, M., Amirahmadi, F., Foster, A. and Li, G. et al. (2012) Irregular rhythm adversely influences calcium handling in ventricular myocardium. *Circ Heart Fail*, 5 (6), pp. 786-793.

Lionetti, V., Linke, A., Chandler, M.P., Young, M.E., Penn, M.S. and Gupte, S. et al. (2005) Carnitine palmitoyl transferase-I inhibition prevents ventricular remodeling and delays decompensation in pacing-induced heart failure. *Cardiovasc Res*, 66 (3), pp. 454-461.

Lipskaia, L., Keuylian, Z., Blirando, K., Mougenot, N., Jacquet, A. and Rouxel, C. et al. (2014) Expression of sarco (endo) plasmic reticulum calcium ATPase (SERCA) system in normal mouse cardiovascular tissues, heart failure and atherosclerosis. *Biochim Biophys Acta*, 1843 (11), pp. 2705-2718.

Little, W.C., Warner, J.G., Rankin, K.M., Kitzman, D.W. and Cheng, C.P. (1998) Evaluation of left ventricular diastolic function from the pattern of left ventricular filling. *Clin Cardiol*, 21 (1), pp. 5-9.

Liu, J., Wang, P., Zou, L., Qu, J., Litovsky, S. and Umeda, P. et al. (2014) High-fat, low-carbohydrate diet promotes arrhythmic death and increases myocardial ischemia-reperfusion injury in rats. *Am J Physiol Heart Circ Physiol*, 307 (4), pp. H598-H608.

Liu, P.P., Liu, J., Jiang, W.Q., Carew, J.S., Ogasawara, M.A. and Pelicano, H. et al. (2016) Elimination of chronic lymphocytic leukemia cells in stromal microenvironment by targeting CPT with an antiangina drug perhexiline. *Oncogene*, 35 (43), pp. 5663-5673.

Liu, Z., Chen, J.M., Huang, H., Kuznicki, M., Zheng, S. and Sun, W. et al. (2016) The protective effect of trimetazidine on myocardial ischemia/reperfusion injury through activating AMPK and ERK signaling pathway. *Metabolism*, 65 (3), pp. 122-130.

Lochner, A., Van Niekerk, I. and Kotze, J.C.N. (1981) Mitochondrial acyl-CoA, adenine nucleotide translocase activity and oxidative phosphorylation in myocardial ischaemia. *J Mol Cell Cardiol*, 13 (11), pp. 991-997.

Lohse, M.J. (1995) G-protein-coupled receptor kinases and the heart. *Trends Cardiovasc Med*, 5 (2), pp. 63-68.

Long, J.P., Fitzgerald, O. and Maurer, B.J. (1980) Hepatotoxicity following treatment with perhexiline maleate. *Ir Med J*, 73 (7), pp. 275-276.

Lonn, E. and McKelvie, R. (2000) Drug treatment in heart failure. *BMJ*, 320 (7243), pp. 1188-1192.

Lopaschuk, G.D., Belke, D.D., Gamble, J., Toshiyuki, I. and Schönekess, B.O. (1994) Regulation of fatty acid oxidation in the mammalian heart in health and disease. *Biochim Biophys Acta*, 1213 (3), pp. 263-276.

Lopaschuk, G.D., Spafford, M.A., Davies, N.J. and Wall, S.R. (1990) Glucose and palmitate oxidation in isolated working rat hearts reperfused after a period of transient global ischemia. *Circ Res*, 66 (2), pp. 546-553.

Lopaschuk, G.D., Ussher, J.R., Folmes, C.D., Jaswal, J.S. and Stanley, W.C. (2010) Myocardial fatty acid metabolism in health and disease. *Physiol Rev*, 90 (1), pp. 207-258.

Lorentz, I.T. and Shortall, M. (1983) Perhexilene neuropathy: a report of two cases. *Int Med J*, 13 (5), pp. 517-518.

Lõster, H. and Punzel, M. (1998) Effects of L-carnitine on mechanical recovery of isolated rat hearts in relation to the perfusion with glucose and palmitate. *Mol Cell Biochem*, 185 (1), pp. 65-75.

Loudon, B.L., Noordali, H., Gollop, N.D., Frenneaux, M.P. and Madhani, M. (2016) Present and future pharmacotherapeutic agents in heart failure: an evolving paradigm. *Br J Pharmacol*, 173 (12), pp. 1911-1924.

Loyer, X., Gómez, A.M., Milliez, P., Fernandez-Velasco, M., Vangheluwe, P. and Vinet, L. et al. (2008) Cardiomyocyte overexpression of neuronal nitric oxide synthase delays transition toward heart failure in response to pressure overload by preserving calcium cycling. *Circulation*, 117 (25), pp. 3187-3198.

Lu, Y.M., Huang, J., Shioda, N., Fukunaga, K., Shirasaki, Y. and Li, X.M. et al. (2011) CaMKIIδB mediates aberrant NCX1 expression and the imbalance of NCX1/SERCA in transverse aortic constriction-induced failing heart. *PLoS One*, 6 (9), p. e24724.

Lu, Z., Xu, X., Hu, X., Fassett, J., Zhu, G. and Tao, Y. et al. (2010) PGC-1α regulates expression of myocardial mitochondrial antioxidants and myocardial oxidative stress after chronic systolic overload. *Antioxid Redox Signal*, 13 (7), pp. 1011-1022.

Luther, J.M., Luo, P., Wang, Z., Cohen, S.E., Kim, H.S. and Fogo, A.B. et al. (2012) Aldosterone deficiency and mineralocorticoid receptor antagonism prevent angiotensin II–induced cardiac, renal, and vascular injury. *Kidney Int*, 82 (6), pp. 643-651.

Lygate, C.A., Schneider, J.E., Hulbert, K., ten Hove, M., Sebag-Montefiore, L.M. and Cassidy, P.J. et al. (2006) Serial high resolution 3D–MRI after aortic banding in mice: band internalization is a source of variability in the hypertrophic response. *Basic Res Cardiol*, 101 (1), pp. 8-16.

Lyon, L., Fisch, S., Nevins, M. and Henry, S. (1971) Perhexilene maleate in treatment of angina pectoris. *Lancet*, 297 (7712), pp. 1272-1274.

Maier, L.S., Layug, B., Karwatowska-Prokopczuk, E., Belardinelli, L., Lee, S. and Sander, J. et al. (2013) RAnoLazIne for the treatment of diastolic heart failure in patients with preserved ejection fraction: the RALI-DHF proof-of-concept study. *JACC Heart Fail*, 1 (2), pp. 115-122.

Maldonado, E.N. and Lemasters, J.J. (2014) ATP/ADP ratio, the missed connection between mitochondria and the Warburg effect. *Mitochondrion*, 19 (Pt A), pp. 78-84.

Man, W., Ming, D., Fang, D., Chao, L. and Jing, C. (2014) Dimethyl Sulfoxide Attenuates Hydrogen Peroxide-Induced Injury in Cardiomyocytes via Heme Oxygenase-1. *J Cell Biochem*, 115 (6), pp. 1159-1165.

Mann, D.L., Kent, R.L., Parsons, B. and Cooper, G. (1992) Adrenergic effects on the biology of the adult mammalian cardiocyte. *Circulation*, 85 (2), pp. 790-804.

Masoud, W.G., Ussher, J.R., Wang, W., Jaswal, J.S., Wagg, C.S. and Dyck, J.R. et al. (2014) Failing mouse hearts utilize energy inefficiently and benefit from improved coupling of glycolysis and glucose oxidation. *Cardiovasc Res*, 101 (1), pp. 30-38.

Martí Massó, J.F.M., Martí, I., Carrera, N., Poza, J.J. and de Munain, A.L. (2005) Trimetazidine induces parkinsonism, gait disorders and tremor. *Therapie*, 60 (4), pp. 419-422.

Massie, B.M., Carson, P.E., McMurray, J.J., Komajda, M., McKelvie, R. and Zile, M.R. et al. (2008) Irbesartan in patients with heart failure and preserved ejection fraction. *N Engl J Med*, 359 (23), pp. 2456-2467.

Masuyama, T., Tsujino, T., Origasa, H., Yamamoto, K., Akasaka, T. and Hirano, Y. et al. (2012) Superiority of long-acting to short-acting loop diuretics in the treatment of congestive heart failure. *Circ J*, 76 (4), pp. 833-842.

Matsuda, T., Zhai, P., Maejima, Y., Hong, C., Gao, S. and Tian, B. et al. (2008) Distinct roles of GSK-3α and GSK-3β phosphorylation in the heart under pressure overload. *Proc Natl Acad Sci U S A*, 105 (52), pp. 20900-20905.

Mattiazzi, A., Mundina-Weilenmann, C., Vittone, L. and Said, M. (2004) Phosphorylation of phospholamban in ischemia-reperfusion injury: functional role of Thr 17 residue. *Mol Cell Biochem*, 263 (1), pp. 131-136.

McDonald, G.S.A. (1977) Liver damage after perhexiline maleate. *Lancet*, 309 (8020), p. 1056.

McFalls, E.O., Sluiter, W., Schoonderwoerd, K., Manintveld, O.C., Lamers, J.M. and Bezstarosti, K. et al. (2006) Mitochondrial adaptations within chronically ischemic swine myocardium. *J Mol Cell Cardiol*, 41 (6), pp. 980-988.

McMurray, J.J., Packer, M., Desai, A.S., Gong, J., Lefkowitz, M.P. and Rizkala, A.R. et al. (2014) Angiotensin–neprilysin inhibition versus enalapril in heart failure. *N Engl J Med*, 371 (11), pp. 993-1004.

Mehta, P.A., Dubrey, S.W., McIntyre, H.F., Walker, D.M., Hardman, S.M. and Sutton, G.C. et al. (2009) Improving survival in the 6 months after diagnosis of heart failure in the past decade: population-based data from the UK. *Heart*, 95 (22), pp. 1851-1856.

Mehta, S.R., Yusuf, S., Díaz, R., Zhu, J., Pais, P. and Xavier, D. et al. (2005) Effect of glucose-insulin-potassium infusion on mortality in patients with acute ST-segment elevation myocardial infarction: the CREATE-ECLA randomized controlled trial. *Jama*, 293 (4), pp. 437-446.

Meier, C., Wahllaender, A., Hess, C.W. and Preisig, R. (1986) Perhexiline-induced lipidosis in the dark Agouti (DA) rat: an animal model of genetically determined neurotoxicity. *Brain*, 109 (4), pp. 649-660.

Meijer, M.K., Spruijt, B.M., Van Zutphen, L.F.M. and Baumans, V. (2006) Effect of restraint and injection methods on heart rate and body temperature in mice. *Lab Anim*, 40 (4), pp. 382-391.

Melenovsky, V., Borlaug, B.A., Rosen, B., Hay, I., Ferruci, L. and Morell, C.H. et al. (2007) Cardiovascular features of heart failure with preserved ejection fraction versus nonfailing hypertensive left ventricular hypertrophy in the urban Baltimore community: the role of atrial remodeling/dysfunction. *J Am Coll Cardiol*, 49 (2), pp. 198-207.

Merit-HF Study Group. (1999) Effect of metoprolol CR/XL in chronic heart failure: metoprolol CR/XL randomised intervention trial in-congestive heart failure (MERIT-HF). *Lancet*, 353 (9169), pp. 2001-2007.

Mielniczuk, L.M., Lamas, G.A., Flaker, G.C., Mitchell, G., Smith, S.C. and Gersh, B.J. et al. (2007) Left Ventricular End-Diastolic Pressure and Risk of Subsequent Heart Failure in Patients Following an Acute Myocardial Infarction. *Congest Heart Fail*, 13 (4), pp. 209-214.

Mishra, S., Sabbah, H.N., Jain, J.C. and Gupta, R.C. (2003) Reduced Ca 2+-calmodulin-dependent protein kinase activity and expression in LV myocardium of dogs with heart failure. *Am J Physiol Heart Circ Physiol*, 284 (3), pp. H876-H883.

Miura, T. and Miki, T. (2009) GSK-3β, a therapeutic target for cardiomyocyte protection. *Circ J*, 73 (7), pp. 1184-1192.

Miyamoto, M.I., Del Monte, F., Schmidt, U., DiSalvo, T.S., Kang, Z.B. and Matsui, T. et al. (2000) Adenoviral gene transfer of SERCA2a improves left-ventricular function in aortic-banded rats in transition to heart failure. *Proc Natl Acad Sci U S A*, 97 (2), pp. 793-798.

Mjøs, O.D., Ichihara, K., Fellenius, E., Myrmel, T. and Neely, J.R. (1991) Fatty acids suppress recovery of function after hypothermic perfusion. *Ann Thorac Surg*, 52 (4), pp. 965-970.

Moens, A.L., Leyton-Mange, J.S., Niu, X., Yang, R., Cingolani, O. and Arkenbout, E.K. et al. (2009) Adverse ventricular remodeling and exacerbated NOS uncoupling from pressure-overload in mice lacking the β3-adrenoreceptor. *J Mol Cell Cardiol*, 47 (5), pp. 576-585.

Mohamed, B.A., Asif, A.R., Schnelle, M., Qasim, M., Khadjeh, S. and Lbik, D. et al. (2016) Proteomic analysis of short-term preload-induced eccentric cardiac hypertrophy. *J Transl Med*, 14 (1), pp. 149-160.

Mohammed, S.F., Borlaug, B.A., Roger, V.L., Mirzoyev, S.A., Rodeheffer, R.J. and Chirinos, J.A. et al. (2012a) Comorbidity and ventricular and vascular structure and function in heart failure with preserved ejection fraction: a community based study. *Circ Heart Fail*, 5 (6), pp. 710-719.

Mohammed, S.F., Storlie, J.R., Oehler, E.A., Bowen, L.A., Korinek, J. and Lam, C.S. et al. (2012b) Variable phenotype in murine transverse aortic constriction. *Cardiovasc Pathol*, 21 (3), pp. 188-198.

Mondal, M.I.H. and Yeasmin, M.S. (2016) Toxicity study of food-grade carboxymethyl cellulose synthesized from maize husk in Swiss albino mice. *Int J Biol Macromol*, 92, pp. 965-971.

Morano, I., Isac, M., Bletz, C., Wojciechowski, R. and Rüegg, J.C. (1989) Perhexiline increases calcium-activated force in skinned psoas fibres by raising calcium affinity of troponin-C. *Biomed Biochim Acta*, 48 (5-6), pp. S329-34.

Morgan, M.Y., Reshef, R., Shah, R.R., Oates, N.S., Smith, R.L. and Sherlock, S. (1984) Impaired oxidation of debrisoquine in patients with perhexiline liver injury. *Gut*, 25 (10), pp. 1057-1064.

Morioka, S. and Simon, G. (1982) Echocardiographic evidence for early left ventricular hypertrophy in dogs with renal hypertension. *Am J Cardiol*, 49 (8), pp. 1890-1895.

Morisco, C., Nappi, A., Argenziano, L., Sarno, D., Fonatana, D. and Imbriaco, M. et al. (1994) Noninvasive evaluation of cardiac hemodynamics during exercise in patients with chronic heart failure: effects of short-term coenzyme Q10 treatment. *Mol Aspects Med*, 15, pp. s155-s163.

Mortensen, S.A., Rosenfeldt, F., Kumar, A., Dolliner, P., Filipiak, K.J. and Pella, D. et al. (2014) The effect of coenzyme Q 10 on morbidity and mortality in chronic heart failure: results from Q-SYMBIO: a randomized double-blind trial. *JACC Heart Fail*, 2 (6), pp. 641-649.

Moyes, A.J., Chu, S.M., Baliga, R.S. and Hobbs, A.J. (2015) Abstract 19478: Endothelial and Cardiomyocyte-derived C-type Natriuretic Peptide Coordinate Heart Structure and Function. *Circulation*, 132, p. A19478.

Mueller, H.S. and Ayres, S.M. (1978) Metabolic responses of the heart in acute myocardial infarction in man. *Am J Cardiol*, 42 (3), pp. 363-371.

Mundiña-Weilenmann, C., Said, M., Vittone, L., Ferrero, P. and Mattiazzi, A. (2003) Phospholamban phosphorylation in ischemia-reperfused heart. Effect of pacing during ischemia and response to a β-adrenergic challenge. *Mol Cell Biochem*, 252 (1), pp. 239-246.

Munkholm, H., Hansen, H.H.T. and Rasmussen, K. (1999) Coenzyme Q10 treatment in serious heart failure. *Biofactors*, 9 (2-4), pp. 285-289.

Münzel, T., Gori, T., Keaney Jr, J.F., Maack, C. and Daiber, A. (2015) Pathophysiological role of oxidative stress in systolic and diastolic heart failure and its therapeutic implications. *Eur Heart J*, 36 (38), pp. 2555-2564.

Murakami, K., Mizushige, K., Noma, T., Tsuji, T., Kimura, S. and Kohno, M. (2002) Perindopril effect on uncoupling protein and energy metabolism in failing rat hearts. *Hypertension*, 40 (3), pp. 251-255.

Murray, A.J., Anderson, R.E., Watson, G.C., Radda, G.K. and Clarke, K. (2004) Uncoupling proteins in human heart. *Lancet*, 364 (9447), pp. 1786-1788.

Murray, A.J., Cole, M.A., Lygate, C.A., Carr, C.A., Stuckey, D.J. and Little, S.E. et al. (2008) Increased mitochondrial uncoupling proteins, respiratory uncoupling and decreased efficiency in the chronically infarcted rat heart. *J Mol Cell Cardiol*, 44 (4), pp. 694-700.

Murray, G.L. and Colombo, J. (2014) Ranolazine preserves and improves left ventricular ejection fraction and autonomic measures when added to guideline-driven therapy in chronic heart failure. *Heart Int*, 9 (2), pp. 66-73.

Muthuramu, I., Lox, M., Jacobs, F. and De Geest, B. (2014) Permanent ligation of the left anterior descending coronary artery in mice: a model of post-myocardial infarction remodelling and heart failure. *J Vis Exp*, (94).

Myers, J.B. and Ronthal, M. (1978) Perhexiline maleate neurotoxicity and weight loss. *Med J Aust*, 2 (10), pp. 465-466.

Nakajima, H., Ishida, T., Satomi-Kobayashi, S., Mori, K., Hara, T. and Sasaki, N. et al. (2013) Endothelial lipase modulates pressure overload–induced heart failure through alternative pathway for fatty acid uptake. *Hypertension*, 61 (5), pp. 1002-1007.

Narula, N., Zaragoza, M.V., Sengupta, P.P., Li, P., Haider, N. and Verjans, J. et al. (2011) Adenine nucleotide translocase 1 deficiency results in dilated cardiomyopathy with defects in myocardial mechanics, histopathological alterations, and activation of apoptosis. *JACC Cardiovasc Imaging*, 4 (1), pp. 1-10.

Nathanson, D., Ullman, B., Löfström, U., Hedman, A., Frick, M. and Sjöholm, Å. et al. (2012) Effects of intravenous exenatide in type 2 diabetic patients with congestive heart failure: a double-blind, randomised controlled clinical trial of efficacy and safety. *Diabetologia*, 55 (4), pp. 926-935.

National Institue of Health (NHS) (2014) *Heart Failure*. Available at: http://www.nhs.uk/Conditions/Heart-failure/Pages/Introduction.aspx (Accessed: 24 March 2015)

National Institute for Health and Care Excellence (NICE) (2010) *Chronic heart failure in adults: management*. Available at: https://www.nice.org.uk/guidance/cg108/chapter/introduction (Accesssed: 15 November 2017).

Neely, J.R., Liebermeister, H., Battersby, E.J. and Morgan, H.E. (1967) Effect of pressure development on oxygen consumption by isolated rat heart. *Am J Physiol*, 212 (4), pp. 804-814.

Neglia, D., De Caterina, A., Marraccini, P., Natali, A., Ciardetti, M. and Vecoli, C. et al. (2007) Impaired myocardial metabolic reserve and substrate selection flexibility during stress in patients with idiopathic dilated cardiomyopathy. *Am J Physiol Heart Circ Physiol*, 293 (6), pp. H3270-H3278.

Neubauer, S. (2007) The failing heart—an engine out of fuel. *N Engl J Med*, 356 (11), pp. 1140-1151.

Neubauer, S., Horn, M., Cramer, M., Harre, K., Newell, J.B. and Peters, W. et al. (1997) Myocardial phosphocreatine-to-ATP ratio is a predictor of mortality in patients with dilated cardiomyopathy. *Circulation*, 96 (7), pp. 2190-2196.

Neubauer, S., Krahe, T., Schindler, R., Horn, M., Hillenbrand, H. and Entzeroth, C. et al. (1992) 31P magnetic resonance spectroscopy in dilated cardiomyopathy and coronary artery disease. Altered cardiac high-energy phosphate metabolism in heart failure. *Circulation*, 86 (6), pp. 1810-1818.

Neubauer, S., Remkes, H., Spindler, M., Horn, M., Wiesmann, F. and Prestle, J. et al. (1999) Downregulation of the Na+-creatine cotransporter in failing human myocardium and in experimental heart failure. *Circulation*, 100 (18), pp. 1847-1850.

Ngo, D.T., Drury, N.E., Pagano, D., Frenneaux, M.P. and Horowitz, J.D. (2011) Abstract 14461: How does perhexiline modulate myocardial energetics and ameliorate redox stress? *Circulation*, 124, p. A14461.

Nguyen, T.D., Shingu, Y., Amorim, P.A., Schwarzer, M. and Doenst, T. (2015) Triheptanoin alleviates ventricular hypertrophy and improves myocardial glucose oxidation in rats with pressure overload. *J Card Fail*, 21 (11), pp. 906-915.

Nicolas, G., Delobel, R., Feve, J.R. and Rozo, L. (1976) Peripheral neuropathy after perhexilene maleate administration. *Ann Med Interne (Paris)*, 127 (8-9), pp. 607-610.

Nicolas-Robin, A., Amour, J., Ibanez-Esteve, C., Coriat, P., Riou, B. and Langeron, O. (2008) Effect of glucose-insulin-potassium in severe acute heart failure after brain death. *Crit Care Med*, 36 (10), pp. 2740-2745.

Nikolaidis, L.A., Elahi, D., Hentosz, T., Doverspike, A., Huerbin, R. and Zourelias, L. et al. (2004) Recombinant glucagon-like peptide-1 increases myocardial glucose uptake and improves left ventricular performance in conscious dogs with pacing-induced dilated cardiomyopathy. *Circulation*, 110 (8), pp. 955-961.

Niu, P., Shindo, T., Iwata, H., Iimuro, S., Takeda, N. and Zhang, Y. et al. (2004) Protective effects of endogenous adrenomedullin on cardiac hypertrophy, fibrosis, and renal damage. *Circulation*, 109 (14), pp .1789-1794.

Nobuhara, M., Saotome, M., Watanabe, T., Urushida, T., Katoh, H. and Satoh, H. et al. (2013) Mitochondrial dysfunction caused by saturated fatty acid loading induces myocardial insulin-resistance in differentiated H9c2 myocytes: a novel ex vivo myocardial insulin-resistance model. *Exp Cell Res*, 319 (7), pp. 955-966.

Noma, T., Nishiyama, A., Mizushige, K., Murakami, K., Tsuji, T. and Kohno, M. et al. (2001) Possible role of uncoupling protein in regulation of myocardial energy metabolism in aortic regurgitation model rats. *FASEB J*, 157), pp.206-1208.

Noordali, H., Loudon, B.L., Frenneaux, M.P. and Madhani, M. (2018) Cardiac metabolism—A promising therapeutic target for heart failure. *Pharmacol Ther*, 182, pp. 95 - 114.

Norton, J.M. (2001) Toward consistent definitions for preload and afterload. *Adv Physiol Edu*, 25 (1), pp. 53-61.

O'Donnell, J.M., Fields, A.D., Sorokina, N. and Lewandowski, E.D. (2008) The absence of endogenous lipid oxidation in early stage heart failure exposes limits in lipid storage and turnover. *J Mol Cell Cardiol*, 44 (2), pp. 315-322.

Oleck, S. and Ventura, H.O. (2016) Coenzyme Q10 and utility in heart failure: just another supplement? *Curr Heart Fail Rep*, 13 (4), pp. 190-195.

Oliveira, A.F., Cunha, D.A., Ladriere, L., Igoillo-Esteve, M., Bugliani, M. and Marchetti, P. et al. (2015) In vitro use of free fatty acids bound to albumin: A comparison of protocols. *Biotechniques*, 58 (5), pp. 228-233.

Omar, M.A., Wang, L. and Clanachan, A.S. (2010) Cardioprotection by GSK-3 inhibition: role of enhanced glycogen synthesis and attenuation of calcium overload. *Cardiovasc Res*, 86 (3), pp. 478-486.

Ono, H., Ohara, N. and Hashimoto, K. (1982) Effect of an antianginal drug, perhexiline, on myocardial oxygen consumption in anesthetized open-chest dogs compared with verapamil and glyceryl trinitrate. *Jpn Circ J*, 46 (6), pp. 559-567.

Osorio, J.C., Stanley, W.C., Linke, A., Castellari, M., Diep, Q.N. and Panchal, A.R. et al. (2002) Impaired myocardial fatty acid oxidation and reduced protein expression of retinoid X receptor-α in pacing-induced heart failure. *Circulation*, 106 (5), pp. 606-612.

Otto, C.M. (2006) Valvular aortic stenosis: disease severity and timing of intervention. *J Am Coll Cardiol*, 47 (11), pp. 2141-2151.

Owan, T.E., Hodge, D.O., Herges, R.M., Jacobsen, S.J., Roger, V.L. and Redfield, M.M. (2006) Trends in prevalence and outcome of heart failure with preserved ejection fraction. *N Engl J Med*, 355 (3), pp. 251-259.

Packer, M., Coats, A.J., Fowler, M.B., Katus, H.A., Krum, H. and Mohacsi, P. et al. (2001) Effect of carvedilol on survival in severe chronic heart failure. *N Engl J Med*, 344 (22), pp. 1651-1658.

Pal, N., Sivaswamy, N., Mahmod, M., Yavari, A., Rudd, A. and Singh, S. et al. (2015) Effect of Selective Heart Rate Slowing in Heart Failure With Preserved Ejection Fraction. *Circulation*, 132 (18), pp. 1719-1725.

Paliard, P., Vitrey, D., Fournier, G., Belhadjali, J., Patricot, L. and Berger, F. (1978) Perhexiline maleate-induced hepatitis. *Digestion*, 17 (5), pp. 419-427.

Paolisso, G., Gambardella, A., Galzerano, D., D'Amore, A., Rubino, P. and Verza, M. et al. (1994) Total-body and myocardial substrate oxidation in congestive heart failure. *Metabolism*, 43 (2), pp. 174-179.

Pascual, F. and Coleman, R.A. (2016) Fuel availability and fate in cardiac metabolism: A tale of two substrates. *Biochim Biophys Acta*, 1861 (10), pp. 1425-1433.

Pasini, E., Ceconi, C., Curello, S., Cargnoni, A. and Ferrari, R. (1991) Toxicity of fatty acids during myocardial reperfusion: a new possible mechanism of action. *Cardiologia*, 36 (3), pp. 237-245.

Patel, K., Fonarow, G.C., Kitzman, D.W., Aban, I.B., Love, T.E. and Allman, R.M. et al. (2013) Aldosterone antagonists and outcomes in real-world older patients with heart failure and preserved ejection fraction. *JACC Heart Fail*, 1 (1), pp. 40-47.

Patel, T.B. and Olson, M.S. (1984) Regulation of pyruvate dehydrogenase complex in ischemic rat heart. *Am J Physiol Heart Circ Physiol*, 246 (6), pp. H858-H864.

Pathak, A., del Monte, F., Zhao, W., Schultz, J.E., Lorenz, J.N. and Bodi, I. et al. (2005) Enhancement of cardiac function and suppression of heart failure progression by inhibition of protein phosphatase 1. *Circ Res*, 96 (7), pp. 756-766.

Paul, M., Mehr, A.P. and Kreutz, R. (2006) Physiology of local renin-angiotensin systems. *Physiol Rev*, 86 (3), pp. 747-803.

Paulus, W.J. and Tschöpe, C. (2013) A novel paradigm for heart failure with preserved ejection fraction. *J Am Coll Cardiol*, 62 (4), pp. 263-271.

Pellieux, C., Aasum, E., Larsen, T.S., Montessuit, C., Papageorgiou, I. and Pedrazzini, T. et al. (2006) Overexpression of angiotensinogen in the myocardium induces downregulation of the fatty acid oxidation pathway. *J Mol Cell Cardiol*, 41 (3), pp. 459-466.

Pepine, C.J., Schang, S.J. and Bemiller, C.R. (1973) Proceedings: Alteration of left ventricular responses to ischemia with oral perhexiline. *Postgrad Med J*, 49 (S3), pp. 43-46.

Pepine, C.J., Schang, S.J. and Bemiller, C.R. (1974) Effects of perhexiline on coronary hemodynamic and myocardial metabolic responses to tachycardia. *Circulation*, 49 (5), pp. 887-893.

Pereira, R.O., Wende, A.R., Crum, A., Hunter, D., Olsen, C.D. and Rawlings, T. et al. (2014) Maintaining PGC-1α expression following pressure overload-induced cardiac hypertrophy preserves angiogenesis but not contractile or mitochondrial function. *FASEB J*, 28 (8), pp. 3691-3702.

Pereira, R.O., Wende, A.R., Olsen, C., Soto, J., Rawlings, T. and Zhu, Y. et al. (2013) Inducible overexpression of GLUT1 prevents mitochondrial dysfunction and attenuates structural remodeling in pressure overload but does not prevent left ventricular dysfunction. *J Am Heart Assoc*, 2 (5), p. e000301.

Pérez, J.E., Borda, L., Schuchleib, R. and Henry, P.D. (1982) Inotropic and chronotropic effects of vasodilators. *J Pharmacol Exp Ther*, 221 (3), pp. 609-613.

Pessayre, D., Bichara, M., Feldmann, G., Degott, C., Potet, F. and Benhamou, J.P. (1979) Perhexiline maleate-induced cirrhosis. *Gastroenterology*, 76 (1), pp. 170-177.

Pfeffer, M.A., Braunwald, E., Moyé, L.A., Basta, L., Brown Jr, E.J. and Cuddy, T.E. et al. (1992) Effect of captopril on mortality and morbidity in patients with left ventricular dysfunction after myocardial infarction: results of the Survival and Ventricular Enlargement Trial. *N Engl J Med*, 327 (10), pp. 669-677.

Phan, T.T., Abozguia, K., Shivu, G.N., Mahadevan, G., Ahmed, I. and Williams, L. et al. (2009a) Heart failure with preserved ejection fraction is characterized by dynamic impairment of active relaxation and contraction of the left ventricle on exercise and associated with myocardial energy deficiency. *J Am Coll Cardiol*, 54 (5), pp. 402-409.

Phan, T.T., Shivu, G.N., Abozguia, K., Davies, C., Nassimizadeh, M. and Jimenez, D. et al. (2010) Impaired heart rate recovery and chronotropic incompetence in patients with heart failure with preserved ejection fraction. *Circ Heart Fail*, 3 (1), pp. 29-34.

Phan, T.T., Shivu, G.N., Choudhury, A., Abozguia, K., Davies, C. and Naidoo, U. et al. (2009b) Multi-centre experience on the use of perhexiline in chronic heart failure and refractory angina: old drug, new hope. *Eur J Heart Fail*, 11 (9), pp. 881-886.

Philpott, A., Chandy, S., Morris, R. and Horowitz, J.D. (2004) Development of a regimen for rapid initiation of perhexiline therapy in acute coronary syndromes. *Int Med J*, 34 (6), pp. 361-363.

Phuong, H., Choi, B.Y., Chong, C.R., Raman, B. and Horowitz, J.D. (2016) Can perhexiline be utilized without long-term toxicity? A clinical practice audit. *Ther Drug Monit*, 38 (1), pp. 73-78.

Pieterse, A.S., Rowland, R. and Dunn, D. (1983) Perhexiline maleate induced cirrhosis. *Pathology*, 15 (2), pp. 201-203.

Pilcher, J. (1978) Comparative trial of perhexiline maleate and oxprenolol in patients with angina pectoris. *Postgrad Med J*, 54 (636), pp. 663-667.

Pilcher, J., Cooper, J.D.H., Turnell, D.C., Matenga, J., Paul, R. and Lockhart, J.D.F. (1985) Investigations of long-term treatment with perhexiline maleate using therapeutic monitoring and electromyography. *Ther Drug Monit*, 7 (1), pp. 54-60.

Pinnell, J., Turner, S. and Howell, S. (2007) Cardiac muscle physiology. *CEACCP*, 7 (3), pp. 85-88.

Pitt, B., Pfeffer, M.A., Assmann, S.F., Boineau, R., Anand, I.S. and Claggett, B. et al. (2014) Spironolactone for heart failure with preserved ejection fraction. *N Engl J Med*, 370 (15), pp. 1383-1392.

Pitt, B., Remme, W., Zannad, F., Neaton, J., Martinez, F. and Roniker, B. et al. (2003) Eplerenone, a selective aldosterone blocker, in patients with left ventricular dysfunction after myocardial infarction. *N Engl J Med*, 348 (14), pp. 1309-1321.

Pitt, B., Zannad, F., Remme, W.J., Cody, R., Castaigne, A. and Perez, A. et al. (1999) The effect of spironolactone on morbidity and mortality in patients with severe heart failure. *N Engl J Med*, 341 (10), pp. 709-717.

Planavila, A., Redondo-Angulo, I., Ribas, F., Garrabou, G., Casademont, J. and Giralt, M. et al. (2015) Fibroblast growth factor 21 protects the heart from oxidative stress. *Cardiovasc Res*, 106 (1), pp. 19-31.

Ponikowski, P., Voors, A.A., Anker, S.D., Bueno, H., Cleland, J.G. and Coats, A.J. et al. (2016) 2016 ESC Guidelines for the diagnosis and treatment of acute and chronic heart failure. *Eur J Heart Fail*, 18 (8), pp. 891-975.

Poupon, R., Rosensztajn, L., de Saint-Maur, P.P., Lageron, A., Gombeau, T. and Darnis, F. (1980) Perhexiline maleate-associated hepatic injury prevalence and characteristics. *Digestion*, 20 (3), pp. 145-150.

Pritchard, T.J., Kawase, Y., Haghighi, K., Anjak, A., Cai, W. and Jiang, M. et al. (2013) Active inhibitor-1 maintains protein hyper-phosphorylation in aging hearts and halts remodeling in failing hearts. *PLoS One*, 8 (12), p. e80717.

Pye, M.P., Black, M. and Cobbe, S.M. (1996) Comparison of in vivo and in vitro haemodynamic function in experimental heart failure: use of echocardiography. *Cardiovasc Res*, 31 (6), pp. 873-881.

Qi, J., Yu, J., Tan, Y., Chen, R., Xu, W. and Chen, Y. et al. (2017) Mechanisms of Chinese Medicine Xinmailong's protection against heart failure in pressure-overloaded mice and cultured cardiomyocytes. *Sci Rep*, 7, p. 42843.

Qin, F., Siwik, D.A., Pimentel, D.R., Morgan, R.J., Biolo, A. and Tu, V.H. et al. (2014) Cytosolic H 2 O 2 mediates hypertrophy, apoptosis, and decreased SERCA activity in mice with chronic hemodynamic overload. *Am J Physiol Heart Circ Physiol*, 306 (10), pp. H1453-H1463.

Ram, R., Mickelsen, D.M., Theodoropoulos, C. and Blaxall, B.C. (2011) New approaches in small animal echocardiography: imaging the sounds of silence. *Am J Physiol Heart Circ Physiol*, 301 (5), pp. H1765-H1780.

Rampe, D., Wang, Z., Fermini, B., Wible, B., Dage, R.C. and Nattel, S. (1995) Voltage-and time-dependent block by perhexiline of K+ currents in human atrium and in cells expressing a Kv1. 5-type cloned channel. *J Pharmaco Exp Ther*, 274 (1), pp. 444-449.

Randle, P.J., Garland, P.B., Hales, C.N. and Newsholme, E.A. (1963) The glucose fatty-acid cycle its role in insulin sensitivity and the metabolic disturbances of diabetes mellitus. *Lancet*, 281 (7285), pp. 785-789.

Rassier, D.E. (2017) Sarcomere mechanics in striated muscles: from molecules to sarcomeres to cells. *Am J Physiol Cell Physiol*. 313 (2), C134-C145.

Razeghi, P., Young, M.E., Alcorn, J.L., Moravec, C.S., Frazier, O.H. and Taegtmeyer, H. (2001) Metabolic gene expression in fetal and failing human heart. *Circulation*, 104 (24), pp. 2923-2931.

Razeghi, P., Young, M.E., Ying, J., Depre, C., Uray, I.P. and Kolesar, J. et al. (2002) Downregulation of metabolic gene expression in failing human heart before and after mechanical unloading. *Cardiology*, 97 (4), pp. 203-209.

Redfield, M.M., Anstrom, K.J., Levine, J.A., Koepp, G.A., Borlaug, B.A. and Chen, H.H. et al. (2015) Isosorbide mononitrate in heart failure with preserved ejection fraction. *N Engl J Med*, 373 (24), pp. 2314-2324.

Redfield, M.M., Jacobsen, S.J., Borlaug, B.A., Rodeheffer, R.J. and Kass, D.A. (2005) Age-and gender-related ventricular-vascular stiffening. *Circulation*, 112 (15), pp. 2254-2262.

Regitz, V., Bossaller, C., Strasser, R., Müller, M., Shug, A.L. and Fleck, E. (1990) Metabolic alterations in end-stage and less severe heart failure—myocardial carnitine decrease. *Clin Chem Lab Med*, 28 (9), pp. 611-618.

Reil, J.C., Hohl, M., Reil, G.H., Granzier, H.L., Kratz, M.T. and Kazakov, A. et al. (2013) Heart rate reduction by I f-inhibition improves vascular stiffness and left ventricular systolic and diastolic function in a mouse model of heart failure with preserved ejection fraction. *Eur Heart J*, 34 (36), pp. 2839-2849.

Relling, D.P., Esberg, L.B., Fang, C.X., Johnson, W.T., Murphy, E.J. and Carlson, E.C. et al. (2006) High-fat diet-induced juvenile obesity leads to cardiomyocyte dysfunction and upregulation of Foxo3a transcription factor independent of lipotoxicity and apoptosis. *J Hyperten*, 24 (3), pp. 549-561.

Remme, W.J. (2000) Overview of the relationship between ischemia and congestive heart failure. *Clin Cardiol*, 23 (7 S4), pp. IV4-8.

Remondino, A., Rosenblatt-Velin, N., Montessuit, C., Tardy, I., Papageorgiou, I. and Dorsaz, P.A. et al. (2000) Altered expression of proteins of metabolic regulation during remodeling of the left ventricle after myocardial infarction. *J Mol Cell Cardiol*, 32 (11), pp. 2025-2034.

Ren, X.R., Wang, J., Osada, T., Mook, R.A., Morse, M.A. and Barak, L.S. et al. (2015) Perhexiline promotes HER3 ablation through receptor internalization and inhibits tumor growth. *Breast Cancer Res*, 17 (1), p. 20.

Renn, C.L., Gallop, D., Cavaletti, G., Rhee, P., Dorsey, S.G. and Carozzi, V.A. (2011) Multimodal assessment of painful peripheral neuropathy induced by chronic oxaliplatin-based chemotherapy in mice. *Mol Pain*, 7 (1), p. 29.

Riehle, C., Wende, A.R., Zaha, V.G., Pires, K.M., Wayment, B. and Olsen, C. et al. (2011) PGC-1β deficiency accelerates the transition to heart failure in pressure overload hypertrophy. *Circ Res*, 109 (7), pp. 783-793.

Roberts, R.K., Cohn, D., Petroff, V. and Seneviratne, B. (1981) Liver disease induced by perhexiline maleate. *Med J Aust*, 2 (10), pp. 553-554.

Robson, R.A. and Wing, L.M. (1983) Perhexiline and liver cirrhosis. *N Z Med J*, 96 (733), p. 447.

Roche, J., Fournet, J., Meullenet, J., Faure, H. and Massot, C. (1979) Acute hepatic failure due to perhexiline maleate. *Nouv Presse Med*, 8 (7), pp. 521-522.

Rockman, H.A., Ross, R.S., Harris, A.N., Knowlton, K.U., Steinhelper, M.E. and Field, L.J. et al. (1991) Segregation of atrial-specific and inducible expression of an atrial natriuretic factor transgene in an in vivo murine model of cardiac hypertrophy. *Proc Natl Acad Sci U S A*, 88 (18), pp. 8277-8281.

Rosca, M.G. and Hoppel, C.L. (2013) Mitochondrial dysfunction in heart failure. *Heart Fail Rev*, 18 (5), pp. 607-622.

Rosca, M.G., Okere, I.A., Sharma, N., Stanley, W.C., Recchia, F.A. and Hoppel, C.L. (2009) Altered expression of the adenine nucleotide translocase isoforms and decreased ATP synthase activity in skeletal muscle mitochondria in heart failure. *J Mol Cell Cardiol*, 46 (6), pp. 927-935.

Rose, B.A., Force, T. and Wang, Y. (2010) Mitogen-activated protein kinase signaling in the heart: angels versus demons in a heart-breaking tale. *Physiol Rev*, 90 (4), pp. 1507-1546.

Rothermel, B.A., Berenji, K., Tannous, P., Kutschke, W., Dey, A. and Nolan, B. et al. (2005) Differential activation of stress-response signaling in load-induced cardiac hypertrophy and failure. *Physiol Genomics*, 23 (1), pp. 18-27.

Ruetten, H., Dimmeler, S., Gehring, D., Ihling, C. and Zeiher, A.M. (2005) Concentric left ventricular remodeling in endothelial nitric oxide synthase knockout mice by chronic pressure overload. *Cardiovasc Res*, 66 (3), pp. 444-453.

Ruiz-Meana, M. and García-Dorado, D. (2009) Pathophysiology of ischemia-reperfusion injury: new therapeutic options for acute myocardial infarction. *Rev Esp Cardiol*, 62 (2), pp. 199-209.

Ruiz-Meana, M., García-Dorado, D., González, M.A., Barrabés, J.A. and Soler-Soler, J. (1995) Effect of osmotic stress on sarcolemmal integrity of isolated cardiomyocytes following transient metabolic inhibition. *Cardiovasc Res*, 30 (1), pp. 64-69.

Ruiz-Meana, M., Garcia-Dorado, D., Juliá, M., González, M.A., Inserte, J. and Soler-Soler, J. (1996) Pre-treatment with trimetazidine increases sarcolemmal mechanical resistance in reoxygenated myocytes. *Cardiovasc Res*, 32 (3), pp. 587-592.

Ruiz-Ramírez, A., López-Acosta, O1., Barrios-Maya, M.A. and El-Hafidi, M. (2016) Cell Death and Heart Failure in Obesity: Role of Uncoupling Proteins. *Oxid Med Cell Longev*, 2016, p. 9340654.

Sabbah, H.N., Gupta, R.C., Kohli, S., Wang, M., Hachem, S. and Zhang, K. (2016) Chronic therapy with elamipretide (MTP-131), a novel mitochondria-targeting peptide, improves left ventricular and mitochondrial function in dogs with advanced heart failure. *Circ Heart Fail*, 9 (2), p. e002206.

Sack, M.N., Rader, T.A., Park, S., Bastin, J., McCune, S.A. and Kelly, D.P. (1996) Fatty acid oxidation enzyme gene expression is downregulated in the failing heart. *Circulation*, 94 (11), pp. 2837-2842.

Safari, F., Anvari, Z., Moshtaghioun, S., Javan, M., Bayat, G. and Forosh, S.S. et al. (2014) Differential expression of cardiac uncoupling proteins 2 and 3 in response to myocardial ischemia-reperfusion in rats. *Life Sci*, 98 (2), pp. 68-74.

Said, G. (1978) Perhexiline neuropathy: a clinicopathological study. *Ann Neurol*, 3 (3), pp. 259-266.

Said, M., Vittone, L., Mundina-Weilenmann, C., Ferrero, P., Kranias, E.G. and Mattiazzi, A. (2003) Role of dual-site phospholamban phosphorylation in the stunned heart: insights from phospholamban site-specific mutants. *Am J Physiol Heart Circ Physiol*, 285 (3), pp. H1198-H1205.

Sallustio, B.C., Westley, I.S. and Morris, R.G. (2002) Pharmacokinetics of the antianginal agent perhexiline: relationship between metabolic ratio and steady-state dose. *Br J Clin Pharmacol*, 54 (2), pp. 107-114.

Sande, J.B., Sjaastad, I., Hoen, I.B., Bøkenes, J., Tønnessen, T. and Holt, E. et al. (2002) Reduced level of serine16 phosphorylated phospholamban in the failing rat myocardium: a major contributor to reduced SERCA2 activity. *Cardiovasc Res*, 53 (2), pp. 382-391.

Sankaralingam, S. and Lopaschuk, G.D. (2015) Cardiac energy metabolic alterations in pressure overload–induced left and right heart failure (2013 Grover Conference Series). *Pulm Circ*, 5 (1), pp. 15-28.

Santos, A.B., Kraigher-Krainer, E., Bello, N., Claggett, B., Zile, M.R. and Pieske, B. et al. (2014) Left ventricular dyssynchrony in patients with heart failure and preserved ejection fraction. *Eur Heart J*, 35 (1), pp. 42-47.

Sato, Y., Fujiwara, H. and Takatsu, Y. (2012) Biochemical markers in heart failure. *J Cardiol*, 59 (1), pp. 1-7.

Satz, N., Täuber, M., Streuli, R., Spycher, M.A. and Maurer, R. (1991) Perhexiline maleate-induced hepatitis. *Hepatogastroenterology*, 38 (4), pp. 314-316.

Sbroggiò, M., Carnevale, D., Bertero, A., Cifelli, G., De Blasio, E. and Mascio, G. et al. (2011) IQGAP1 regulates ERK1/2 and AKT signalling in the heart and sustains functional remodelling upon pressure overload. *Cardiovasc Res*, 91 (3), pp. 456-464.

Schaff, H.V., Gott, V.L., Goldman, R.A., Frederiksen, J.W. and Flaherty, J.T. (1981) Mechanism of elevated left ventricular end-diastolic pressure after ischemic arrest and reperfusion. *Am J Physiol*, 240 (2), pp. H300-H307.

Scheubel, R.J., Tostlebe, M., Simm, A., Rohrbach, S., Prondzinsky, R. and Gellerich, F.N. et al. (2002) Dysfunction of mitochondrial respiratory chain complex I in human failing myocardium is not due to disturbed mitochondrial gene expression. *J Am Coll Cardiol*, 40 (12), pp. 2174-2181.

Schmidt, U., Hajjar, R.J., Kim, C.S., Lebeche, D., Doye, A.A. and Gwathmey, J.K. (1999) Human heart failure: cAMP stimulation of SR Ca 2+-ATPase activity and phosphorylation level of phospholamban. *Am J Physiol Heart Circ Physiol*, 277 (2), pp. H474-H480.

Schmidt-Schweda, S. and Holubarsch, C. (2000) First clinical trial with etomoxir in patients with chronic congestive heart failure. *Clin Sci (Lond)*, 99 (1), pp. 27-35.

Schnell, S.A., Ambesi-Impiombato, A., Sanchez-Martin, M., Belver, L., Xu, L. and Qin, Y. et al. (2015) Therapeutic targeting of HES1 transcriptional programs in T-ALL. *Blood*, 125 (18), pp. 2806-2814.

Schönfeld, P. and Wojtczak, L. (2007) Fatty acids decrease mitochondrial generation of reactive oxygen species at the reverse electron transport but increase it at the forward transport. *Biochim Biophys Acta*, 1767 (8), pp. 1032-1040.

Schou, S.C. (2010) Influence of [2H]-labelled acetic acid as solvent in the synthesis of [2H]-labelled perhexiline. *J Labelled Comp Radiopharm*, 53 (1), pp. 31-35.

Schrauwen, P., Saris, W.H. and Hesselink, M.K. (2001) An alternative function for human uncoupling protein 3: protection of mitochondria against accumulation of nonesterified fatty acids inside the mitochondrial matrix. *FASEB J*, 15 (13), pp. 2497-2502.

Schwarz, K., Siddiqi, N., Singh, S., Neil, C.J., Dawson, D.K. and Frenneaux, M.P. (2014) The breathing heart—mitochondrial respiratory chain dysfunction in cardiac disease. *Int J Cardiol*, 171 (2), pp. 134-143.

Schwarzer, M., Faerber, G., Rueckauer, T., Blum, D., Pytel, G. and Mohr, F.W. et al. (2009) The metabolic modulators, Etomoxir and NVP-LAB121, fail to reverse pressure overload induced heart failure in vivo. *Basic Res Cardiol*, 104 (5), p. 547-557.

Schwinger, R.H., Böhm, M., Schmidt, U., Karczewski, P., Bavendiek, U. and Flesch, M. et al. (1995) Unchanged protein levels of SERCA II and phospholamban but reduced Ca2+ uptake and Ca2+-ATPase activity of cardiac sarcoplasmic reticulum from dilated cardiomyopathy patients compared with patients with nonfailing hearts. *Circulation*, 92 (11), pp. 3220-3228.

Selim, A., Zolty, R. and Chatzizisis, Y.S. (2017) The Evolution of Heart failure with Reduced Ejection Fraction Pharmacotherapy: What do we Have and Where are we Going? *Pharmacol Ther*, 178, pp. 67-82.

Senanayake, E.L., Howell, N.J., Ranasinghe, A.M., Drury, N.E., Freemantle, N. and Frenneaux, M. et al. (2015) Multicentre double-blind randomized controlled trial of perhexiline as a metabolic modulator to augment myocardial protection in patients with left ventricular hypertrophy undergoing cardiac surgery. *Eur J Cardiothorac Surg*, 48 (3), pp. 354-362.

Senni, M., Greene, S.J., Butler, J., Fonarow, G.C. and Gheorghiade, M. (2017) Drug Development for Heart Failure With Preserved Ejection Fraction: What Pieces Are Missing From the Puzzle? *Can J Cardiol*, 33 (6), pp. 768-776.

Sequeira, V. and van der Velden, J. (2015) Historical perspective on heart function: the Frank–Starling Law. *Biophys Rev*, 7 (4), pp. 421-447.

Seymour, A.M.L. and Chatham, J.C. (1997) The effects of hypertrophy and diabetes on cardiac pyruvate dehydrogenase activity. *J Mol Cell Cardiol*, 29 (10), pp. 2771-2778.

Seymour, A.M.L., Giles, L., Ball, V., Miller, J.J., Clarke, K. and Carr, C.A. et al. (2015) In vivo assessment of cardiac metabolism and function in the abdominal aortic banding model of compensated cardiac hypertrophy. *Cardiovasc Res*, 106 (2), pp. 249-260.

Shah, R.R. (2006) Can pharmacogenetics help rescue drugs withdrawn from the market? *Pharmacogenomics*, 7 (6), pp. 889-908.

Shah, R.R., Oates, N.S., Idle, J.R., Smith, R.L. and Lockhart, J.D.F. (1982) Impaired oxidation of debrisoquine in patients with perhexiline neuropathy. *Br Med J (Clin Res Ed)*, 284 (6312), pp. 295-299.

Shah, R.R., Oates, N.S., Idle, J.R., Smith, R.L. and Lockhart, J.D.F. (1983) Prediction of subclinical perhexiline neuropathy in a patient with inborn error of debrisoquine hydroxylation. *Am Heart J*, 105 (1), pp. 159-161.

Sharma, A., Fonarow, G.C., Butler, J., Ezekowitz, J.A. and Felker, G.M. (2016) Coenzyme Q10 and Heart Failure: A State-of-the-Art Review. *Circ Heart Fail*, 9 (4), p. e002639.

Sharma, K. and Kass, D.A. (2014) Heart failure with preserved ejection fraction: mechanisms, clinical features, and therapies. *Circ Res*, 115 (1), pp. 79-96.

Shibayama, J., Yuzyuk, T.N., Cox, J., Makaju, A., Miller, M. and Lichter, J. et al. (2015) Metabolic remodeling in moderate synchronous versus dyssynchronous pacing-induced heart failure: integrated metabolomics and proteomics study. *PLoS One*, 10 (3), p. e0118974.

Shimizu, T., Narang, N., Phetcharat Chen, B.Y., Knapp, M. and Janardanan, J. et al. (2017) Fibroblast deletion of ROCK2 attenuates cardiac hypertrophy, fibrosis, and diastolic dysfunction. *JCI Insight*, 2 (13), p. 93187.

Shiojima, I. and Walsh, K. (2006) Regulation of cardiac growth and coronary angiogenesis by the Akt/PKB signaling pathway. *Genes Dev*, 20 (24), pp. 3347-3365.

Siddiqi, N., Singh, S., Beadle, R., Dawson, D. and Frenneaux, M. (2013) Cardiac metabolism in hypertrophy and heart failure: implications for therapy. *Heart Fail Rev*, 18 (5), pp. 595-606.

Singh, S., Beadle, R., Cameron, D., Rudd, A., Bruce, M. and Jagpal, B. et al. (2014) Randomized double-blind placebo-controlled trial of perhexiline in heart failure with preserved ejection fraction syndrome. *Future Cardiol*, 10 (6), pp. 693-698.

Singlas, E., Goujet, M.A. and Simon, P. (1978a) Perhexilline maleate: relationship between side-effects, plasma concentrations and rate of metabolism (author's transl). *Nouv Presse Med*, 7 (19), pp. 1631-1632.

Singlas, E., Goujet, M.A. and Simon, P. (1978b) Pharmacokinetics of perhexiline maleate in anginal patients with and without peripheral neuropathy. *Eur J Clin Pharmacol*, 14 (3), pp. 195-201.

Sjölin, H., Tomasello, E., Mousavi-Jazi, M., Bartolazzi, A., Kärre, K. and Vivier, E. et al. (2002) Pivotal role of KARAP/DAP12 adaptor molecule in the natural killer cell–mediated resistance to murine cytomegalovirus infection. *J Exp Med*, 195 (7), pp. 825-834.

Smith, C.S., Bottomley, P.A., Schulman, S.P., Gerstenblith, G. and Weiss, R.G. (2006) Altered creatine kinase adenosine triphosphate kinetics in failing hypertrophied human myocardium. *Circulation*, 114 (11), pp. 1151-1158.

Sokos, G.G., Nikolaidis, L.A., Mankad, S., Elahi, D. and Shannon, R.P. (2006) Glucagon-like peptide-1 infusion improves left ventricular ejection fraction and functional status in patients with chronic heart failure. *J Card Fail*, 12 (9), pp. 694-699.

Soldatow, V.Y., LeCluyse, E.L., Griffith, L.G. and Rusyn, I. (2013) In vitro models for liver toxicity testing. *Toxicol Res*, 2 (1), pp. 23-39.

Solomon, S.D., Anavekar, N., Skali, H., McMurray, J.J., Swedberg, K. and Yusuf, S. et al. (2005) Influence of ejection fraction on cardiovascular outcomes in a broad spectrum of heart failure patients. *Circulation*, 112 (24), pp. 3738-3744.

Solomon, S.D., Zile, M., Pieske, B., Voors, A., Shah, A. and Kraigher-Krainer, E. et al. (2012) The angiotensin receptor neprilysin inhibitor LCZ696 in heart failure with preserved ejection fraction: a phase 2 double-blind randomised controlled trial. *Lancet*, 380 (9851), pp. 1387-1395.

SOLVD Investigators, Yusuf, S., Pitt, B., Davis, C.E., Hood, W.B. and Cohn, J.N. (1991) Effect of enalapril on survival in patients with reduced left ventricular ejection fractions and congestive heart failure. *New Engl J Med*, 325 (5), pp. 293-302.

Sopontammarak, S., Aliharoob, A., Ocampo, C., Arcilla, R.A., Gupta, M.P. and Gupta, M. (2005) Mitogen-activated protein kinases (p38 and c-Jun NH 2-terminal kinase) are differentially regulated during cardiac volume and pressure overload hypertrophy. *Cell Biochem Biophys*, 43 (1), pp. 61-76.

Sørensen, L.B., Sørensen, R.N., Miners, J.O., Somogyi, A.A., Grgurinovich, N. and Birkett, D.J. (2003) Polymorphic hydroxylation of perhexiline in vitro. *Br J Clin Pharmacol*, 55 (6), pp. 635-638.

Sorokina, N., O'Donnell, J.M., McKinney, R.D., Pound, K.M., Woldegiorgis, G. and LaNoue, K.F. et al. (2007) Recruitment of compensatory pathways to sustain oxidative flux with reduced carnitine palmitoyltransferase I activity characterizes inefficiency in energy metabolism in hypertrophied hearts. *Circulation*, 115 (15), pp. 2033-2041.

Soufer, R., Wohlgelernter, D., Vita, N.A., Amuchestegui, M., Sostman, H.D. and Berger, H.J. et al. (1985) Intact systolic left ventricular function in clinical congestive heart failure. *Am J Cardiol*, 55 (8), pp. 1032-1036.

Sparagna, G.C., Hickson-Bick, D.L., Buja, L.M. and McMillin, J.B. (2000) A metabolic role for mitochondria in palmitate-induced cardiac myocyte apoptosis. *Am J Physiol Heart Circ Physiol*, 279 (5), pp. H2124-H2132.

Spillmann, F., Trimpert, C., Peng, J., Eckerle, L.G., Staudt, A. and Warstat, K. et al. (2015) High-density lipoproteins reduce palmitate-induced cardiomyocyte apoptosis in an AMPK-dependent manner. *Biochem Biophys Res Commun*, 466 (2), pp. 272-277.

Stanley, W.C., Recchia, F.A. and Lopaschuk, G.D. (2005) Myocardial substrate metabolism in the normal and failing heart. *Physiol Rev*, 85 (3), pp. 1093-1129.

Stapel, B., Kohlhaas, M., Ricke-Hoch, M., Haghikia, A., Erschow, S. and Knuuti, J. et al. (2017) Low STAT3 expression sensitizes to toxic effects of β-adrenergic receptor stimulation in peripartum cardiomyopathy. *Eur Heart J*, 38 (5), pp. 349-361.

Steggall, A., Mordi, I.R. and Lang, C.C. (2017) Targeting Metabolic Modulation and Mitochondrial Dysfunction in the Treatment of Heart Failure. *Diseases*, 5 (2), p. 14.

Steigen, T.K., Aasum, E., Myrmel, T. and Larsen, T.S. (1994) Effects of fatty acids on myocardial calcium control during hypothermic perfusion. *J Thorac Cardiovasc Surg*, 107 (1), pp. 233-241.

Steinberg, B.A., Zhao, X., Heidenreich, P.A., Peterson, E.D., Bhatt, D.L. and Cannon, C.P. et al. (2012) Trends in Patients Hospitalized with Heart Failure and Preserved Left Ventricular Ejection Fraction-Prevalence, Therapies, and Outcomes. *Circulation*, 126 (1), pp. 65-75.

Stenger, R.J. and Spiro, D. (1961) Structure of the cardiac muscle cell. *Am J Med*, 30 (5), pp. 653-665.

Su, Y.R., Chiusa, M., Brittain, E., Hemnes, A.R., Absi, T.S. and Lim, C.C. et al. (2015) Right ventricular protein expression profile in end-stage heart failure. *Pulm Circ*, 5 (3), pp. 481-497.

Sumimoto, T., Jikuhara, T., Hattori, T., Yuasa, F., Kaida, M. and Hikosaka, M. et al. (1997) Importance of left ventricular diastolic function on maintenance of exercise capacity in patients with systolic dysfunction after anterior myocardial infarction. *Am Heart J*, 133 (1), pp. 87-93.

Sutherland, F.J., Shattock, M.J., Baker, K.E. and Hearse, D.J. (2003) Mouse isolated perfused heart: Characteristics and cautions. *Clin Exp Pharmacol Physiol*, 30 (11), pp. 867-878.

Sutton, M.S.J. (2010) A Comprehensive Noninvasive Hemodynamic Assessment of Systolic Heart Failure. *Circ Heart Fail*, 3 (3), pp. 337-339.

Swedberg, K., Komajda, M., Böhm, M., Borer, J., Robertson, M. and Tavazzi, L. et al. (2012) Effects on outcomes of heart rate reduction by ivabradine in patients with congestive heart failure: is there an influence of beta-blocker dose?: findings from the SHIFT (Systolic Heart failure treatment with the If inhibitor ivabradine Trial) study. *J Am Coll Cardiol*, 59 (22), pp. 1938-1945.

Szeto, H.H. (2014) First-in-class cardiolipin-protective compound as a therapeutic agent to restore mitochondrial bioenergetics. *Br J Pharamcol*, 171 (8), pp. 2029-2050.

Tan, Y.T., Wenzelburger, F., Lee, E., Heatlie, G., Leyva, F. and Patel, K. et al. (2009) The pathophysiology of heart failure with normal ejection fraction: exercise echocardiography reveals complex abnormalities of both systolic and diastolic ventricular function involving torsion, untwist, and longitudinal motion. *J Am Coll Cardiol*, 54 (1), pp. 36-46.

Tanno, M.1., Bassi, R., Gorog, D.A., Saurin, A.T, Jiang J. and Heads RJ. et al. (2003) Diverse mechanisms of myocardial p38 mitogen-activated protein kinase activation: evidence for MKK-independent activation by a TAB1-associated mechanism contributing to injury during myocardial ischemia. *Circ Res*, 93 (3), pp. 254-261.

Tassoni, E., Giannessi, F., Dell, U.N., Gallo, G., Conti, R. and Tinti, M.O. (2007) *Inhibitors of CPT in the Central Nervous System as Antidiabetic and/or Anti-Obesity Drugs*. Patent number: WO2007096251 A1.

Taylor, A.L., Ziesche, S., Yancy, C., Carson, P., D'Agostino Jr, R. and Ferdinand, K. et al. (2004) Combination of isosorbide dinitrate and hydralazine in blacks with heart failure. *N Engl J Med*, 351 (20), pp. 2049-2057.

Tenenbaum, A. and Fisman, E.Z. (2004) Impaired Glucose Metabolism in Patients with Heart Failure. *Am J Cardiovasc Drugs*, 4 (5), pp. 269-280.

The Japan Society of Ultrasonics in Medicine, 2006. Standard measurement of cardiac function indexes. *J Med Ultrason*, 33 92), pp. 123-127.

Toischer, K., Teucher, N., Unsöld, B., Kuhn, M., Kögler, H. and Hasenfuss, G. (2010) BNP controls early load-dependent regulation of SERCA through calcineurin. *Basic Res Cardiol*, 105 (6), pp. 795-804.

Tomita, H., Hoshino, K., Fuchimoto, Y., Ebinuma, H., Ohkuma, K. and Tanami, Y. et al. (2013) Acoustic radiation force impulse imaging for assessing graft fibrosis after pediatric living donor liver transplantation: a pilot study. *Liver Transpl*, 19 (11), pp. 1202-1213.

Tomlinson, I.W. and Rosenthal, F.D. (1977) Proximal myopathy after perhexiline maleate treatment. *Br Med J*, 1 (6072), pp.1319-1320.

Torp-Pedersen, C., Metra, M., Spark, P., Lukas, M.A., Moullet, C. and Scherhag, A. et al. (2007) The safety of amiodarone in patients with heart failure. *J Card Fail*, 13 (5), pp. 340-345.

Triposkiadis, F., Karayannis, G., Giamouzis, G., Skoularigis, J., Louridas, G. and Butler, J. (2009) The sympathetic nervous system in heart failure: physiology, pathophysiology, and clinical implications. *J Am Coll Cardiol*, 54 (19), pp. 1747-1762.

Tseng, C.C., Noordali, H., Sani, M., Madhani, M., Grant, D.M. and Frenneaux, M.P. et al. (2017) Development of Fluorinated Analogues of Perhexiline with Improved Pharmacokinetic Properties and Retained Efficacy. *J Med Chem*, 60 (7), pp. 2780-2789.

Tsutsui, H., Kinugawa, S. and Matsushima, S. (2011) Oxidative stress and heart failure. *Am J Physiol Heart Circ Physiol*, 301 (6), pp. H2181-H2190.

Tuomainen, T. and Tavi, P. (2017) The role of cardiac energy metabolism in cardiac hypertrophy and failure. *Exp Cell Res*, 360 (1), pp. 12-18.

Turcani, M. and Rupp, H. (1997) Etomoxir improves left ventricular performance of pressure-overloaded rat heart. *Circulation*, 96 (10), pp. 3681-3686.

Turcani, M. and Rupp, H. (1999) Modification of left ventricular hypertrophy by chronic etomoxir treatment. *Br J Pharmacol*, 126 (2), pp. 501-507.

Turner, P.V., Brabb, T., Pekow, C. and Vasbinder, M.A. (2011) Administration of substances to laboratory animals: routes of administration and factors to consider. *J Am Assoc Lab Anim Sci*, 50 (5), pp. 600-613.

Tuunanen, H., Engblom, E., Naum, A., Någren, K., Hesse, B. and Airaksinen, K.J. et al. (2006) Free fatty acid depletion acutely decreases cardiac work and efficiency in cardiomyopathic heart failure. *Circulation*, 114 (20), pp. 2130-2137.

Tuunanen, H., Engblom, E., Naum, A., Någren, K., Scheinin, M. and Hesse, B. et al. (2008) Trimetazidine, a metabolic modulator, has cardiac and extracardiac benefits in idiopathic dilated cardiomyopathy. *Circulation*, 118 (12), pp. 1250-1258.

Unger, S.A., Kennedy, J.A., McFadden-Lewis, K., Minerds, K., Murphy, G.A. and Horowitz, J.D. (2005) Dissociation between metabolic and efficiency effects of perhexiline in normoxic rat myocardium. *J Cardiovasc Pharmacol*, 46 (6), pp. 849-855.

Unger, S.A., Robinson, M.A. and Horowitz, J.D. (1997) Perhexiline improves symptomatic status in elderly patients with severe aortic stenosis. *Int Med J*, 27 (1), pp. 24-28.

Upadhya, B. and Kitzman, D.W. (2017) Management of Heart Failure with Preserved Ejection Fraction: Current Challenges and Future Directions. *Am J Cardiovasc Drugs*, 17(4), pp. 283-298.

Ussher, J.R., Wang, W., Gandhi, M., Keung, W., Samokhvalov, V. and Oka, T. et al. (2012) Stimulation of glucose oxidation protects against acute myocardial infarction and reperfusion injury. *Cardiovasc Res*, 94 (2), pp. 359-369.

Valmalle, R., Bacq, Y., Furet, Y., Dorval, E., Barbieux, J.P. and Metman, E.H. (1989) Fatal acute hepatitis during treatment with perhexiline maleate and bezafibrate. *Gastroenterol Clin Biol*, 13 (5), pp. 530-531.

Vamos, M., Erath, J.W. and Hohnloser, S.H. (2015) Digoxin-associated mortality: a systematic review and meta-analysis of the literature. *Eur Heart J*, 36 (28), pp. 1831-1838.

van Bilsen, M., Smeets, P.J., Gilde, A.J. and van der Vusse, G.J. (2004) Metabolic remodelling of the failing heart: the cardiac burn-out syndrome?. *Cardiovasc Res*, 61 (2), pp. 218-226.

van der Vusse, G.J., van Bilsen, M. and Glatz, J.F. (2000) Cardiac fatty acid uptake and transport in health and disease. *Cardiovasc Res*, 45 (2), pp. 279-293.

van Heerebeek, L., Hamdani, N., Falcão-Pires, I., Leite-Moreira, A.F., Begieneman, M.P. and Bronzwaer, J.G. et al. (2012) Low myocardial protein kinase G activity in heart failure with preserved ejection fraction. *Circulation*, 126 (7), pp. 830-839.

van Riet, E.E., Hoes, A.W., Wagenaar, K.P., Limburg, A., Landman, M.A. and Rutten, F.H. (2016) Epidemiology of heart failure: the prevalence of heart failure and ventricular dysfunction in older adults over time. A systematic review. *Eur J Heart Fail*, 18 (3), pp. 242-252.

van Veldhuisen, D.J. and de Boer, R.A. (2016) Ischaemia in heart failure with preserved ejection fraction; is it important? *Eur J Heart Fail*, 18 (5), pp. 577-578.

van Veldhuisen, D.J., van den Heuvel, A.F., Blanksma, P.K. and Crijns, H.J. (1998) Ischemia and left ventricular dysfunction: a reciprocal relation?. *J Cardiovasc Pharmacol*, 32 (S1), pp. S46-S51.

Varnavas, V.C., Kontaras, K., Glava, C., Maniotis, C.D., Koutouzis, M. and Baltogiannis, G.C. et al. (2011) Chronic skeletal muscle ischaemia preserves coronary flow in the ischemic rat heart. *Am J Physiol Heart Circ Physiol*, 301 (4), pp. 1229-1235.

Vary, T.C. and Randle, P.J. (1984) The effect of ischaemia on the activity of pyruvate dehydrogenase complex in rat heart. *J Mol Cell Cardiol*, 16 (8), pp. 723-733.

Vedin, O., Lam, C.S., Koh, A.S., Benson, L., Teng, T.H.K. and Tay, W.T. et al. (2017) Significance of Ischemic Heart Disease in Patients With Heart Failure and Preserved, Midrange, and Reduced Ejection Fraction. *Circ Heart Fail*, 10 (6), p. e003875.

Veitch, K., Maisin, L. and Hue, L. (1995) Trimetazidine effects on the damage to mitochondrial functions caused by ischemia and reperfusion. *Am J Cardiol*, 76 (6), pp. 25B-30B.

Vella, S., Penna, I., Longo, L., Pioggia, G., Garbati, P. and Florio, T. et al. (2015) Perhexiline maleate enhances antitumor efficacy of cisplatin in neuroblastoma by inducing over-expression of NDM29 ncRNA. *Sci Rep*, 5, p. 18144

Ventura-Clapier, R., Garnier, A., Veksler, V. and Joubert, F. (2011) Bioenergetics of the failing heart. *Biochim Biophys Acta*, 1813 (7), pp. 1360-1372.

Vettor, R., Fabris, R., Serra, R., Lombardi, A.M., Tonello, C. and Granzotto, M. et al. (2002) Changes in FAT/CD36, UCP2, UCP3 and GLUT4 gene expression during lipid infusion in rat skeletal and heart muscle. *Int J Obes Relat Metab Disord*. 26 (6), pp. 838-847.

Vinereanu, D., Nicolaides, E., Tweddel, A.C. and Fraser, A.G. (2005) "Pure" diastolic dysfunction is associated with long-axis systolic dysfunction. Implications for the diagnosis and classification of heart failure. *Eur J Heart Fail*, 7 (5), pp. 820-828.

Walker, B.D., Valenzuela, S.M., Singleton, C.B., Tie, H., Bursill, J.A. and Wyse, K.R. et al. (1999) Inhibition of HERG channels stably expressed in a mammalian cell line by the antianginal agent perhexiline maleate. *Br J Pharmacol*, 127 (1), pp. 243-251.

Wang, B.F. and Yoshioka, J. (2017) The Emerging Role of Thioredoxin-Interacting Protein in Myocardial Ischemia/Reperfusion Injury. *J Cardiovasc Pharmacol Ther*, 22 (3), pp. 219-229.

Wang, C.M., Almsherqi, Z.A., McLachlan, C.S., Matthews, S., Ramachandran, M. and Tay, S.K. et al. (2011) Acute starvation in C57BL/6J mice increases myocardial UCP2 and UCP3 protein expression levels and decreases mitochondrial bio-energetic function. *Stress*, 14 (1), pp. 66-72.

Wang, P.X., Li, Z.M., Cai, S.D., Li, J.Y., He, P. and Huang, Y. et al. (2017) C33 (S), a novel PDE9A inhibitor, protects against rat cardiac hypertrophy through upregulating cGMP signaling. *Acta Pharmacol Sin*, 38 (9), pp. 1257-1268.

Wang, X., Chen, W., Zhang, J., Khan, A., Li, L. and Huang, F. et al. (2017) Critical Role of ADAMTS2 (A Disintegrin and Metalloproteinase With Thrombospondin Motifs 2) in Cardiac Hypertrophy Induced by Pressure Overload. *Hypertension*, 69 (6), pp. 1060-1069.

Wang, Y., Ebermann, L., Sterner-Kock, A., Wika, S., Schultheiss, H.P. and Dörner, A. et al. (2009) Myocardial overexpression of adenine nucleotide translocase 1 ameliorates diabetic cardiomyopathy in mice. *Exp Physiol*, 94 (2), pp. 220-227.

Wei, C.D., Li, Y., Zheng, H.Y., Tong, Y.Q. and Dai, W. (2013) Palmitate induces H9c2 cell apoptosis by increasing reactive oxygen species generation and activation of the ERK1/2 signaling pathway. *Mol Med Rep*, 7 (3), pp. 855-861.

Wei, H., Bedja, D., Koitabashi, N., Xing, D., Chen, J. and Fox-Talbot, K. et al. (2012) Endothelial expression of hypoxia-inducible factor 1 protects the murine heart and aorta from pressure overload by suppression of TGF-β signaling. *Proc Natl Acad Sci U S A*, 109 (14), pp. E841-E850.

Wei, W.Y., Ma, Z.G., Xu, S.C., Zhang, N. and Tang, Q.Z. (2016) Pioglitazone protected against cardiac hypertrophy via inhibiting AKT/GSK3β and MAPK signaling pathways. *PPAR Res*, 2016, p. 9174190.

Weng, Y.C., Chuang, C.F., Chuang, S.T., Chiu, H.L., Kuo, Y.H. and Su, M.J. (2012) KS370G, a synthetic caffeamide derivative, improves left ventricular hypertrophy and function in pressure-overload mice heart. *Eur J Pharmacol*, 684 (1-3), pp. 108-115.

Westenbrink, B.D., Ling, H., Divakaruni, A.S., Gray, C.B., Zambon, A.C. and Dalton, N.D. et al. (2015) Mitochondrial Reprogramming Induced by CaMKIIδ Mediates Hypertrophy DecompensationNovelty and Significance. *Circ Res*, 116 (5), pp. e28-e39.

Westermann, D., Kasner, M., Steendijk, P., Spillmann, F., Riad, A. and Weitmann, K. et al. (2008) Role of left ventricular stiffness in heart failure with normal ejection fraction. *Circulation*, 117 (16), pp. 2051-2060.

Westley, I.S., Licari, G. and Sallustio, B.C. (2015) Validation of a High-Performance Liquid Chromatography-Tandem Mass Spectrometry Method for the Determination of Perhexiline and Cis-Hydroxy-Perhexiline Plasma Concentrations. *Ther Drug Monit*, 37 (6), pp. 821-826.

Wettschureck, N., Rütten, H., Zywietz, A., Gehring, D., Wilkie, T.M. and Chen, J. et al. (2001) Absence of pressure overload induced myocardial hypertrophy after conditional inactivation of Gαq/Gα11 in cardiomyocytes. *Nat Med*, 7 (11), pp. 1236-1240.

White, H.D. and Lowe, J.B. (1983) Antianginal efficacy of perhexiline maleate in patients refractory to beta-adrenoreceptor blockade. *Int J Cardiol*, 3 (2), pp. 145-155.

Wijesekera, J.C., Critchley, E.M.R., Fahim, Y., Lynch, P.G. and Wright, J.S. (1980) Peripheral neuropathy due to perhexilene maleate. *J Neurol Sci*, 46 (3), pp. 303-309.

Willoughby, S.R., Stewart, S., Chirkov, Y.Y., Kennedy, J.A., Holmes, A.S. and Horowitz, J.D. (2002) Beneficial clinical effects of perhexiline in patients with stable angina pectoris and acute coronary syndromes are associated with potentiation of platelet responsiveness to nitric oxide. *Eur Heart J*, 23 (24), pp. 1946-1954.

Winsor, T. (1970) Clinical evaluation of perhexiline maleate. *Clinl Pharmacol Ther*, 11 (1), pp. 85-89.

Wright, G.J., Leeson, G.A., Zeiger, A.V. and Lang, J.F. (1973) Proceedings: The absorption, excretion and metabolism of perhexiline maleate by the human. *Postgrad Med J*, 49 (S3), pp. 8-15.

Wroge, J. and Williams, N.T. (2016) Glucagon-like peptide-1 (GLP-1) receptor agonists in cardiac disorders. *Ann Pharmacother*, 50 (12), pp. 1041-1050.

Wu, H., Zhu, Q., Cai, M., Tong, X., Liu, D. and Huang, J. et al. (2014) Effect of inhibiting malonyl-coa decarboxylase on cardiac remodeling after myocardial infarction in rats. *Cardiology*, 127 (4), pp. 236-244.

Wu, J., Chen, P., Li, Y., Ardell, C., Der, T. and Shohet, R. et al. (2013) HIF-1α in heart: protective mechanisms. *Am J Physiol Heart Circ Physiol*, 305 (6), pp. H821-H828.

Wu, J., Cheng, Z., Gu, Y., Zou, W., Zhang, M. and Zhu, P. et al. (2015) Aggravated cardiac remodeling post aortocaval fistula in unilateral nephrectomized rats. *PLoS One*, 10(8), p.e0134579.

Xiong, Q., Zhang, P., Guo, J., Swingen, C., Jang, A. and Zhang, J. (2015) Myocardial ATP hydrolysis rates in vivo: a porcine model of pressure overload-induced hypertrophy. *Am J Physiol Heart Circ Physiol*, 309 (3), pp. H450-H458.

Xu, X., Hu, X., Lu, Z., Zhang, P., Zhao, L. and Wessale, J.L. et al. (2008) Xanthine oxidase inhibition with febuxostat attenuates systolic overload-induced left ventricular hypertrophy and dysfunction in mice. *J Cardiac Fail*, 14 (9), pp. 746-753.

Xu, X., Hua, Y., Nair, S., Bucala, R. and Ren, J. (2013) Macrophage migration inhibitory factor deletion exacerbates pressure overload–induced cardiac hypertrophy through mitigating autophagy. *Hypertension*, 63 (3), pp. 490-499.

Xu, X., Hua, Y., Nair, S., Bucala, R. and Ren, J. (2014) Macrophage migration inhibitory factor deletion exacerbates pressure overload–induced cardiac hypertrophy through mitigating autophagy. *Hypertension*, 63 (3), pp. 490-499.

Yamamoto, K., Masuyama, T., Sakata, Y., Nishikawa, N., Mano, T. and Yoshida, J. et al. (2002) Myocardial stiffness is determined by ventricular fibrosis, but not by compensatory or excessive hypertrophy in hypertensive heart. *Cardiovasc Res*, 55 (1), pp. 76-82.

Yamamoto, K., Origasa, H. and Hori, M. (2013) Effects of carvedilol on heart failure with preserved ejection fraction: the Japanese Diastolic Heart Failure Study (J-DHF). *Eur J Heart Fail*, 15 (1), pp. 110-118.

Yamamoto, R., Matsushita, M., Kitoh, H., Masuda, A., Ito, M. and Katagiri, T. et al. (2013) Clinically applicable antianginal agents suppress osteoblastic transformation of myogenic cells and heterotopic ossifications in mice. *J Bone Miner Metab*, 31 (1), pp. 26-33.

Yazaki, Y., Isobe, M., Takahashi, W., Kitabayashi, H., Nishiyama, O. and Sekiguchi, M. et al. (1999) Assessment of myocardial fatty acid metabolic abnormalities in patients with idiopathic dilated cardiomyopathy using 123 I BMIPP SPECT: correlation with clinicopathological findings and clinical course. *Heart*, 81 (2), pp. 153-159.

Ye, Y., Gong, H., Wang, X., Wu, J., Wang, S. and Yuan, J. et al. (2015) Combination Treatment With Antihypertensive Agents Enhances the Effect of Qiliqiangxin on Chronic Pressure Overload–induced Cardiac Hypertrophy and Remodeling in Male Mice. *J Cardiovasc Pharmacol*, 65 (6), pp. 628-639.

Yin, X., Dwyer, J., Langley, S.R., Mayr, U., Xing, Q. and Drozdov, I. et al. (2013) Effects of perhexiline-induced fuel switch on the cardiac proteome and metabolome. *J Mol Cell Cardiol*, 55, pp. 27-30.

Yoshioka, J., Chutkow, W.A., Lee, S., Kim, J.B., Yan, J. and Tian, R. et al. (2012) Deletion of thioredoxin-interacting protein in mice impairs mitochondrial function but protects the myocardium from ischemia-reperfusion injury. *J Clin Invest*, 122 (1), pp. 267-279.

Yoshioka, J., Imahashi, K., Gabel, S.A., Chutkow, W.A., Burds, A.A. and Gannon, J. et al. (2007) Targeted deletion of thioredoxin-interacting protein regulates cardiac dysfunction in response to pressure overload. *Circ Res*, 101 (12), pp. 1328-1338.

Yoshioka, J., Schulze, P.C., Cupesi, M., Sylvan, J.D., MacGillivray, C. and Gannon, J. et al. (2004) Thioredoxin-interacting protein controls cardiac hypertrophy through regulation of thioredoxin activity. *Circulation*, 109 (21), pp. 2581-2586.

Young, M.E., Patil, S., Ying, J., Depre, C., Ahuja, H.S. and Shipley, G.L. et al. (2001) Uncoupling protein 3 transcription is regulated by peroxisome proliferator-activated receptor α in the adult rodent heart. *FASEB J*, 15 (3), pp. 833-845.

Yu, C.M., Lin, H., Yang, H., Kong, S.L., Zhang, Q. and Lee, S.W.L. (2002) Progression of systolic abnormalities in patients with "isolated" diastolic heart failure and diastolic dysfunction. *Circulation*, 105 (10), pp. 1195-1201.

Yu, F.X., Chai, T.F., He, H., Hagen, T. and Luo, Y. (2010) Thioredoxin-interacting protein (Txnip) gene expression: sensing oxidative phosphorylation status and glycolytic rate. *J Biol Chem*, 285 (33), pp. 25822-25830.

Yudate, H.T., Kai, T., Aoki, M., Minowa, Y., Yamada, T. and Kimura, T. et al. (2012) Identification of a novel set of biomarkers for evaluating phospholipidosis-inducing potential of compounds using rat liver microarray data measured 24-h after single dose administration. *Toxicology*, 295 (1), pp. 1-7.

Yusuf, S., Pfeffer, M.A., Swedberg, K., Granger, C.B., Held, P. and McMurray, J.J. et al. (2003) Effects of candesartan in patients with chronic heart failure and preserved left-ventricular ejection fraction: the CHARM-Preserved Trial. *Lancet*, 362 (9386), pp. 777-781.

Zahabi, A., Picard, S., Fortin, N., Reudelhuber, T.L. and Deschepper, C.F. (2003) Expression of constitutively active guanylate cyclase in cardiomyocytes inhibits the hypertrophic effects of isoproterenol and aortic constriction on mouse hearts. *J Biol Chem*, 278 (48), pp. 47694-47699.

Zamani, P., Akers, S., Soto-Calderon, H., Beraun, M., Koppula, M.R. and Varakantam, S. et al. (2017) Isosorbide dinitrate, with or without hydralazine, does not reduce wave reflections, left ventricular hypertrophy, or myocardial fibrosis in patients with heart failure with preserved ejection fraction. *J Am Heart Assoc*, 6 (2), p. e004262.

Zannad, F., McMurray, J.J., Krum, H., van Veldhuisen, D.J., Swedberg, K. and Shi, H. et al. (2011) Eplerenone in patients with systolic heart failure and mild symptoms. *N Engl J Med*, 364 (1), pp. 11-21.

Zhabyeyev, P., Gandhi, M., Mori, J., Basu, R., Kassiri, Z. and Clanachan, A. et al. (2013) Pressure-overload-induced heart failure induces a selective reduction in glucose oxidation at physiological afterload. *Cardiovasc Res*, 97 (4), pp. 676-685.

Zhang, L., Ding, W.Y., Wang, Z.H., Tang, M.X., Wang, F. and Li, Y. et al. (2016) Early administration of trimetazidine attenuates diabetic cardiomyopathy in rats by alleviating fibrosis, reducing apoptosis and enhancing autophagy. *J Transl Med*, 14 (1), p. 109.

Zhang, L., Jaswal, J.S., Ussher, J.R., Sankaralingam, S., Wagg, C. and Zaugg, M. et al. (2013) Cardiac insulin resistance and decreased mitochondrial energy production precede the development of systolic heart failure following pressure overload hypertrophy. *Circ Heart Fail*, 6 (5), pp. 1039-1048.

Zhang, L., Lu, Y., Jiang, H., Zhang, L., Sun, A. and Zou, Y. et al. (2012) Additional use of trimetazidine in patients with chronic heart failure: a meta-analysis. *J Am Coll Cardiol*, 59 (10), pp. 913-922.

Zhao, C.Z., Zhao, X.M., Yang, J., Mou, Y., Chen, B. and Wu, H.D. et al. (2016) Inhibition of farnesyl pyrophosphate synthase improves pressure overload induced chronic cardiac remodeling. *Sci Rep*, 6, p. 39186.

Zhao, L., Cheng, G., Jin, R., Afzal, M.R., Samanta, A. and Xuan, Y.T. et al. (2016) Deletion of interleukin-6 attenuates pressure overload-induced left ventricular hypertrophy and dysfunction. *Circ Res*, 118 (12), 1918-1929.

Zhou, N., Ma, B., Stoll, S., Hays, T.T. and Qiu, H. (2017) The valosin-containing protein is a novel repressor of cardiomyocyte hypertrophy induced by pressure overload. *Aging Cell*, 16 (5), pp. 1168-1179.

Zile, M.R., Baicu, C.F. and Gaasch, W.H. (2004) Diastolic heart failure—abnormalities in active relaxation and passive stiffness of the left ventricle. *N Engl J Med*, 350 (19), pp. 1953-1959.

Zile, M.R., Baicu, C.F., Ikonomidis, J., Stroud, R.E., Nietert, P.J. and Bradshaw, A.D. et al. (2015) Myocardial stiffness in patients with heart failure and a preserved ejection fraction: contributions of collagen and titin. *Circulation*, 131 (14), pp. 1247-1259.

Zou, Y., Hiroi, Y., Uozumi, H., Takimoto, E., Toko, H. and Zhu, W. et al. (2001) Calcineurin plays a critical role in the development of pressure overload–induced cardiac hypertrophy. *Circulation*, 104 (1), pp. 97-101.